METAGENOMICS OF POLAR MARINE SEDIMENTS: STUDY OF MICROBIAL BIODIVERSITY AND ISOLATION OF NEW BIOCATALYSTS FOR USE IN INDUSTRIAL PROCESSES

Concetta De Santi

Dottorato in Scienze Biotecnologiche – XXVI ciclo
Indirizzo Biotecnologie Industriali
Università di Napoli Federico II

Dottorato in Scienze Biotecnologiche – XXVI ciclo
Indirizzo Biotecnologie Industriali
Università di Napoli Federico II

METAGENOMICS OF POLAR MARINE SEDIMENTS: STUDY OF MICROBIAL BIODIVERSITY AND ISOLATION OF NEW BIOCATALYSTS FOR USE IN INDUSTRIAL PROCESSES

Concetta De Santi

Dottoranda: Concetta De Santi

Relatore: Prof. Giovanni Sannia

Correlatore: Dott. Donatella de Pascale

Coordinatore: Prof. Giovanni Sannia

There will be a time
when you believe everything is finished.
That will be the beginning.
Louis L'Amour

Ai miei genitori

INDEX

SUMMARY 1
RIASSUNTO 2

GENERAL INTRODUCTION 7

1. Understanding Bioprospecting 8
2. Metagenomic and Genomic Approach 10
3. Psychrophilic Enzymes 13
4. Lipases and Esterases 15
5. Biotechnological Application of Lipolytic Enzymes 16
6. Aim of the thesis 19
7. References 19

Chapter I: Bioprospecting around arctic islands: Marine bacteria as rich source of biocatalysts

1.1 Introduction 27
1.2 Results and Discussion 28
1.3 Experimental Section 38
1.4 Conclusions 41
1.5 References 41

Chapter II: Biochemical characterization and structural analysis of a new cold-active and salt tolerant esterase from the marine bacterium *Thalassospira* sp.

2.1 Introduction 47
2.2 Material and Methods 49
2.3 Results 51
2.4 Discussion 55
2.5 References 57

Chapter III: Identification of a new cold-active and salt tolerant esterase isolated by functional screening of arctic metagenomic libraries

3.1 Introduction 74
3.2 Material and Methods 75
3.3 Results 80
3.4 Discussion 81
3.5 References 83

PUBLICATIONS 99

COMMUNICATIONS 99

EXPERIENCES IN FOREIGN LABORATORIES 100

SUMMARY

Marine bioprospecting is a highly topical research subject since the marine ecosystem is a relatively unexplored source of enzymes with potential biocatalytic activity. Development of new biocatalysts from marine extreme environments, such as Polar Regions, can be considered value-added. In fact, there is an increasing demand in bio discovering powerful biocatalysts for biotechnological applications in terms of esterase/lipases from cold environments. This is due to their salt tolerance, hyperthermostability, barophilicity, cold adaptivity, substrate specificity and affinity.
The first session of the research project was focused on functional-based screening method to screen a collection of 100 marine bacteria isolated from Svalbard and Lofoten islands for their ability to produce a broad spectrum of cold-active enzymes. The isolated bacteria were classified by 16S rRNA sequencing and the phylogenetic distribution of the detected activities was evaluated with the interest for finding new cold-active biocatalysts.
In the second session of the project, a gene encoding for an esterase was amplified by PCR from a bacterial sequenced genome belonging to *Thalassospira* sp. GB04J01. After cloning and gene heterologous expression in *E. coli,* the recombinant protein was obtained as high level in soluble form and then purified to homogeneity. A full structural and functional protein characterization was carried on and in addition, the enzyme was able to form diamond crystals which diffracted at 1.7 Å.
This was the first biochemical characterization and structural analysis of a cold-active esterase isolated from the genus *Thalassospira.*
A parallel session of the project was aimed at identifying and at characterizing a new cold-active and salt tolerant esterase isolated from Arctic metagenomic libraries. Taking advantage of an “omic” technique, such as Metagenomics, it was possible to access to unculturable microbes in such extreme environment, the Arctic.
A fosmid containing an ORF encoding a gene with potential esterase/lipase activity was detected by functional screening on tributyrin agar plates. The positive clones employing the largest halo size were sequenced and a gene encoding a putative lipase was found.
Gene cloning and expression were followed by a production of the recombinant protein in a soluble form. A biochemical approach highlighted protein features with a functional characterization methodology.
To achieve the summarized results several expertise in different research fields were required. The research activity was realized through short exchanges of researchers between Italy and Norway. This research project and the data obtained strongly represent a contribution to enhance the market of cold-active lipolytic enzymes of white biotechnology field as powerful biocatalysts.

RIASSUNTO

Ambienti definiti “estremi” come quelli Polari rappresentano una notevole risorsa in termini di biodiversitá microbica. Date le condizioni estreme di temperatura, pressione e salinitá, a cui gli organismi sopravvivono, non risulta sempre possibile accedere geneticamente ad un’ampia parte di microrganismi perché non coltivabili in laboratorio. Con l’interesse, dunque, di voler esplorare tale biodiversitá, é nata e si é poi sviluppata e perfezionata nel corso degli anni, una tecnica “omica” che affianca la genomica. Questa tecnica, definita metagenomica, ha permesso, con le sue notevoli potenzialitá, di esaminare la biodiversitá completa su una scala molto piú ampia, applicando differenti metodi di analisi, consentendo una valutazione diretta della diversitá dei gruppi e fornendo una serie di dati rilevanti per misurare e modellare i processi biologici. Piattaforme sempre più ricercate, con un ridotto impatto in termini di costi e di tempi di sequenziamento, hanno portato all’identificazione di un gran numero di genomi.
Questa tecnica trova il suo maggior impiego non solo nell’identificazione di composti naturali bioattivi, che possono trovare largo impiego nelle industrie farmaceutiche, ma anche di enzimi particolarmente interessanti per aziende operanti nel settore delle biotecnologie industriali.
Un’analisi volta all’identificazione di biocatalizzatori dotati di particolari caratteristiche, come una migliore efficienza catalitica in particolari condizioni di reazione, é infatti favorita dall’utilizzo di collezioni metagenomiche derivanti da siti contaminati o da ambienti polari, quest’ultimi dotati di particolari caratteristiche come estremi di pH, temperatura o concentrazione salina.
L’impiego di enzimi come biocatalizzatori per i moderni processi industriali si prospetta, dunque, come una vantaggiosa alternativa ai tradizionali processi chimici per diversi motivi. In primo luogo, data la loro specificitá, restituiscono un prodotto di maggiore qualità attraverso processi produttivi “puliti” a ridotto impatto ambientale in quanto non rilasciano prodotti di scarto inquinanti e sono essi stessi biodegradabili. Inoltre, dal punto di vista economico, il ridotto consumo di energia, materie prime ed acqua richiesto nelle bioconversioni, consente l’ottenimento di prodotti di qualità superiori a costi sostanzialmente ridotti. Le molte potenzialità offerte dalle peculiari caratteristiche di batteri e biocatalizzatori psicrofili che li rendono vantaggiosi, in molti processi industriali, risultano in sintonia con gli obiettivi della *white biotechnology* e rappresentano dunque un campo in cui é interessante continuare a investire. Esterasi e lipasi sono alcuni dei maggiori biocatalizzatori utilizzati. Le ragioni di questo successo sono numerose e relative all’ampia varietà di substrati riconosciuti, combinata all’esclusiva chemoselettivitá, regioselettivitá e stereoselettivitá frequentemente mostrata da questa classe di enzimi.
A tal proposito, il lavoro svolto durante il mio dottorato di ricerca é stato dedicato all’identificazione di nuovi biocatalizzatori, da fonti microbiche artiche, da utilizzare nel campo della *white biotechnology*. A tale scopo sono stati utilizzati due diversi approcci, genomico e metegenomico, per arrivare all’isolamento di due esterasi psicrofile, a partire da una collezione di batteri marini isolati da sedimenti marini. Le metodologie sperimentali adottate e i risultati conseguiti sono elencati di seguito.

1) Identificazione di una serie di classi enzimatiche mediante *functional screening*, a partire da una collezione di batteri marini psicrofili isolati in Artide.

Avvalendoci di una collezione di 100 batteri marini psicrofili, abbiamo investigato il potenziale biotecnologico di tali microganismi come produttori di enzimi quali cellulasi, xilanasi, chitinasi, DNasi, proteasi ed esterasi/lipasi.

Tutti i batteri, identificati mediante sequenziamento del gene del 16S rRNA, sono stati isolati nell'ambito di due spedizioni artiche, presso le Lofoten e le isole Svalbard e messi a nostra disposizione dall'Universitá di Tromsø in Norvegia.

La metodologia sperimentale, che ci ha permesso di arrivare all'identificazione delle attivitá enzimatiche extracellulari d'interesse, é stata quella del *functional screening*.

Diversi substrati sintetici sono stati aggiunti al terreno di crescita, su piastre solide di agar, in funzione dell'attività enzimatica di interesse.

La concentrazione di substrato utilizzata é stata scelta in base al suo grado di tossicitá nei confronti dei vari batteri. Le piastre sono state incubate per diversi giorni a due temperature: 4°C e 20°C. L'attivitá é stata valutata in base alla presenza di un alone su piastra, in corrispondenza della colonia, indice di una degradazione del substrato da parte dell'enzima. Per la determinazione di alcune attivitá enzimatiche é stata necessaria l'aggiunta di un colorante, Congo Red o blu di Coomassie. L'incubazione delle piastre, in presenza dei coloranti e la successiva decolorazione, é stata ottimizzata per meglio evidenziare, laddove presente, l'attivitá extracellulare. I risultati ottenuti sono stati messi a confronto e analizzati per identificare i batteri migliori quali produttori delle diverse classi di enzimi. Un approccio futuro prevede il sequenziamento del genoma dei batteri selezionati e l'isolamento di enzimi di potenziale interesse biotecnologico.

Risultati conseguiti

Sulla base delle attivitá enzimatiche riscontrate, una percentuale superiore al 45% dei batteri analizzati é risultata in grado di produrre enzimi quali esterasi, proteasi e DNasi. Il 41%, 23%, 9% e 7% dei batteri é stato in grado di produrre enzimi quali: amilasi, chitinasi, cellulasi, xilanasi rispettivamente.

Tutti i batteri sono cresciuti in maniera ottimale in presenza del terreno di crescita commerciale *Marine broth* senza richiedere alcuna ulteriore aggiunta di cloruro di sodio.

L'analisi filogenetica della collezione di batteri é stata condotta sulla base delle sequenze dei 16S rRNA. Un albero filogenetico é stato costruito per meglio determinare le loro affiliazioni. Il risultato ottenuto ha evidenziato come dei 60 batteri gram-negativi, 53 appartengano al phylum dei *Proteobacteria* mentre 9 a quello dei *Bacteroidetes.* Dei 40 batteri classificati come gram-positivi, 29 erano appartenenti al phylum degli *Actinobacteria* e 12 a quello dei *Firmicutes.*

Analizzando i risultati ottenuti, é stata riscontrata un'attivitá esterasica, proteasica e DNasica ugualmente distribuita tra *Proteobacteria, Bacteroidetes, Actinobacteria* e *Firmicutes* mentre differenze sono state rivelate per le altre attivitá analizzate. In tabella sono stati elencati gli enzimi di interesse ricercati e le diverse specie batteriche produttori di tali enzimi come esito del *functional screening* effettuato.

Enzimi di interesse	Specie batteriche
ESTERASI	*Pseudoalteromonas, Pseudomonas, Shewanella, Acinetobacter, Roseovarius, Psychrobacter*
CELLULASI	*Serratia, Photobacterium, Moritella, Pseudoalteromonas*
XILANASI	*Promiconospora, Serratia, Pseudoalteromonas, Clavibacter*
CHITINASI	*Pseudomonas, Photobacterium, Serratia, Brevundimonas, Roseobacter, Shewanella*
AMILASI	*Pseudoalteromonas,Serratia, Flavobacterium, Photobacterium, Psychrobacter*

2) Identificazione e caratterizzazione strutturale e funzionale di una esterasi psicrofila isolata dal batterio marino artico *Thalassospira* sp.

Il ceppo batterico *Thalassospira* sp. GB04J01 é stato isolato da una gorgonia a ventaglio (*Paramuricea placomus*) nell'ambito di una spedizione scientifica lungo il Vestfjorden, Norvegia del Nord.
Il genoma del batterio é stato interamente sequenziato e messo a nostra disposizione, da parte dell'universitá di Tromsø, con l'intento di isolare una sequenza codificante per un enzima ad attivitá lipolitica. La scelta é ricaduta su di un gene, annotato come *putative carboxylesterase*, la cui sequenza amminoacidica é risultata identica al 36% per 114 amminoacidi, ad una carbossilesterasi Est2 da *Alicyclobacillus acidocaldarius* (1QZ3A). Il gene é stato clonato ed espresso in opportuno vettore e la proteina, ThaEst2349, prodotta ad alte rese in forma solubile. La presenza di una coda di sei istidine all'estremitá C-terminale ha facilitato la procedura di purificazione della proteina, in termini qualitativi e quantitativi, che é risultata pura al 98%.
Un'ampia caratterizzazione funzionale e strutturale della proteina ricombinante é stata effettuata per identificare il pH ottimale, la temperatura ottimale, e valutare la termostabilitá, l'attivitá esterasica in presenza di cationi metallici, possibili inibitori, detergenti e solventi organici. Tutti i saggi di attivitá spettrofotometrici sono stati condotti in presenza di substrati sintetici quali esteri del p-nitrofenile con catene aciliche a lunghezza variabile misurando spettrofotometricamente a 405 nm il rilascio del prodotto, paranitrofenolo, a seguito della reazione enzimatica.

Risultati conseguiti

L'enzima ThaEst2349 si é rivelato particolarmente attivo a pH 8,5 in presenza del tampone Tris-HCl. L'attivitá elevata riscontrata a pH alcalino é dovuta alla protonazione del residuo di istidina coinvolto nella triade catalitica; questo risultato ci ha permesso di considerare l'enzima una esterasi alcalina. La temperatura ottimale dell'enzima é risultata pari a 45°C mentre una completa inattivazione dell'enzima é stata riscontrata ad una temperatura pari a 70°C.

Un'altra interessante proprietá enzimatica riscontrata é stata l'elevata termostabilitá a 40°C dopo un'incubazione di 2 ore. Una spiegazione di tale comportamento risiede nell'elevata flessibilitá strutturale dell'enzima psicrofilo, dovuta a un numero ridotto di legami idrogeno e ad un aumento del numero di residui di metionina, se comparato con altre strutture di esterasi.
L'enzima ricombinante ha mostrato specificitá di substrato verso esteri del p-nitrofenile a catena corta dai due ai cinque atomi di carbonio (C2-C5). Il substrato p-nitrofenil acetato (C2) é risultato quello ottimale. Questo dato conferma la natura esterasica dell'enzima.
Per meglio comprendere le caratteristiche dell'enzima, in vista di un suo possibile utilizzo come catalizzatore di sintesi organica, siamo andati a valutarne l'attivitá in presenza di solventi organici. Una notevole inattivazione si é avuta in presenza di solventi quali metanolo, acetonitrile, etanolo e acetone. Tuttavia, l'enzima ha mostrato attivitá in presenza di DMSO (dimetilsolfossido), glicerolo ed etere dietilico.
Saggi effettuati in presenza di un agente chelante, quale l'EDTA (etilediamminotetracetico), non hanno mostrato alcun effetto sull'attivitá enzimatica a differenza di cationi metallici quali Fe^{2+} e Cr^{2+} che hanno totalmente inibito l'enzima se presenti ad una concentrazione pari a 10mM. Invece, l'aggiunta di cloruri metallici quali, $CuCl_2$, $MnCl_2$, $HgCl_2$, $SnCl_2$, $CoCl_2$, LiCl, $NiCl_2$, non ha portato ad alcun effetto inibitorio nei confronti dell'esterasi.
Detergenti non ionici testati hanno incrementato l'attivitá enzimatica a differenza di quelli ionici, quali SDS (sodio dodecil solfato) o del CTAB (bromuro di cetil-trimetilammonio) quale surfattante cationico con effetti tossici sull'esterasi.
Considerando che l'enzima é stato isolato da un batterio marino, siamo andati a valutare la stabilitá e solubilitá dell'enzima in presenza di elevate concentrazioni di sale. Questo dato avvalora in suo possibile impiego di biocatalizzatore in determinati settori industriali.
Il cristallo della proteina é stato ottenuto con una buona risoluzione pari a 1.7 Å. Da una cromatografia ad esclusione molecolare la proteina é risultata essere un dimero in soluzione ed, in termini di struttura cristallografica, le due catene A e B formano un dimero funzionale. Nota la struttura cristallografica, l'analisi strutturale sulle caratterisitiche psicrofile dell'enzima é stata portata avanti per confronto con altre esterasi ipertermofile, PcEstE, StoEst ed Est2, isolate da *Pyrobaculum calidifontis*, *Sulfolobus tokodaii* ed *Alicyclobacillus acidocaldarius,* rispettivamente.

3) Identificazione e caratterizzazione funzionale di una nuova esterasi psicrofila isolata mediante *functional screening* a partire da una *library* metagenomica.

Una delle tecniche "omiche" nota come metageomica é stata utilizzata per l'identificazione di un nuovo enzima ad attivitá lipasica da utilizzare come biocatalizzatore nel campo delle biotecnologie industriali. L'intento é stato quello di voler isolare il gene da quella parte di microrganismi, esistenti ma non coltivabili in laboratorio, che popola le regioni artiche; nello specifico, sedimenti marini prelevati nell'ambito di una spedizione scientifica presso le Lofoten e le isole Svalbard.
L'estrazione del DNA metagenomico é stato effettuato a partire da tre campioni ambientali di natura diversa: CTD241-86, CTD249-119 e HH596.
Il protocollo di estrazione é stato ottimizzato per ottenere un DNA qualitativamente ottimale e quantitativamente sufficiente per la costruzione di tre librerie metageomiche. I frammenti di DNA delle dimensioni di circa 40 Kb sono stati clonati

all'interno di un vettore fosmidico. Il DNA cosí ottenuto é stato impacchettato in particelle fagiche, utilizzate poi per infettare cellule di *E. coli* EPI300. Le cellule sono state piastrate in presenza di un agente selettivo, quale il cloramfenicolo, ed un numero pari a 384, 1000 e 2500 di cloni fosmidici é stato ottenuto per ciascuna *library*, rispettivamente.
Le colonie ottenute sono state trasferite su piastre contententi un substrato sintetico, la tributirrina, per identificare i cloni fosmidici contenenti geni codificanti per esterasi e lipasi. I cloni risultati positivi su piastra sono stati sequenziati e, mediante analisi bioinformatica, é stato individuato un gene codificante per una putativa lipasi di classe 3.
Si é deciso pertanto di clonare il gene ed esprimerlo, tramite un opportuno vettore, in un ospite eterologo quale *E. coli* BL21DE3. La resa di produzione della proteina ricombinante, Lip3, in forma solubile, non é stata elevata ma sufficiente ad effettuare una caratterizzazione biochimica per meglio comprenderne un possibile utilizzo quale biocatalizzatore.

Risultati conseguiti

L'effetto del pH sull'attivitá enzimatica é stato valutato in un ampio intervallo che va da pH 5,0 a pH 10,5 in presenza di vari tamponi. L'attivitá piú elevata per Lip3 é stata osservata a pH 8,0. La temperatura ottimale dell'enzima é risultata invece pari a 35°C mentre una completa inattivazione dell'enzima é stata riscontrata ad una temperatura pari a 70°C.
L'enzima si é mostrato, inoltre, particolarmente stabile alle alte temperature. Infatti, persino a 60°C, dopo un'incubazione di 1 ora, il catalizzatore manteneva un'attivitá pari quasi al 90% rispetto a quella rivelata, nelle stesse condizioni sperimentali, in assenza di incubazione. Ancora una volta, la spiegazione di tale fenomeno risiede nell'elevata flessibilitá strutturale dell'enzima psicrofilo, soprattutto in corrispondenza del sito attivo, rispetto alle controparti mesofile.
L'enzima ricombinante ha mostrato una migliore specificitá di substrato verso il paranitrofenilacetato ma é stato in grado di degradare anche esteri del paranitrofenile a catena piú lunga, fino ad un massimo di otto atomi di carbonio.
L'effetto dell'attivitá di Lip3 in presenza del cloruro di sodio a varie concentrazioni, ha portato ad individuare un notevole incremento dell'attivitá enzimatica sia in termini di solubilitá che di stabilitá.
L'attivitá di Lip3 in presenza di EDTA, DTT (ditiotreitolo), PMSF (fenil-metil-sulfonil-fluoruro) e β-mercaptoetanolo ha mostrato un decremento dovuto ad un effetto inibitorio dei vari composti se aggiunti ad una concentrazione pari a 10mM.
L'inibizione da PMSF puó essere spiegata in termini di inattivazione della serina, presente nella triade catalitica, e coinvolta in qualitá di nucleofilo nella reazione catalitica che avviene nel sito attivo. L'inibizione da DTT, invece, é da attribuirsi ad un ipotetico ponte disolfuro esistente. Non disponendo della struttura cristallografica, é stato costruito un modello di struttura 3D tramite *modelling* per omologia della sequenza dell'enzima di interesse con altri templati.
Le strutture scelte appartengono ad una triacilglicerolo lipasi da *Yarrowia lipolytica* (PDB ID: 3O0D), una lipasi da *Gibberella zeae* (3NGM), una lipasi da *Penicillium expansum* (3G7N) e da *Serratia marcescens* (2QUB).
Un'analisi della superfice accessibile al solvente, ne mostra una natura idrofobica del 59,6%, che lascia presagire una possibile interazione con solventi organici.

General introduction

1. Understanding Bioprospecting

The earth is rich in biological material that may not be completely understood. It's often the case that remote areas use biological cures for disease that are not produced in laboratory and have not yet been packaged and patented by some companies. Great potential exists in these traditional medicines from small countries, and this has led to increased interest, in particular by advanced countries, in finding prospective beneficial biological substances, developing them through biotechnology and patenting them.

This methodical search in nature for novel bioactive compounds is called *bioprospecting* and includes whole organisms, genes, chemical compounds, micro and macroorganisms. The term "bioprospecting" is usually credited to Thomas Eisner, a chemical ecologist who wrote an article in 1989 entitled "Prospecting for nature's chemical riches" [1]. Years later, the Convention on Biological Diversity (CBD) Secretariat defines bioprospecting as "the exploration of biodiversity for commercially valuable genetic and biochemical resources" [2].

In recent years, the bioprospecting efforts are often characterized by high-throughput approaches, where robotized technologies are used to screen through large numbers of samples from specific environments or class of organisms. The screening of microbial natural products continues to represent the main route in order to discover novel bioactive and therapeutic compounds.

A prospecting program might include collection of the material, screening to protect intellectual property interests and the eventual development of a commercial process or new products which may include modification of the chemical structure to increase efficacy.

Bioprospecting may also include downstream testing and the development of other substances derived from the initial discovery. Final stages of the process include manufacturing and plans for larger scale production and marketing of the product [3].

Bioprospecting usually requires the collection of a very limited amount of biomass for the initial discovery. Even if further collections may be required after a promising discovery, bioprospecting generally does not involve risks to biodiversity in comparison with the large biomass removals involved in harvesting resources for food or mineral exploitation.

Hence, the commercialization aspects of bioprospecting and potential profitability remain the critical aspects regarding its legal definition. The distinction lies between Marine Scientific Research (MSR) [4] and bioprospecting, as concerns any property rights arising from the planned future development of marine genetic resources discovered on scientific expeditions, is the subject of ongoing debate.

The concerns are that:

- Very little is known about the conservation status of many species used as sources of marine genetic resources
- Many species occur in vulnerable and fragile ecosystems
- The effect on ecosystems of removal of marine genetic resources is poorly understood

Marine bioprospecting

Marine environments, including the subsurface, are believed to contain a total of approximately 3.67×10^{30} microorganisms. Roughly 71% of the earth's surface covered by the ocean, this environment represents 80% of life on earth, and an

enormous pool of potential microbial biodiversity and exploitable biotechnology or *blue* biotechnology [5].
Marine bioprospecting is the action of searching for unknown organisms or genes that can constitute the basis of a new biological product, such as a drug or cosmetic. It has increased rapidly in recent years. Today, more than 18,000 natural products have to date been developed from about 4,800 marine organisms, and the number of natural products from marine species is growing at a rate of 4% per year. The marine environment represents a likely source of future products, as life there has been much less extensively explored than on land.
Much of the marine biome under-investigated and the prospect for new and unique findings is high, especially in the microbial realm with a very rich variety of organisms, mostly of them undescribed [6].
Advances in technologies for observing and sampling the deep ocean, such as remotely operated vehicles (ROVs), have given access to unexplored areas to scientific research. Coordinated scientific efforts such as the Census of Marine Life (Census of Marine Life: http://www.coml.org) have contributed to scientific research, resulting in many new and exciting discoveries. At the same time, high throughput genome sequencing, metagenomics and bioinformatics, have increased our ability to investigate and make use of marine genetic material.
Since 1999, the number of patents of genetic material from marine species has increased at the rate of 12% per year. Marine species are about twice as likely to yield at least one gene in a patent than their terrestrial counterparts. 97% of natural products of marine origin are from eukaryotic sources (organisms with complex cells), and sponges alone accounting for 38% of the products [6].
By the end of 2007, only 10 compounds had been reported from deep ocean and ocean trench environments, with a further seven identified in 2010. Fewer than 10 marine natural products have so far been reported from hot vent bacteria [7].
It is expected that the rate of discovery will continue to increase as technology develops. Conservation and sustainably use of marine biological diversity in areas beyond national jurisdiction (ABNJ) is one of the most long debated issue in international forum.

Bioprospecting in polar regions
Bioprospecting of marine environments is conducted almost exclusively in regions at extreme depths in the high seas or on the deep seabed below, specifically around sub-marine trenches, cold seeps, seamounts and hydrothermal vents.
Polar regions are home to an enormous diversity of organisms, which are well adapted to the extreme conditions of their marine habitats. This makes these arctic species very attractive for marine bioprospecting.
As a process, marine bioprospecting generally consists of four phases:

- Phase 1: on-site collection of samples;
- Phase 2: isolation, characterization and culture of specific compounds;
- Phase 3: screening for potential uses, such as pharmaceutical or other uses;
- Phase 4:product development and commercialization, including patenting, trials, sales and marketing [8].

Due to their location and characteristics, extremophilic organisms are difficult and expensive to access and study. Pure research projects have difficulty financed expeditions. Companies can be unwilling to undertake the financial risks of exploration in the absence of clear rules regarding ownership of the genetic resources in these areas. The significant expenses involved have led to a number of

public/private partnerships in which private companies finance public research expeditions, which then pass samples to the companies for commercial research.
The biotechnology based on polar genetic and molecular aspects includes several key areas including enzymes, anti-freeze proteins, bioremediation, pharmaceuticals and other health related applications such as dietary supplements (nutraceuticals) and cosmetics. The commercialization of research expedition results based on marine bio-prospecting requires a long-term perspective, a cross-disciplinary approach, business expertise, sufficient capital and a willingness to take risk.

2. Metagenomic and genomic approach

This record of discovery on bioactive organisms and compounds, coupled with the knowledge that there is a largely undiscovered diversity of microorganisms, supports the issue for bioprospecting in polar regions. There is a particular interest in marine species that live in extreme environments, such as hydrothermal vents and seamounts. The capacity of deep, cold and hot vent ecosystems to produce novel chemistry and genes have been under-investigated, despite indications that biodiversity is high.
The challenge is to access the organisms, by bringing them into laboratory culture, or to access the genetic information, through genomics and metagenomics [9].
The combination of a culture-dependent and culture-independent technique has been considered the best approach towards a better understanding of how microorganisms survive and function in such extreme environments [10]. Two different approaches, genomics and metagenomics, can be utilized to implement a culture dependent or independent approach respectively.
Genomics can be defined as the study of the genetic complement of a single organism.
Metagenomics refers to all of the genetic information of a natural assemblage equivalent to the genomes of all of the organisms in the sample [11].

Culture-dependent method

The development of techniques for analysis of 16S rRNA gene sequences unnatural samples has enhanced our ability to identify bacteria in terms of unique and previously unrecognized microorganisms [12]. The most application of culture-dependent procedure in community analysis were carried out using synthetic medium supplemented with various nutrients [13,14].
Cultured microbes remain useful as they provide a mechanism to help pair genetic potential with physiology of isolated organisms but they do not necessarily provide comprehensive information on the composition of microbial communities and on the assessment the significance of cultured members in resident microbial communities.
For example, culture-independent molecular methods have been employed to show that cultivated microorganisms from both temperate and extreme environments often may represent very minor components of the microbial community [15] because the most abundant environmental microbes are often the most difficult to grow in the laboratory since their metabolic and physiological requirements cannot be reproduced in vitro [16].
Hence, efforts are now underway to improve cultivation and sequencing technologies. Most of the marine compounds that have been successfully screened and structurally elucidated so far originate from isolated and culturable microorganisms, especially bacteria [17].

It is easy to understand that, if the scientific aim is to explore extreme environments with respect to the presence of novel biocatalysts, then there is a need to introduce metagenomic as culture-independent approach paired to an optimized heterologous expression system.

Culture-independent method

It has been reported that only 0.001–0.1% of the microorganisms which live in seawater, 0.25% in fresh water, 0.25% in sediments and only 0.3% of soil microorganisms are cultivable. Contrarily, typically 99% of the microbial diversity in any habitat is not accessible using classical microbiological cultivation technologies. So it stands to reason that many more genetic sequences valuable for products are yet to be discovered [18,19].

Metagenomics is an extremely useful technique to access the uncultured majority, and can be broadly defined as the study of microbial communities using high-throughput DNA sequencing technology without requirement for laboratory culture [20]. Metagenomics revolves around two categories of discovery:

- Microbial biocatalysts for synthesis and production of secondary metabolites as bioactive products;
- Genes or gene clusters encoding enzymes or enzyme systems applicable to product synthesis and development [21].

Methodology and strategy in metagenomics

The experimental methodology for metagenomics consist of collecting desired samples and involves direct extraction of the entire genomic DNA from an environmental sample. Then, after a size-selection of the total DNA, DNA fragments are cloned into a suitable vector and then transferred into host cells, followed by sequence-based or function-based screening (**Fig1**). Although *E. coli* is commonly used, other hosts are also employed for additional expression capabilities.

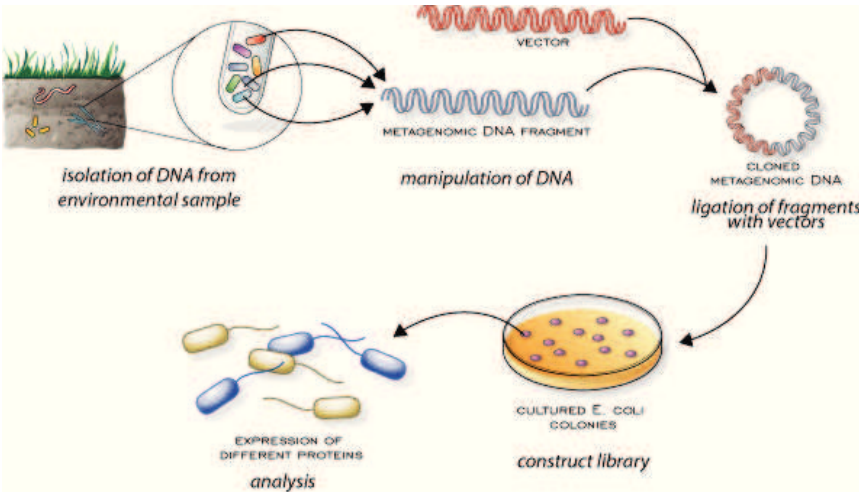

Fig1: Metagenomic expression library construction (www.scq.ubc.ca/?p=509)

DNA is sequenced at random and the genome sequences assembled using the most sophisticated computer technology available. The development of next generation DNA sequencing technologies in many centers has provided greatly enhanced capabilities for sequencing large meta-datasets.

This technology has created new opportunities for the pursuit of large scale sequencing projects that were difficult to imagine just several years ago. With this extraordinary and powerful set of sequencing tools now available, it is not a surprise that metagenomics has become one of the fastest growing scientific disciplines.
The new generation of sequencing technology (NGS) and Massively Parallel Sequencing (MPS) are often used interchangeably to refer to high throughput sequencing technologies. Sequencing by Synthesis (SBS) refers specifically to Illumina sequencing technology with its ability to sequence thousands of organisms in parallel. As a result, the sequencing of microbial genomes has become routine. Recent technical improvements allow nearly complete genome assembly from individual microbes directly from environmental samples or clinical specimens, without the need to develop cultivation methods [22].
At the moment, six platforms from the second and the third generation sequencing technologies are available with most platforms requiring short template DNAs (200–1000 bp) and with each template containing a forward and reverse site (Table 1) [23,24].

Platform	454	Illumina	Life technologies ABI/SOLID	Helicos biosciences heliscope	Ion torrent	Pacific biosciences
Year of availability	2005	2006	2006	2007	2010	2010
Sequencing length	200–700 bp	Up to 150 bp	35–50 bp	25–55 bp	~200 bp	1500 bp
Sequence yield per run	700 Mb	2–600 Gb[a]	120 Gb	35 Gb	20–50 Mb on 314 chip 100–200 Mb on 316 chip Gb on 318 chip	100 Mb
Run time	23 h	27 h–11 days	7-8 days	3–6 days	2 h	2 h
Technology	emPCR, pyrosequencing	Polonies, cleavable dye terminators	emPCR, ligation with cleavable dye terminators	True Single Molecule Sequencing (tSMS) Single base, reversible dye terminator extension reactions	emPCR, H+ detection	Single Molecule Real Time (SMRT) sequencing dyes that are phospholinked to the nucleotide, very sensitive fluorescent detection in zero mode waveguides

[a]2 Gb for the MiSeq and 600 Gb for the HiSeq2000.

Table1: Technical specifications of Next Generation Sequencing platforms (Nikolaki et al., 2013)

The biotechnological implications result from the possibility of recognizing new and heretofore unknown genes, gene products and processes suggested from the sequence. Once identified, the ‘lead genes’ can be isolated, cloned and expressed in suitable microbial hosts using existing molecular tools [25].
A huge number of natural products exist in non-culturable microbes with chemical, biological, and functional activities for potential uses in various industrial and biomedical applications [11]. In fact, unique bioactive compounds have been discovered through metagenomic cloning and expression of genomic DNA of uncultured terrestrial microbes, including terragines, violacein, indirubin, and turbomycins. Similar works on uncultured marine microorganisms such as sponges and ascidians introduced drugs such as cephalosporins (anti-microbial), cytarabine (anti-cancer), and vidarabine (antivirus), which are well established on the pharmaceutical market [26].

Novel biocatalysts from metagenome

Functional analysis of the metagenomic data plays a central role in such studies by providing important clues about functional and metabolic diversity [27].

Sequence-similarity-based screening and activity-based screening may retrieve valuable catalysts from the metagenome but the activity based approach holds more potential for identifying entirely novel active sequence [19].

There is clearly demand for novel enzymes and biocatalysts, and metagenomics is currently thought to be one of the most likely technologies to provide the candidate molecules required. In the industrial field, metagenomics is focused on prokaryotes since their genomes can easily be targeted by the functional screening tools available today [28-30].

In particular, useful biocatalysts from microbial resources are becoming popular with chemical industries as indispensable for the modern organic chemistry [31]. It is estimated that in 10% of processes may provide a superior synthetic solution over classical chemistry [32] and for this reason, the availability of an appropriate biocatalyst is now thought to be a limiting factor for any biotransformation process [33]. To be employed in any industrial application, enzymes need to function well according to several specific parameters, as activity, stability, specificity and efficiency.

Metagenomics and the derived biomolecules can offer industry a specific contribution to every industrial field:

- For industries that produce bulk products, for example in terms of detergent formulas. An enzyme backbone with peculiar functionality with a new sequence would be very attractive for patenting [34].
- For the pharmaceutical fine chemicals industries which need often to find multiple diverse biocatalysts to build internal toolboxes for biotransformations [35].
- For the discovery of elusive metabolites: many pharmacologically active secondary metabolites are produced by bacteria that live in complex consortia, or by bacteria that inhabit niches that are difficult to reconstitute *in vitro* [36].

This overview on Metagenomic applications in the discovery and development of novel enzymes highlights this omic technique as factors that could change the landscape of enzyme technology [21].

As for any technique there are advantages, it has been reported that in highly diverse environments, metagenomic approaches have not been so successful since the assembly is extremely challenging due to the highly heterogeneity of these samples. A way to overcome this issue is to use a single cell genomics approach that has been recently developed to permit the genome analysis of individual community members [37,38].

3. Psychrophilic enzymes

Microorganisms represent a powerful resource for novel enzymes, biocatalysts and biologically active compounds [39]. Some microorganisms are able to survive in unusual environmental conditions, including the high temperatures of volcanic hot springs, the low temperatures of polar regions, high pressures in deep seas, very high salt concentrations, or very high and low pH values [40]. These microorganisms can be divided into three groups: psychrophiles, mesophiles, and thermophiles, depending on their optimal growth temperatures.

Psychrophiles are one of the most underutilized resources and there is not so much reported in the literature, about the biology of microorganisms in cold environments, especially in Polar Regions, but this scenario is changing. The new high-throughput DNA sequencing technologies have revolutionized the exploration of polar microbiology revealing microbial ecosystems with unexpectedly high levels of diversity and complexity.

Large proportion of our planet is cold and most ecosystems are subjected to low temperatures since ~70% of the Earth's surface is covered by oceans that have a constant temperature of 4–5°C below a depth of 1,000 meters. In order to maintain metabolic rates even at low temperatures, psychrophiles contain thermolabile enzymes, named “cold-active enzymes”.

The high specific activity at low temperature of cold-adapted enzymes is a key adaptation to compensate the exponential decrease in chemical reaction rates when the temperature is reduced. Such high biocatalytic activity arises from the disappearance of various non-covalent stabilizing interactions, resulting in an improved flexibility of the enzyme conformation. It is known that this adaptive feature is genetically encoded within the protein sequence and results from a long-term selection.

Most psychrophilic enzymes have in common one property: a heat-labile activity, unrelated to the protein structural stability. Furthermore, the active site seems to be the most heat-labile structural element of these proteins. Activity of the cold-active enzyme is lost before the protein unfolds [41,42].

Due to their high specific activity at low temperatures and their rapid inactivation at higher temperatures, extremozymes offer a great potential as biocatalysts in biotechnology and in food processing [43].

These specific traits are responsible for the three main advantages of cold active enzymes in biotechnology:

- lower concentration of the enzyme is required due to their high activity and this can reduce the amount of costly enzyme preparation in an industrial process;
- efficient activation in tap water or room temperature, therefore avoiding heating during a process, either at domestic or industrial levels;
- efficient inactivation due to their heat lability.

Directed evolution experiments have highlighted that, in theory, cold activity of enzymes can be gained by several subtle adjustments of the protein structure [44]. Amino acids present on the protein surface of cold marine active enzymes have been shown to play critical roles in both activity in cold and in high salinity, with increased activity and improved folding at higher concentrations of salt [45,46]. In fact, halophilic proteins have also been found to contain a low content of bulky hydrophobic side chains on their surface, due to a reduced number of larger hydrophobic amino acid residues (phenylalanine, isoleucine, and leucine) compared to non-halophilic proteins [47-49].

Published studies of extremophilic enzymes have also shown a mechanism of adaptation of enzymes to function in organic solvent [50]. Such enzymes may be useful for both biofuel and bioenergy applications, where large quantity of ethanol or other organic solvents are produced [51] and for synthetic chemistry, especially when catalysis of desired chemical reactions requires the presence of organic solvents [52,53].

The high activity of psychrophilic enzymes at low and moderate temperatures offers potential economic benefits, for example, through substantial energy savings in large-scale processes that would not require the expensive heating of reactors.

4. Lipases and esterases

Carboxylesterases (carboxyl ester hydrolase) include two groups of enzymes, namely non-specific esterases (EC 3.1.1.1) and lipases (EC 3.1.1.3) which have been early differentiated on the basis of their substrate specificity [54].
Lipases are ubiquitous enzymes that catalyze the breakdown of fats and oils with subsequent release of free fatty acids, diacylglycerols, monoglycerols and glycerol (**Fig.2**) [55].

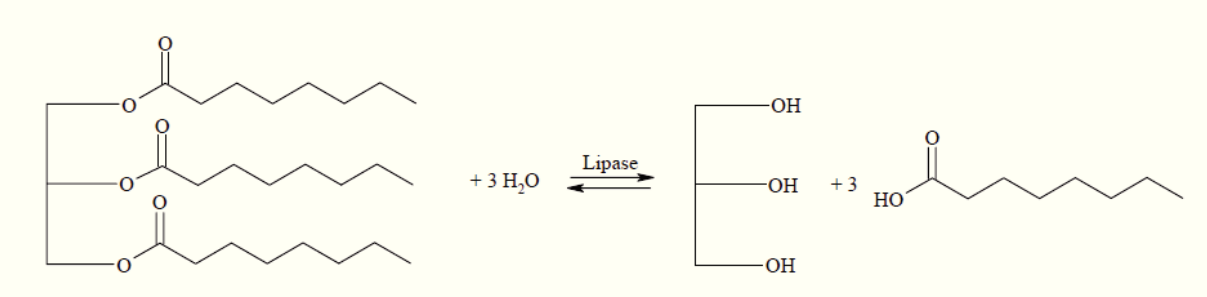

Fig.2 The catalytic action of lipases. A triglyceride can be hydrolyzed to form glycerol and fatty acids, or the reverse (synthesis) reaction can combine glycerol and fatty acids to form the triglyceride**. (Jaeger et al.1998).**

Lipases and esterases have received attention, as evidenced by the increasing amount of information about these enzymes from the current literature.
One important aspect of lipolytic enzymes is the unique physico-chemical character of the reactions they catalyse at lipid-water interfaces. Lipases were previously defined in kinetic terms, based on the "interfacial activation" phenomenon, in terms of the increase in the activity which occurs when a partially water-soluble substrate becomes water-insoluble [56]. This process was not observed among esterases.
The first microbial lipase was found from *Penicillium Oxalicum* and *Aspergillus flavus* in 1935 by Kirsh [57]. Thereafter, four cold-adapted lipases were isolated from *Moraxella* by Feller *et al.* (1990).
Lipases were classified by Vorderwulbecke, Kieslich and Erdmann (1992) as enzymes that hydrolyze and also synthesize esters; they can also act regardless of the presence of an interface, under well-established conditions, retaining catalytic activity in either organic or non-organic solvents. This new definition poses a challenge to define lipolytic activity, and to select the standard assay [58].
Arpigny and Jeager categorized prokaryotes-derived lipolytic enzymes into 8 families [59] on the base of sequence identity and biochemical properties and revealed to be useful against the increasing number of bacterial lipases and esterases.
Family I covered the 6 subfamilies of true lipase which principally catalyzed the hydrolytic reactions on substrates with long acyl chains. Carboxyl esterase families were grouped into Family II, called GDSL family. Family III and Family IV (also called HSL family). Subsequent studies led to the discovery of new enzymes that could not be classified in the previous discovered 8 families. The 9th family of bacterial esterases (Family IX) was created when nPHB depolymerase PhaZ7 was discovered [60]. The hyperthermophilic esterase EstD from *Thermotoga maritime* was categorized into Family X. Metagenomic derived lipolytic enzymes LipG [61] and LipEH166 [62] were identified as 1th and 12th bacterial esterase family members. Family XIII started from the discovery of esterase Est30 from *Geobacillus stearothermophilus* [63,64] through 3D structural characterisation that revealed a three-helix cap domain and an a/b hydrolase fold domain with a peculiar topological

structure. The most recently found bacterial lipolytic family is Family XIV with thermostable esterase EstA3 as typical member [65]. Recently, two novel thermostable bacterial lipases, LipS and LipT, have been identified by functional metagenomic screenings [66].

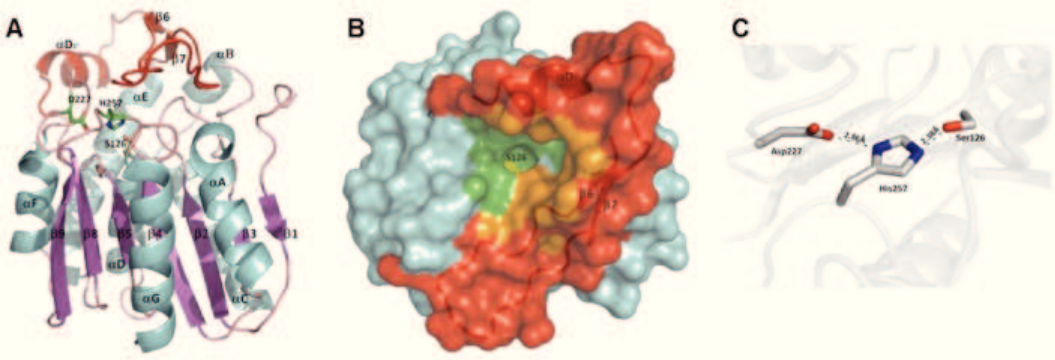

Fig.3 Protein structure of LipS. A) LipS monomer according to secondary structure elements. **B)** Surface representation of the LipS monomer with the lid-domain (β6, β7, $\alpha D_1'$) in red. The active site pocket identified by green colour. **C)** The catalytic triad residues of LipS are properly placed to establish hydrogen bond. **(Chow et al. 2012).**

The lypolitic enzymes active site is formed by a catalytic triad, highly conserved, consisting of the amino acids serine, aspartic (or glutamic) acid and histidine; the nucleophilic Ser residue is located at the C-terminal end of strand β5 in a highly conserved pentapeptide GXSXG, forming a characteristic β–turn–α motif named the "nucleophilic elbow". The conserved pentapeptide and the reaction mechanism is the same as for esterases [55].
In most lipases, a mobile element covers the catalytic site in the inactive form of the lipase. This 'lid' consists of one or two short α-helices linked to the body of the lipase by flexible structure elements. In the open, active form of the lipase, the lid moves away and makes the binding site accessible to the substrate. The lid is not found in some lipases and esterases [67].
Esterases accept esters with an acyl side chain shorter than ten carbon atoms as a substrate; esterase activity is found to be highest towards more water-soluble substrates. Like lipases, esterases have been shown to be stable and active in organic solvents, though this feature is more pronounced with lipases.
Lipases and esterases features portend their employment as valuable biocatalysts in biotechnological applications.

5. Biotechnological applications of lipolytic enzymes

Microorganisms are able to produce high yields of lipases. The hydrolysis and usually, the synthesis of esters catalized by lipolytic enzymes, proceed with high region- and/or enantioselectivity. The biotechnological potential, assigned to this class of enzymes, is due to some peculiar properties: stability in organic solvents, broad substrate specificity, no cofactor requirement, activity over range of pH and temperature, high enantioselectivity.

Microbial lipases are mostly extracellular and they can be produced by fermentation. After the purification step, the enzyme is ready to be tested as biocatalyst [68].
Sometimes purification costs are too high and companies prefer to use the whole cells as biocatalyst [69].
Nowadays commercial use of lipase is a billion dollar business that comprises a wide variety of different applications (Table 2) [70].

Table 2 : industrial applications of microbial lipases (Sharma et al. 2011).

Industry	Action	Product or application
Detergents	Hydrolysis of fats	Removal of oil stains from fabrics
Dairy foods	Hydrolysis of milk fat, cheese ripening, modification of butter fat	Development of falvoring agents in milk, cheese and butter
Bakery foods	Flavor improvement	Shelf-life prolongation
Beverages	Improved aroma	Beverages
Food dressings	Quality improvement	Mayonnaise, dressings and whippings
Health foods	Transesterification	Health foods
Meat and fish	Flavor development	Meat and fish products; fat removal
Fats and oils	Transesterification; hydrolysis	Cocoa butter, margarine, fatty acids, glycerol, mono- and diglycerides
Chemicals	Enantioselectivity, synthesis	Chiral builidng blocks, chemicals
Pharmaceuticals	Transesterification, hydrolysis	Specialty lipids, digestive aids
Cosmetics	Synthesis	Emulsifiers, moisturizers
Leather	Hydrolysis	Leather products
Paper	Hydrolysis	Paper with improved quality
Cleaning	Hydrolysis	Removal of fats

Lipases in food industry

Lipases have become an integral part of the modern food industry [71]. It is useful for the production of flavours in cheese and for interesterification of fats and oils. It also accelerates the seasoning of cheese and lipolysis of butter, fats and cream.
Lipases are also used for the conversion of triacylglycerols to diacylglycerols and monoacylglycerols and these products gives rise to non-esterified fatty acids and fatty acid propan-2-yl esters. Another use of these enzymes is the production of maltose-and lactose-like sugar fatty acid esters.
Some methods utilizes the immobilized *Rhizomucor miehei* lipase for transesterification reaction that replaces the palmitic acid in palm oil with stearic acid. Immobilized lipases from *Candida antarctica* (CAL-B), *C. cylindracea AY*30, *Humicola lanuginosa*, *Pseudomonas* sp. and *Geotrichum candidum* are being used for the esterification of functionalized phenols for synthesis of lipophilic antioxidants that can be used in sunflower oil [72].

Lipases in the resolution of chiral compounds

In all biological system chirality is predominant. When these enantiomers are present in equimolecular amounts within a mixture, the resultant mixture is named racemic. The lipases are used in organic chemistry for the resolution of enantiomeric compounds. Lipases have been used for the production of pure biologically active S-enantiomer of Sulcatol transesterification of cyanohydrin compounds and epoxyesters. Lipases from *Candida cylindracea* has been applied to the resolution of 2-Bromopropionic acids and 2-Chloropropionic acids which are starting materials for the synthesis of phenoxy propionic herbicides.
Members of the lipase family have been found to be particularly suitable for such applications and lipases from *Candida cylindracea*, *C. antarctica*, Porcine pancreas lipase have been used to resolve the enantiomers of flurbiprofen, naproxen, ibuprofen and suprofen [73,74].

The S-enantiomer of flurbiprofen (2-fluoro-α-methyl-[1,1-biphenyl]-4-acetic acid) possesses most of its antiinflammatory action, but the presence of the R-enantiomer is reported to greatly enhance its gastrointestinal toxicity [75]. This makes the resolution of the enantiomers of this drug particularly desirable.

Lipases as biosensor

The quantitative determination of triacylglycerol by lipases as biosensor is of great importance in clinical diagnosis and in food industry, compared to the chemical methods, for the determination of tryacylglycerols. An analytical biosensor was developed for the determination of lipids for the clinical diagnosis [76]. *Candida rugosa* lipase biosensor from *Candida rugosa* has been developed as a DNA probe [77].

Lipase in detergents

Enzymes can reduce the environmental load of detergent products saving energy by working at lower wash temperature. These enzymes are biodegradable, so they do not leave any harmful residues and risks for aquatic life [78]. Lipases have also been used to clean clogged drain which is due to the food and non-food material deposition. In 1992, Novo Nordisk introduced the first commercial recombinant lipase 'Lipolase' originating from fungus *Thermomyces lanuginose* which was expressed in *Aspergillus oryzae* [55].

Lipases in bioremediation

Oil spills in refinery could be handled by the use of lipases [79]. Another important application has been reported for the degradation of polyester waste, removal of biofilm deposits from cooling water systems and also to purify the waste gasses from factories [80].

Lipases in cosmetics and perfumery

Lipases have potential application in cosmetics and perfumeries because they shows activity in surfactants and in aroma production [81]. Their use in personal care gives products of much higher quality with minimum downstream in refining process.

Lipases in paper making industry

The hydrophobic components of wood, named picht, can be removed by lipases during paper making processes. *Candida rugosa* lipases were used by Nippon Paper Industry, Japan, to develop a pitch control method to hydrolyse 90% of wood tryglycerides [55].

With the above showed prospect of recombinant lipase enzyme and the employment of lipolytic enzymes in other industrial fields, there is a need in improving the properties of existing lipases for established improved technical applications. The modern methods of genetic engineering combined with an increasing knowledge of structure and function are allowing further adaptation to industrial needs and the exploration of novel applications [70].

6. Aim of the thesis

The aim of this project was to discovery new biocatalysts isolated from marine bacterial strains and sediments samples collected in the Arctic region by using two different approaches: genomic and metagenomic respectively.
Work description has been organised in the following sections:
SECTION I

- Analysis of 100 marine bacteria collection in terms of bacterial 16S phylogeny;
- Implementation of functional-based screenings methods to identify novel cold active extracellular classes of enzymes (cellulase, amylase, chitinase, xylanase, esterase, DNase, protease and gelatinase) from the above mentioned bacteria collection;
- Isolation of an esterase/lipase encoding gene from an Arctic genome sequenced bacterium;
- Recombinant production of selected enzyme;
- Purification, structural/functional characterization of selected enzyme.

SECTION II

- Optimization of protocols for extracting environmental DNA and constructing metagenomic libraries;
- Optimization of functional screening procedure to isolate positive fosmid clones containing genes encoding novel cold-adapted biocatalysts;
- Identification of a fosmid containing an ORF encoding a gene with potential esterase/lipase activity;
- Recombinant production of the selected enzyme;
- Purification, structural/functional characterization of the selected enzyme.

7. REFERENCES

1. **Eisner T.** Prospecting for nature's chemical riches.1989. Issues in Science and Technology. 6:31-34.
2. **Jabour-Green J, Nicol, D.** Bioprospecting in areas outside national jurisdiction: Antarctica and the southern ocean. 2003. Melbourne journal of international law. 4:76-111.
3. **Bull A**. Microbial Diversity and Bioprospecting. 2004. Washington, D.C.: ASM Press.
4. UNEP/CBD/COP/5/INF/7.
5. **Whitman WB, Coleman DC, Wiebe WJ.** Prokaryotes: the unseen majority. 1998. Proc Natl Acad Sci U S A. 95:6578-6583.
6. **Arrieta JM, Arnaud-Haond S, Duarte CM.** What lies underneath: conserving the oceans' genetic resources. 2010. PNAS. 107:18318–18324.
7. **Jaspars M.** 2013. The Marine Biodiscovery Pipeline, PharmaSea Cons.
8. **Jabour-Green J, Nicol D.** Bioprospecting in areas outside national jurisdiction: Antartica and the Southern Ocean. 2003. Melbourne Journal of international law 76.
9. **Glöckner FO, Joint I.** Marine microbial genomics in Europe: current status and perspectives. 2010. Microbial Biotechnology. 3:523–530.
10. **Rampelotto PH.** Polar Microbiology: Recent Advances and Future Perspectives. 2014. Biology. 3:81-84.

11. **Handelsman J.** Metagenomics: Application of Genomics to Uncultured Microorganisms. 2004. Microbiol. Mol. Biol. Rev. 68:669-685.
12. **Pace NR.** A molecular view of microbial diversity and the biosphere.1997. Science 276:734-740.
13. **Burns DG, Camakaris HM, Janssen PH, Dyall-Smith ML.** Combined use of cultivation-dependent and cultivation-independent methods indicates that members of most haloarchaeal groups in an Australian crystallizer pond are cultivable. 2004. Appl Environ Microbiol. 70:5258-65.
14. **Simbahan J, Kurth E, Schelert J, Dillman A, Moriyama E, Jovanovich S, Blum P.** Community analysis of a mercury hot spring supports occurrence of domain-specific forms of mercuric reductase. 2005. Appl Environ Microbiol. 71:8836-45.
15. **Orphan VJ, Taylor LT, Hafenbradl D, Delong EF.** Culture-Dependent and Culture-Independent Characterization of Microbial Assemblages Associated with High-Temperature Petroleum Reservoirs. 2000. Appl. Environ. Microbiol. 66:700-711.
16. **Nadkarni FE, Martin N, Hunter NA, Jacques MA.** Methods for optimizing DNA extraction before quantifying oral bacterial numbers by real-time PCR. 2009. FEMS Microbiol. Lett. 296:45–51.
17. **Schweder T, Lindequist U, Lalk M.** Screening for new metabolites from marine microorganisms. 2005. Marine Biotechnology. 96:1–48.
18. **de la Calle F.** Marine genetic resources, a source of new drugs: the experience of the biotechnology sector. 2009. International Journal of Marine and Coastal Law. 24:209–220.
19. **Langer M, Gabor EM, Liebeton K, Meurer G, Niehaus F, Schulze R, Eck J, Lorenz P.** Metagenomics: An inexhaustible access to nature's diversity. 2006. J. Biotechnol. 1:815–821.
20. **Amann RI, Ludwig W, Schleifer KH.** Phylogenetic identification and *in situ* detection of individual microbial cells without cultivation. 1995. Microbiol. Rev. 59:143–169.
21. **Wong D.** Applications of metagenomics for industrial bioproducts. 2010. In Metagenomics: Theory, methods and applications.1st edition. Edited by Marco D. Norfolk, UK: Caister Academic Press. 141-158.
22. **Lasken RS.** Single-cell sequencing in its prime. 2013. Nat Biotechnol. 31:211-212.
23. **Niedringhaus TP, Milanova D, Kerby MB, Snyder MP, Barron AE.** Landscape of next-generation sequencing technologies. 2011. Analytical Chemistry. 83:4327–4341.
24. **Nikolaki S, Tsiamis G.** Microbial Diversity in the Era of Omic Technologies. 2013. BioMed Research International. Review article ID 958719, 15 pages.
25. **Gutnick D.** Exploiting biodiversity in the marine environment: a personal perspective file exploiting biodiversity. 2010. Microbial Biotechnology. 3:491–492.
26. **Haefner B.** Drugs from the deep: marine natural products as drug candidates. 2003. Drug Discov. 8:536-544.
27. **Prakash T, Taylor TD.** Functional assignment of metagenomic data: challenges and applications. 2012. Briefings in Bioinformatics Advance. doi:10.1093/bib/bbs033.
28. **Curtis TP, Sloan WT, Scannell JW.** Estimating prokaryotic diversity and its limits. 2002. Proc. Natl. Acad. Sci. 99:10494–10499.

29. **Ward BB.** How many species of prokaryotes are there? 2002. Proc. Natl. Acad. Sci. 99:10234–10236.
30. **Schloss PD, Handelsman J.** 2004. Status of the microbial census. Microbiol. Mol. Biol. Rev. 68:686–691.
31. **Schoemaker HE, Mink D, Wubbolts MG.** Dispelling the myths–biocatalysis in industrial synthesis. 2003. Science. 299:1694–1697.
32. **Roberts SM.** Biocatalysts in synthetic organic chemistry. 2004. Tetrahedron. 60:499–500.
33. **Schmid A, Dordick JS, Hauer B, Kiener A.** Industrial biocatalysis. Today and tomorrow. 2001. Nature. 409:258–268.
34. **Maurer KH.** Detergent proteases. 2004. Curr. Opin. Biotechnol.15:330–334.
35. **Homann MJ, Vail RB, Previte E, Tamarez M.** Rapid identification of enantioselective ketone reductions using targeted microbial libraries. 2004. Tetrahedron. 60:789–797.
36. **Piel J.** Metabolites from symbiotic bacteria. 2004. Nat. Prod. Rep. 21:519–538.
37. **Dean FB, Nelson JR, Giesler TL, Lasken RS.** Rapid amplification of plasmid and phage DNA using Phi29 DNA polymerase and multiply-primed rolling circle amplification. 2001. Genome Research. 1:1095–1099.
38. **R. S. Lasken.** Single-cell genomic sequencing using multiple displacement amplification. 2007. Current Opinion in Microbiology. 10:510–516.
39. **Lorenz P, Eck J.** Metagenomics and industrial applications. 2005. Nat. Rev. Microbiol. 3:510–516.
40. **Fujiwara S.** Extremophiles: Developments of their special functions and potential resources. 2002. J. Biosci. Bioeng. 94:518-525.
41. **Georlette D, Damien B, Blaise V.** Structural and functional adaptations to extreme temperatures in psychrophilic, mesophilic, and thermophilic DNA ligases. 2003. Journal of Biological Chemistry. 278:37015–37023.
42. **Siddiqui KS, Feller G, D'Amico S, Gerday C, Giaquinto L, Cavicchioli R.** The active site is the least stable structure in the unfolding pathway of a multidomain cold-adapted α-amylase. 2005. Journal of Bacteriology. 187:6197–6205.
43. **Suresh Kumar P, Mrinmoy Ghosh , Pulicherla KK, Sambasiva Rao KRS.** Cold Active Enzymes from the Marine Psychrophiles: Biotechnological Perspective 2011. Advanced Biotech. 10:43-45.
44. **Wintrode, PL, Arnold, FH.** Temperature adaptation of enzymes: lessons from laboratory evolution. 2000. Adv. Protein Chem. 55:161–225.
45. **Srimathi S, Jayaraman G, Feller G, Danielsson B, Narayanan PR.** Intrinsic halotolerance of the psychrophilic alpha-amylase from *Pseudoalteromonas haloplanktis.* 2007. Extremophiles. 11:505-515.
46. **Sivakumar N, Li N, Tang JW, Patel BK, Swaminathan K.** Crystal structure of AmyA lacks acidic surface and provide insights into protein stability at poly-extreme condition. 2006. FEBS. 11:2646-2652.
47. **Lanyi JK.** Salt dependent properties of proteins from extremely halophilic bacteria. 1974. Bacteriol Rev. 38:272-290.
48. **Bolhuis A, Kwan D, Thomas JR.** Halophilic adaptations of proteins. 2008. In: Siddiqui KS, Thomas T (eds). Protein Adaptation in Extremophiles. Nova Biomedical Books: New York, pp 71–104.
49. **Rao JKM, Argos P.** Structural stability of halophilic proteins. 1981. Biochemistry. 20:6536-6543.

50. **Ogino H, Uchiho T, Doukyu N, Yasuda M, Ishimi K, Ishikawa H.** Effect of exchange amino acid residues of the surface region of the PST-01 protease on its organic solvent-stability. 2007. Biochem Biophys Res Commun. 358:1028-1033.
51. **Shah S, Gupta MN.** Lipase catalyzed preparation of biodiesel from Jatropha oil in a solvent-free system. 2007. Process Biochem. 3:409-414.
52. **Gupta A, Khare SK.** Enzymes from solvent-tolerant microbes: Useful biocatalysts for non-aqueous enzymology. 2009. Crit Rev Biotechnol. 29:44-54.
53. **Doukyua N, Ogino H.** Organic solvent-tolerant enzymes. 2010. Biochem Eng J. 48:270-282.
54. **Chahinian H, Sarda L.** Distinction between esterases and lipases: comparative biochemical properties of sequence-related carboxylesterases. 2009. Protein Pept Lett. 16:1149-61.
55. **Jaeger KE, Reetz MT.** Microbial lipases form versatile tools for biotechnology. 1998. Trends Biotechnol.16:396-403.
56. **Beisson F, Tiss A, Rivière C, Verger R.** Methods for lipase detection and assay: a critical review. 2000. Eur. J. Lipid Sci. Technol. 133–153.
57. **Zhang C, Kim SK.** Research and Application of Marine Microbial Enzymes: Status and Prospects. 2010. Marine drugs. 8:1920-1934.
58. **Lopes GB, Fraga LP, Fleuri LF, Macedo GA.** Lipase and esterase - to what extent can this classification be applied accurately? 2011. Ciênc. Tecnol. Aliment., Campinas. 31: 608-613.
59. **Arpigny JL, Jaeger KE.** Bacterial lipolytic enzymes: classification and properties. 1999. Biochem J. 1: 177–183.
60. **Handrick R, Reinhardt S, Focarete ML, Scandola M, Adamus G.** A new type of thermoalkalophilic hydrolase of *Paucimonas lemoignei* with high specificity for amorphous polyesters of short chain-length hydroxyalkanoic acids. 2001. J Biol Chem. 276: 36215–36224.
61. **Lee MH, Lee CH, Oh TK, Song JK, Yoon JH.** Isolation and characterization of a novel lipase from a metagenomic library of tidal flat sediments: evidence for a new family of bacterial lipases. 2006. Appl Environ Microbiol. 72: 7406–7409.
62. **Kim EY, Oh KH, Lee MH, Kang CH, Oh TK.** Novel cold-adapted alkaline lipase from an intertidal flat metagenome and proposal for a new family of bacterial lipases. 2009. Appl Environ Microbiol. 75:257–260.
63. **Ewis HE, Abdelal AT, Lu CD.** Molecular cloning and characterization of two thermostable carboxyl esterases from *Geobacillus stearothermophilus*. 2004. Gene 329:187–195.
64. **Liu P, Wang YF, Ewis HE, Abdelal AT, Lu CD.** Covalent reaction intermediate revealed in crystal structure of the Geobacillus stearothermophilus carboxylesterase Est30. 2004. J Mol Biol 342:551–561.
65. **Rao L, Xue Y, Zheng Y, Lu JR, Ma Y.** A Novel Alkaliphilic *Bacillus* Esterase Belongs to the 13th Bacterial Lipolytic Enzyme Family. PLoS One. 8:e60645.
66. **Chow J, Kovacic F, Dall Antonia Y, Krauss U, Fersini F, Schmeisser C, Lauinger B, Bongen P, Pietruszka J, Schmidt M, Menyes I, Bornscheuer UT, Eckstein M, Thum O, Liese A, Mueller-Dieckmann J, Jaeger KE, Streit WR.** The metagenome-derived enzymes LipS and LipT increase the diversity of known lipases. 2012. PLoS One. 7:e47665.

67. **Pleiss J, Fischer M, Schmid RD.** Anatomy of lipase binding sites: the scissile fatty acid binding site. 1998. Chemistry and Physics of Lipids. 93:67–80.
68. **Balaji V, Ebenezer P.** Optimization of extracellular lipase production in *Colletotrichum gloeosporioides* by solid state fermentation. 2008. Ind. J. Sci. Technol. 1:1-8.
69. **Iftikhar T, Niaz M, Ikram-ul-Haq MA, Rajoka MI.** Maximization of intracellular lipase production in a lipase-overproducing mutant derivative of *Rhizopus oligosporus* DGM 31: a kinetic study. 2008. Food Technol. Biootechnol. 46:402-412.
70. **Sharma D, Sharma B, Shukla AK.** Biotechnological Approach of Microbial Lipase: A Review. 2011. Biotechnology.10:23-40.
71. **Theil, F.** Lipase-supported synthesis of biologically active compounds. 1995. Chem. Rev. 95:2203-2227.
72. **Xu H, Li M, He B.** Immobilization of *Candida cylindracea* lipase on methyl acylate-divinyl benzene copolymer and its derivatives. 1995. Enzyme Microbiol. Technol.17:194-199.
73. **Mustranta A.** Use of lipases in resolution of racemic ibuprofen. 1992. Applied Microbiol. Biotechnol. 38:61-66.
74. **Mertoli P, Nicolosi G, Patti A, Piattelli M.** Convenient lipase-assisted preparation of both enantiomers of suprofen, a non-steroidal anti-inflammatory drug. 1996. Chirality. 8:377-380.
75. **Wechter WJ, Bigornia AE, Murray ED, Levine BH, Young JW.** Rac-flurbiprofen is more ulcerogenic than its (S)-enantiomer. 1993. Chirality. 5:492-494.
76. **Masahiko A, Masahiro K, Takasi K, Kenji M, Ayari M.** Process for preparation of polyol fatty acid ester and glyceride mixture obtained. 1995. Pat., EP-658629.
77. **Benjamin S, Pandey A.** Isolation and characterization of three distinct forms of lipases from *Candida rugosa* produced in solid state fermentation. 2001. Braz. Arch. Biol. Technol. 44:213-221.
78. **Falch EA.** Industrial enzymes: Developments in production and application. 1991. Biotechnol. Adv. 9:643-658.
79. **Nakamura K, Yoda M, Fukase T.** Treatment process for drainage containing fats and oils. 1994. Japan Patent, JP-06246295. http://www19.ipdl.inpit.go.jp/PA1/cgi-bin/PA1DETAIL.
80. Anonymous. Methods for decomposing polyv fatty acid esters. 1995. Jpn. Pat., Jp-07165977.
81. **Metzger JO, Bornscheuer U.** Lipids as renewable resources: Current state of chemical and biotechnological conversion and diversification. 2006. Applied Microbiol. Biotechnol. 71:13-22.

Chapter 1

Bioprospecting around Arctic islands: Marine bacteria as rich source of biocatalysts

Bioprospecting around Arctic islands: Marine bacteria as rich source of biocatalysts

Concetta De Santi[1, 2]*, Bjørn Altermark[2], Donatella de Pascale[1], Nils-Peder Willassen[2]*

[1] Institute of Protein Biochemistry, National Research Council, Via P. Castellino, 111. I-80131, Naples, Italy; E-mails: c.desanti@ibp.cnr.it (C.D.S.); d.depascale@ibp.cnr.it (D.d.P.)
[2] NorStruct, Department of Chemistry, Faculty of Science and Technology, University of Tromsø, Tromsø, Norway; E-Mail: bjorn.altermark@uit.no (B.A.)

Authors to whom correspondence should be addressed; E-Mail: nils-peder.willassen@uit.no (N-P.W.); E-Mail: c.desanti@ibp.cnr.it (C.D.S.)

Tel.: +47-77644651; Fax: 77645350

Abstract:

We have investigated the biotechnological potential of marine Arctic bacteria for their ability to produce a broad spectrum of cold-active enzymes. Marine bacteria exhibiting these features are of great interest for both fundamental research and industrial applications. Biota and sediment samples has been collected during recent expeditions around the Lofoten and Svalbard islands and bacteria were also isolated from this material and identified through 16S rRNA sequence analysis for the purpose of establishing a culture collection of marine Arctic bacteria.
Herein, we present the functional screening for different extracellular enzymatic activities from 100 diversely chosen microbial isolates incubated at 4- and 20°C. The production of esterase, DNase and protease activities were revealed in more than 45% of the strains, while approximately 41%, 23%, 9% and 7% of the strains possessed amylase, chitinase, cellulase and xylanase activities, respectively. Our findings indicated that phylogenetically diverse bacteria including many new species could be cultured from the marine arctic environment. The Arctic polar environment is still an untapped reservoir of biodiversity for bioprospecting.

Keywords: Marine bacteria; Cold-active enzymes; Extracellular activities

1.1 Introduction

High-latitude Arctic oceans and seas have been shown to be important sites for the investigation of marine-derived enzymes. Despite the fact that the Arctic is a region with broad interest as a climate indicator, comparatively little is known about the bacterial diversity [1]. In these areas, microorganisms are exposed to several conditions of extreme temperature and high salinity. Microbial adaptations (expressed constantly) such as intracellular processes allow them to thrive or survive in presence of those geochemical polar conditions [2,3]. The composition of these communities varies by depth, season and location in the ocean. Heterotrophic microbial communities are responsible for a substantial proportion of the main productivity in the ocean due to their role in the marine carbon cycle [4]. In order to avail of this organic matter, members of microbial communities have adapted themselves by producing extracellular enzymes of the correct structural specificity to hydrolyze high molecular weight substrates to small sizes to be transported into the cell. The ability of microorganisms to produce extracellular enzymes is

homogeneously distributed [5], but the extent to which enzymatic capabilities change among whole microbial communities in the ocean needs to be largely explored.

The aim of this work was to investigate the diversity of cultivable Arctic marine bacteria and their extracellular hydrolytic enzymes in the deep-sea sediments and biota samples with the aim to highlight the phylogenetic distribution of the detected activities.
Furthermore, we focused our attention on the extracellular enzymes, produced by the isolated bacteria. It is well established that psychrophilic enzymes, produced by cold-adapted bacteria, display a high catalytic efficiency. This feature is not only important for *in situ* biogeochemical processes, but in particular for their powerful relevance in biotechnological and industrial fields [6,7]. A bioprospecting methodology using functional screening has been performed to explore the extent of microbial enzymatic activity along the coast of the Arctic Svalbard archipelago and Lofoten's islands.

1.2 Results and Discussion

Isolation of marine bacteria from Arctic environments
A collection of 354 bacteria had previously been obtained during two separate research-cruises to the Lofoten area (Northern Norway) and around the Svalbard archipelago. The bacteria had been classified by 16s rRNA sequencing and stored in an in-house bacterial collection at the University of Tromsø. The growth temperature range for 100 selected isolates was tested on marine 2216 broth and all the isolates were able to grow in this medium without any additional requirement of sodium chloride or seawater. The result pointed out the ability of these isolates to survive and proliferate in the low temperature and constant salinity. We noticed however that the Gram-positives, in general, needed longer time at low temperatures to reach the same colony size as the Gram-negative bacteria.

Bacterial phylogenetic diversity
The phylogenetic diversity of 100 selected arctic bacterial isolates was determined by 16S rRNA sequence analysis. Based upon the 16S sRNA sequences a phylogenetic tree was constructed to visualize their affiliations (Fig. 1). Out of 60 Gram-negative phylotypes, 53 belonged to the phylum *Proteobacteria*, 9 to the phylum *Bacteroidetes.* Out of 40 Gram-positive phylotypes, 29 belonged to the phylum *Actinobacteria* and 12 belonged to the phylum *Firmicutes*.

Figure 1. Phylogenetic tree showing the relationships among the arctic marine bacterial isolates based on 16S rRNA gene homology. Reference sequences of type strains (●). GeneBank accession numbers of 16S rRNA sequences are shown in parentheses.

Screening and detection of extracellular enzymatic activities

The bacterial isolates were screened for the production of extracellular enzymes at 4°C and 20°C. We detected extracellular activities of all 100 isolates on marine agar plates. The ability to degrade substrates was tested on tributyrin, skim milk, chitin, carboxymethylcellulose, gelatin, starch, xylan and DNA (Fig. 2). In the tables 1 and 2, we showed all the hydrolase enzymatic activities production, in terms of halo size, corresponding to each isolate. This activity overview highlight the multiple enzyme activities mainly localized in the Gram-negative bacteria group.

Table 1. Hydrolase activities of 40 Gram-positive marine bacterial isolates from Lofoten and Svalbard. Halo size is indicated by: (+) small halo, (++) medium halo and (+++) large halo.

		Lipase	Gelatinase	Protease	Xylanase	Chitinase	Amylase	DNase	Cellulase
		20°C	20°C	20°C	20°C	20°C	20°C	20°C	20°C
GRAM +									
Microbacterium	AW28M07	+					+	+	
Microbacterium	AW28M15	+						+	
Filibacter	KH04J17								
Rhodococcus	AW19M46	+		+					
Rhodococcus	MP02J07	+							
Rhodococcus	GB23J02	+							
Arthrobacter	GB04J08	+						+	
Bacillus	AW25M04	+		+				+	
Staphylococcus	AW02J12	++		+					
Nesterenkonia	AW19M55	++	+	+			+		
Streptomyces	AW19M35								
Planomicrobium	AW19M56			++			+		
Arthrobacter	SP003	+		+			++	+	
Clavibacter	SP011	+			++		++	+	
Clavibacter	SP033	+			++		++	+	
Leifsonia	SP050	+		+				+	
Microbacterium	SP006						++	+	
Micrococcus	SP063	++		++					
Rhodococcus	SP061	+	+						
Salinibacterium	SP028					+		+	

Table 1. Cont.

	Lipase	Gelatinase	Protease	Xylanase	Chitinase	Amylase	DNase	Cellulase
	20°C	20°C	20°C	20°C	20°C	20°C	20°C	20°C
GRAM +								
Staphylococcus SP052								
Tomitella SP012	+	+						
Leifsonia AW28M06	+						+	
Leifsonia AW02J23	+	+	+				+	
Arthrobacter AW25M11	+							
Arthrobacter AW19M24			+			++		
Filibacter AW28M30							+	
Bacillus GB04J31		+						
Plantibacter AW25M38							++	
Planococcus AW02J18	+		+++				++	
Planococcus GB02J13			+			++		
Micrococcus AW19M49	+		+				++	
Nocardiopsis BA19M08	+		+					
Streptomyces BA19M03	+	+	+					
Arthrobacter AW19M34		+	+	+				++
Rhodococcus AW25M09		++	++					++
Streptomyces AW19M42		++	++	++				++
Knoellia SP073		++	++	++				++
Psycrobacillus AW28M34		+						++
Sanguibacter SP022		++	++					++

Table 2. Hydrolase activities of 60 Gram-negative marine bacterial isolates from Lofoten and Svalbard. Halo size is indicated by: (+) small halo, (++) medium halo and (+++) large halo.

	Lipase		Gelatinase		Protease		Xylanase		Chitinase		Amylase		DNase		Cellulase	
	4°C	20°C	4°C	20°C	4°C	20°C	4°C	20°C	4°C	20°C	4°C	20°C	4°C	20°C	4°C	20°C
GRAM -																
Thalassopsira AW25M45	+	+	+	+	++	++							+	++		
Thalassospira AW19M11													+	++		
Thalassospira KH04J01																
Thalassospira BA19M05														+		
Pseudomonas GB04J27	+	+		++	+	+				++						
Pseudomonas AW28M04	+	+	+	+						++		+		+		
Roseobacter GB02J23				+		+				++						
Roseobacter GB02J24	+	+								++				+		
Roseobacter AW25M03	+	+		++						++			+	++		
Roseobacter AW19M09																
Shewanella KH04J08	++	+		++	++	+++						+	+	+		
Shewanella AW25M33	+	+		++	++	++							+	+		
Shewanella MP02J10	+	+				+			+	++	+	+	+	+		
Stenotrophomonas AW25M54	+	+	++	++	++	++			+	++			+	++		
Stenotrophomonas AW25M14	+	+			++	++				+	+	+	+	++		
Achromobacter GB02J42			+	+								+	+	++		
Achromobacter AW28M02																
Gelidibacter GB04J26			++	++	++	+++								++		
Polaribacter KH04J14	+	+	++	++	++	++					+	+		++		
Pseudoalteromonas GB02J33	+	+	++	++	++	+++					++	+ ++	+	++		

Table 2. Cont.

	Lipase		Gelatinase		Protease		Xylanase		Chitinase		Amylase		DNase		Cellulase	
	4°C	20°C	4°C	20°C	4°C	20°C	4°C	20°C	4°C	20°C	4°C	20°C	4°C	20°C	4°C	20°C
GRAM -																
Pseudoalteromonas AW25M26	+	++	++	++	++	++							+	++		
Serratia GB02J45	+	+	+	++	++	++					+	++				
Psychrobacter AW25M27	+	+	+	++	++	++					+	++	+	++		
Psychrobacter GB04J30	+	+														
Brevundimonas KH11J01	+	+	+	+++	++	++				+++			+	++		
Rhodobacter AW25M51	+	+			++	++							+	++		
Sulfitobacter AW25M05	+	+							+	++						
Acinetobacter GB02J46	+	++	+	++					+	++		+		++		
Roseovarius GB02J02	+	++										+		++		
Photobacterium GB02J53	+	++							+	++						
Halomonas R5-57	+			+						+				+		
Marinobacter CK-1	+	++	+	++	++	++						+	+	++		
Pseudoalteromonas AW28M34b	+	++	+	++	++	++						+	+	++		
Oceanisphaera SP013															+	++
Polaribacter SP072	+	+			+	++			+		+	+		+		
Psychromonas SP041	+	++		+					+			+		++	+	++
Shewanella SP035	+	+			++	+								++		++
Vibrio SP025	+	+				+	+				++	+	+	++		
Promiconospora AW19M33	+		+		+		+	+++	++				+			

Table 2. Cont.

		Lipase		Gelatinase		Protease		Xylanase		Chitinase		Amylase		DNase		Cellulase	
		4°C	20°C	4°C	20°C	4°C	20°C	4°C	20°C	4°C	20°C	4°C	20°C	4°C	20°C	4°C	20°C
GRAM -																	
Halomonas	SP051													+	+		
Flavobacterium	SP045					+						+	++				
Flavobacterium	SP046					++						+	++	+	+		
Moritella	SP016	+	+			++						+	++	+	+	+	++
Marinomonas	SP036		+												+		
Mesorizhobium	SP068																
Photobacterium	SP001									+	++						
Photobacterium	SP044		+				+	+				+	+		++	+	++
Photobacterium	SP005									+	++	+	++	+	+		
Pseudoalteromonas	SP007	+	+			++	++					+		+	++		
Pseudoalteromonas	SP077	+	++							+	+	+	++	+	++		
Psychrobacter	SP009	+	+				++			+		+	++				
Psychrobacter	SP042	+	++			+	++					+	++	+	+		
Psychromonas	SP017	+	+			++	++							++	++		
Shewanella	SP023											+	+				
Shewanella	SP043	++	+	++		++	+					+	+	++	++		
Sulfitobacter	SP069	+	+							+	+	+	+				
Serratia	SP010	+	+					++	+++	++	++	+	++	+	++	+	++
Pseudomonas	KH04J19	+	+	++		+	++										
Pseudomonas	AW25M15	+	++	++		+	++										
Sphingopyxis	GB02J19																

Figure 2. Functional screening of marine bacteria on marine agar plates for: (**A**) protease activity; (**B**) esterase/lipase activity (**C**) chitinase activity; (**D**) amylase activity; (**E**) xylanase activity; (**F**) gelatinase activity; (**G**) DNase activity; (**H**) cellulase activity.

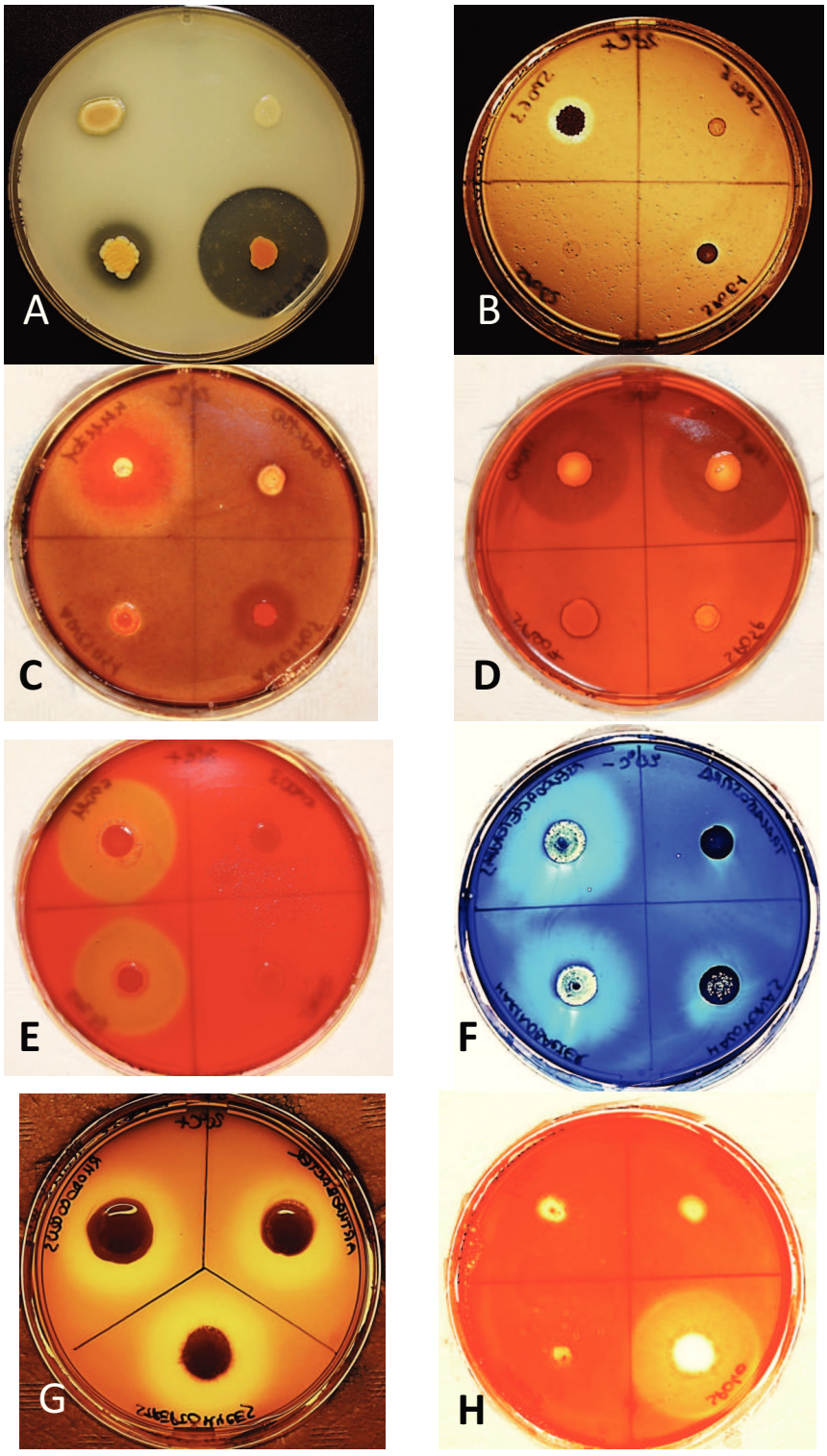

A functional-based screening method was performed to detect the extracellular enzyme activities. A suitable concentration of substrate was chosen to decrease possible toxic effects for bacteria growth. Hydrolytic activities were easily detected on tributyrin and skim milk plates. All other activities that required a staining/post-staining experimental step were detected after an optimization of the already known protocols according to the visible halos we got on the marine broth agar plates. The size of halos was used to compare enzymatic activities. Analyzing our results, the ability to degrade tributyrin, skim milk and DNA was almost equally distributed among the isolates of *Proteobacteria*, *Bacteroidetes*, *Actinobacteria* and *Firmicutes*. When the same activities were analyzed at 4°C, *Shewanella* SP043 displayed the highest esterase activity while *Pseudoalteromonas*, *Pseudomonas*, *Acinetobacter*, *Roseovarius* and *Psychrobacter* isolates showed a high esterase activity at 20°CThe protease activity was detected at 4- and 20°C. Concerning the activity detected at 4°C, the halo size was bigger than what we observed for the other enzymatic activities. The biggest size of the halo was reached at 20°C when *Shewanella*, *Gelidibacter* and *Pseudoalteromonas* isolates were spotted on the plates. The chitinase activity was detected in members of *Proteobacteria* such as *Pseudomonas*, *Photobacterium* and *Serratia*, which indicate that these bacteria may be important degraders of chitin in the soil ecosystem and contribute to the recycling of vital carbon and nitrogen resources. At 20°C the best chitinase activity was detected in *Brevundimonas* sp. while a lower activity was observed for *Pseudomonas*, *Roseobacter*, *Shewanella, Photobacterium and Serratia.* At 4°C the best chitinase activity was observed in *Serratia* sp. The functional screening for chitinases on Gram-positive bacteria gave only negative results, in terms of halos.The xylanase activity was exclusively detected by the members of *Promiconospora*, *Serratia*, *Pseudolateromonas* and *Clavibacter*. In our experiments large halos was observed at 20°C for the *Serratia* and *Promiconospora* isolates. A very low activity, sometimes faint, was showed at 4°C for the Gram-negative bacteria. *Clavibacter* was the only Gram-positive bacteria that showed xylanase activity.

The gelatin and starch were more hydrolyzed by Gram-negative bacteria. The best gelatinase activity was detected for the *Brevundimonas* strain at 20°C. *Pseudoalteromans* showed the best amylase activity at 20°C compared to *Serratia, Flavobacterium, Photobacterium* and *Psychrobacter*.

A very few isolates were able to produce extracellular cellulase enzymes from Gram-negative bacteria. The cellulase activity was detected among the isolates of *Proteobacteria*. Cellulase positive isolates were members of *Serratia*, *Photobacterium*, *Moritella* and *Pseudoalteromonas*. No cellulase activity was identified from the functional screening performed for the Gram-positive bacteria at 20°C.

It is worth noting that in the functional screenings carried out, sometimes bacteria that had highly similar 16s rRNA sequences, isolated from different cold environments, displayed different behavior referring to the same enzymatic activity. Environmental temperature not only has effects on microbial activity, but can also affect activity indirectly by changing the temperature dependency of the whole community [8]. This is an additional evidence of the prodigious and extraordinary ability of the bacteria to adapt themselves and to develop new strategies to survive in such extreme and changeable microenvironment and community composition.

Enzymes industrial applications

The experimental approach described in this paper could be considered propaedeutic in order to introduce in the industrial market new psychrophilic and psychrotolerant enzymes produced by a wide range of isolated Arctic bacteria. Sometimes there is a difficult in growing bacterial isolates in the laboratory and an essential prerequisite for biodiscovery comes to fail [9,10]. To summarized in percentage the production of hydrolytic enzymes: more than 45% of the isolates were positive for esterase-, DNase- and protease activity while approximately 41%, 23%, 9% and 7% of the isolates showed the ability to produce amylase, chitinase, cellulase and xylanase activity respectively (Fig. 3). The high number of bacterial isolates we analyzed gave use the opportunity to explore the connection between extracellular activity and biodiversity in the Arctic regions. A huge number of cold-active enzymes detected in this study indicated that many bacteria are able to hydrolyze the major constituents of the organic matter such as esters, proteins, α- and β-linked polysaccharides.

The increased interest for cold-active enzymes in academia and research industry is due to their peculiar features such as salt tolerance, high activity at low temperatures in addition to their novel chemical and stereo-chemical features [12]. The applications of cold active enzymes are becoming more and more interesting for industry sectors such as consumer products, pharmaceutical, cosmetic, and fine chemicals. Cold-active hydrolytic enzymes can be used in detergents applied for cold washing with a reduction of energy consumption and prevents wear and tear of textile fibers [13]. Other potential applications of cold-active enzymes are evident in processes such as the hydrolysis of lactose in milk by using galactosidase or the taste improvement of refrigerated meat using proteases and betterment of bakery products using glycosidase such as amylases, proteases and xylanases. Brewing and wine industries use cold-active enzymes as an alternative to warm-active enzymes. The reason is that cold-active enzymes in food industry reduce the risk of contamination without destroying the flavor at high temperatures. By this way it is possible to preserve the nutritional quality of foods. The identification of marine bacteria with the ability to degrade cellulose could lead to improved processes in the quest for cellulosic ethanol.

Figure 3. Pie Chart representation showing the percentages of total enzymatic activities

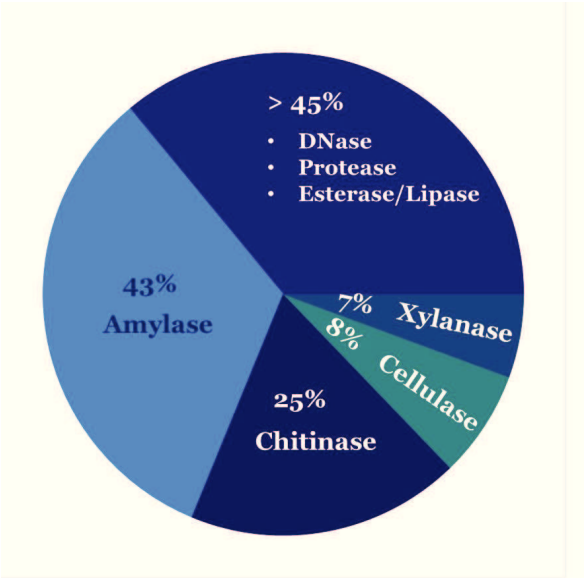

1.3 Experimental Section

The isolation, culturing and preliminary classification of the bacterial isolates was performed by scientist at the University of Tromsø. The bacteria are stored in an in-house collection together with all meta-data. The procedures were:

Isolation and culturing of bacteria

Samples of various biota and sea-sediment were collected during two separate scientific expeditions onboard R/V Helmer Hanssen (University of Tromsø, Norway). The first cruise was carried out in the Lofoten area (Northern Norway) in April 2010 and the second was focused on the costal areas around the Svalbard archipelago in October 2011. The samples were used as inoculum on selective agar plates: IM5 (humic acid agar [21], with sea water), humic acid (1 g), K2HPO4 (0.5 g), FeSO4•7H2O (1 mg), agar (20 g), vitamin B solution (1 mL), natural sea water (0.5 L) and distilled water (0.5 L); IM6 glycerol (0.5 g), starch (0.5 g), sodium propionate (0.5 g), KNO3 (0.1 g), asparagine (0.1 g), casein (0.3 g), K2HPO4 (0.5 g), FeSO4•7H2O (1 mg), agar (20 g), vitamin B solution (1 mL), natural sea water (0.5 L) and distilled water (0.5 L); IM7 (chitin agar [9], with sea water) chitin (Sigma), K2HPO4 (0.5 g), FeSO4•7H2O (1 mg), agar (20 g), vitamin B solution (1 mL), natural sea water (0.7 L) and distilled water (0.3 L); IM8, malt extract (1 g), glycerol (1 g), glucose (1 g), peptone (1 g), yeast extract (1 g), agar (20 g), natural sea water (0.5 L) and distilled water (0.5 L). All isolation media were amended with filtered (0.2-µm pore size) cycloheximide (50 µg/mL), nystatin (75 µg/mL) and nalidixic acid (30 µg/mL) [14]. On land the bacteria was re-stroked onto new plates and single colonies were used to inoculate 5 ml cultures. One ml of dense culture was cryopreserved in 20% glycerol, while one ml of culture was harvested by centrifugation using a table-top centrifuge at 12,000 rpm for 3 min, washed once with 1 ml of distilled water and re-centrifuged for 3 min. Tubes were afterwards frozen at -20°C for later extraction of genomic DNA.

Genomic DNA extraction and partial sequencing of the 16S rRNA gene

Two hundreds µL of premixed cold Instagene matrix (BioRad, Hercules, CA) were added to the frozen bacterial pellets and tubes vortexed to dissolve the pellets. Samples were then heated for 30 min at 56°C, vortexed for 10 s and then heated again for 8 min at 100°C with a final vortexing for 10 s. Tubes containing genomic DNA and cell debris were centrifuged for 3 min and approximately 0.5 µl of supernatant was used as template for PCR reactions. To generate a PCR product

0.2 µM of universal primers 27F (5′-AGAGTTTGATCCTGGCTCAG-3′) and 1492R (5′- TACGGYTACCTTGTTACGACTT -3′) were combined with 1.5 mM $MgCl_2$, 0.2 mM dNTP mix, 0.5µl genomic DNA, 1X Taq buffer and 1.25U Taq polymerase in a 0.2 ml PCR tube. Water was added to a final volume of 50 µl. PCR was conducted using an initial denaturation for 3 min at 94°C followed by 30 cycles of 94°C for 30 s, 55°C for 30 s and 72°C for 2 min. A final extension step for 7 min at 72°C was performed before cooling to 4°C. Presence of amplified product was checked by running 5 µl on a 1% agarose gel. PCR product was purified using ExoSap-IT (Affymetrix, Santa Clara, CA) or PureLink Pro 96 PCR Purification Kit (Invitrogen-Life Technologies, Carlsbad, CA) following manufacturers protocols. In sequencing PCR about 50-100 ng template was mixed with buffer and 2 µl BigDye v 3.1 together with 1 µl (10 µM) sequencing primer 515F (5′- GTGCCAGCAGCCGCGGTAA-3′). Water was added to a final volume of 20 µl. PCR program was set up according to the BigDye Terminator v 3.1 Cycle Sequencing Kit protocol (Applied Biosystems, Carlsbad, CA) and further handling was done at the University of Tromsø's DNA sequencing core facility.

Bacterial 16S phylogeny

The ABI2FASTA converter v 1.1.2 (available online) was used to extract FASTA sequence files from ABI output files and low quality ends were trimmed (http://www.dnabaser.com).

The trimmed sequences were then checked for chimeras using DECIPHER's Find Chimeras web tool (http://decipher.cee.wisc.edu/FindChimeras.html). Sequence search against GenBank using BLAST [15] was performed to identify the genus each bacterium belongs to.

The sequences, around 800-900 bp, depending on the isolate, were compared with those data available in the RDPII (Ribosomal Database Project II) to determine the relative phylogenetic positions. Multiple alignments were generated using CLUSTAL W [16]. Alignments were edited using BioEdit Sequence Alignment Editor version 3.0.3 [17] and regions of ambiguous alignment were removed. The sequences were then entered into the MEGA version 5 program [18] to produce a phylogenetic tree. The phylogenetic tree was constructed using the maximum likelihood method [19] with General Time Reversible and complete-deletion model analysis. The resultant tree topologies were evaluated by bootstrap analysis based on 500 replicates. DNA sequences are deposited in GenBank under Accession numbers KF313361-KF313377, KF313380-KF313402, KF313404-KF313463.

Growth Temperature

Bacterial strains were growth in marine 2216 broth (Difco) at two different temperatures according to their classification. Gram-positive were grown at 20°C and Gram-negative were grown at 4°C using a Heidolph tube shaker (Heidolph, Germany) at 600 rpm.

Extracellular enzymatic activities

Protease, esterase, lipase, chitinase, cellulase, gelatinase, amylase, xylanase, DNase were detected on marine agar assay plates. 10 µl of log-phase bacteria cultures were spotted onto assay plates which were incubated at 4- and 20°C. The appearance of a halo was evaluated after one week.

Screening of protease producing bacteria

Screening of bacteria isolates for protease activity was performed on marine 2216 broth agar supplemented with 1% (w/v) skimmed milk [20]. Skimmed milk was prepared using a 10% (w/v) stock solution of commercially available nonfat milk powder. Marine broth agar was autoclaved at 121°C for 15 min, while 10 % (w/v) milk powder solution was autoclaved at 115°C for 10 min.
Exactly 10% (w/v) milk solution was mixed with marine broth agar to a final concentration of 1% (w/v) while still hot. Protease producing bacteria were selected based on the formation of halo zone of clearance around the colony.

Screening of esterase/lipase producing bacteria
Screening of bacteria isolates for esterase/lipase activity was performed on marine 2216 broth agar supplemented with 1% (w/v) tributyrin [21]. Marine broth agar was autoclaved at 121°C for 15 min and 100% (w/v) glyceryl tributyrate solution (Sigma) was mixed after sonication with marine broth agar to a final concentration of 1% (w/v). Esterase/lipase producing bacteria were selected based on the formation of halo zone of clearance around the colony.

Screening of chitinase producing bacteria
Screening of bacteria isolates for chitinase activity was performed on marine 2216 broth agar supplemented with 0.5% (w/v) colloidal chitin. Colloidal chitin was prepared using commercial chitin (Sigma-Aldrich) from shrimp shells [22]. Marine broth agar was autoclaved at 121°C for 15 min and mixed with 5% (w/v) colloidal chitin solution to a final concentration of 0.5% (w/v). Chitinase producing bacteria were selected based on the formation of halo zone of clearance around the colony. For the visualization of the chitinolytic activity the agar plates were flooded with 0.5% Congo red solution for 30 minutes and destained with 1M NaCl for 20 min [23].

Screening of cellulase producing bacteria
Screening of bacteria isolates for cellulase activity was performed on marine 2216 broth agar supplemented with 1.5% (w/v) carboxymethylcellulose (CMC) low viscosity sodium salt (Sigma). After incubation, the plates were flooded with 0.5% Congo red for 15–20 min followed by destaining with 1 M NaCl for 15–20 min. The extracellular cellulase activity was detected by the presence of clear zone around the growing colony against the dark red background [24].

Screening of gelatinase producing bacteria
Screening of bacteria isolates for gelatinase activity was performed on marine 2216 broth agar supplemented with 0.4% (w/v) gelatin (Sigma)[25]. Marine broth agar was autoclaved at 121°C for 15 min and sterilized aqueous solution of gelatin (8% w/v) was added to the medium before pouring to obtain 0.4% gelatin concentration in the medium. Gelatinase producing bacteria were selected based on the formation of halo zone of clearance around the colony after staining with Comassie blue (0.25% w/v) in methanolacetic acid-water 5:1:4 (v/v/v) and destained by using methanol and acetic acid. The extracellular gelatinase activity was detected by the presence of clear zone around the growing colony against the dark blue background.

Screening of amylase producing bacteria
Screening of bacteria isolates for amylase activity was performed on marine 2216 broth agar supplemented with 2% (w/v) starch (Sigma). Marine broth agar and starch were autoclaved at 121°C for 15 min. After incubation, the plates were flooded with

0.5% Congo red for 15–20 min followed by destaining procedure with 1 M NaCl for 15–20 min [26]. The extracellular amylase activity was detected by the presence of clear zone around the growing colony against the dark red background.

Screening of xylanase producing bacteria
Screening of bacteria isolates for xylanase activity was performed on marine 2216 broth agar supplemented with 2.5 g/L xylan from beechwood (Sigma) [27]. Marine broth agar and xylan were autoclaved at 121°C for 15 min. After incubation, the plates were flooded with 0.5% Congo red for 15–20 min followed by destaining with 1 M NaCl for 15–20 min. The extracellular xylanase activity was detected by the presence of yellow zone around the growing colony against the dark red background.

Screening of DNase producing bacteria
The extracellular bacterial DNases were screened using DNase test agar (Merck) and all plates were supplemented with extra 0.3 M NaCl. For the detection of DNase-producer bacterial strains, the plates were flooded with 0.1 M HCl solution. A clear or dim halo around a colony after one week indicated a positive exoenzyme-producing isolate [28].

1.4 Conclusions

This work provides insight into the microbial diversity that populates the Arctic region and further shows the vast genetic potential of these psychrophilic microorganisms to produce hydrolytic enzymes for processes of biotechnologically added value.

Acknowledgments
We thank Drs. Adele K. Williamson, Marcin Pierechod, Gro EK. Bjerga and Seila Pandur for their contributions regarding sampling, bacterial isolation and classification. This study is part of a research project (No. 219710/F11) within the YGGDRASIL mobility program and the MARZymes project (No. 192123) funded by the Research Council of Norway.

Conflict of Interest

"The authors declare no conflict of interest".

1.5 References

1. Jankowska, K.; Wlodarska-Kowalczuk, M.; Wieczorek, P. Abundance and biomass of bacteria in two Arctic glacial fjords. *Pol Polar Res/Pol Badania Polarne.* **2005**, *26*, 77–84.
2. Sahm, K.; Berninger, U. Abundance, vertical distribution, and community structure of benthic prokaryotes from perma-nently cold marine sediments (Svalbard, Arctic Ocean). *Mar EcolProgr Ser.* **1998**, *165*, 71–80.
3. Feller, G.; Gerday, C. Psychrophilic enzymes: hot topics in cold adaptation. *Nat Rev Microbiol.* **2003**, *1*, 200–208.
4. Azam, F. Microbial control of oceanic carbon flux: The plot thickens. *Science* **1998**, *280*, 694–96.

5. Zimmerman, A. E.; Martiny, A. C.; Allison, S. D. Microdiversity of extracellular enzyme genes among sequenced prokaryotic genomes. *ISME J.* **2013**, *7*, 1187–1199.
6. Gerday, C.; Aittaleb, M.; Bentahir, M.; Chessa, JP.; Claverie, P.; Collins, T.; D'Amico, S.; Dumont, J.; Garsoux, G.; Georlette, D.; Hoyoux, A.; Lonhienne, T.; Meuwis, MA.; Feller, G. Cold-adapted enzymes: from fundamentals to biotechnology. *Trends Biotechnol.* **2000,** *3,* 103-107.
7. Van der Burg, B. Extremophiles as a source for novel enzymes. *Current Opinion in Microbiology.* **2003**, *6*, 213–218.
8. Barcenas-Moreno, G.; Gomez-Brandon, M.; Rousk, J.; Erland L. Adaptation of soil microbial communities to temperature: comparison of fungi and bacteria in a laboratory experiment. In Global Change Biology **2009,** *15*, 2950-2957.
9. Joint, I.; Muibling, M.; Querellon, J. Culturing marine bacteria an essential prerequisite for biodiscovery. *Microbi. Biotechnol*. **2010**, *5*, 564-575.
10. Shigematsu, T.; Hayashi, M.; Kikuchi, I.; Ueno, S.; Masaki, H.; Fujii, T. A culture dependent bacterial community structure analysis based on liquid cultivation and its application to a marine environment. *FEMS Microbial Lett.* **2009**, *293*, 240-247.
11. Trincone, A. Marine biocatalysts: enzymatic features and applications. *Marine drugs.* **2011**, *9*, 478-499.
12. Huston, A.L. Biotechnological Aspects of Cold-Adapted Enzymes. In psychrophiles: from biodiversity to biotechnology; Margesin, R.; Schinner, F.; Max, J.C., Gerday, C.; Eds.; Springer-Verlag: Berlin, Germany, **2008**; pp 347-363.
13. Hasan, F.; Shah, A.A.; Javed, S.; Hameed, A. Enzymes used in detergents: lipases. *African Journal of Biotechnology*. **2010**, *31*, 4836-4844.
14. Bredholt, H.; Fjaervik E.; Johnsen G.; Zotchev, S.B. Actinomycetes from sediments in the Trondheim fjord, Norway: diversity and biological activity. *Marine Drugs*. **2008**, 6, 12-24.
15. Altschul, S.F.; Gish, W.; Miller, W.; Myers, E.W.; Lipman, D.J. Basic local aligment search tool. *Journal of Molecular Biology.* **1990**, *215*, 403–410.
16. Thompson, J.D.; Higginns, D.G.; Gibson, T.J. CLUSTAL W: improving the sensitivity oed progressive multiple sequence alignment through sequence weighting, position-specific gap penalties and weight matrix choice. *Nucleic Acids Res*. **1994**, *22*, 4673–4680.
17. Hall, T.A. BioEdit: a user-friendly biological sequence alignment editor and analysis program for windows 95/98/NT. *Nucleic Acids Symp. Ser*. **1999**, *41*, 95–98.
18. Tamura, K.; Peterson, D.; Peterson, N.; Stecher, G.; Nei, M.; Kumar, S. MEGA5: Molecular Evolutionary Genetics Analysis using Maximum Likelihood, Evolutionary Distance, and Maximum Parsimony Methods. *Molecular Biology and Evolution*. **2011**, *28*: 2731-2739.
19. Myung, I.J. Tutorial on *maximum likelihood* estimation. *Journal of Mathematical Psychology.* **2003**, *47*, 90–100.

20. Lee, D.G.; Jeon, J.H.; Jang, M.K.; Kim, S.J.; Kim, G.D.; Lee, S.H. Screening and characterization of a novel fibrinolytic metalloprotease from a metagenomic library. *Biotechnol Lett.* **2007**, *29*, 465–472.
21. Henne, A.; Schimtz, R.A.; Bömeke, M.; Gottschalk, G.; Daniel R. Screening of environmental DNA libraries for the presence of genes conferring lipolytic activity on *Escherichia coli*. *Appl Environ Microbiol.* **2000**, *66*, 3113–3116.
22. Usharani, T.R.; Gowda, T.K.S. Cloning of chitinase gene from *Bacillus thuringiensis. Indian Journal of Biotechnology.* **2011**, *10*, 264–269.
23. Devokta, H.K.; Maharjan, B.L.; Baral, B.; Singh, A.; Yami, K.D. Invitro screening of antifungal activity of rhizosperic bacteria and possible role of chitinase in antifungal activity. *Nepal Journal of Science and Technology.* **2011**, *12*, 304–311.
24. Rawat, R.; Tewari, L. Purification and characterization of an acidothermophilic cellulose enzyme produced by *Bacillus subtilis* strain LFS3. *Extremophiles.* **2012**, *16*, 637.
25. Vermelho, A.B.; Meirelles, M.N.L; Lopes, A.; Petinate, S.D.G.; Chaia, A.A.; Branquinha, M.H. Detection of extracellular proteases from microorganisms on agar plates*. Mem Inst Oswaldo Cruz.* **1996**, *91*, 755–760.
26. Mishra, S.; Behera, N. Amylase activity of a starch degrading bacteria isolated from soil receiving kitchen wastes. *African Journal of Biotechnology.* **2008**, *18*, 3326-3331.
27. Rajashri, D.K.; Anandrao, R.J. Isolation, purification and characterization of xylanase produced by a new species of *Bacillus* in solid state fermentation.. *International Journal of Microbiology.* **2012**, *3*, 189–194.
28. Dang, H.; Zhu, H.; Wang, J.; Li, T. Extracellular hydrolytic enzyme screening of culturable heterotrophic bacteria from deep-sea sediments of the Southern Okinawa Trough. *World Journal Microbiol Biotechnol.* **2009**, *25*, 71-79.

Chapter 2

Biochemical characterization and structural analysis of a new cold-active and salt tolerant esterase from the marine bacterium *Thalassospira* sp.

Biochemical characterization and structural analysis of a new cold-active and salt tolerant esterase from the marine bacterium *Thalassospira* sp.

Concetta De Santi [1,2] *, Hanna-Kirsti S. Leiros [2], Alessia Di Scala [1], Donatella de Pascale [1], Bjørn Altermark [2], Nils-Peder Willassen [2] *

1 Institute of Protein Biochemistry, National Research Council, Via P. Castellino, 111. I-80131, Naples, Italy
2 NorStruct, Department of Chemistry, Faculty of Science and Technology, UiT The Arctic University of Norway, 9037 Tromsø, Norway

*Authors to whom correspondence should be addressed;
E-Mail: nils-peder.willassen@uit.no (N-P.W.); Tel.: +47-77644651
c.desanti@ibp.cnr.it (C.D.S.); Tel.: +39-6132629

Abstract
An esterase ThaEst2349 was isolated from the marine arctic psychrophilic bacterium *Thalassospira* sp. GB04J01. The gene was cloned and successfully overexpressed in *E. coli* as a His-tagged fusion protein. The recombinant enzyme showed optimal activity at 45°C and the thermal stability displayed a retention of 75% relative activity at 40°C after 2 h. The optimal pH was 8.5 but the enzyme kept more than 75% of its maximal activity between pH 8 and 9.5. ThaEst2349 also showed remarkable tolerance towards high concentrations of salt and it was active against short-chain *p*-nitrophenyl esters (C2–C5), displaying optimal activity with the acetate (C2). The enzyme has been tested for tolerance of organic solvents and different ions and the results are suggesting it could function as an interesting candidate for biotechnological applications. The crystal structure of ThaEst2349 was determined to 1.69 Å revealing an asymmetric unit containing two chains, which also is the biological unit. Further the structure has a characteristic lid domain and a catalytic triad comprising Ser158, His285 and Asp255. The cold active nature of the enzyme can be explained by the high methionine content, less hydrogen bonds and less ion pairs. The water exposed channel leading into the active site of ThaEst2349 is enclosed by helix α1 and α2 in the lid and determines the substrate binding properties.

Keywords:
Cold-active, esterase, psychrophilic micro-organism, biotechnological applications, crystal structure

Abreviations
Esterase from *Thalassospira* sp, ThaEst2349

2.1 Introduction
The screening of microbes from extreme environments frequently reveals novel enzymes useful for biotechnological applications. Biocatalysts of bacterial origin represent the majority which are used in industrial and biotechnological processes due to the ability of prokaryotes to populate and adapt to a plethora of extreme environments (Uchiyama et al. 2009). In this respect, marine microorganisms are

often dramatically different from terrestrial organisms regarding their various and special living habitats and provide a rich and unique source to be tapped for industrial use (Kim et al. 2006). Biocatalysts of great potential are represented by the microbial esterases, which is comprised of two enzymes groups: carboxylesterases (carboxylester hydrolases, E.C. 3.1.1.1) and lipases (triacylglycerol acylhydrolase E.C. 3.1.1.3), widely named lipolytic enzymes. This enzyme class has been comprehensively studied and classified (Arpigny et al. 1999). Both esterases and lipases are members of α/β hydrolase superfamily and the classification into eight families is based on some fundamental biological properties and specific amino acid residues that constitute the catalytic triad site: Ser, His and Glu/Asp where one of those residues is within a highly conserved pentapeptide GXSXG motif. The serine is part of a "nucleophilic elbow and believed to be the active site performing a nucleophilic attack during the catalysis (Fu et al. 2013; Ollis et al. 1992). A recent paper describes how mutations in the conserved motif altered the biochemical properties and substrate specificity (Pérez et al. 2012).

In the recent years, an increasing number of lipolytic enzymes with different enzymological properties and substrate specificity have been isolated from psychrophilic microorganisms by a genomic approach (Do et al. 2013; Lee et al. 2013; Kim et al. 2013). This interest is mostly due to the high activity of psychrophilic lipolytic enzymes at low and moderate temperature that can offer huge potential economic benefits compared to mesophilic microorganisms (Fuciños et al. 2012).

Many cold adapted proteins have a low temperature optimum and a low thermal stability (Smalås et al. 2000). Still there is no common structural determinant for all cold active protein, but the trend seems to be fewer interactions within these proteins. This can be achieved through: a decrease in the number of ion-pair interactions; fewer intersubunit hydrogen bonds; an increase in surface charge, mostly a negative charge; a decrease in the fraction of accessible surface area (ASA) of side-chains; a higher proportion of hydrophobic residues at the surface; longer surface loops with reduced number of proline residues; a reduced Arg/(Lys+Arg) ratio; and, for some, a higher methionine content (Smalås et al. 2000, Siddiqui et al. 2006b, Gianese et al. 2002). Flexibility has been discussed for many cold active enzymes and particularly the local flexibility around the active site. The theory is that the increased flexibility is translated into lower activation enthalpy, lower substrate affinity, and higher specific activity at low temperatures compared to mesophilic and thermophilic homologues (Lonhienne et al. 2000).

The temperature stability of lipolytic enzymes is particularly regarded to be one of the most characteristics to be biotechnological (Joseph et al. 2008).

Besides, bacterial esterases display a more broad range of substrate specificity and regiospecificity than those from eukaryotes, a basic requirement to be used in versatile industrial applications, such as additives in laundry detergents and catalysts for organic synthesis of unstable compounds at low temperatures (Bornscheuer 2002).

In the present study, we focused our attention on the structural and functional properties of a novel cold-active esterase that was cloned, recombinantly expressed, biochemically characterised and its crystal structure was solved at high resolution, highlighting new peculiar features of the psychrophilic enzyme.

2.2 Materials and Methods

Bacterial Strains, DNA manipulation and gene cloning

The strain *Thalassospira* sp. GB04J01 was isolated from a sea fan (*Paramuricea placomus*) during a research-cruise with R/V Helmer Hanssen to the Vestfjorden area (Northern Norway and it is preserved and available from an in-house collection at the University of Tromsø, Norway (database index GB04J01).

The whole genome of *T*. sp GB04J01 has been sequenced and annotated (data not published). The genome was analysed using the Artemis software suit (Rutherford et al. 2000) to search for new genes encoding for esterases and lipases. This revealed an open reading frame (ORF) of 1029 bp, the *ThaEst2349* lipolytic gene that encodes for a protein of 343 amino acids and herein determined ThaEst2349. The gene contains a N-terminal leader sequence (27 amino acids long) that was not included in the cloning construct. The gene has been deposited in GenBank under accession number KJ365310.

Thalassospira sp. GB04J01 was grown in marine 2216 broth (Difco) at 4°C using a Heidolph tube shaker (Heidolph, Germany) at 600 rpm. Genomic DNA from *Thalassospira* sp. GB04J01 was purified by using Sigma's Gen Elute Bacterial Genomic kit. The *ThaEst2349* gene was amplified from genomic DNA by using a cloning method termed FastCloning (Li. et al. 2011). The following primer pairs were used to PCR amplify pET-26b vector and insert separately:

VecFw 5'-ACCGCCCTTCACGGGAAGCACCACCACCACCACCAC-3',

VecRv 5'-GGTGGGTTCAAGAACCGGCATATGTATATCTCCTTCTTAAAG-3',

InsertFw 5'-CTTTAAGAAGGAGATATACATATGCCGGTTCTTGAACCCACC-3',

InsertRv 5'-GTGGTGGTGGTGGTGGTGCTTCCGGTGAAGGGCGGT-3'. The expression cassette includes an in-frame C-terminal fusion purification 6xHis-Tag and the PCR reaction conditions used were: 1 cycle (98°C for 3 min), 20 cycles (98°C 15 sec, 55°C 30 sec, and 72°C 1 min), and a final cycle at 72°C for C 10 min. *Dpn*I enzyme (Sigma-Aldrich, USA) was added into the PCR insert- and vector product separately. Vector and insert were mixed with a 1:3 ratio and incubated at 37°C for 2 h. The mixture was then added into NovaBlue GigaSingles competent cells (Novagen, Germany). The DNA sequence of the resulting construct was verified by bidirectional DNA sequencing. The recombinant plasmid was then transformed into *E.coli* BL21 (DE3) cells.

Production and purification of ThaEst2349

E. coli BL21(DE3) carrying pET-26b-ThaEst2349 vector was grown in Luria Broth (LB) medium with 50 *μ*g/mL kanamycin until OD_{600} reached 0.5, and induced by 0.2 mM IPTG at 20°C overnight. Cells were harvested by centrifugation at 3,200x*g* at 4°C for 30 min and the cell pellet was resuspended in lysis buffer (50 mM Tris-HCl pH 8.0, 500 mM NaCl and 10% glycerol). The cells were disrupted by sonication at 6 m/s for ten bursts of 60 seconds and ultra centrifuged at 75,000 *g* at 4°C for 45 min. The recovered supernatant was loaded on a HisTrap HP 1ml column (GE Healthcare, England) equilibrated with 50 mM Tris-HCl pH 8.0, 500 mM NaCl, 30 mM imidazole, 10% glycerol. A linear gradient of 0-500 mM imidazole over 10 column volumes was applied to elute the protein. Fractions containing the recombinant enzyme were analyzed by SDS-PAGE and dialyzed against 50 mM Tris-HCl pH 8.0, 500 mM NaCl and 10% glycerol.

Enzyme Assays

The esterase activity of the recombinant enzyme was measured spectrophotometrically at 405 nm in 1 cm path-length cells with a Cary 100 spectrophotometer (Varian, Australia) equipped with a temperature controller. Assays were performed in 1 mL mixture containing purified enzyme (50 μg/mL), 100 mM Tris-HCl buffer (pH 8.0), 3% acetonitrile and *p*-NP esters at different concentrations. Assays were carried out in duplicate or triplicate and one unit of enzymatic activity was defined as the amount of protein that released 1 μmol of *p*-nitrophenoxide/min from *p*-NP esters. The absorption coefficient used for *p*-nitrophenoxide was 19,000 M^{-1} cm^{-1}.

Kinetic Measurements

The kinetic parameters K_M and k_{cat} of the ThaEst2349 were determined using *p*-NP esters as substrates at the condition described in the enzyme assays paragraph. The following substrate concentration ranges were used: *p*-NP acetate (C2, in a range of 30-1000 μM), *p*-NP butanoate (C4, 600-1500 μM), *p*-NP pentanoate (C5, 600-1800 μM). The kinetic parameters were determined from the rates of hydrolysis by fitting the rates to a Lineweaver-Burk double reciprocal plot. All kinetic data were analyzed by linear regression using SigmaPlot 10.0.

Determination of pH and optimal temperature of ThaEst2349

The pH dependence of the esterase activity was monitored at 348 nm (the pH-independent isosbestic point of *p*-nitrophenol and the *p*-nitrophenoxide ion), with *p*-NP pentanoate (100 μM) as substrate. A molar absorption coefficient of 5000 M^{-1} cm^{-1} at 25°C was introduced. The following 0.1 M buffers were used: MES (pH: 5.0-6.0), Na-phosphate (pH: 6.0-7.5), Tris-HCl (pH: 7.5-9.5) and CAPS (pH: 9.5-10.5). The temperature optimum was determined in the range of temperature from 10 to 70°C in 0.1 M Tris-HCl (pH 8.5), containing 3% acetonitrile, using *p*-NP pentanoate (100 μM) as substrate.

Determination of the thermostability and residual activity

The thermostability of the enzyme was examined by testing the residual activity after incubation of the enzyme in a microcentrifuge tube at 10, 20, 30, 40 and 50°C. Aliquots of the reactions were withdrawn at 0, 20, 40, 60, 80, 100, 120 min. The activity was also evaluated after a pre-incubation of 24 hours at 4°C in presence of methanol, acetone, 2-Propanol, butanol, ethanol, dimethyl sulfoxide (DMSO), dimethyl formamide (DMFA), glycerol, acetonitrile and dietilic ether. Each assay was performed in duplicate using a final organic solvent concentration of 10% (v/v).

The enzyme activity was also measured by using an increasing concentration of several solvents: acetonitrile, DMSO, methanol, acetone, ethanol, butanol and 2-propanol from 0 to 20% (v/v) in the assay mixture.

The effect of detergents on ThaEst2349 enzymatic activity was evaluated after an incubation of the protein for 1 h at 4°C in presence of TRITON X, CTAB, Tween80, Tween20, SDS at 0.1% and 1% (v/v). β-mercaptoethanol, EDTA, DTT and PMSF were included in the mixture at a final concentration of 1 mM and 10 mM. Preferences for metal cations, $CuCl_2$, $CrCl_2$, $MgCl_2$, $MnCl_2$, KCl, $CaCl_2$, $CdCl_2$, $FeCl_2$, $ZnCl_2$, $HgCl_2$, $SnCl_2$, $CoCl_2$, LiCl, CsCl, $NiCl_2$, were analyzed by adding them at a final concentration of 1 and 10 mM after an incubation at 4°C for 1h. The effect of NaCl on enzymatic activity was evaluated by increasing the salt concentration in a range of 0-4 M at 45°C and also after incubation in presence of 0, 1, 2, 2.5 and 3 M NaCl for 24 h at 4°C.

Sequence Analysis
Sequence similarity and analysis for conserved domains were performed using BLAST programs on the National Center for Biotechnology Information (NCBI) website (http://www.ncbi.nlm.nih.gov) and Pfam protein families database (Bateman et al. 2002**)**. Sequence alignments were created using the tools of the T-Coffee server (http://www.ebi.ac.uk/Tools/msa/tcoffee/) and ClustalW2 (http://www.ebi.ac.uk/Tools/msa/clustalw2/). The N-terminal signal peptide was predicted using SignalP 3.0 (http://www.cbs.dtu.dk/services/SignalP/). Molecular weights were determined using Protein Calculator V3.3 (http://www.scripps.edu/~cdputnam/protcalc.html).

Crystallization, Data collection, structure determination
Crystallization experiments on pure ThaLip2349, was performed at room temperature using a Phoenix crystallization robot (Art Robbins Instruments) in 96-well format MRC plates with 60 µl reservoir solution per well and drops made by mixing 0.5 µl well solution and 0.5 µl protein solution. The protein was at 10 mg/ml in a buffer with 50 mM Tris-HCl pH 8.0, 500 mM NaCl and 10% glycerol. In total 96 different in-house made conditions were screened, and 2 hit were optimized by hand using the hanging drop method. The best crystal obtained had a reservoir solution with 25% PEG 3350 and 0.2 M $MgCl_2$ (Figure 1b), and the crystal was harvested straight from the drop and flash frozen in liquid nitrogen. X-day data were collected at BESSY, Berlin at BL 14.2 with a wavelength of 0.91705 Å, a crystal to detector distance of 150 mm, 0.5 degree oscillation per frame and 90° of data (Table 6).
The phase problem was solved by PHASER (McCoy et al. 2007) using the structure of carboxyl esterase 2 (EST2) from *Alicyclobacillus acidocaldarius* (AcEst2)(PDB 1QZ3)(De Simone et al. 2004) with 36% sequence identity as a search model, the structure was refined in Phenix (Adams et al. 2010) and manually built in WinCoot (Emsley & Cowtan, 2004).

Structural analysis and accessible surface areas calculations
Prior to these calculations all double conformations were removed. Then hydrogen bonds were calculated using the program HBPLUS (McDonald & Thornton, 1994) v3.2 and the following parameters for Donor (D), Acceptor (A), Acceptor Antecedents (AA) and (calculated) Hydrogens (H) were applied: maximum distances for D-A 3.5 Å, H-A 2.5 Å; minimum angle for D-H-A, D-A-AA and H-A-AA of 90°. All ion pairs were included in the calculations. Accessible surface areas were calculated using on line server PISA at the European Bioinformatics Institute (Krissinel & Henrick, 2007).
Ionic interactions were analyzed using the WHAT IF server (http://swift.cmbi.ru.nl/servers/html/shosbr.html), and maximum cut off distances of 4 and 6 Å were applied. Inter-subunit salt bridges were found from the same server with a 4 Å cut-off distance.

2.3 Results

Sequence analysis
Sequence analysis using the Pfam protein families identified an α/β-hydrolase family sequence (Pfam07859) that spans the full length of ThaEst2349. The amino acid sequence exhibited the highest full-length identity to a carboxylesterase Est2 from the *Alicyclobacillus acidocaldarius* (1QZ3A, 36% identity for 114 AA) (De Simone et al. 2004). The *Thalip* gene was cloned in the expression vectors pET-26b(+). After

confirming the correct ORF by DNA sequencing, the gene was expressed as a C-terminal His-tag fusion protein.

Purification and physical properties of ThaEst2349

Heterologous expression of ThaEst2349 in *E. coli* BL21(DE3) resulted in the production of about 30 mg soluble recombinant protein per 500 ml culture, and the purity was estimated to be 98% pure from SDS-PAGE analysis (Figure 1a). The apparent molecular mass of about 35 kDa is in agreement with the theoretical mass from the sequence of 35.04 kDa.

Esterase activity of ThaEst2349: pH dependence, temperature optimum and thermostability

The optimal pH for the esterase activity was determined using *p*-NP pentanoate as a substrate in the pH range from 8.0 to 12.0, and the kinetics were followed spectrophotometrically at 348 nm, which is the pH independent isosbestic wavelength between the *p*-nitrophenol and *p*-nitrophenolate ion produced by the reaction. As shown in Fig. 2a, the maximum activity was recorded at pH 8.5 in Tris-HCl buffer. The effect of temperatures on esterase activity was determined using *p*-NP pentanoate as substrate in the temperature range of 10 to 70°C. As shown in Fig. 2b, the highest percentage activity was observed at 45°C. No catalytic activity was detectable at 70°C.

The ThaEst2349 hydrolysed *p*-NP esters with acyl-chain lengths from two to five carbon atoms (C2–C5). All the characterization was performed at 45°C and in presence of 3% acetonitrile. In this condition, the enzyme displays highest activity towards *p*-NP acetate (Table 1) with a highest k_{cat} and k_{cat}/K_M value. The results indicated that the enzyme is an esterase and *p*-NP acetate was used as preferential substrate for further studies.

To analyse the thermostability of the recombinant enzyme, we incubated the enzyme in the range 10-50°C for 0-140 min before measuring the residual esterase activities at its optimal temperature, using *p*-NP acetate as substrate (Fig. 2c). After 2 h of incubation we observed a little decrease of activity at 10 and 20°C. At 30 and 40°C the residual enzymatic activity did not significantly decrease and it was about 70-80%. A 10% of enzymatic activity was recorded after 20 min of incubation at 50°C (Fig. 2c).

The enzyme was strongly inhibited by 10 mM Cr^{2+} and Fe^{2+}, while the activity increased in presence of 1 mM Li^{+}, Sn^{2+}, Ca^{2+}, Cr^{2+}, Co^{2+}. The relative activity was weakly reduced in presence of 10 mM Li^{+} and Co^{2+} but not in presence of 10 mM Sn^{2+} and Ca^{2+} (Table 2). Tween80 at 0.1% concentration had no effect on the activity, whereas 0.1% Tween20 and 1% Tween80 gave a modest reduction of esterase activity. Strong decrease in activity was observed with SDS and cetyltrimethylammonium bromide (CTAB). Moreover, higher concentration of CTAB (1%) showed an increased activity of ThaEst2349 (Table 3). The enzyme appears not to be effected by the presence of low and high concentration EDTA, PMSF and β-mercaptoethanol. A significant activation was observed with 10 mM DTT.

The effect of the NaCl presence on ThaEst2349 enzymatic activity was evaluated by using *p*-NP-acetate as substrate at 45°C in 0.1 M Tris-HCl pH 8.5. We observed an improved activity with the highest concentration of 3 M NaCl (Table 4). This behaviour was even confirmed after incubation for 24 h at 4°C in presence of 3M NaCl when the relative activity was five times higher than the activity in absence of NaCl. The esterase stability profile in presence of 10% organic solvents and glycerol

was evaluated (Table 5). In comparison, controls in presence of DMSO and glycerol did not affect the enzyme activity. Methanol showed an inhibitory effect on the enzyme activity. The decrease of the relative activity was even displayed when the assay was performed in presence of 5, 10, 15 and 20% of organic solvents. A remarkable reduction of the activity was obtained in the range of 5-20% of methanol, butanol, 2-propanol and ethanol (Figure 2d).

Crystal structure of ThaLip2349

The characterized ThaEst2349 esterase was crystalized (Figure 1b) and the crystal structure was resolved to 1.69 Å with an R-factor of 14.3% and an R-free value of 18.4% (Table 6). The model has satisfactory geometry for the two molecules in the asymmetric unit and 915 water molecules. The overall structure of one ThaEst2349 monomer includes eight β-strands and eleven α-helices (Figure 3a, b). The eight β-strands surrounded by five adjacent α-helices together form a central α/β-hydrolase domain and where the central β-sheet has a typical left-handed superhelical twist with β1 and β8 oriented at an angle close to 90° (Figure 3b).

Comparison with other esterases

By use of the DALI server (Holm & Rosenström, 2010) and Chain A of ThaLip2349 we identified many structures with high Z-scores (40 PDB entries with Z score of 40-44), thus the ThaLip2349 has the same fold as these. The ones used for comparison in this paper include:

The esterase from the hyperthermophilic microorganism *Pyrobaculum calidifontis* VA1 (PcEstE; PDB 3ZWQ, Z=44.3, RMSD=1.5 Å for 303 CA-atoms, 35% sequence identity)(Palm et al. 2011), the archaeon thermostable carboxylesterase from *Sulfolobus tokodaii* (StoEst; PDB 3AIL, Z=42.9, RMSD=1.4 Å for 283 CA-atoms, 35% sequence identity)(Angkawidjaja et al. 2012), the carboxyl esterase 2 (Est2) from *Alicyclobacillus acidocaldarius* (AcEst2; PDB 1QZ3; Z=43.7, RMSD=1.9 Å for 305 CA-atoms, 36% sequence identity)(De Simone et al., 2004) and the cold-adapted esterase from an Arctic intertidal metagenomic library (Est97; PDB 4AO8; Z=18.1 RMSD=2.6 Å for 197 CA atoms, 14% sequence identity)(Fu et al. 2013). The latter is included since it is from a cold environment.

Active site

ThaEst2349 was from the characterization found to be an esterase and the proposed active site residues from the structure (Figure 3c) and sequence alignment (Figure 4) are: Ser158, His285 and Asp255 These residues overlap with catalytic triad in the esterases, PcEst (PDB 3ZWQ), StoEst (PDB 3AIL) and AcEst2 (PDB 1QZ3)(De Simone et al. 2004) and also the cold-adapted esterase Est97 (PDB 4AO6)(Fu et al. 2013). Ser158 is then the most likely candidate to perform a nucleophilic attack on the substrate during the catalysis, stabilized by His285 as proton carrier and Asp255 in a charge-relay system. Ser158 is part of a GXSXG sequence motif typical for a nucleophilic elbow (Ollis et al. 1992) in lipolytic enzymes. An oxyanion hole, needed to stabilize the negatively charged substrate intermediate can be composed of the main-chain nitrogen atoms of Ala86 and Gly87 in ThaEst2349 (Figure 3c), which are similar to the compared structures.

Lid domain

Many lipolytic enzymes has a lid domain which play an important role in substrate specificity, thermostability, regulation of access to the active site or facilitation of

product release (Uppenberg et al. 1994; Santarossa et al. 2005; Nam et al. 2009). In Est97 the lid includes 35 residues forming one α-helix and loops (Fu et al., 2013). For PcEstE the cap domain includes α1 and α2 (in part), and α6, α7, α8 and α9 plus several random coils inserted between strands β6 and β7 (Palm et al. 2011). In ThaEst2349 this corresponds to α1, α2, and α6, α7, α8 and α10 in addition to α10 (Figure 3b). Since the lid is situated adjacent to the active site is can contribute to substrate access and activity, as illustrated in figure 3e.

Dimer

ThaEst2349 was in solution found to be a dimer and in the crystal structure chain A and chain B form a functional dimer. The dimer interface of 1 977 $Å^2$ is 9% of the total solvent-accessible area of one dimer (Table 7). The interface is held together by nine hydrogen bonds where five are main-chain to main chain interactions (Arg279 O to Arg279 N, Arg279 N to Arg279 O, Val277 O to Asn281 N, Asn281 N to Val277 O, and Ala304 O to Gln308 N (Figure 3d). In addition there are strong ionic interactions (<4 Å) involving Glu253 to Arg266 and vice versa Arg266 to Glu253 (Figure 3d). The two β8 strands (residues 275-284) are involved in a many of these interface interactions.

A similar dimer interface with interactions at the same side of the molecule and also involving a β8-β8 interactions, are also found for PcEstE from a hyperthermophilic microorganism (PDB 3ZWQ) (Palm et al. 2011), and the thermostable StoEst (PDB 3AIL) (Angkawidjaja et al. 2012), thus not unique to ThaLip2349.

Analysis of the PcEstE dimer (PDB 3ZWQ) reviled a larger buried intersubunit surface, 22 hydrogen bonds and 4 ion pairs, and in StoEst (PDB 3AIL; AD chains) a similar intersubunit surface was found, with 15 hydrogen bonds and 4 ion pairs (Table 7). One ThaEst2349 dimer is then less stabilized by fewer interactions than in both PcEstE and StoEst (Table 7).

Cold adaptation features

ThaEst2349 has a clear cold active profile with substantial activity below 10°C and a relatively low temperature optimum of 45°C (Figure 2b). In addition no enzyme activity was present after heating the enzyme to 50°C (Figure 2c), also showing that no refolding occurs after thermal denaturation. In order to find structural explanations to this we set off to analyze the crystal structures of ThaEst2349, PcEstE and StoEst (Table 7).

One ThaLip2349 monomer is stabilized by less hydrogen bonds per residue (0.88/0.89) than in PcEstE (1.02/1.03) and StoEst (0.95-0.99). There are also less strong ion pair per residue (< 4Å) in ThaLip2349 (0.054/0.054) than in in the PcEstE (0.086/0.085) and in StoEst (0.071-0.081) crystal structures (Table 7). The Arg/(Lys+Arg) ratio is high for ThaEst2349 (0.65) and similar to StoEst (0.67) and lowest in PcEst (0.38). In one StoEst monomer there is one di-sulfide bond not present in the two other structures. The glycine and proline content cannot explain the low thermal stability of ThaEst2349. The methionines are investigated underneath.

Taken together then the reduced number of hydrogen bonds and ion pairs within one monomer and at the dimer interface and the lack of the di-sulfide bond found in StoEst all sems to contribut to the low thermal stability of ThaEst2349.

Methionine residues

Met1 is not defined in the ThaEst2349 and StoEst crystal structures, whereas Met90, Met 163, Met212 and Met289 in ThaEst2349 in are all found partly buried in the structure. Met1 in PcEstE is found at the dimer interface, one methionine is party buried (Met214) and the remaining four (Met24, Met43, Met169, Met310) are situated at the surface of the molecule. The role of the metheonines then seems different in the hyperthermophile PcEstE and ThaEst2349 with marine origin, and in the latter they might explain the observed low temperature optimum at 45°C (Figure 2b) and loss of enzymatic activity after 20 min at 50°C (Figure 2c).

Substrate binding

The crystal structure of AcEst2 from *Alicyclobacillus acidocaldarius* (PDB 1QZ3)(De Simone et al. 2004) is a complex with an inhibitor covalently bound to the active site serine. Herein the 1-Hexadecanesulfonyl is protruding from the active site. The same channel is also found in ThaEst2349 (Figure 3e) but the size is different and for ThaEst2349 the “walls“ are constrained by Asp286 (Gly283 in AcEst2), Met90 (Val87 in AcEst2), Trp206 (Leu205 in AcEst2).

For AcEst2 residues Phe30, Phe37, Met210 and Phe214 form import parts of this channel.

The inhibitor is protruding out to the solvent between α1 and α1 in AcEst2 and in the modeled with ThaEst2349 (Figure 3e), thus these two helices seems important for the enzyme specificity. The enzyme kinetics of ThaEst2349 found *p*NP-acetate to bind stronger than *p*NP-pentanoate and *p*NP-butanoate, the smallest substrate also gave the highest catalytic turnover (k_{cat}) and highest catalytic efficiency (k_{cat}/K_M) of the three substrates tested (Table 1). In terms of size they should all fit into the observed channel, still Asp286, Trp206 and Met90 are determinants for the channel properties (Figure 3e).

2.4 Discussion

In this study, we report the biochemical characterization and structure analysis of an esterase from the arctic marine bacteria *Thalassospira* sp. To our knowledge, this is the first biochemical characterization and structural analysis of a cold-active isolated from the genus *Thalassospira*.

The optimal pH activity was lost at pH 6 most probably due to protonation of His285 in the catalytic triad. The observed of a pH dependent enzyme activity fits with fact that the catalytic triad must be in the correct protonation state to be active. The pH optimum of ThaEst2349 is higher than for Est97 which had an optima around pH 7.5 (Fu et al. 2013); for the ThaEst2349 enzyme activity was found at pH 8.5 (Figure 2a) and it maintained more than 80% maximal activity at pH 9.5, which indicates that this protein may be considered as an alkaline esterase.

Similarly, a carboxylesterase was reported to be active and stable in neutral to alkaline pH range (Lv et al. 2010). This property makes this enzyme very attractive for its tremendous potentiality in industrial processes (Chakraborty et al. 2011).

Another remarkable property of ThaEst2349 is its high thermostability after incubation at 40°C. This result can be explained considering that cold-active enzymes possess a high level of structural flexibility (Siddiqui et al. 2006). It has even been previously reported that structural flexibility and rigidity of psychrophilic enzymes may co-exist in the same molecule (Lonhienne et al. 2000) and this hypothesis has been supported by several studies on other characterized cold-active enzymes (Kulakova et al. 2004; Wu et al. 2013). The low thermal stability and activity at low temperature of ThaEst2349 can be related to the reduced number of hydrogen

bonds and ion pairs, and more methionine residue than in the compared esterase structures. The methionine residue is special in the fact that it has high degree of rotational freedom, it lacks branching, has no charge and no dipole interactions. In some cold-adapted proteins a high methionine content have been proposed as one cold-adaptation mechanism (Siddiqui & Cavicchioli, 2006a; Smalås et al. 2000). The increased methionine content, however, might also be attributed to halophilic (salt loving) adaptation since a higher content in this residue has been found in many fish enzymes (Leiros et al. 1999, 2000, Smalås et al. 2000) and in the estease Est97 from intertidal metagenomic library (Fu et al. 2013). Also the Isocitrate dehydrogenase from the psychrophilic bacterium Desulfotalea psychrophila (Fedoy et al. 2007) has many methinines and enhanced methionine cluster. However, this phenomenon is also reported for cold-adapted archaeal proteins (Thomas & Cavicchioli, 1998), and Isocitrate dehydrogenase from the hyperthermophilic Thermotoga maritima (Fedoy et al. 2007). The recombinant esterase showed substrate specificity toward short acyl chain-length (C2-C5) of *p*-NP esters, and higher activity was displayed on short acyl chain-length (C2). The observed water exposed channel cannot explain why the enzyme has higher efficiency for short acyl chain-length compared to longer (C4 and C5).

ThaEst2349 activity was not affected by EDTA chelation, suggesting that the enzyme is not a metalloenzyme (Zhang et al 2009). In addition, ThaEst2349 displayed significant resistance to inhibition by most of all heavy metal that were tested (Cu^{2+}, Mn^{2+}, Hg^{2+}, Sn^{2+}, Co^{2+}, Li^{+} and Ni^{2+}). A similar behaviour was recently reported in another esterase (Yasmine et al. 2013). A total inhibition was observed in presence of higher concentrations of Fe^{2+} and Cr^{2+}. A strong inhibition was also revealed with 10 mM zinc ions (less than 20% residual activity). This effect was also found in other lipolytic enzymes (Jeon et al. 2009).

The enzyme activity was completely inhibited by SDS and enhanced by low concentration of Tween80 and high concentration of Tween20. Non-ionic detergents can help the substrate interaction with the catalytic triad while ionic detergents such as SDS may inhibit inter- and intra-molecular protein-protein interaction (Fu et al. 2011). Another surfactant, CTAB, had a toxic effect on esterase activity. This result has been recently reported in another esterase (Ghati et al. 2013).

ThaEst2349, isolated from marine environment, displayed particular features including stability and solubility in high salt concentrations by acquiring a relatively large number of charged amino residues on their surfaces to prevent precipitation (Madern et al. 2000; Rao et al. 2009). This unique property suggested that the enzyme is also a halotolerant enzyme.

We tested the enzyme activity in organic solvents that is an essential requirement for applications in organic synthesis (Doukyu et al. 2010). A significant inactivation was observed in presence of hydrophilic organic solvents such as methanol, acetonitrile, ethanol and acetone, as reported also for another enzyme (Ogino et al. 2001). However the enzyme showed an increased activity in presence of DMSO, glycerol and dietilic ether suggesting that there is no relationship with the polarity of the organic solvent. This is in agreement with the organic solvent stability of some esterases already studied (Ji et al. 2010).

In conclusion the biochemical and structural characterization of the α/β idrolase protein ThaEst2349 from the psychrophilic marine bacterium Thalassospira sp. revealed to be a cold-active, alkaline and salt tolerance carboxylesterase. Extremophilic salt- and cold-adapted enzymes have enlarged the understanding of enzyme stability and activity mechanisms, protein structure-function relationships,

enzyme engineering and evolution. The enzyme displays a high potential for biotechnological applications and this was confirmed by extensive biochemical characterization. The emerged ThaEst2349 futures regarding the protein-solvent interactions may suggest it can cause the development of new catalysts for use in novel synthetic applications, including enzymes operating in low water activity and organic solvents for applications in bioenergy and biotechnology. The crystal structure revealed a dimeric structure held together by nine hydrogen bonds and two strong ionic interactions. Helix α1 and α2 in the lid domain along with Asp286, Trp206 and Met90 all define properties of the channel into the active site which comprisie Ser158, His285 and Asp255.

Acknowledgements
We thank the Research Council of Norway for supporting part of this work by the grant (No. 219710/F11) within the YGGDRASIL mobility program. This study was supported by The Research Council of Norway, the Functional Genomics Program (FUGE) through The Norwegian Structural Biology Centre (NorStruct). Provision of beam time at Bessy II, Berlin Germany at BL14.2 is gratefully acknowledged.

2.5 References

Adams PD, Afonine PV, Bunkoczi G, Chen V B, Davis IW, Echols N, Headd JJ, Hung LW, Kapral GJ, Grosse-Kunstleve RW, McCoy AJ, Moriarty NW, Oeffner R, Read RJ, Richardson DC, Richardson JS, Terwilliger TC & Zwart PH (2010) PHENIX: a comprehensive Python-based system for macromolecular structure solution Acta crystallographica. Section D, Biological crystallography D66: 213-221

Arpigny JL, Jaeger KE (1999) Bacterial lipolytic enzymes: classification and properties. Biochem J 343:177-183

Angkawidjaja C, Koga Y, Takano K & Kanaya S (2012) Structure and stability of a thermostable carboxylesterase from the thermoacidophilic archaeon Sulfolobus tokodaii. Febs J 279: 3071-3084

Bateman A, Birney E, Cerruti L, Durbin R, Etwiller L, Eddy SR, Griffiths-Jones S, Howe KL, MarshallM, Sonnhammer EL (2002) The Pfam protein families database. Nucleic Acids R Res 30:276–280

Bornscheuer UT (2002) Microbial carboxylesterases: classification, properties and applications in biocatalysts. FEMS Microbiol Rev 26:73-81

Chakraborty S, Khopade A, Biao R, Jian W, Liu XY, Mahadik K, Chopade B, Zhang LX, Kokare C (2011) Characterization and stability studies on surfactant, detergent and oxidant stable α-amilase from marine haloalkaliphilic Saccharopolyspora sp. J Mol Catal B-Enzym 68:52-58

De Simone G, Mandrich L, Menchise V, Giordano V, Febbraio F, Rossi M, Pedone C & Manco G (2004) A substrate-induced switch in the reaction mechanism of a thermophilic esterase: kinetic evidences and structural basis. The Journal of biological chemistry 279:815-6823

Do H, Lee JH, Kwon MH, Song HE, An JY, Eom SH, Lee SG, Kim HJ (2013) Purification, characterization and preliminary X-ray diffraction analysis of a cold-active lipase(CpsLip) from the psychrophilic bacterium *Colwellia psychrerythraea* 34H. Acta Crystallogr Sect F Struct Biol Cryst Commun 69:920-924

Doukyu N, Ogino H (2010) Organic sovent tolerant enzymes. Biochem Eng J 48:270-282

Emsley P & Cowtan K (2004) Coot: model-building tools for molecular graphics. Acta Crystallogr D Biol Crystallogr 60:2126-2132

Fedoy AE, Yang N, Martinez A, Leiros HK & Steen IH (2007) Structural and functional properties of isocitrate dehydrogenase from the psychrophilic bacterium Desulfotalea psychrophila reveal a cold-active enzyme with an unusual high thermal stability. J Mol Biol 372:130-149

Fu C, Hu Y, Xie F, Guo H, Ashforth EJ, Polyak SW, Zhu B, Zhang L (2011) Molecular cloning and characterization of a new cold-active esterase from a deep-sea metagenomic library. Appl Microbiol Biotechnol 90:961-970

Fu J, Leiros, HK S, de Pascale D, Johnson KA, Blencke HM & Landfald B (2013) Functional and structural studies of a novel cold-adapted esterase from an Arctic intertidal metagenomic library. Applied microbiology and biotechnology 97:3965-3978

Fuciños P, Gonzáles R, Altanes E, Sestelo ABF, Pérez-Guerra, Pastrana L, Rúa L (2012) Lipases and esterases from extremophiles: overview and case example of the production and purification of an esterase from *Thermus thermophilus* HB27. Methods in Molecular Biology 861: 239-266

Ghati A, Sarkar K, Paul G (2013) Production and characterization of an alkalothermostable, organic solvent tolerant and surfactant tolerant esterase produced by a thermophilic bacterium *Geobacillus* sp. AGP-04, isolated from Bakreshwar Hot Spring, India. JMBFS 3:155-162

Gianese G, Bossa F & Pascarella S (2002) Comparative structural analysis of psychrophilic and meso- and thermophilic enzymes. Proteins 47:236-249

Holm L & Rosenström P (2010) Dali server: conservation mapping in 3D. Nucleic Acids Res 38:W545-549.

Jeon JH, Kim JT, Kang SG, Lee JH, Kim SJ (2009) Characterization and its potential application of two esterases derived from the arctic sediment metagenome. Mar Biotechnol (NY) 11:307–316

Ji Q, Xiao S, He B, Liu X (2010) Purification and characterization of an organic solvent tolerant lipase from *Pseudomonas aeruginosa* LX1 and its application for biodiesel production. J Mol Catal B-Enzym 66:264-269

Joseph B, Ramteke PW, Thomas G (2008) Cold active microbial lipases: some hot issues and recent developments. Biotechnol Adv 26:457-470

Kim YO, Heo YL, Nam BH, Kim DG, Jee YJ, Lee SJ, An CM (2013) Molecular cloning, purification and characterization of a cold-adapted esterase from *Photobacterium* sp. MA1-3. Fish Aquat Sci 16:311-318

Kim JT, Kang SG, Woo JH, Lee JH, Jeong BC, Kim SJ (2006) Screening and its potential application of lipolytic activity from a marine environment: characterization of a novel esterase from *Yarrowia lipolytica* CL180. Appl Microbiol Biotechnol 74:820-828

Krissinel E & Henrick K (2007) Inference of macromolecular assemblies from crystalline state. Journal of molecular biology 372:774-797

Kulakova L, Galkin A, Nakayama T, Nishino T, Esaki N (2004) Cold-active esterase from *Psychrobacter* sp. Ant300: gene cloning, characterization, and the effects of Gly-->Pro substitution near the active site on its catalytic activity and stability. Biochimica et Biophysica acta 1696: 59-65

Lee C, Kim J, Hong S, Goo B, Lee S, Jang SH (2013) Cloning, expression and characterization of a recombinant esterase from cold-adapted Pseudomonas mandelii. Appl Biochem Biotechnol 169:29-40

Leiros HK S, Willassen NP & Smalås AO (2000) Structural comparison of psychrophilic and mesophilic trypsins. Elucidating the molecular basis of cold-adaptation. Eur. J. Biochem. 267:1039-1049

Leiros HK S, Willassen NP & Smalås AO (1999) Residue determinants and sequence analysis of cold-adapted trypsins. Extremophiles 3:205-219

Li C, Wen A, Shen B, Lu J, Huang Y, Chang Y (2011) FastCloning: a highly simplified, purification-free, sequence- and ligation-independent PCR cloning method. BMC Biotechnology, 11:92

Lonhienne T, Gerday C, Feller G (2000) Psychrophilic enzymes: revisiting the thermodynamic parameters of activation may explain local flexibility. Biochimica et Biophysica Acta (BBA) - Protein Structure and Molecular Enzymology 1543:1-10

Lv XY, Guo LZ, Song L, Fu Q, Zhao K, Li AX, Luo XL, Lu WD (2010) Purification and characterization of a novel extracellular carboxylesterase from moderately halophilic bacterium *Thalassobacillus* sp. Strain DF-E4. Ann Microbiol 61:281-290

Madern D, Ebel C, Zaccai G (2000) Halophilic adaptation of enzymes. Extremophiles 2:91-98

McDonald IK & Thornton JM (1994) Satisfying hydrogen bonding potential in proteins. J Mol Biol 238:777-793

McCoy AJ, Grosse-Kunstleve RW, Adams PD, Winn MD, Storoni LC & Read RJ (2007) Phaser crystallographic software. J Appl Crystallogr 40:658-674

Mohamed YM, Ghazy MA, Sayed A, Ouf A, El-Dorry H, Siam R (2013) Isolation and characterization of a heavy metal-ressitant, thermophilic esterase from a Red Sea Brine Pool. Scientific Reports 3:3358

Nam KH, Kim MY, Kim SJ, Priyadarshi A, Lee WH & Hwang KY (2009) Structural and functional analysis of a novel Est5 belonging to the subfamily of hormone-sensitive lipase. Biochem Bioph Res Co 379:553-556

Ogino H, Ishikawa H (2001) Enzymes which are stable in the presence of organic solvents. J Biosci Bioeng 91:109-116

Ollis DL, Cheah E, Cygler M, Dijkstra B, Frolow F, Franken SM, Harel M, Remington SJ, Silman I, Schrag J & Sussman JL (1992) The alpha/beta hydrolase fold. Protein engineering 5:197-211

Palm GJ, Fernandez-Alvaro E, Bogdanovic X, Bartsch S, Sczodrok J, Singh RK, Bottcher D, Atomi H, Bornscheuer UT & Hinrichs W (2011) The crystal structure of an esterase from the hyperthermophilic microorganism Pyrobaculum calidifontis VA1 explains its enantioselectivity. Appl Microbiol Biot 91:1061-1072

Pérez D, Kovacic F, Wilhelm S, Jaeger KE, Garcia MT, Ventosa A, Mellado E (2012) Identification of amino acids involved in the hydrolitic activity of lipase LipBL from *Marinobacter lipolyticus*. Microbiology 158:2192-2203

Rao L, Zhao X, Pan F, Li Y, Xue Y, Ma Y, Lu JR (2009) Solution behavior and activity of a halophilic esterase under high salt concentration. PloS ONE 4: 1-10

Rutherford K, Parkhill J, Crook J, Horsnell T, Rice P, Rajandream MA, Barrell B (2000) Artemis: Sequence visualization and annotation. Bioinformatics 16:944-945

Santarossa G, Lafranconi PG, Alquati C, DeGioia L, Alberghina L, Fantucci P & Lotti M (2005). Mutations in the "lid" region affect chain length specificity and thermostability of a *Pseudomonas fragi* lipase. FEBS letters 579:2383-2386

Siddiqui KS, Cavicchioli R (2006) Cold-adapted enzymes. Annual review of biochemistry 75:403-433

Smalås AO, Leiros HK S, Os V & Willassen NP (2000) Cold adapted enzymes. Biotechnol. Annu. Rev. 6:1-57

Thomas T & Cavicchioli R (1998) Archaeal cold-adapted proteins: structural and evolutionary analysis of the elongation factor 2 proteins from psychrophilic, mesophilic and thermophilic methanogens. FEBS Lett 439:281-286

Uchiyama T, Miyazaki K (2009) Functional metagenomics for enzyme discovery: challenges to efficient screening. Curr Opin Biotechnol 20:616-622

Uppenberg J, Hansen MT, Patkar S & Jones TA (1994) The sequence, crystal structure determination and refinement of two crystal forms of lipase B from *Candida antarctica*. Structure 2:293-308

Wu G, Wu G, Zhan T, Shao Z, Liu Z (2013) Characterization of a cold-Adapted and salt-tolerant esterase from a psychrotrophic bacterium *Psychrobacter pacificensis*. Extremophiles 17:809-819

Zhang T, Han WJ (2009) Gene cloning and characterization of a novel esterase from activated sludge metagenome. Microb. Cell Fact. 8:18

Figure legends

Fig 1. **a)** SDS-PAGE analysis of the purified esterase from *Thalassospira*. Lane 1, Opti-Protein XL protein molecular mass marker; Lane 2, the purified esterase. ThaEst2349. **b)** Crystals of ThaLip2349 resulting from a hanging drop experiment.

Fig 2. Characterization of the esterase ThaEst2349. **a)** Effect of pH on esterase activity. **b)** Effect of temperatures on esterase activity. **c)** The residual activity of ThaEst2349 studied over the range 10-50°C using *p*-NP acetate as substrate. **d)** The effect of organic solvents on ThaEst2349 activity**.**

Fig 3. The ThaLip2349 structure. **a)** Ribbon diagram of one ThaLip2349 dimer composed of Chain A (dark red) and Chinn B (Sand), and **b)** only one monomer (Chain A) with the proposed cap domain in green and methionine residues in black (carbon) and yellow (sulfur). **c)** The active site residues Ser185, His285 and Asp255, the oxyanion hole composed by Gly87 N and Ala86 N. **d)** The dimer interface of Chain A (dark red) and Chain B (Sand) with hydrogen bonds (red lines) and ionic interactions (black line). **e)** A modeled inhibitor 1-hexadecanesulfonyl (pink from AcEst2; PDB 1QZ3) in ThaLip2349, was found to fit into a water exposed channels that lead into the active site, and the channel entrance is lined by Asp286, Trp206 and Met90.

Fig 4. Sequence alignment and secondary structure elements of ThaLip2349 (top), StoEst and PcEstE (bottom). The figure was created by EsPript (http://espript.ibc).

Figure/Table legends

Table 1. Substrate specificities of the purified esterase. Esterase activities were measured toward various p-nitrophenyl esters in presence of Tris-HCl 0.1 M pH 8.5.

	Kinetic parameters		
Substrate	**k_{cat} (s^{-1})**	**K_M ($M \cdot 10^{-3}$)**	**$s = k_{cat} / K_M$ ($sec^{-1} \cdot M^{-1} \cdot 10^3$)**
***p*NP-acetate**	**47.7±4.4**	**0.94±0.15**	**50.6±13.3**
***p*NP-butanoate**	**5.0±0.4**	**4.9±0.8**	**1.0±0.2**
***p*NP-pentanoate**	**3.38±0.2**	**1.4±0.2**	**2.4±0.6**

Table 2. Effect of various metals on esterase activity.

	1mM compound	10mM compound
	Relative activity %	**Relative activity %**
Control	100.0 ± 0.009	100.0 ± 0.009
$CuCl_2$	108.7 ± 0.015	147.6 ± 0.018
$CrCl_2$	130.2 ± 0.188	0
$MgCl_2$	73.4 ± 0.082	82.4 ± 0.024
$MnCl_2$	97.2 ± 0.010	61.1 ± 0.007
KCl	85.9 ± 0.040	89.7 ± 0.029
$CaCl_2$	126.3 ± 0.196	150.2 ± 0.217
$NiCl_2$	88.4 ± 0.003	82.8 ± 0.034
$FeCl_2$	47.9 ± 0.010	0
$CdCl_2$	76.5 ± 0.010	42.1± 0.10
$HgCl_2$	100.9 ± 0.052	15.2 ± 0.004
$ZnCl_2$	50.3 ± 0.027	17.0 ± 0.001
$SnCl_2$	129.0 ± 0.126	133.2 ± 0.024
LiCl	172.6 ± 0.143	140.1 ± 0.163
CsCl	93.4 ± 0.012	101.0 ± 0.101
$CoCl_2$	159.8 ± 0.143	54.3 ± 0.046

Table 3. Effect of **a)** various detergents and **b)** additives on esterase activity.

a)

	0.1% reagent	1% reagent
	Relative activity %	**Relative activity %**
Control	100.0 ± 0.009	100.0 ± 0.009
TRITON X	56.5 ± 0.039	61.4 ± 0.012
CTAB	11.5 ± 0.014	101.4 ± 0.000
Tween 80	84.3 ± 0.031	61.8 ± 0.047
Tween 20	62.7 ± 0.013	120.3 ± 0.019
SDS	1.7 ± 0.003	0

b)

	1mM reagent	10mM reagent
	Relative activity %	**Relative activity %**
β-mercaptoethanol	99.1 ± 0.058	90.8 ± 0.0001
EDTA	86.1 ± 0.019	94.9 ± 0.003
DTT	113.1 ± 0.011	257.2 ± 0.035
PMSF	109.2 ± 0.054	99.9 ± 0.006

Table 4. a) Effect of NaCl concentration on the ThaEst2349 activity. **b)** Activity profile of ThaEst2349 with NaCl. ThaEst2349 activity was evaluated after an incubation in presence of NaCl at 4 °C for 24 h.

a)

NaCl (M)	Relative activity %
0	100.0 ± 0.093
0.5	132.5 ± 0.092
1	156.5 ± 0.107
1.5	165.5 ± 0.107
2	213.9 ± 0.003
2.5	230.5 ± 0.023
3	283.1 ± 0.021
3.5	123.9 ± 0.051
4	40.9 ± 0.007

b)

NaCl (M)	Relative activity (%)
0	100.0 ± 0.036
1	284.6 ± 0.006
2	402.4 ± 0.012
2.5	453.6 ± 0.018
3	506.4 ± 0.015

Table 5. Activity profile of ThaEst2349 with organic solvents ThaEst2349 activity was evaluated after an incubation in presence of organic solvents at 4°C for 24h.

Solvents 10%	Residual activity (%)
Control	100.0 ± 0.003
Methanol	8.0 ± 0.0007
Acetone	42.9 ± 0.005
2-Propanol	27.6 ± 0.046
Butanol	41.9 ± 0.045
Ethanol	10.1 ± 0.0014
DMSO	108.7 ± 0.003
DMFA	34.0 ± 0.008
Glycerol	99.6 ± 0.016
Acetonitrile	35.9 ± 0.042
Dietilic ether	87.4± 0.035

Table 6. Statistics from the X-ray data collections and refinement of ThaEst2349. The numbers in parentheses represent values in the highest resolution shells.

X-ray statistics	**ThaEst2349**
PDB Entry	
Beamline	Bessy, BL14.2
Space group	$P2_12_12_1$
Unit cell (Å)	a=73.33, b=85.43, c=91.75
Resolution (Å) (highest bin)	25-1.69 (1.79-1.69)
Wavelength (Å)	0.91705
No of Unique reflections	61 330 (6 648)
Completeness (%)	93.4 (63.3)
Mean ($\langle I \rangle / \langle \sigma_I \rangle$)	13.6 (2.4)
R_{merge} (%)	9.9 (62.0)
Wilson B-factor (Å^2)	12.9
Refinement	
Resolution (Å)	25-1.69
R-factor (all reflections) (%)	14.26
R-free (%)	18.42
No of protein residues	630
No of water molecules / other solvent	926 HOH/ 3 Mg^{2+}
R.m.s.d. bond lengths (Å)	0.008
R.m.s.d. bond angles (°)	1.16
Average B-factor (Å^2) protein/solvent	10.0/23.2

Table 7. Dimer interface analysis performed by the PISA server (http://www.ebi.ac.uk/msd-srv/prot_int/).

	ThaEst2349	PcEstE	StoEst
PDB entry	#	3ZWQ	3AIL
Organism	Marine origin *Thalassospira*	Hyperthermophile *P. calidifon*	Archaeon *S. tokodaii*
Resolution (Å)	1.69	2.00	1.91
Observed T_m (°C)			86.6
Temperature optimum (°C)	45	90	70
% of Gly/Met/Pro in gene	8.0/1.6/6.4	7.3/1.9/6.4	8.3/0.3/5.0
No. of H-bonds per residue in [a]: **Chain A/B/C/D**	0.883/0.886/-/-	1.022/1.030/-/-	0.989/0.982/0.951/0.982
No. ion pairs per residue [a, b] **Chain A/B/C/D (< 4Å)**	0.054/0.054/-/-	0.086/0.085/-/-	0.081/0.074/0.081/0.071
Arg/(Lys+Arg)	0.65	0.38	0.67
No of di-sulfide bond **Chain A/B/C/D**	0/0/-/-	0/0/-/-	1/1/0/1
Dimer interface for chains:	AB	AB	AD
Buried intersubunit surface in Å^2 (% of dimer)	1 977 (8.9%)	2707 (11.9%)	1 993 (8.9%)
No. of H-bonds [b]	9	22	15
No. Salt bridges [c] / Ion pairs [b] (<4Å)	3/2	6/4	6/4

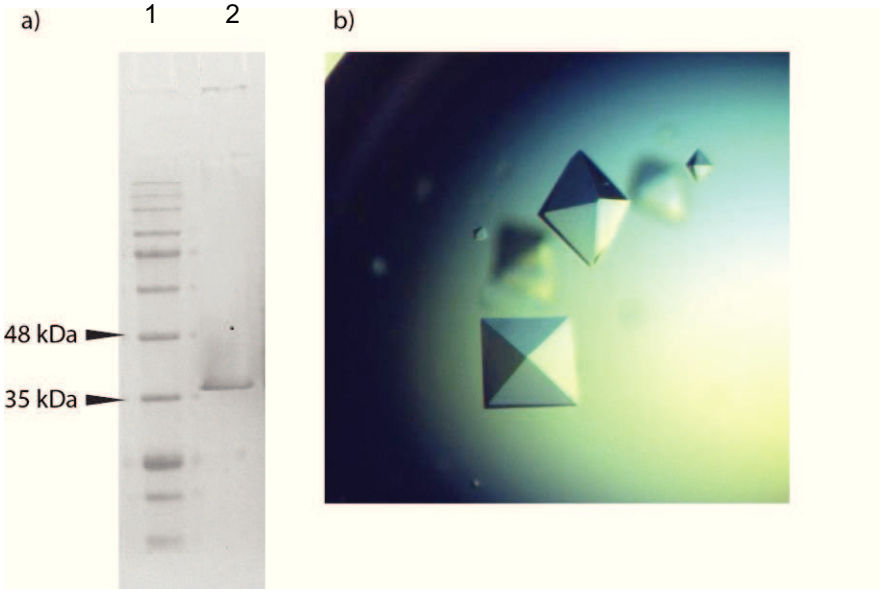

Fig 1. a) SDS-PAGE analysis of the purified esterase from *Thalassospira*. Lane 1, Opti-Protein XL protein molecular mass marker; Lane 2, the purified esterase. ThaEst2349. **b)** Crystals of ThaLip2349 resulting from a hanging drop experiment.

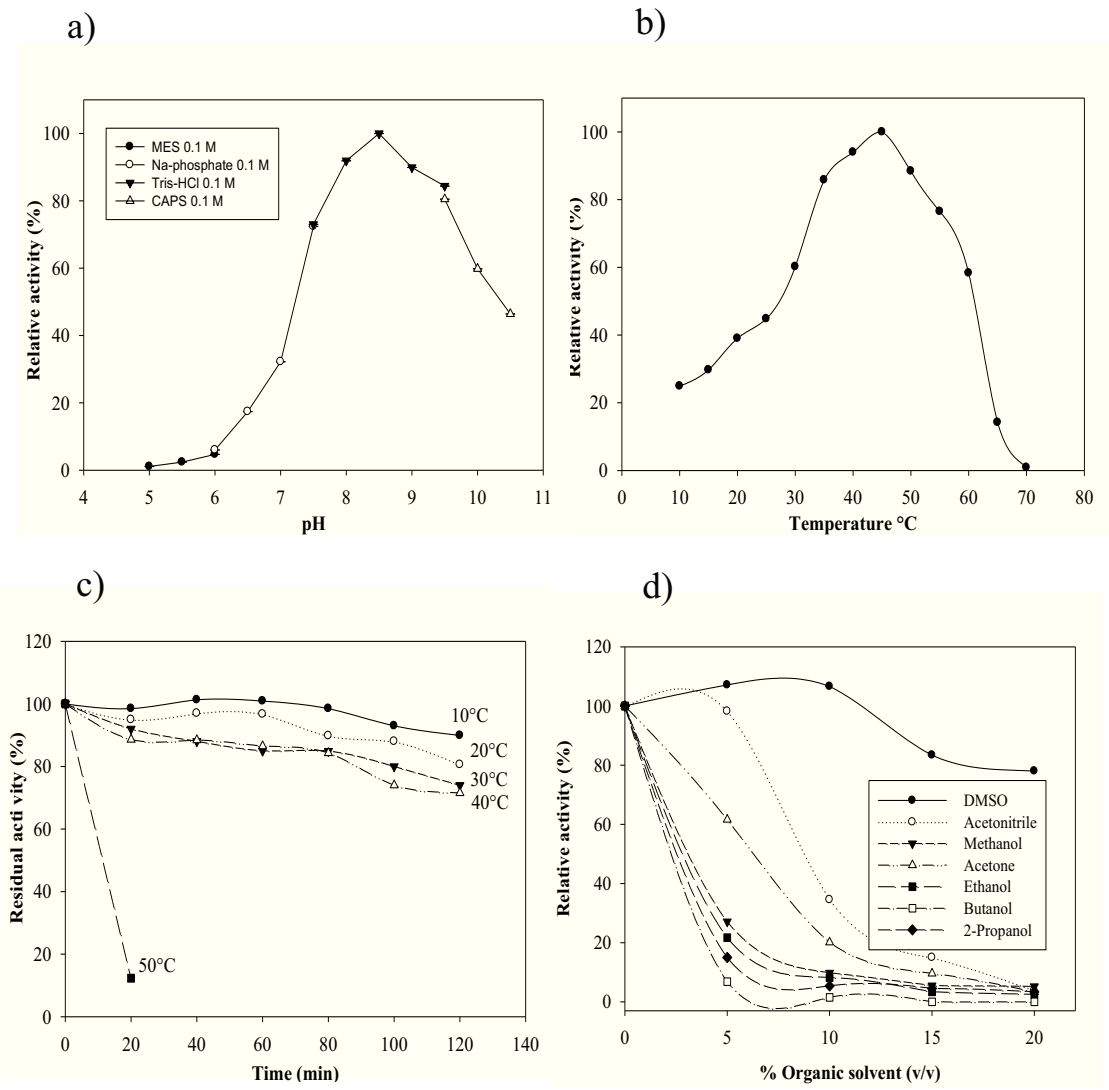

Fig 2. Characterization of the esterase ThaEst2349. **a)** Effect of pH on esterase activity. **b)** Effect of temperatures on esterase activity. **c)** the residual activity of ThaEst2349 studied over the range 10-50°C using *p*-NP acetate as substrate. **d)** The effect of organic solvents on ThaEst2349 activity**.**

Fig 3. The ThaLip2349 structure. **a)** Ribbon diagram of one ThaLip2349 dimer composed of Chain A (dark red) and Chinn B (Sand), and **b)** only one monomer (Chain A) with the proposed cap domain in green and methionine residues in black (carbon) and yellow (sulfur). **c)** The active site residues Ser185, His285 and Asp255, the oxyanion hole composed by Gly87 N and Ala86 N. **d)** The dimer interface of Chain A (dark red) and Chain B (Sand) with hydrogen bonds (red lines) and ionic interactions (black line). **e)** A modeled inhibitor 1-hexadecanesulfonyl (pink from AcEst2; PDB 1QZ3) in ThaLip2349, was found to fit into a water exposed channels that lead into the active site, and the channel entrance is lined by Asp286, Trp206 and Met90.

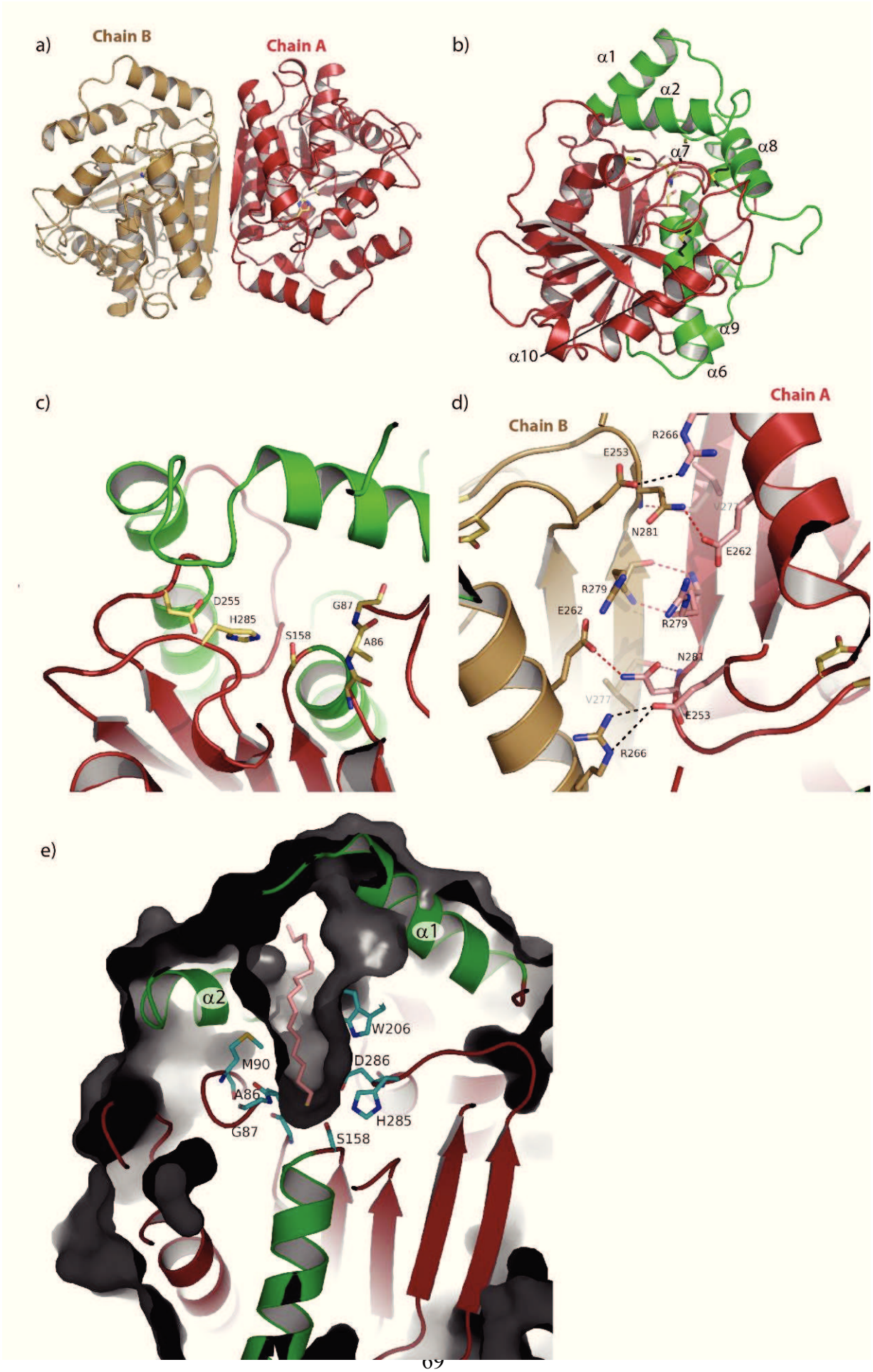
a)
Chain B
Chain A
b)
α1
α2
α7
α8
α9
α10
α6
c)
D255
H285
S158
G87
A86
d)
Chain B
Chain A
R266
E253
V277
N281
E262
R279
E262
R279
N281
V277
E253
R266
e)
α1
α2
W206
M90
D286
A86
H285
G87
S158

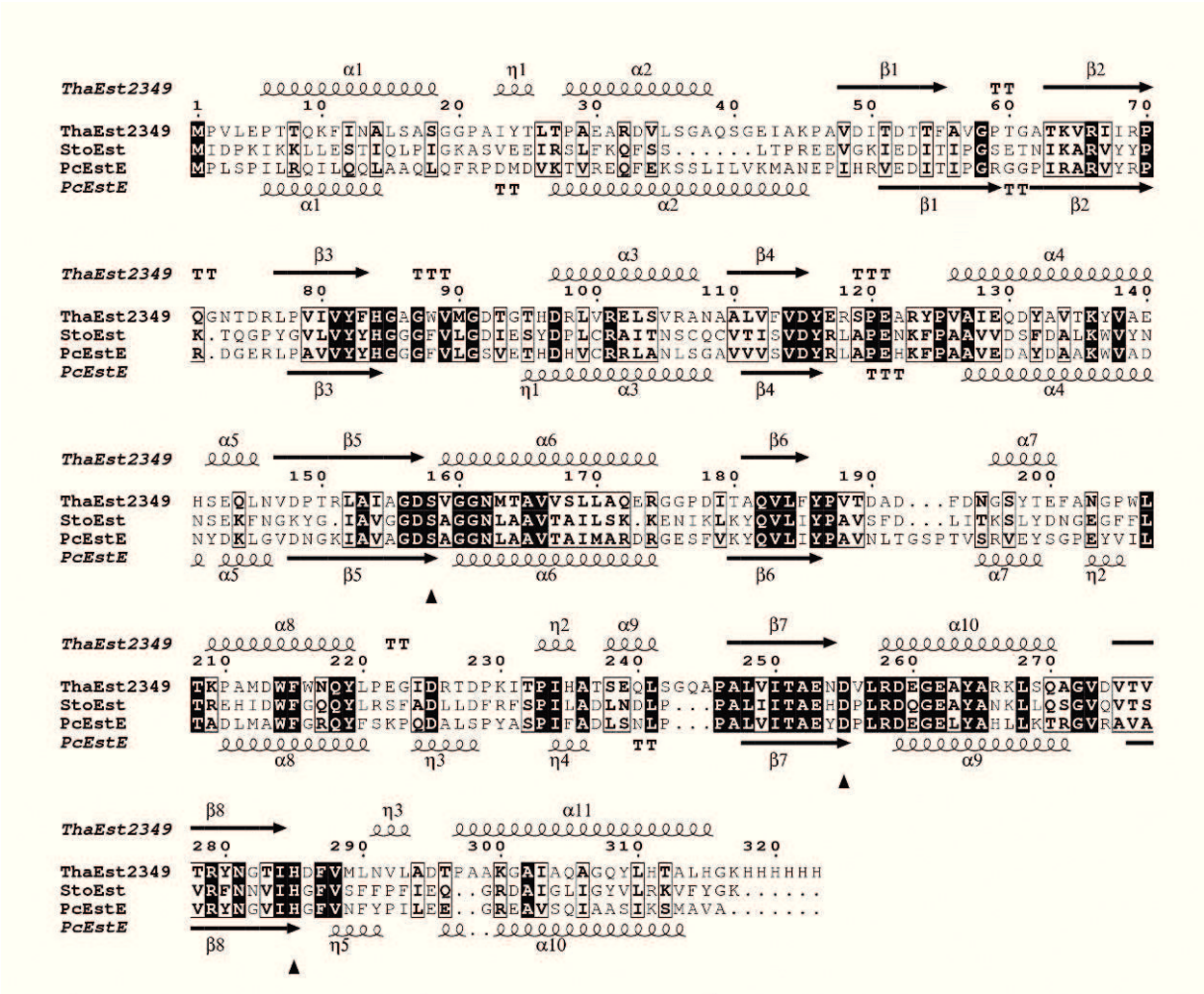

Fig 4. Sequence alignment and secondary structure elements of ThaLip2349 (top), StoEst and PcEstE (bottom). The figure was created by EsPript (http://espript.ibc).

Chapter 3

Identification of a new cold-active and salt tolerant esterase isolated by functional screening of Arctic metagenomic libraries

MANUSCRIPT TO BE SUBMITTED TO
APPLIED AND ENVIRONMENTAL MICROBIOLOGY

Identification of a new cold-active and salt tolerant esterase isolated by functional screening of Arctic metagenomic libraries

Concetta De Santi[1,2], Bjørn Altermark[2], Marcin Pierechod[2], Luca Ambrosino[1], Donatella de Pascale[1], Nils-Peder Willassen[2]*

1 Institute of Protein Biochemistry, National Research Council, Via P. Castellino, 111. I-80131, Naples, Italy
2 NorStruct, Department of Chemistry, Faculty of Science and Technology, UiT The Arctic University of Norway, 9037 Tromsø, Norway

*Authors to whom correspondence should be addressed;
E-Mail: nils-peder.willassen@uit.no (N-P.W.); Tel.: +47-77644651

Abstract
The use of metagenomics in enzyme discovery constitutes a powerful approach. A novel esterase gene (*lip3*) was identified by functional screening of three fosmid metagenomic libraries constructed from three marine sediment samples. The sequenced positive fosmid revealed an enzyme of 281 amino acids with similarity to class 3 lipases. The catalytic triad of Lip3 was predicted to be Asp207 and His267 and the catalytic nucleophile Ser150 in a conserved pentapeptide (GXSXG). The recombinant Lip3 esterase, expressed and purified from *Escherichia coli*, preferred to hydrolyze short and medium length *p*-nitrophenyl esters with the best substrate being *p*-nitrophenyl acetate. Further characterization revealed a temperature optimum of 35°C and a pH optimum of 8.0. Lip3 exhibits a broad temperature stability range and tolerates the presence of DTT, EDTA, PMSF, β-mercaptoethanol and high concentrations of salt. These features render this enzyme as a highly valuable candidate for biotechnological applications.

Keywords:
Metagenomics, functional screening, cold-active, esterase, biotechnological applications

3.1 Introduction
Extreme environments represent a great microbial resource of novel enzymes, most of which remains to be discovered.
Metagenomics, the technique to access the genome resource of non-cultivated microbes, is a powerful tool used in the discovery of novel industrial enzymes for biotechnological and pharmaceutical applications (1,2,3,4).
Since more than 99% of microorganisms cannot be cultivated (6), the possibilities of making new discoveries using metagenomics are huge.
Modern biotechnology has an emerging demand for new and better biocatalysts, which has driven the development of novel approaches to isolate biocatalyst from extreme environments. Metagenomics is an alternative approach to traditional microbial screening methods (7,8,9).
Based on the direct cloning of the metagenomic DNA (10) for the construction of large clone libraries, the above mentioned omic technique gives access to new

genes, complete pathways and their products by multiple screening methods. Even if there are several limitations in screening, such as the functional expression of genes in a heterologous, screening host, the metagenome-approach has led to the dicovery of many novel enzymes such as esterases (carboxyl ester hydrolases, EC 3.1.1.1) and lipases (triacylglycerol lipases, EC 3.1.1.3) (11,12). Lipolytic enzymes are found in all living organisms and most of the commercially produced enzymes originate from microbial sources. Lipolytic enzymes can be grouped into 8 different families based on their sequence, structure and biological function (13). All these enzymes families are characterized by a typical catalytic triad formed of a nucleophilic serine, a catalytic acid (aspartate or glutamate) and a histidine residue and located among a conserved Gly-Xaa-Ser-Xaa-Gly pentapeptide which forms a sharp elbow in the center of the α/β-fold (14).
True lipases are distinguished from esterases by having a lid domain that covers the hydrophobic catalytic cleft (15,16). This lid moves to expose the catalytic cleft at the lipid-water interface according to the activation mechanism typical of lipases. However, there are exceptions such as the studied *Candida antarctica* Lip B (17).
Until now, numerous novel lipolytic enzymes have been identified by functional metagenomic analysis of various microbial habitats, such as soil (18,19,20), hot springs (21), lake water (22) and marine sediments (23, 24).
In this study, we screened three small metagenomic libraries constructed from marine sediment samples in order to identify new esterases. After sequencing of a positive clone we found the gene responsible for the esterase activity seen on tributyrin plates. After recombinant expression in *E. coli*, the enzyme was characterized for its substrate specificity, optimal pH and temperature, thermal stability, and effect of different additives on the enzymatic activity. Moreover, homology modelling was performed to investigate structural features of the enzyme.

3.2 Materials and Methods

Sampling in the marine Arctic

During two research-cruises in the high Arctic on board R/V Helmer Hanssen, belonging to the University of Tromsø, Norway, samples of seawater, sediment and various biota were taken. For the sediment sampling a Van-Veen grab was used and two 50 ml tubes of the top 10 cm layer was filled at each sampling location and frozen first at -20°C and later at -80°C. Three of these sediment-samples, described in table 1, were used to extract total DNA. The first sampling was conducted in the Barents Sea area in May 2010 and the second around Svalbard in October 2011.

High molecular weight DNA extraction and purification

The frozen sediments were aliquoted using a solid mortar prechilled with liquid nitrogen. A soft lysis protocol (25) was followed with some modifications. Five grams of sediment was resuspended in 10mL of DNA extraction buffer and 100 µl of proteinase K (10 mg/ml) was added. Sample was incubated in a 56°C water bath for 2 h with an occasional, gentle mixing. Then, 1.5mL 20% SDS was added and samples were incubated at 60°C for another 2 h. After centrifugation at 5000 g for 20 min, the DNA-containing supernatant was extracted with phenol: chloroform: isoamyl alcohol mixture (25:24:1 volume ratio). Next, the aqueous phase was precipitated with isopropanol (0.7 volumes). The pellet was then washed with 70% EtOH, air-dried and dissolved in TE buffer (pH 8.0). At this stage the raw-DNA had a brown color, especially the DNA from the two clayish samples**.**

To purify the DNA further, two procedures were followed; for sediment sample nr. 1 an ion-exchange hydroxyapatite column was used. Dry HTP-hydroxyapatite (Bio-Rad, USA) was resuspended in TE-phosphate buffer (25mM Na-phosphate, pH 8.0), swirled and decanted 3 to 4 times to get rid of ultra-fine particles. Then, empty, hypodermic syringe plugged with wet glass wool was packed with medium by centrifugation. The maximum RCF used in all centrifugation steps was below 1000xg to prevent compression of the resin. Final volume of the resin was between 0.6 and 0.8ml. Column was than equilibrated with TE-phosphate buffer. DNA solution was loaded onto the column and washed with an increasing concentration of sodium phosphate in TE-phosphate buffer (25mM, 50mM, 100mM, 200mM Na-phosphate pH 8.0). DNA was then eluted with TE-phosphate buffer containing 300mM of Na-phosphate. Buffer exchange was performed by using Centricone 4ml spin cartridge with 100 kDa cut-off (Millipore, Germany). For sediment samples nr. 2 and 3 the Aurora DNA purifier from Boreal genomics, USA, utilizing the SCODA DNA extraction technology (26), was used. Raw DNA was diluted to 5ml in milliQ water and applied to the sample well of a precasted gel cassette (1% 0.25 X TBE agarose gel, and 0.25X TBE buffer). The run parameters were as stated in the AURORA_HMW_DNA_SOIL_PROTOCOL, provided by the manufacturer.
The purified metagenomic DNA was quality checked by performing standard PCR with Taq polymerase using universal primers (27F and 1492R) targeting the 16s rRNA gene.

Creation of fosmid library, storage of clones and functional screening
The purified DNA was used with the CopyControl Fosmid Library Production Kit with pCC1FOS Vector (Epicentre, USA) following the manufacturers protocol to obtain the three metagenomic fosmid libraries. Colonies were picked and grown in 400µl LB containing 12.5 µg/ml chloramphenicol and 10% glycerol using 1.2ml deepwell blocks (squared wells) and sealed with “breathable” film (BREATHseal, Greiner bio-one, USA). Incubation was done in a plate shaker at 37°C and 300rpm. Plates were afterwards re-sealed with alumina sealing film (alumaseal, Sigma-aldrich, USA) and a lid was put on before the plates were transferred to -80°C for storage.
For detecting the esterase activity, EPI300TM-T1R *Escherichia coli* fosmid clones were transferred to omni trays containing LB agar medium, 12.5 µg/ml chloramphenicol and 1% tributyrin as synthetic substrate. The replication of fosmid libraries was made by a 96 pin library copier (Thermo Scientific, USA). The appearance of a clear halo zone around colonies within 4 days at 20°C was considered a positive indication of esterase activity.

Fosmid purification and sequencing
The fosmid from the clone showing strongest esterase/lipase activity (evaluated by halo size) was included together with 167 randomly selected fosmids to be sequenced. Deepwell blocks (2.2ml square wells) containing 1.5ml of LB medium containing 12.5 µg/ml chloramphenicol supplemented with 1X autoinduction solution (Epicentre, USA) were inoculated with the 168 fosmid bearing clones. The plates were incubated with shaking at 37°C for 16hrs. The fosmid DNA were then purified using the Montage 96 well kit from Millipore following the vacuum suction protocol. The resulting fosmid DNA was resuspended in 100µl Tris buffer pH 8.0. The DNA concentration was measured using a Nanodrop Spectrophotometer at 260nm. The concentration of DNA in each well was then adjusted to 120ng/µl by adding more buffer. Pools of 7 X 24 fosmids were made by pipetting 4µl of each of the 24 fosmid

into 7 separate tubes. The pools of DNA was sent to the Norwegian Sequencing centre (NSC) in Oslo where 7 individually tagged libraries were made, pooled and sequenced on the 454 GS-FLX machine (Roche, USA) using one half of a picotiter plate. The remaining fosmid DNA in the 96 well plates was utilized in end-sequencing by the Sanger method using BigDye chemistry and the primers T7 or EpiFOSF (forward) and EpiFOSR (reverse). All sequencing was performed at the Norwegian Sequencing Centre (NSC) in Oslo.

Assembly and analysis of fosmid sequences

The sequence reads were screened for vector- and *E. coli* DNA and assembled using the Newbler Assembler software (454 Life Sciences), accessed remotely through the Bioportal in Oslo (now changed to Lifeportal, https://lifeportal.uio.no/). The 7 pools of sequences were separated according to their MID and assembled individually. The Sanger end-sequences were then used to distinguish what fosmid-clone the contigs in each pool originally came from. This was done by local nucleotide blast searches against the assembled fosmid DNA. The complete insert belonging to the fosmid-clone showing esterase activity was further annotated and analyzed online using GeneMark (http://opal.biology.gatech.edu/GeneMark/). The GC content profile of the fosmid-DNA was analyzed online using EMBOSS Isochore with default settings (http://www.ebi.ac.uk/Tools/seqstats/emboss_isochore/). The fosmid insert containing the *lip3* gene has been deposited in GenBank under accession number KJ538549.

Gene cloning strategy

The *Lip3* gene was amplified from purified fosmidic DNA by using a cloning method termed FastCloning (27). The following primer pairs were used to PCR amplify pET-26b vector and insert separately:
VecFw 5'-TGTCTTAAGAGCTTACTGCACCACCACCACCACCAC -3',
VecRv 5'-CTATCTATTATGTAATTATTCATATGTATATCTCCTTCTTAAAGTT-3',
InsertFw 5'-AACTTTAAGAAGGAGATATACATATGAATAATTACATAATAGATAG-3',
InsertRv 5'-GTGGTGGTGGTGGTGGTGCAGTAAGCTCTTAAGACA-3'. The expression vector encodes an in-frame C-terminal 6xHis-Tag.The PCR reaction conditions used were: 1 cycle (98°C for 3 min), 20 cycles (98°C 15 sec, 55°C 30 sec, and 72°C 1 min), and a final cycle at 72°C for C 10 min. PCR reactions were performed in a MJ Research PTC 200 thermal cycler (MJ Research, Canada). *Dpn*I (Sigma-Aldrich, USA) was added to the PCR insert- and vector product separately. Vector and insert were mixed at a 1:4 ratio and incubated for 2 h at 37°C. The mixture was then used to transform NovaBlue Giga Singles competent cells (Novagen, Germany). The DNA sequence of the resulting construct was verified by bidirectional DNA sequencing. The expression vector containing *lip3* was then transformed into *E.coli* BL21 (DE3) cells.

Recombinant production and purification of Lip3

E. coli BL21(DE3) cells carrying pET-26b-Lip3 vector were cultivated in Luria Broth (LB) medium with 50 *μ*g/mL kanamycin for 16 h at 37°C. To induce protein expression, overnight culture was diluted to an OD 600nm of 0.1 in 3-L shake flasks containing 600 ml LB medium and antibiotic (50 *μ*g/ml kanamycin). Culture was grown at 37°C with an agitation rate of 140 rpm until the OD 600 nm reached 0.6. IPTG was then added to a concentration of 0.2 mM to induce the expression. The culture was incubated further for 16 h at 20°C. Cells were then harvested by

centrifugation at 3,200x*g* at 4°C for 30 min and frozen at −20°C. The pellet was resuspended in 50 mM Tris-HCl pH 8.0, 500 mM NaCl and 10% glycerol, sonicated, and cleared by ultracentrifugation at 75,000 *g* for 40 min. The crude extract was filtered using a 0.45 µm membrane, and loaded on a HisTrap HP 1ml column (GE Healthcare, England) equilibrated with 50 mM Tris-HCl pH 8.0, 500 mM NaCl, 30 mM imidazole, 10% glycerol. Lip3 was eluted with a linear imidazole gradient (10 ml of 0–500 mM). Fractions of 1 mL were collected and analyzed by SDS-PAGE. Fractions containing the recombinant enzyme were dialyzed against 20 mM Tris-HCl pH 8.0, 10 mM NaCl and 5% glycerol.
The recombinant protein was further purified using a 1-ml HiTrap Q HP column (GE Healthcare, England) equilibrated with buffer A (20 mM Tris-HCl pH 8, 10 mM NaCl, 5% glycerol) and eluted with a linear gradient of 0–100% of buffer B (20 mM Tris-HCl pH 8, 1 M NaCl, 5% glycerol) at a flow rate of 1 ml/min. The proteins containing the esterase activity eluted at approximately 50% buffer B.

Analytical methods, determination of protein concentration
SDS-PAGE was performed using 5 % polyacrylamide-stacking gel and a 12 % polyacrylamide-resolving gel with a Bio-Rad Mini-Protean II cell unit, at room temperature essentially as described by Laemmli. ‘‘Opti-Protein XL protein molecular mass marker” (ABM, Canada) was used as molecular weight standard. The protein concentration was determined according to the Bradford method with bovine serum albumin as the standard (28). The protein content was measured by monitoring the optical density at 595 nm.

Lypolitic activity assays
The lipolytic activities of the purified enzyme was determined by measuring at 405 nm in 1-cm path-length cells with a Cary 100 spectrophotometer (Varian, Australia) equipped with a temperature controller. To check the linearity of the reaction, two different concentrations of enzyme were tested for each condition. Stock solutions of p-NP esters were prepared by dissolving the substrates in pure acetonitrile. Assays were performed in 1 mL mixture containing purified enzyme (2 µg/mL), 100 mM Tris-HCl buffer (pH 8.0), 3% acetonitrile and p-nitrophenyl (p-NP) esters at different concentrations.
One unit of esterase activity was defined as the amount of enzyme needed to release 1µmol p-nitrophenol in 1 min. All experiments were performed in triplicate. Results are expressed as mean values ± SE of the mean.

Substrate specificity and enzyme kinetics
The substrate specificity of the esterase was investigated. The enzyme activity was assayed at 450 nm at 35°C toward a variety of p-NP esters of various carbon chain lengths: pNP acetate (C2), pNP butanoate (C4), pNP pentanoate (C5), pNP octanoate (C8), pNP decanoate (C10). Assays were done in duplicate and the kinetic parameters were determined from the rates of hydrolysis by fitting the rates to a Lineweaver-Burk double reciprocal plot. All kinetic data were analyzed by linear regression using SigmaPlot 10.0.

Effects of pH and temperature on Lip3 activity
Esterase activity was measured at different pH values by using the buffers 0.1 M MES (pH 5.0-6.0), 0.1 M Na-phosphate (pH 6.0-7.5), 0.1 M Tris-HCl (pH 7.5-9.5) and 0.1 M CAPS (pH 9.5-10.5). The esterase activity was monitored by the amount of p-

nitrophenol released from p-nitrophenyl (pNP) esters at 348 nm, which is the pH-independent isosbestic wavelength of p-nitrophenoxide and p-nitrophenol. A molar extinction coefficient t of 5000 M^{-1} cm^{-1} at 25°C was used in the calculations.
The activity was expressed as percent relative activity with respect to maximum activity which was considered as 100%. Esterolytic activity, as a function of temperature, was determined in a temperature range of 10-65°C with 5°C increments at the optimum pH value in 0.1 M Tris-HCl (pH 8.0), containing 3 % acetonitrile, using p-NP pentanoate (100 µM) as substrate.

Thermal stability of the esterase
The thermostability of the enzyme was examined at temperatures ranging from 25°C to 70°C. The enzyme was incubated at different temperatures for a total time of 2 h, and the residual activity was measured at every 20-min intervals**.**

Effect of compounds and NaCl on enzyme activity
The effect of various compounds on esterase activity was tested by incubating the protein for 1 h at 4°C in presence of β-mercaptoethanol, EDTA, DTT and PMSF at final concentrations of 1 mM and 10 mM. The residual activities were measured by comparison with standard assay activity containing no compounds and defined as 100%.
The effect of NaCl on esterase activity was investigated by increasing the salt concentration in a range from 0-4 M at 35°C in standard assay conditions and also after incubation in presence of 0, 1, 2, 3 M NaCl for 24 h at 4°C.

Sequence Analysis
The identified sequence was investigated for protein similarity by searching the complete non-redundant protein databases (www.ncbi.nlm.nih.gov) using the BLAST software (29). A multiple sequence alignment was constructed using the JalView software (30). The N-terminal signal peptide prediction was made using SignalP 3.0 (http://www.cbs.dtu.dk/services/SignalP/). Molecular weights were determined using Protein Calculator V3.3 (http://www.scripps.edu/~cdputnam/protcalc.html).

Lip3 Modeling
Lip3 was modeled using 4 templates, obtained by scanning the Protein Data Bank database with the HHpred server (31): a triacylglycerol lipase from *Yarrowia lipolytica* (3O0D PDB entry), a lipase from *Gibberella zeae* (3NGM), a lipase from *Penicillium expansum* (3G7N) and a lipase from *Serratia marcescens* (2QUB). The atomic coordinates of the templates were obtained from the Protein Data Bank. In order to create the 3D-model, the multiple alignment between Lip3 and the sequences of the four templates, obtained in PIR format by HHpred server (31), was submitted to the comparative protein structure modeling software Modeller 9v11 (32). This software extracts information about spatial relationships between amino acids of the templates, and uses this information to create a mathematical function that describes the free energy of the protein. Modeller algorithm was set to generate fifty models. To select the best model, structure validation was carried out by PDBSum pictorial database. Models were uploaded, using standard PDB file format, on the PDBsum server, to carry out a full set of Procheck structural analyses (33) in order to evaluate the stereochemical quality of the generated structures. Moreover, Z-score of Lip3 model was calculated by the web server WhatIf (34). Z-score expresses how well the backbone conformations of all residues correspond to the known allowed

areas in the Ramachandran plot. Furthermore the Solvent Accessible Surface Area of Lip3 model was calculated by POPS algorithm (35). Finally the molecular graphics software VMD (36) was used to display the obtained model.

3.3 Results

Construction metagenomic libraries and screening for lipolytic enzymes

Three small fosmid libraries were created from marine sediment samples. The total number of fosmid clones and the number of positive hits in the screening are shown in table 1.

A total of 19 fosmid clones showed a clear halo zone indicative of putative lipolytic activity. The clone employing the largest halo size were sequenced and a gene encoding a putative class3 lipase was found. As shown in table 3, we could not detect any clear phylogenetic relatedness of the ORFs encoded by the fosmid. Each ORF is similar to a variety of unrelated bacteria and no phylogenetic marker gene is present. The presence of four transposase genes in the fosmid indicates that the region which is cloned comes from a region within the host DNA with rearrangements/insertions due to the transposases. The highly variable GC-content profile also supports this. An 843-bp ORF encoding a putative esterase/lipase (designated Lip3) was identified by GeneMark. The low sequence conservation, between Lip3 and the eight lipolytic families described by Arpigny (13), did not allow the construction of a meaningful phylogenetic tree for the full dataset. Anyway, a sequence analysis using the Pfam protein families identified a α/β-hydrolase family sequence (Pfam01764) belonging to class 3 lipase. The lipase consensus sequence (GHSLG) and the catalytic triad (serine, aspartate and histidine) are indicated (Fig. 9, 12). Lip3 contain no signal peptide as predicted by SignalP.

Expression and purification of recombinant Lip3

In order to study the biochemical properties of the enzyme, the *Lip3* gene was cloned into pET26b in frame with the C-terminal 6x His tag encoded by the vector.

High amounts of active protein was achieved when *E. coli* BL21 (DE3) was induced overnight with 0.2 mM IPTG at 20°C. The expressed protein was purified to homogeneity and a SDS-PAGE analysis showes that under denaturing condition the molecular weight (MW) is around 31.2 kDa (Fig. 3).

Effect of pH and temperature on enzyme activity and stability

The effect of pH on esterase activity was assessed at 25°C (Fig. 4) using p-NP-C5 as substrate. The enzyme in the pH range of 5.0–10.5 showed maximal activity at pH 8.0 in Tris-HCl buffer.

The effect of temperature on esterase activity was determined using *p*-NP-C5 as substrate. Lip3 was active over a temperature range from 7 to 65°C (Fig. 5), with an optimum temperature of 35°C. No catalytic activity was detectable at 70°C.

Lip3 hydrolysed *p*-NP esters with acyl-chain lengths from two to ten carbon atoms (C2–C10). All the characterization was performed at 35°C and in presence of 3% acetonitrile. In this condition, the enzyme displays highest activity towards *p*-NP acetate (Table 3) with a highest k_{cat} and k_{cat}/K_M value. The results indicated that the enzyme is an esterase and *p*-NP acetate was used as preferential substrate for further studies.

To examine the thermal stability of Lip3 esterase, we preincubated the enzyme at at different temperatures and measured the residual activity under standard assay conditions. The enzyme displayed a high thermal stability at 60°C. It lost only

approximately 20% of its activity, even after incubation for 120 min (Fig. 6). However, the stability of the enzyme decreased tremendously after 20 min at 70°C.

Lip3 activity in presence of compounds and NaCl

The enzyme was unaffected by the presence of low concentration β-mercaptoethanol and DTT. PMSF and EDTA seemed to reduce the enzyme activity at lower concentrations but not in a noticeably way. The corresponding relative activity decreased by half of its original value when the compound concentration was ten times more (Table 4).

Lip3 activity was evaluated in presence of NaCl under the above mentioned assay conditions in 0.1 M Tris-HCl pH 8.0. Results show (Table 5) the activation effect of Lip3 when NaCl was added in the assay mixture. The highest activity value was obtained with 3M NaCl.

To test the stability of the enzyme with NaCl we measured the relative activity after incubation for 24h at 4°C. The activity increased by a factor of about four in presence of 3M NaCl (Fig. 7) and a factor of about two in presence of 2M NaCl.

Analysis of the Lip3 sequence

A multiple sequence alignment consisting of Lip3 together with the most similar amino acid sequences is shown in Fig. 8. Similarities were found with lipases from *Vibrio scophthalmi* and *Vibrio ichthyoenteri*, hypothetical proteins from *Flexthrix Dorotheae* and *Pseudanabaena sp. PCC 6802*, and a putative lipase from *Vibrio nigripulcritudo*. These sequences had about 30% of identity and 50% of positive matches with Lip3 sequence. The alignment revealed that Lip3 contains the lipase-conserved catalytic triad residues, Asp207 and His267 and the catalytic nucleophile Ser150, in the typical consensus pentapeptide G-X-S-X-G, also known as “nucleophilic elbow”.

Lip3 modeling

The 3D-modeling of Lip3 was performed by homology modeling using as templates the structures of a triacylglycerol lipase from *Yarrowia lipolytica* (PDB ID: 3O0D), a lipase from *Gibberella zeae* (3NGM), a lipase from *Penicillium expansum* (3G7N) and a lipase from *Serratia marcescens* (2QUB). These structures were chosen because they showed a significant structural homology with Lip3, calculated by HHpred server, despite a low percentage of sequence identity. Starting from the alignment of Lip3 sequence with the reference structures, a set of 50 all atoms models was generated. The best model (Fig. 9) was selected in terms of energetic and stereochemical quality. In details, it has 86.3% of residues in most favored regions and no residues in disallowed regions of the Ramachandran plot according to PROCHECK program provided with PDBSum. Moreover this model has a WhatIf Z-score of -0.297, which is within expected ranges for well-refined structures. These values, compared with those of the template structures, indicated that a good quality model was created. The Lip3 model displayed an alpha-beta structure characterized by 9 alpha-helices (Fig. 10: H1-H6, H9, H10, H12), three 310-helices (Fig. 10: H7, H8, H11) and 11 beta-strands forming three sheets (Fig. 10: A-C), corresponding to 35%, 5.4% and 16.8% of sequence, respectively. Moreover Lip3 structure is stabilized by a disulfide bond (Cys179-Cys210). Finally, the SASA analysis of Lip3 model carried out by POPS algorithm revealed an exposed surface more hydrophobic than hydrophilic (59.6% versus 40.4%).

3.4 Discussion

In the current study we have identified a cold-active esterase (Lip3) originating from marine clay sediment as result of a functional screening of three small fosmid libraries. The choice of sampling area was based on the knowledge that marine habitats are really a vast resource of novel lipolytic genes because of the numerous microorganisms living there. Lipids from phytoplankton are one of the principal nutrition sources in marine food chains (37) and they can be removed from the surface layers by microbial activity when falling through the water column and lying on the benthos (38, 39). The number of positive clones for esterase activity is really high for sample number 1 (11 out of 384). We do not have an explanation for this, however the sample sites were not carefully inspected, and there are probably huge variations in what available nutrients exists at the respective sites. The occurrence of false positives is a well-known fenomenon when using tributyrin as substrate. As we did not sequence more of the positive fosmids, we can only speculate the reasons for this high hit-rate.

To address the biotechnological potential of Lip3 as a biocatalyst, we performed a biochemical and structural characterization. Lip3 showed activity at temperatures as low as 10°C and has an optimum temperature of 35°C, so it can be defined as a cold-active esterase. The highest relative activity was observed at pH 8.0 while a loss of activity at pH<7 (40). The activity value at alkaline pH can be explained by deprotonation of His267. The drop at alkaline pH could be due to protonation of Lys or Arg residues crucial for the enzyme integrity by being involved in salt bridges or in proximity to the active site.

The substrate specificity experiment revealed that the enzyme was an esterase with a preference for pNP esters of short- and medium chain fatty acids and could not hydrolyze substrates with long-chain fatty acids. In agreement with our results, another esterase from sea sediment metagenome was also found to have the highest hydrolytic activity with short- and middle- length *p*-NP esters (41). In addition, Lip3 activity was evaluated in the presence of DTT, EDTA, β-mercaptoethanol and PMSF, at low and high compounds concentration. An inhibitory effect was observed when high concentration of the compounds was added. The inhibition of esterase activity in the presence of EDTA can be attributed to its metal chelating effect.

The weak inhibition of esterase activity caused by PMSF may be attributed to the attack of Ser150 responsible for the hydrolytic reaction in the active site since this inhibitor interact selectively and irreversibly with the serine hydroxyl groups (42). The relatively low reactivity could be explained by the low stability of PMSF in the assay conditions. A hypthetical disulphide bond between Cys179 and Cys210 was seen in the model, and the high concentrations of DTT and β-mercaptoethanol probably reduce this bond, thereby lowering the enzyme activity. Being an intracellular enzyme, the disulphide bonds rarely forms due to the reducing environment. The surface exposure of the disulphide bond might be low, so that it is more shielded towards being naturally reduced.

Lip3 enzyme stability studies showed a quite stable behavior up to 60°C for 1 h and decreased at higher temperature while stability of published cold active lipase EstF, from deep-sea metagenomic library, was up to 50°C and a dramatic decrease thereafter (43).

The Lip 3 enzyme thus showing stability at moderate temperature can be used because of its high catalytic efficiency and specificity at low and moderate temperatures for biotechnological or industrial applications. These include their use as catalyst for organic synthesis of unstable compounds at low temperature (44).

Structural analysis was carried out and we focused our attention to the most conserved regions in the sequence alignment (Fig. 8). In Fig. 11, the catalytic triad of Lip3, formed by Ser150, Asp207 and His267, is highlighted in yellow. The three amino acids forming the catalytic triad seem to be located in three different loops connecting three strands to three helices. In particular Ser150 is within a conserved motif called “nucleophilic elbow”.
The solvent accessible surface area analysis suggests that this enzyme, thanks to its prevailing hydrophobic surface (59.6%), could be adapted to hydrophobic environments, such as organic solvents. In particular, the active site is covered by a mobile element, the lid, which opens when the enzyme binds a hydrophobic interface (45). The surface exposed to the active site of the lid is hydrophobic, whereas the surface exposed to the outside of the enzyme is hydrophilic (46, 47, 48). When the lid opens and exposes its hydrophobic surface, the SASA increases drastically (49). Depending on the structure of the lid, different transition mechanisms were proposed. In lipases with a simple one-helix lid, it’s assumed that the transition is a fast rigid body movement (50). In lipases with a more complex lid, instead, the secondary structure of this mobile element changes when it opens, undergoing a partial refolding (48) which might be a kinetic bottleneck (15). Lip3 seems to belong to the first category, having a single-helix lid (Fig. 9,11).
In summary, a novel cold-active esterase, Lip3, was isolated from a metagenomic library constructed from an Arctic marine sediment sample. Lip3 has high activity at low temperatures and in presence of high salt concentration. These are very useful characteristics for biotechnological processes. This study highlights the potential of metagenomic approach to discover and isolate, from extreme environments, novel biocatalysts for industrial applications.
Our esterase with its characteristics is a valuable contribution to the expanding enzymatic toolbox used by academia and the biotechnological industry.

3.5 References

1. **Schloss PD, Handelsman J.** 2003. Biotechnological prospects from metagenomics, Curr. Opin. Biotechnol. **14**:303–310.
2. **Lorenz P, Schleper C.** 2002. Metagenome—a challenging source of enzyme discovery, J. Mol. Catal. B: Enzymatic **19**:13–19.
3. **Streit WR, Daniel R, Jaeger KE.** 2004. Prospecting for biocatalysts and drugs in the genomes of non-cultured microorganisms, Curr. Opin. Biotechnol. **15**:285–290.
4. **Daniel R.** 2004. The soil metagenome—a rich resource for the discovery of novel natural products, Curr. Opin. Biotechnol. **15**:199–204.
5. **Alcade M, Ferrer M, Plou FJ, Ballesteros A.** 2006**.** Environmental biocatalysis: from remediation with enzymes to novel green processes. Trends in Biotechnology **24**:6.
6. **Handelsman J, Rondon MR, Brady SF, Clardy J, Goodman RM**. 1998. Molecular biological access to the chemistry of unknown soil microbes: a new frontier for natural products. Chem Biol. **5:**R245-R249.
7. **Daniel, R.** 2005. The metagenomics of soil. Nat. Rev. Microbiol. **3**:470–478.
8. **Lorenz P, Eck J.** 2005. Metagenomics and industrial applications. Nat. Rev. Microbiol. **3**:510.
9. **Streit WR, Schmitz RA.** 2004. Metagenomics-the key to the uncultured microbes. Curr. Opin. Microbiol. **7**:492–498.

10. **Handelsman J.** 2004. Metagenomics: application of genomics to uncultured microorganisms. Microbiol Mol Biol Rev. **68:**669-685.
11. **Jeon JH, Kim JT, Kim YJ, Kim HK, Lee HS, Kang SG, Kim SJ, Lee JH.** 2009. Cloning and characterization of a new cold-active lipase from a deep-sea sediment metagenome. Appl Microbiol Biotechnol. **81**:865-874.
12. **Glogauer A, Martini V, Faoro H, Couto G, Müller-Santos M, Monteiro R, Mitchell D, de Souza E, Pedrosa F, Krieger N**. 2011. Identification and characterization of a new true lipase isolated through metagenomic approach. Microbial Cell Factories. **10**:54.
13. **Arpigny JL, Jaeger KE**. Bacterial lipolytic enzymes: classification and properties. 1999. Biochem J. **343**:177–183.
14. **Brault G, Shareck F, Hurtubise Y, Lepine F, Doucet N**. 2012. Isolation and Characterization of EstC, a New Cold-Active Esterase from Streptomyces coelicolor A3(2). PLoS ONE **7**: e32041. doi:10.1371/journal.pone.0032041.
15. **Verger R**. 1997. Interfacial activation of lipases: facts and artifacts. Tibtech **15**: 32–38.
16. **Fojan P, Jonson PH, Petersen MT, Petersen SB**. 2000. What distinguishes an esterase from a lipase: a novel structural approach. Biochimie **82**:1033–1041.
17. **Uppenberg J, Hansen MT, Patkar S, Jones TA**. 1994. The sequence crystal structure determination and refinements of two crystal forms of lipase B of Candida antarctica. Structure **15**:293–308.
18. **Hu XP, Heath C, Taylor MP, Tuffin M, Cowan D**. 2012. A novel, extremely alkaliphilic and cold-active esterase from Antarctic desert soil. Extremophiles **16**:79-86.
19. **Berlemont R, Jacquin O, Delsaute M, La Salla M, Georis J, Verté F, Galleni M, Power P**. 2013. Novel Cold-Adapted Esterase MHlip from an Antarctic Soil Metagenome. Biology. **2**:177- 188.
20. **Wanga S, Wangb K, Lia L, Liua Y**. 2013. Isolation and characterization of novel organic solvent-tolerant and halotolerant esterase from a soil metagenomic library. Journal Molecular Catalysis B: Enzymatic. **95**:1–8.
21. **Tirawongsaroj P, Sriprang R, Harnpicharnchai P, Thongaram T, Champreda V, Tanapongpipat S, Pootanakit K, Eurwilaichitr L**. 2008. Novel thermophilic and thermostable lipolytic enzymes from a Thailand hot spring metagenomic library. J Biotechnol. **133**:42–49.
22. **Martínez-Martínez M, Alcaide M, Tchigvintsev A, Reva O, Polaina J, Bargiela R, Guazzaroni ME, Chicote A, Canet A, Valero F, Rico Eguizabal E, Guerrero Mdel C, Yakunin AF, Ferrer M.** 2013. Biochemical diversity of carboxyl esterases and lipases from Lake Arreo (Spain): a metagenomic approach. Appl Environ Microbiol. **79**:3553-3562.
23. **Xiawei J, Xiawei J, Xuewei X, Yingyi H, Yuehong W, Xufen Z, Xinqi Z, Min W**. 2012. Identification and characterization of novel esterases from a deep-sea sediment metagenome. Arch Microbiol. **194**:207–214.
24. **Zhu Y, Li J, Cai H, Ni H, Xiao A, Hou L.** 2013. Characterization of a new and thermostable esterase from a metagenomic library. Microbiol Res. **168**:589-597.
25. **Zhou J, Bruns MA, Tiedje JM**. 1996. DNA recovery from soils of diverse composition. Appl. Environ. Microbiol. **62**: 316-322.

26. **Pel J, Broemeling D, Mai L, Poon HL, Tropini G, Warren RL, Holtand RA, Marziali A.** Nonlinear electrophoretic response yields a unique parameter for separation of biomolecules. PNAS. vol. 106 no. 35.
27. **Li C, Wen A, Shen B, Lu J, Huang Y, Chang Y**. 2011. FastCloning: a highly simplified, purification-free, sequence- and ligation-independent PCR cloning method. BMC Biotechnology. **11**:92.
28. **Kruger NJ**. 1994. The Bradford method for protein quantitation. Methods in molecular biology **32**:9-15.
29. **Altschul SF, Gish W, Miller W, Myers EW, Lipman DJ.** 1990. Basic local alignment search tool. J Mol Biol. **215**:403-410.
30. **Waterhouse AM, Procter JB, Martin DMA, Clamp M, Barton GJ.** 2009. Jalview Version 2-a multiple sequence alignment editor and analysis workbench. Bioinformatics. **25**: 1189-1191.
31. **Soding J, Biegert A, Lupas AN.** 2005. The HHpred interactive server for protein homology detection and structure prediction. Nucleic Acids Res. **33**:W244-248.
32. **Sali A, Blundell TL.** 1993. Comparative protein modelling by satisfaction of spatial restraints. J. Mol. Biol. **234**:779-815.
33. **Laskowski RA, MacArthur MW, Moss DS, Thornton JM.** 1993. PROCHECK: a program to check the stereochemical quality of protein structures. J. Appl. Crystal. **26**: 283-291.
34. **Vriend G.** 1990. WHAT IF: A molecular modeling and drug design program. J. Mol. Graphics. **8**:52-56.
35. **Cavallo L, Kleinjung J, Fraternali F.** 2003. POPS: a fast algorithm for solvent accessible surface areas at atomic and residue level. Nucleic Acids Res. **31**:3364-3366.
36. **Humphrey W, Dalke A, Schulten K.** 1996. VMD: Visual molecular dynamics. J. Mol. Graphics. **14**:33-38.
37. **Bergé JP, Barnathan G**. 2005. Fatty acids from lipids of marine organisms: molecular biodiversity, roles as biomarkers, biologically active compounds, and economical aspects. Adv Biochem Engin Biotechnol. **96**:1–x.
38. **Kiriakoulakis K, Fisher E, Wolff GA, Freiwald A, Grehan A, Roberts JM. Freiwald A, Roberts JM**. 2005. Lipids and nitrogen isotopes of two deep-water corals from the North-East Atlantic: initial results and implications for their nutrition. Cold-water Corals and Ecosystems. Springer-Verlag Berlin Heidelberg, pp 715-729.
39. **Russell NJ, Nichols DS**. 1999. Polyunsaturated fatty acids in marine bacteria--a dogma rewritten.Microbiology. **145**: 767-79.
40. **Petersen MTN, Fojan P, Petersen SB.** 2001. How do lipases and esterases work: the electrostatic contribution. Journal of Biotechnology **85**: 115–147.
41. **Jiang X, Xu X, Huo Y, Wu Y, Zhu X, Zhang X, Wu M**. 2012. Identification and characterization of novel esterases from a deep-sea sediment metagenome. Arch Microbiol. **194**:207–214.
42. **Ghati A, Sarkar K, Pau G**. 2013. Production and characterization of an alkalothermostable, organic solvent tolerant and surfactant tolerant esterase produced by a thermophilic bacterium geobacillus sp. agp-04 isolated from bakreshwar hot spring, India. Journal of Microbiology, Biotechnology and Food Sciences. **3**:55-162.

43. **Fu C, Hu Y, Xie F, Guo H, Ashforth EJ, Polyak SW, Zhu B, Zhang L.** 2011. Molecular cloning and characterization of a new cold-active esterase from a deep-sea metagenomic library; Appl Microbiol Biotechnol. **90**:961–970.
44. **Joseph B, Ramteke PW, Thomas G, Shrivastava N**. 2007. Cold-active microbial Lipases: Aversatile tool for industrial applications. Biotech. Mol. Bio. Rev. **2**:39–48.
45. **Brady L, Brzozowski AM, Derewenda ZS, Dodson E, Dodson G, Tolley S, Turkenburg JP, Christiansen L, Huge-Jensen B, Norskov L.** 1990. A serine protease triad forms the catalytic center of a triacylglycerol lipase. Nature. **343**:767–770.
46. **Brzozowski AM, Savage H, Verma CS, Turkenburg JP, Lawson DM, Svendsen A, Patkar S.** 2000. Structural origins of the interfacial activation in *Thermomyces (Humicola) lanuginosa* lipase. Biochemistry. **39**:15071–15082.
47. **Brzozowski AM, Derewenda U, Derewenda ZS, Dodson GG, Lawson DM, Turkenburg JP, Bjorkling F, Huge-Jensen B, Patkar SA, Thim L.** 1991. A model for interfacial activation in lipases from the structure of a fungal lipase-inhibitor complex. Nature. **351**:491–494.
48. **Grochulskis P, Li Y, Schrags JD, Cygler M.** 1994. Two conformational states of *Candida rugosa* lipase. Protein Sci. **3**:82–91.
49. **Van Tilbeurgh H, Egloff M, Martinez C, Rugani N, Verger R, Cambillau C.** 1993. Interfacial activation of the lipase procolipase complex by mixed micelles revealed by x-ray crystallography. Nature. **362**:814–820.
50. **Peters GH, Toxvaerd S, Olsen OH, Svendsen A.** 1997. Computational studies of the activation of lipases and the effect of a hydrophobic environment. Protein Eng. **10**:137–147.
51. **Rehm S, Trodler P, Pleiss J.** 2010. Solvent-induced lid opening in lipases: A molecular dynamics study. Protein Sci. **19**:2122–2130.

Figure legends

Fig. 1. Arrangement of open reading frames (ORFs) encoded by the fosmid-insert. The Lip3 encoding gene is marked in red color.

Fig. 2. GC content profile of the lip3 fosmid-DNA.

Figure/Table legends

Table 1. Sample description, number of positive hits and total number of screened clones

Sample number	Grain size	Number of positive clones	Total number of screened clones
1. CTD241-86	Clay	11	384
2. CTD249-119	Clay	-	1000
3. HH596-1	Sand	8	2500

Table 2. Predicted function of the ORFs in the lip3-fosmid predicted by GeneMark. The GC content of each fosmid gene is compared with the GC content of the gene with best blast score.

ORF #	Putative function	Best hit (organism)	Acc. nr.	E-value
1	GMC oxidoreductase	Hyphomicrobium nitrativorans NL23	YP_008864948.1	5e-31
2	Transposase ISSpo9	Candidatus Entotheonella sp. TSY1	ETW96891.1	7e-35
3	IS5 family transposase	Octadecabacter arcticus 238	YP_007701055.1	9e-48
4	Acyl-CoA synthase	marine gamma proteobacterium HTCC2080	WP_007234422.1	8e-136
5	Unknown			
6	Transposase	Clostridium clariflavum DSM 19732	YP_005047631.1	1e-24
7	Type-1 restriction enzyme	Microcystis aeruginosa	WP_004268210.1	1e-10
8	Type-1 restriction enzyme	Methanosarcina barkeri str. Fusaro	YP_304562.1	4e-61
9	Unknown			
10	Unknown			
11	Unknown			
12	PBS lyase HEAT dom. containing protein	Leptolyngbya sp. PCC 7375	WP_006514873.1	5e-06
13	Unknown			
14	Unknown			
15	Dehydrogenase	Shewanella piezotolerans WP3	YP_002310053.1	2e-59
16	Radical SAM domain protein	Pedosphaera parvula	WP_007414050.1	1e-86
17	ATP-bind. protein of ABC transporter	Glaciecola nitratireducens FR1064	YP_004873353.1	1e-71
18	Unknown			
19	Transposase	Desulfobacterium autotrophicum HRM2	YP_002605365.1	4e-31
20	Serine/threonine protein kinase	Candidatus Solibacter usitatus Ellin6076	YP_826265.1	8e-07
21	Transposase, Mutator family protein	Mycobacterium avium MAV_061107_1842	ETZ43836.1	4e-14
22	Putative lipase, class 3	Vibrio nigripulchritudo	WP_022612571.1	3e-33
23	Dihydroorotate dehydrogenase	Pseudomonas sp. GM49	WP_007999884.1	2e-60
24	Hypothetical protein	Amorphus coralli	WP_018701069.1	1e-63

Table 3. Turnover rate, Michaelis constant and specificity constant for Lip3 using different p-nitrophenyl esters as substrate. Esterase activity was measured at 35°C in presence of Tris-HCl 0.1 M pH 8.0.

Substrate	k_{cat} (s^{-1})	K_M ($M \cdot 10^{-3}$)	$s = k_{cat} / K_M$ ($sec^{-1} \cdot M^{-1} \cdot 10^3$)
***p*NP-acetate**	**1198±200**	**2.38±0.56**	**503.3±214.5**
***p*NP-butanoate**	**218.0±15.5**	**1.05±0.16**	**206.5±48.6**
***p*NP-pentanoate**	**152.8±9.82**	**1.52±0.20**	**100.2±19.7**
***p*NP-octanoate**	**100.0±3.8**	**0.36±0.04**	**271.0±44.0**
***p*NP-decanoate**	**29.9±1.5**	**1.03±0.12**	**29.3±10.1**

Table 4. Esterase activities were measured toward various compounds at 35°C in presence of Tris-HCl 0.1 M pH 8.0.

	Relative activity %	
	Concentration 1mM	**Concentration 10mM**
Control	100± 0.007	100± 0.004
β-mercaptoethanol	96.0 ± 0.005	56.0 ± 0.002
EDTA	91.0 ± 0.001	78.7 ± 0.003
DTT	106.0 ± 0.021	59.0 ± 0.005
PMSF	77.0 ± 0.011	55.0 ± 0.004

Table 5. Effect of NaCl on Lip3 activity.

NaCl (M)	Relative activity (%)
0	100.0 ± 0.093
1	284.3± 0.107
2	334.3± 0.003
3	675.0± 0.021
4	528.0± 0.007

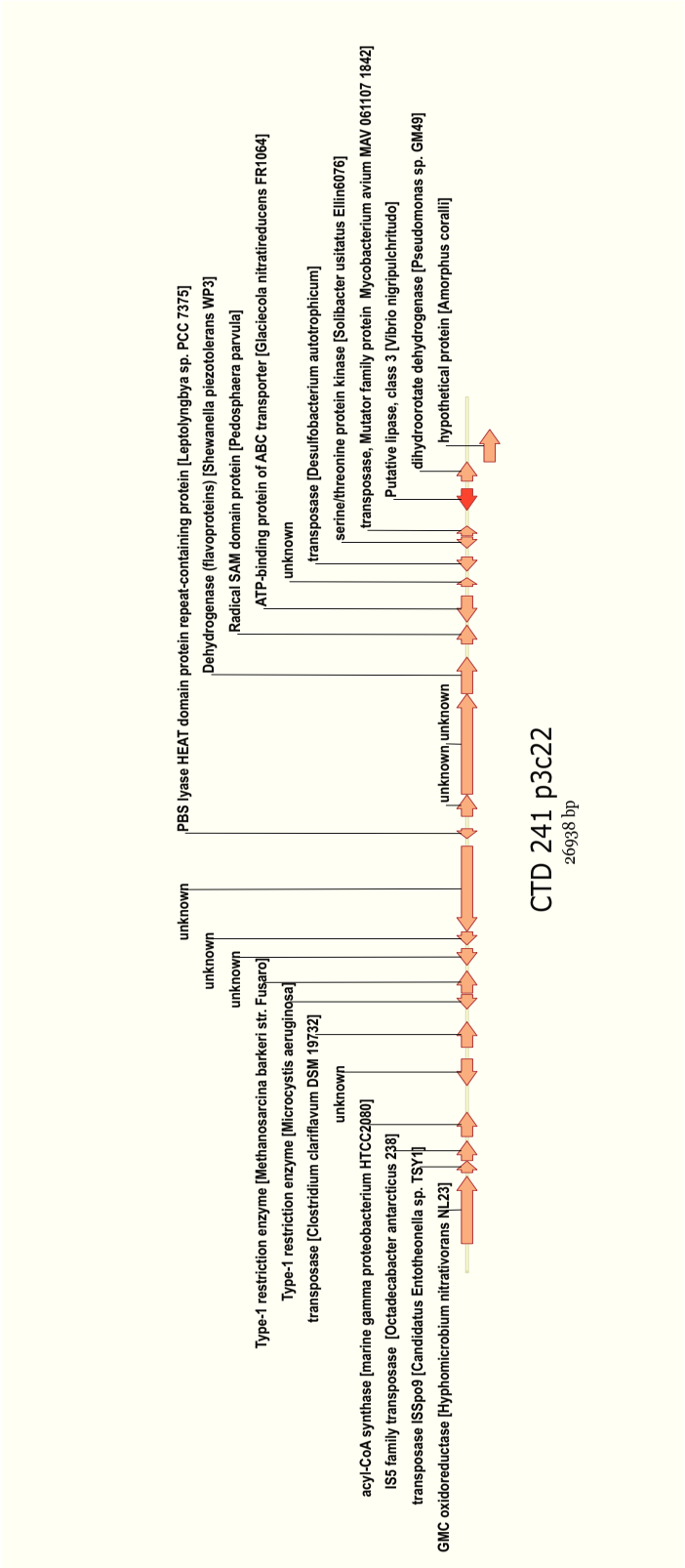

Fig. 1. Arrangement of open reading frames (ORFs) encoded by the fosmid-insert. The Lip3 encoding gene is marked in red color.

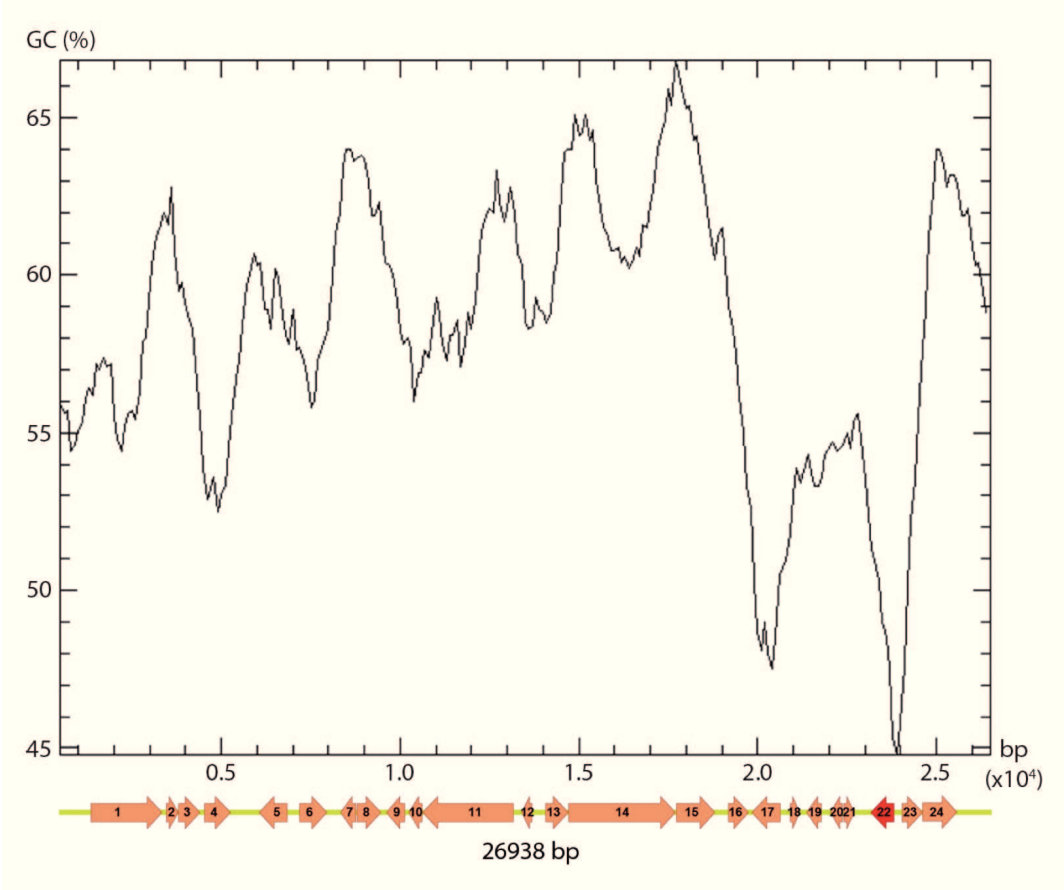

Fig. 2. GC content profile of the lip3 fosmid-DNA.

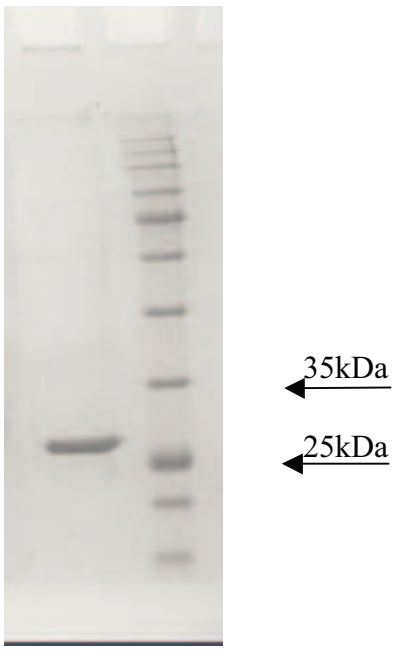

Fig 3. SDS-PAGE analysis of the purified recombinant esterase. Lane 1, purified esterase; Lane 2, Opti-Protein XL protein molecular mass marker.

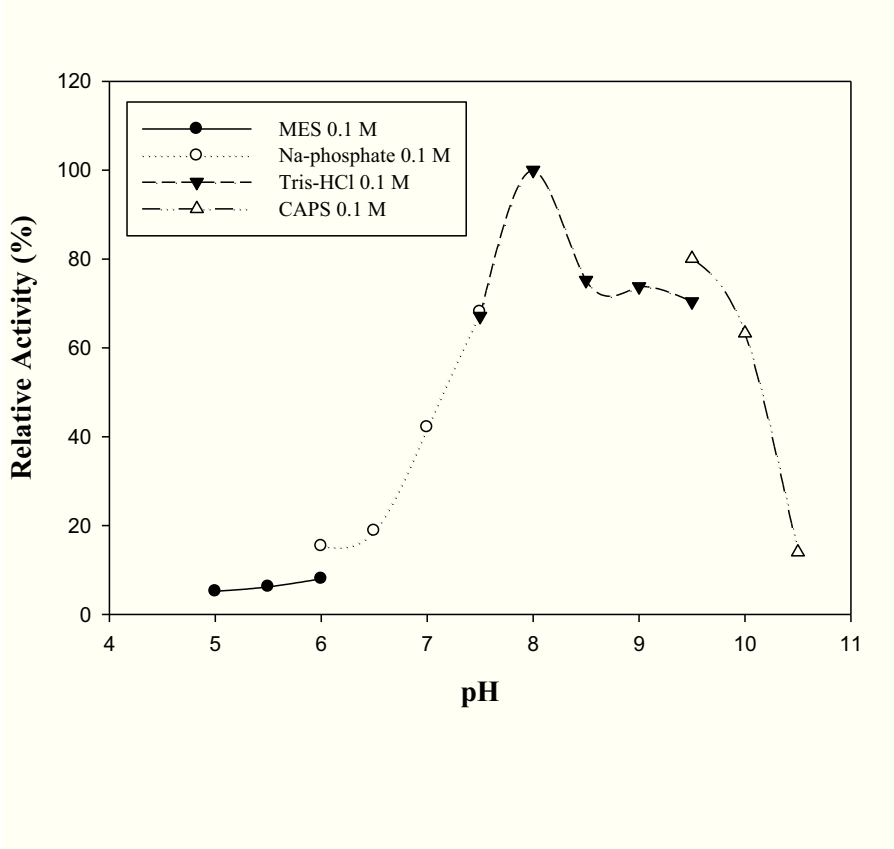

Fig 4. Effect of pH on esterase activity.

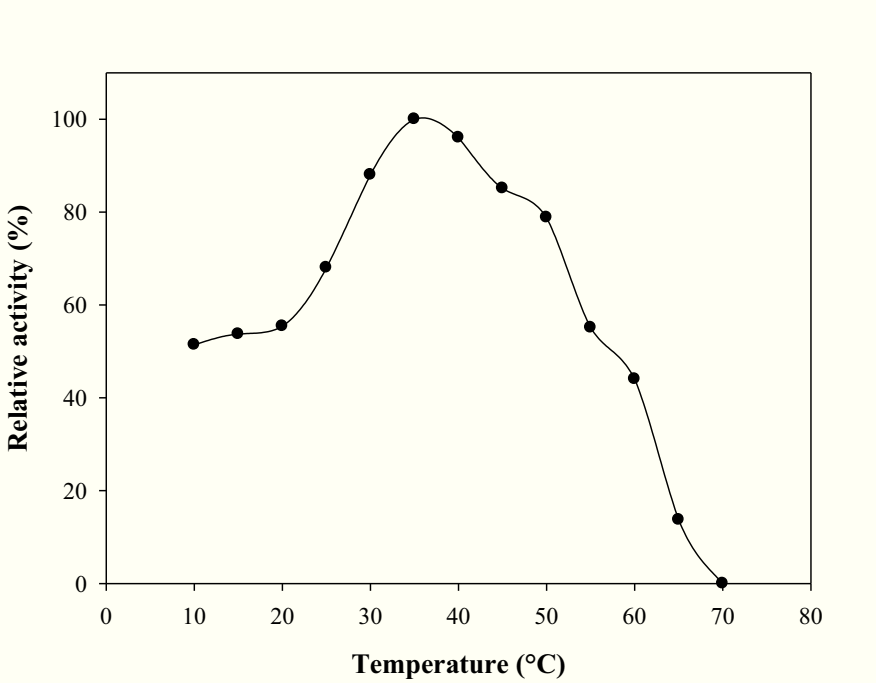

Fig 5. Effect of temperatures on esterase activity.

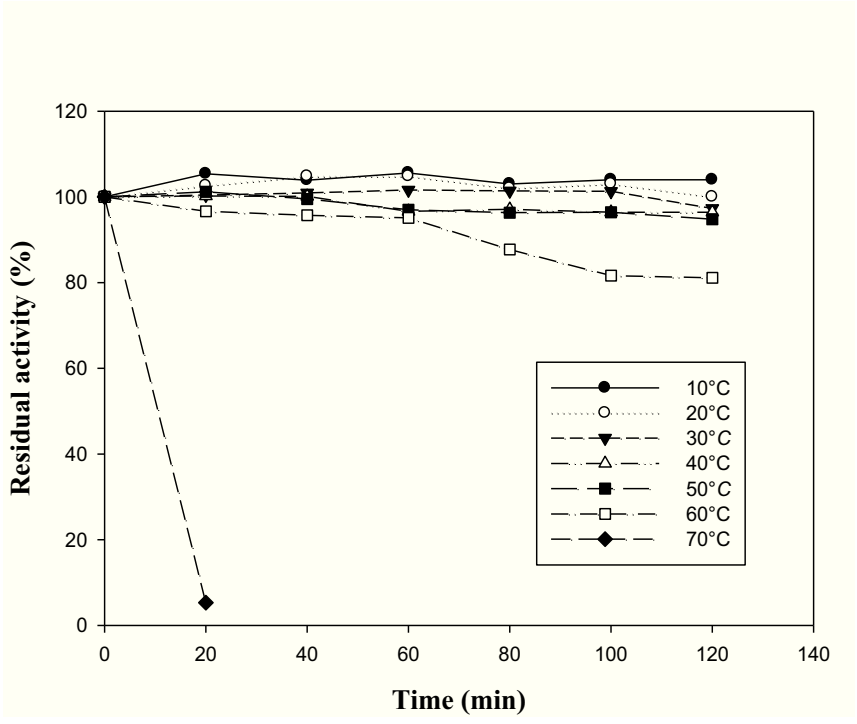

Fig 6. Thermal stability of Lip3 in the range from 10-70°C using *p*NP-acetate as substrate.

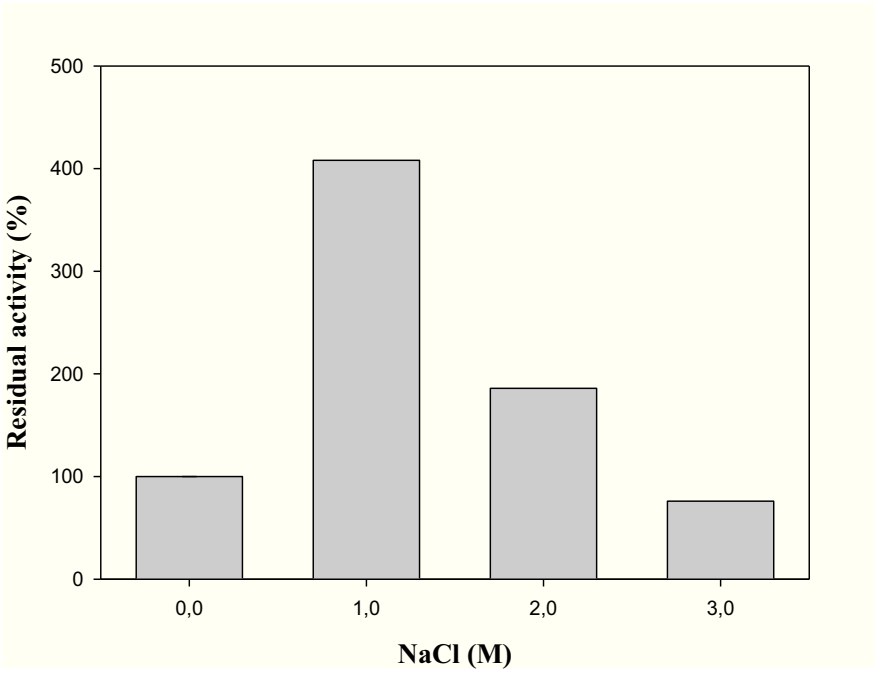

Fig 7. Bar Graph showing the stability profile of Lip3 with NaCl.
Lip3 activity was evaluated after preincubation in presence of NaCl at 4°C for 24h.

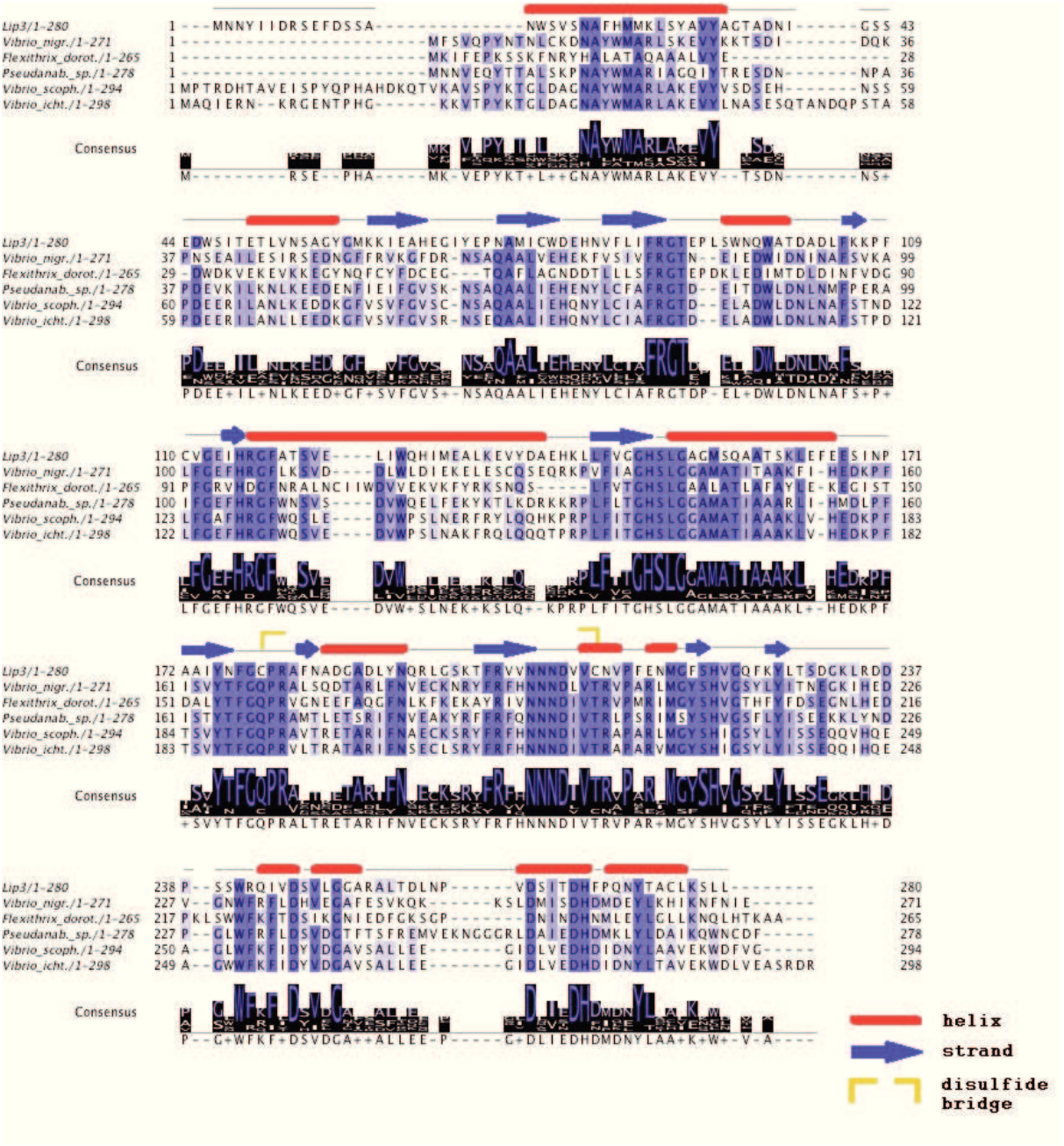

Fig 8. Multiple alignment of Lip3 and the most similar sequences found using BLASTp against the non-redundant protein database. The most conserved residues are shown in dark blue. The level of sequence identity, the quality of the alignment and the consensus histograms are also shown

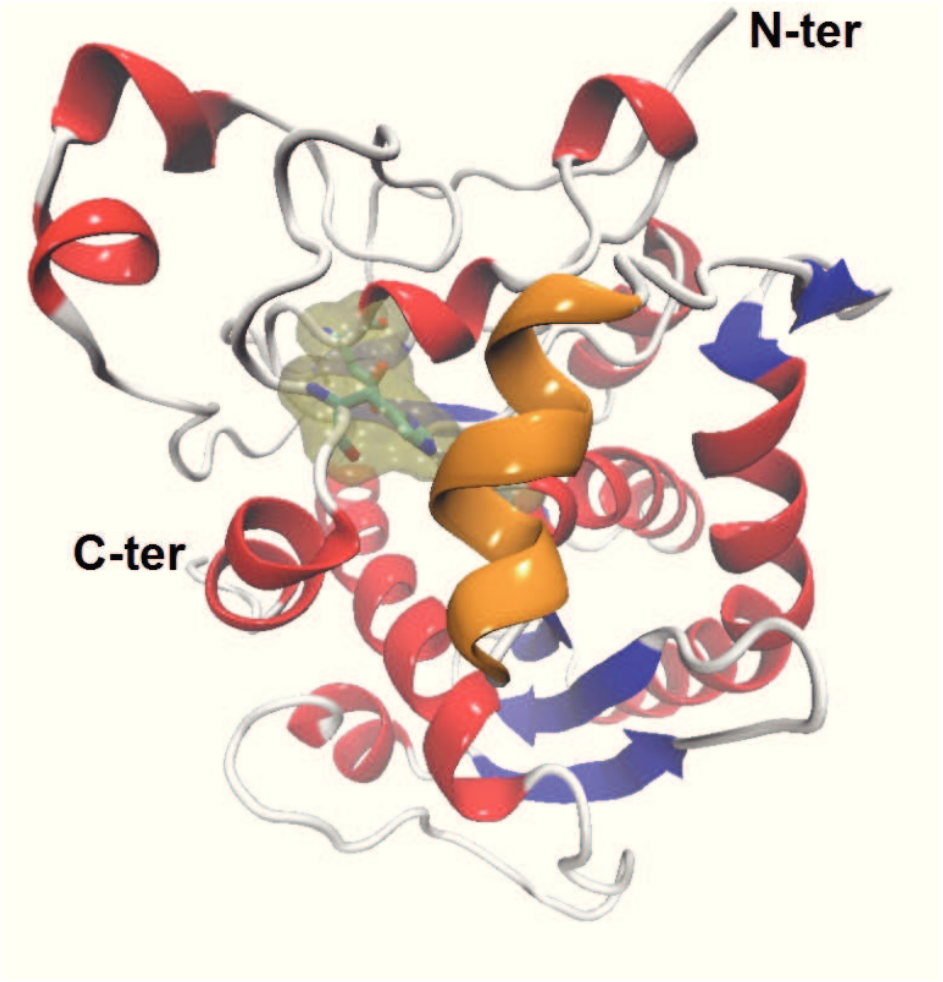

Fig 9. 3D-model of Lip3. Helices are shown in red. Strands are shown in blue. The one-helix lid is shown in orange. The catalytic triad is shown in yellow.

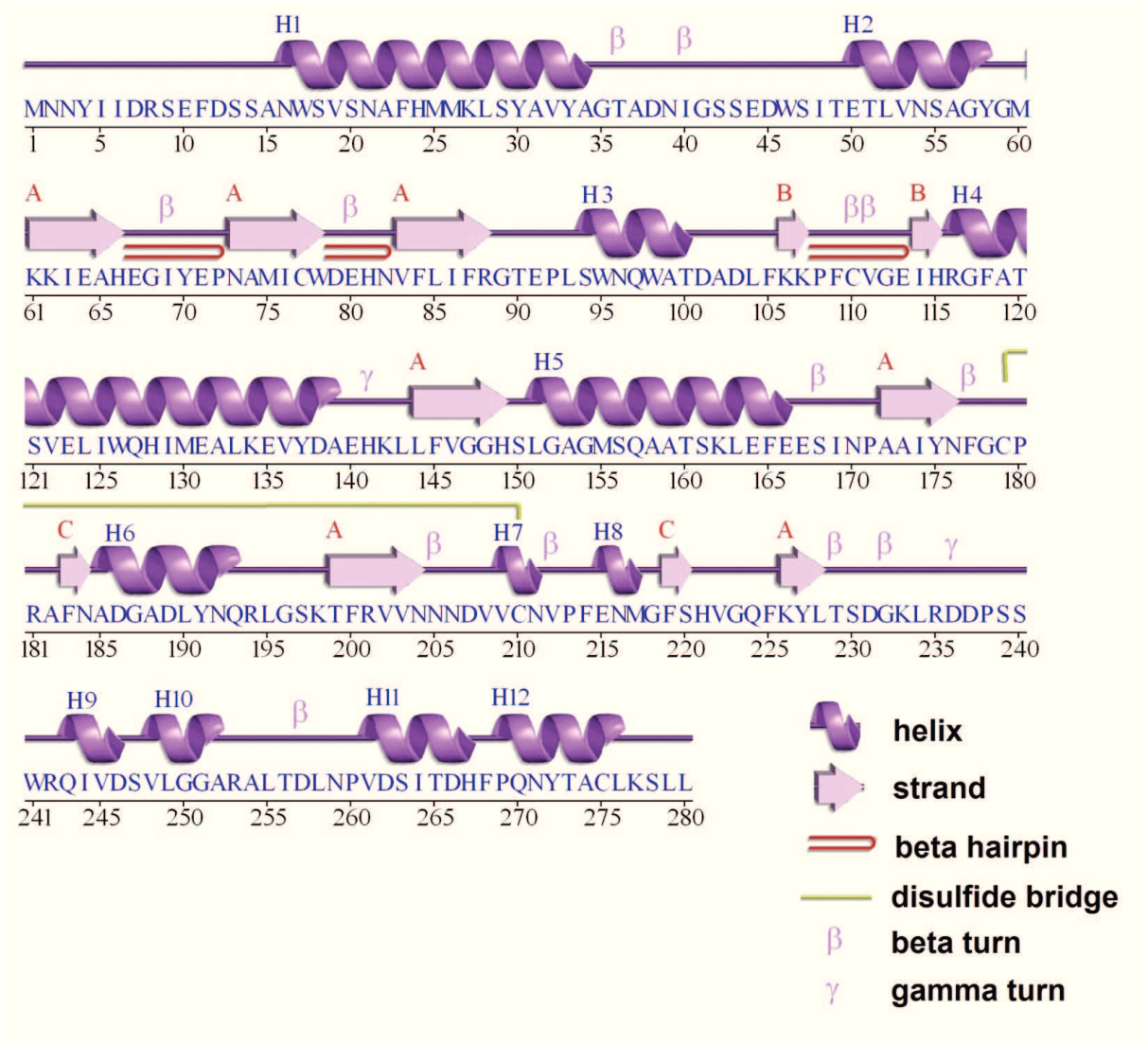

Fig 10. Secondary structure belonging to Lip3 model.

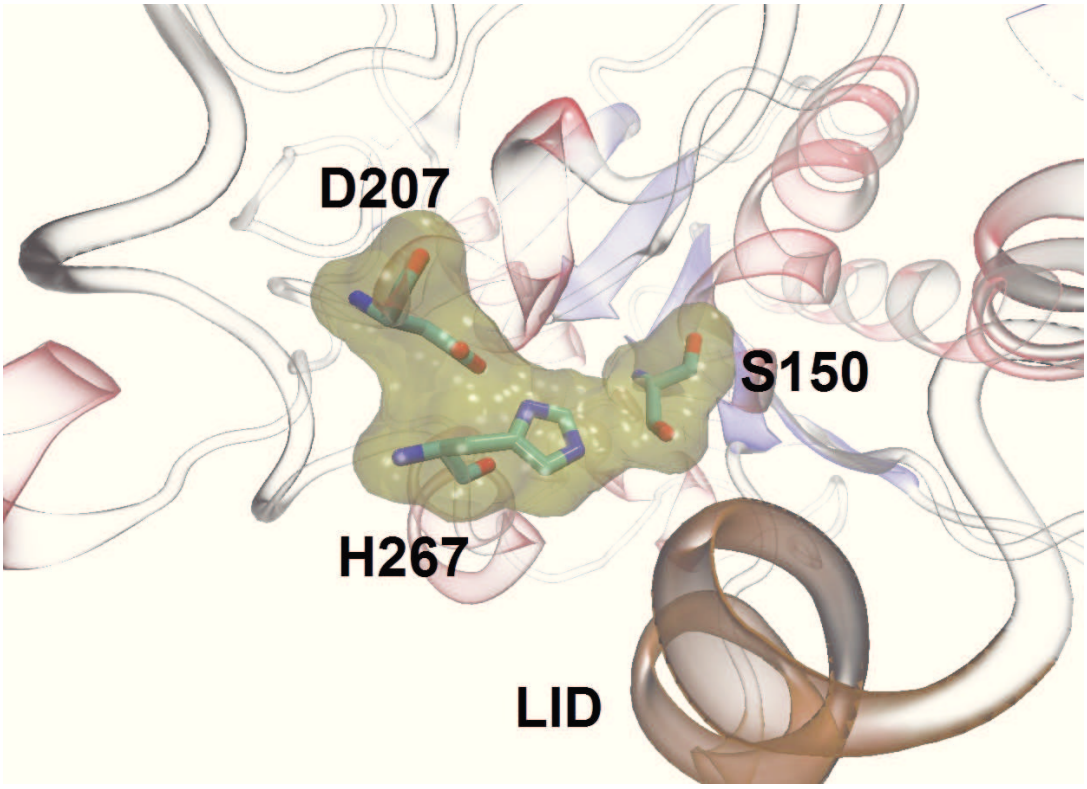

Fig 11. Close-up view of Lip3 catalytic triad. In yellow are shown the residues forming the catalytic triad. In orange is shown the one-helix lid.

PUBLICATIONS

• Ascione G, de Pascale D, **De Santi C**, Pedone C, Dathan NA, Monti SM (2012) Native expression and purification of hormone-sensitive lipase from Psychrobacter sp. TA144 enhances protein stability and activity. Biochem Biophys Res Commun. 420:542-6.
• Mandrich L, **De Santi C**, de Pascale D, Manco G (2012) Effect of low organic solvents concentration on the stability and catalytic activity of HSL-like carboxylesterases: Analysis from psychrophiles to (hyper) thermophiles. Journal of Molecular Catalysis B: Enzymatic. 82:46–52.
• **De Santi C**, Durante L, Vecchio PD, Tutino ML, Parrilli E, de Pascale D (2012) Thermal stabilization of psychrophilic enzymes: a case study of the cold-active hormone-sensitive lipase from Psychrobacter sp. TA144. Biotechnol Prog. 28:946-52.
• Buonocore F, Randelli E, Casani D, Picchietti S, Belardinelli MC, de Pascale D, **De Santi C**, Scapigliati G (2012) A piscidin-like antimicrobial peptide from the icefish Chionodraco hamatus (Perciformes: Channichthyidae): molecular characterization, localization and bactericidal activity. Fish Shellfish Immunol. 33:1183-91.
• de Pascale D, **De Santi C**, Fu J, Landfald B (2012) The microbial diversity of Polar environments is a fertile ground for bioprospecting. Mar. Genomics. 8:15-22.
• Yang G, **De Santi C**, de Pascale D, Pucciarelli S, Pucciarelli S, Miceli C (2013) Characterization of the first eukaryotic cold-adapted patatin-like phospholipase from the psychrophilic Euplotes focardii: Identification of putative determinants of thermal-adaptation by comparison with the homologous protein from the mesophilic Euplotes crassus. Biochimie. 95:1795-806.
• **De Santi C**, Tedesco P, Ambrosino L, Altermark B, Willassen NP, de Pascale D (2014) A New Alkaliphilic Cold-Active Esterase from the Psychrophilic Marine Bacterium Rhodococcus sp.: Functional and Structural Studies and Biotechnological Potential. Appl Biochem Biotechnol.
• Bjerga GEK, Hjerde E, **De Santi C**, Williamson AK, Smalås AO, Willassen NP, Altermark B (2014) High quality draft genome sequence of Streptomyces sp. strain AW19M42 isolated from a sea squirt in Northern Norway. Stand. Genomic Sci. 9:3.

Oral communications

• **C. De Santi,** D. de Pascale. Metagenomic approaches to cold environments: discovery of new extremozymes. Cortona Procarioti. Cortona, Italy, May 3-5th, 2012.

Poster communications:

• **C. De Santi**, B. Landfald, J. Fu, M.L. Tutino, E. Parrilli and D. de Pascale. Bioprospecting from Polar Marine Sediments. CAREX – Conference on life in Extreme Environments. Dublin, Ireland, 2011.
• G. Ascione, D. de Pascale, **C. De Santi**, C. Pedone, N.A. Dathan, S.M. Monti. Optimized expression of *Psychrobacter* sp. TA144 hormone-sensitive lipase and subsequent purification generates a stable, active protein. 13th Workshop on Bioactive Peptides - Cirpeb, Naples, 2012.

• L. Zhai, **C. De Santi**, P. Tedesco, Y. Xue, Z. Cheng, D. de Pascale. Exploring Tibetan glaciers: lipolytic enzymes from metagenomic libraries. Conference - Marine Microbiology & Biotechnology: Biodiscovery, Biodiversity and Bioremediation. Cork, Ireland, 2012,
• **C. De Santi**, P. Tedesco, B. Altermark, N.P. Willassen, D. de Pascale. Marine Biotechnology in the Arctic context: new hydrolytic enzymes for challenging reactions. Conference - Marine Microbiology & Biotechnology: Biodiscovery, Biodiversity and Bioremediation. Cork, Ireland, 2012.
• **C. De Santi**, B. Altermark, A.K. Williamson, D. de Pascale, N.P. Willassen. Bioprospecting around Arctic islands: marine bacteria as a rich source of biocatalysts and polyunsaturated fatty acids. Conference - Marine Bioprospecting from cold marine environment. Tromsø, Norway, 2013.
• A.K. Williamson, B. Altermark, M. Pierechod, G. Bjerga, H. Pedersen, **C. De Santi**, N.P. Willassen, A. Smalås. Hot investigations into cold-sourced enzymes". Conference: Marine Bioprospecting from cold marine environment. Tromsø, Norway, 2013.
• H. Pedersen, B. Altermark, E. Hjerde, A.K. Williamson, M. Pierechod, G.E.K. Bjerga, **C. De Santi**, N.P. Willassen, A. Smalås. Genome Sequencing of Bacteria Isolated from the Arctic Marine Environment. Conference: Marine Bioprospecting from cold marine environment. Tromsø, Norway, 2013.
• **C. De Santi**, B. Altermark, A.K. Williamson, D. de Pascale, N.P. Willassen. Bioprospecting around Arctic islands: marine bacteria as a rich source of biocatalysts and polyunsaturated fatty acids. Conference: SIMGBM. Ischia, Naples, 2013.

RESEARCH ACTIVITY IN FOREIGN LABORATORIES

• From September 1st 2011 to February 20th 2012 and from September 4th 2012 to March 3rd 2013 my research activity was carried out in Prof. Nils-Peder Willassen's laboratory at the University of Tromsø, Department of Chemistry, NorStruct, MabCent & SYSBIO, Norway.

Biochemical and Biophysical Research Communications 420 (2012) 542–546

Contents lists available at SciVerse ScienceDirect

Biochemical and Biophysical Research Communications

journal homepage: www.elsevier.com/locate/ybbrc

Native expression and purification of hormone-sensitive lipase from *Psychrobacter* sp. TA144 enhances protein stability and activity

Giuseppina Ascione [a], Donatella de Pascale [b], Concetta De Santi [b], Carlo Pedone [a], Nina Alayne Dathan [a,*], Simona Maria Monti [a]

[a] Institute of Biostructures and Bioimaging, National Research Council, Via Mezzocannone 16, I-80134 Naples, Italy
[b] Institute of Protein Biochemistry, National Research Council, Via Pietro Castellino 111, I-80131 Naples, Italy

ARTICLE INFO

Article history:
Received 21 February 2012
Available online 13 March 2012

Keywords:
Lipase
Psychrophile
Trehalose
Benzyl alcohol
Molecular chaperones
Protein stability

ABSTRACT

Psychrobacter, a micro-organism originally isolated from Antarctic sea water, expresses an extremely active hormone-sensitive lipase (HSL) which catalyzes the hydrolysis of fatty acid esters at very low temperature and is therefore of great potential industrial and pharmaceutical interest. An insoluble form of the entire enzyme has previously been cloned and expressed in *Escherichia coli*, subsequently refolded and shown to be active, whilst a shorter but completely inactive version, lacking the N-terminal 98 amino acids has been expressed in soluble form. In this study the entire enzyme has been expressed as a fully soluble protein in *E. coli* in the presence of either the osmolyte trehalose, plus high salt concentration, or the membrane fluidizer benzyl alcohol. Trehalose promotes protein mono-dispersion by increasing the viscosity of the growth medium for bacterial cells, thereby helping circumvent protein aggregation, whilst the heat-shock inducer benzyl alcohol stimulates the production of a network of endogenous chaperones which actively prevent protein misfolding, whilst also converting recombinant aggregates to native, correctly folded proteins. The resultant recombinant protein proved to be more stable than its previously expressed counterpart, as shown by CD and enzymatic activity data which proved the enzyme to be more active at a higher temperature than its refolded counterpart. By light scattering analysis it was shown that the newly expressed protein was monomeric. The stability of the full length native protein will help in understanding the structure of *Psy*HSL and the role of its regulatory N-terminal for eventual application in a myriad of biotechnological processes.

1. Introduction

Lipases play a crucial role in lipid metabolism, catalyzing the hydrolysis of acylglycerides and a range of other fatty acid esters [1]. They are produced by organisms in a wide range of environments and are fully functional, often in an extreme range of conditions [2,3]. Due to their catalytic activities and adaptable nature they are potentially extremely useful enzymes for an ever growing number of industrial and pharmaceutical applications [4–6]. Cold-active enzymes produced by micro-organisms often show high catalytic efficiency at low temperatures, frequently associated with low stability at moderate and high temperatures. The specific activity of psychrophylic enzymes is higher than that of their mesophylic homologues at 0–30 °C. Over the past decade, the attention of many researchers has been focused on the biotechnological applications of these enzymes [5], thanks to the numerous economical and ecological advantages of enzymes that operate at lower temperatures.

The bacterial species TA144 of *Psychrobacter* is a micro-organism which has been isolated from Antarctic sea water, where it efficiently catalyzes the hydrolysis of acylglycerides and other fatty acid esters in the process of degradation of organic matter via its highly active hormone-sensitive lipase [7]. Cold-adapted micro-organisms normally grow very slowly, but with the aid of genetic engineering it has become possible to clone their highly catalytic genes in host strains such as *Escherichia coli* as has been the case for the *lip2* gene, normally expressed in *Psychrobacter* sp. TA144, hereafter referred to as recombinant *Psy*HSL [8]. As with other members of the HSL family *Psy*HSL contains a highly conserved sequence of His-Gly-Gly-Gly upstream of the catalytic site, shown to be homologous to the corresponding region of human HSL, Gly-Asp-Ser-Ala-Gly [9]. In fact *Psy*HSL shows a surprising degree of homology around the catalytic domain, displaying 42% identity and 60% similarity over a span of 87 amino acids, this region being proposed to be a common feature in triacylglycerol lipases and esterases [10].

* Corresponding author. Fax: +39 0812534574.
E-mail address: nina.dathan@unina.it (N.A. Dathan).

0006-291X/$ - see front matter © 2012 Elsevier Inc. All rights reserved.
http://dx.doi.org/10.1016/j.bbrc.2012.03.028

PsyHSL has previously been expressed in the bacterial vector pET22b, but proved to be highly insoluble. It has however been successfully refolded and shown to be catalytically active, although this activity does not confirm the true nature of the enzyme; all attempts to crystallize the refolded protein have proved unsuccessful [8]. However a deleted version of *Psy*HSL, lacking the initial 98 residues has been expressed in fully soluble form but not extensively characterized since this deleted version was completely inactive [8]; suggesting that the N-terminal region of HSL, like its human counterpart, could be considered as a regulative domain of the protein, rendering the attainment of the soluble full length protein to be of considerable potential interest [9].

The aim of this study was to find suitable expression conditions in order to provide us with a high level of native, soluble and fully active protein for extensive biochemical characterization and, eventually, crystallographic studies. For this purpose *PsyHSL* was initially re-cloned in two simple 6×His-tag (N-terminal and C-terminal) modified pET vectors pETM11 and pETM13 (EMBL, Heidelberg) via PCR using specific oligonucleotide primers and their soluble expression levels were confronted with that obtained from pET22b. Further to altering growth conditions two additives were also used to encourage correct folding of the recombinant protein expressed in *E. coli*. These were benzyl alcohol, a membrane fluidizer [11] known to artificially cause a heat-shock response in the modified membrane of bacterial cells, causing severe stress and inducing the expression of the cells own chaperone network, as well as the osmolyte trehalose which exerts an anti-aggregation effect on proteins in the presence of high salt concentration thereby encouraging uptake of the osmolyte into individual bacterial cells [12]. The addition of these compounds proved to be decisive in procuring a high expression level of stable, soluble, full length recombinant protein.

2. Materials and methods

2.1. Materials

Oligonucleotide primers for PCR were purchased from PRIMM srl (Milan), DNA extraction and purification kits were from Qiagen (Germany), Phusion polymerase (Finnzymes, Milan), expression vectors pETM11 and pETM13 were kindly provided by the Protein Expression and Purification Core Facility, EMBL (Heidelberg), restriction enzymes were from New England Biolabs (Milan), anti-His-HRP conjugated mouse monoclonal IgG from Santa Cruz (USA), HisTrapHP and Superdex 200 columns from GE Healthcare (Milan), Bio-Sep SEC3000 from Phenomenex (Germany). Bacterial expression strains were from Novagen, whilst the cloning strain TOP10F' was from Invitrogen (Milan). Benzyl alcohol, trehalose and other chemicals were from Sigma–Aldrich (Milan).

2.1.1. Construction of pETM11-HSL and pETM13-HSL

HSL ([8] GenBank X53868.1) cDNA was PCR-amplified from pET22b-HSL with Phusion polymerase using the site-specific oligonucleotide primers: HSL-F CGCGCGCCATGGGCATGCCTATTCTACCAGTACCGGC with HSL-11R CGCGCGCTCGAGTTACTACGCTCTGAGATTTGGCTTATCAC and again HSL-F with HSL-13R CGCGCGCTCGAGCGCTCTGAGATTTGGCTTATCAC and inserted in the appropriately cut expression vectors pETM11 and pETM13 before being transformed in TOP10F'. The resulting plasmids were named 11-HSL and 13-HSL, whilst the original was known as 22-HSL.

2.1.2. Expression screening of recombinant clones

Expression of recombinant HSL was screened in strains: BL21(DE3), BL21(DE3)pLysS, Rosetta(DE3), Rosetta(DE3)pLysS and Rosettagami2(DE3), using various bacterial growth media. Cultures were induced in exponential phase for 16 h at 20 °C with 0.2 mM IPTG. All pellets were lysed in B-PER (Pierce, Milan) to obtain soluble and insoluble fractions and loaded on 12% SDS/PAGE. Expression was confirmed by Western Blot with anti-His-HRP conjugated antibody before scaling-up optimized conditions.

2.1.3. Purification of recombinant HSL

Expression was scaled up under sequentially optimized conditions to 400 ml cultures grown in 1.8 L baffled shake flasks, with vigorous shaking, inducing HSL expression 16 h at 20 °C with 0.2 mM IPTG, before harvesting 15 min at 3000*g*, 4 °C. One gram pellets were resuspended in 10 ml of: 50 mM Tris–HCl, 40 mM imidazole, 0.1% Tween 20, 30 mM $MgCl_2$, 5 mM DTT, 1 mM PMSF, 10 μg/ml lysozyme, 5 μg/ml DNaseI, pH 8.0. The lysate was adjusted to 500 mM NaCl and sonicated gently on ice. The soluble fraction was recovered by centrifugation and loaded on a 1 ml HisTrapHP column, connected to an FPLC ÄKTA system, in the presence of 50 mM Tris–HCl, 500 mM NaCl, 40 mM imidazole, 2 mM DTT, 100 μM PMSF, pH 8.0. Peak fractions eluted at 100 mM and 250 mM imidazole, concentrated on Amicon 10 kDa MWCO and loaded on Superdex 200, Superose 6 or Bio-Sep SEC 3000 columns in 50 mM Tris–HCl, 150 mM NaCl, 2 mM DTT, pH 8.0.

2.1.4. Enzymatic activity of 13-HSL

13-HSL was tested for esterase activity as previously described [8].

2.1.5. Optimization of expression for correct protein folding

Recombinant HSL underwent growth and expression in the presence of additives to optimize the level of correct protein folding in bacteria. Either trehalose or benzyl alcohol were added at the initiation of the exponential stage of bacterial growth at various concentrations. Growth was continued and 13-HSL expression induced with IPTG. Lysates from 2 ml cultures were prepared in B-PER and 100 μg from each soluble fraction was subjected to 2 h digestion at 25 °C in the presence of 5 ng trypsin to determine optimal additive concentration.

Once optimized, growth was scaled up to 400 ml cultures as above and followed either to OD_{600} = 0.2 at 37 °C, before adding 50 mM trehalose and 400 mM NaCl, switching to 20 °C for 45 min before adding 0.2 mM IPTG and expressing 24 h at 16 °C; or to OD_{600} = 0.4 at 37 °C, before adding 20 mM benzyl alcohol, switching to 20 °C for 20 min before adding 0.2 mM IPTG and expressing 24 h at 16 °C. Pelleted cells were resuspended and treated as before, although following HisTrap purification, concentrated samples were further purified directly on Bio-Sep SEC 3000. Using this new purification procedure the protein yield was 1.6 mg/g cells, while refolding from inclusion bodies yielded 20 mg/g cells.

2.1.6. Circular dichroism

All CD spectra were recorded with a Jasco J-715 spectropolarimeter equipped with a Peltier temperature control system [Model PTC-423-S]. Molar ellipticity per mean residue, $[\theta]$ in deg $cm^2 \times dmol^{-1}$, was calculated from the equation: $[\theta] = [\theta]_{obs} \times mrw/10 \times l \times C$, where $[\theta]_{obs}$ is the ellipticity measured in degrees, mrw is the mean residue molecular mass, *C* is the protein concentration in mg × mL^{-1}, and l is the optical path length of the cell in cm. Far-UV measurements (183–250 nm) were carried out at 20 °C, at time constant of 4 s, 2 nm band width, scan rate of 10 nm min^{-1}, using a 0.1 cm optical path length cell and a protein concentration of 0.2 mg × mL^{-1} in 6.6 mM buffer phosphate pH 8.0. CD spectra were signal averaged over at least three scans, and the baseline was corrected by subtracting a buffer spectrum. Thermal unfolding curves were determined by recording the molar ellipticity at 222 nm, using a scanning rate of 1 °C/min.

2.1.7. Light scattering

The oligomeric form of recombinant HSL was determined by combining size exclusion chromatography with Light Scattering equipment; experiments were run at 0.5 ml/min in 50 mM Tris, 150 mM NaCl, 2 mM DTT, pH 8.0 buffer using a Bio-Sep SEC 3000 size exclusion column (Phenomenex) connected to an FPLC ÄKTA purifier system which in turn was connected to a Refractive index (Shodex RI 101) followed by a Mini Dawn Treos (Wyatt Technology, USA) Light Scattering instrument. All data collected were interpreted with an ASTRA V software package.

3. Results

11-HSL and 13-HSL were obtained by cloning PCR-amplified HSL cDNA in NcoI/XhoI cleaved pETM11 and pETM13. Resulting clones were verified by bidirectional sequencing.

Initial levels of expression were confronted with that of the original clone in pET22b [8] in various bacterial expression strains, being induced 16 h at 20 °C with 0.2 mM IPTG. The presence of recombinant HSL was checked by SDS/PAGE. Levels of expression were so low that the HSL could only be detected by Western blotting with an anti-His-HRP conjugated antibody. Expression levels were observed to be clearly higher in pETM13, despite there being a minimal difference between this vector and the commercial pET22b vector using the codon-optimized strain Rosetta(DE3) so all further optimization was carried out using this combination of vector/strain. Expression was further optimized by using enriched TB growth media [13], obtaining a visible expression level on Coomassie Blue stained SDS/PAGE.

Purification of 13-HSL on 1 ml HisTrap revealed two species of the 48 kDa protein, being eluted at 100 mM and 250 mM imidazole (Fig. 1). Both species were initially loaded on a Superdex G200 or Superose 6 column. In both cases 13-HSL eluted with the front, suggesting that the protein was highly aggregated, despite being run in reducing conditions to eliminate any covalent interactions. Although *Psy*HSL contains eight cysteine residues they are all predicted to be reduced (re. DiANNA 1.1 web server) so any aggregation is likely due to remaining non-covalent interactions brought about by incorrect folding of the protein at the expression level.

There are numerous alternatives available in attempting to reduce the level of misfolded protein expressed during bacterial growth [14–16] either by reducing the level of aggregated protein formed in the bacterial cells or by scavenging any misfolded proteins and converting them into a correctly folded species [17–20]. Lowering the induction temperature and optimizing the growth medium had minimal effects on the level of soluble recombinant *Psy*HSL expressed in *E. coli*. It was therefore decided to try two alternative approaches; firstly using the osmolyte trehalose [12] alone or in conjunction with a high salt concentration in the growth medium to encourage its uptake into the bacterial cells and create a more viscous environment, thereby helping stabilize cells under stress and improve protein stability overall [21–23]. The second approach was to use the membrane fluidizer benzyl alcohol [11] which alters the structure of the cytoplasmic membrane, creating stress and inducing the production of endogenous chaperones to prevent aggregation [24,25].

A series of concentrations of trehalose +/− NaCl and benzyl alcohol were added to the growth medium in early log phase. Optimal trehalose and benzyl alcohol concentrations were selected based on the results of trypsin digests of the supernatant collected from cell lysates: 5 ml cultures were treated initially with additive at the appropriate OD_{600} followed by 24 h induction in the presence of 0.2 mM IPTG. Trypsin treated lysates were loaded on 12% SDS/PAGE. The least digested full-length *PsyHSL* observed on SDS/PAGE were: 50 mM trehalose + 400 mM NaCl and 20 mM benzyl alcohol.

As before, trehalose and benzyl alcohol treated cultures were purified on 1 ml HisTrapHP and eluted at 100 and 250 mM imidazole. The four individual peak fractions were purified on Bio-Sep SEC 3000, together with untreated 100 mM and 250 mM imidazole fractions (Fig. 2). The 250 mM imidazole fractions were discarded, since they contained almost exclusively aggregated protein which eluted with the front (as verified by a standard calibration curve with proteins run in the same buffer, Fig. 2), but both the trehalose treated and benzyl alcohol treated 100 mM fractions showed a clear improvement over untreated cells since most of the protein eluted at the expected retention time for a 48 kDa protein, implying that the protein was correctly folded. Benzyl alcohol treatment provided a cleaner band, although trehalose + NaCl treatment also clearly improved the level of correctly folded protein.

3.1. Circular dichroism

Secondary structure of soluble HSL purified from benzyl alcohol treatment was investigated by means of CD in the far-UV region. The spectrum suggested that native HSL displays a high degree of secondary structure, showing a large negative band at 222 nm. Estimation of the secondary structure of native HSL performed on the basis of the CD spectrum, was carried out according to the Variable Selection Method (CDSSTR) using DICHROWEB and

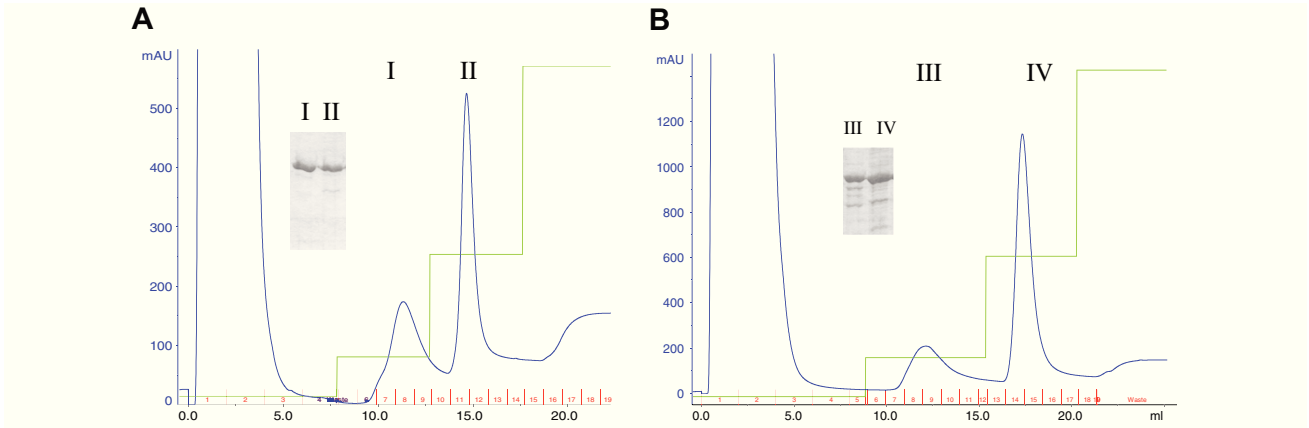

Fig. 1. Purification scheme of soluble 13-HSL. (A) 13-HSL HisTrap purification in the presence of 20 mM benzyl alcohol: I and II indicate 13-HSL fractions eluted with 100 mM and 250 mM imidazole respectively (B) 13-HSL HisTrap purification expression in the presence of 50 mM trehalose + 400 mM NaCl.: III and IV indicate 13-HSL fractions eluted with 100 mM and 250 mM imidazole respectively.

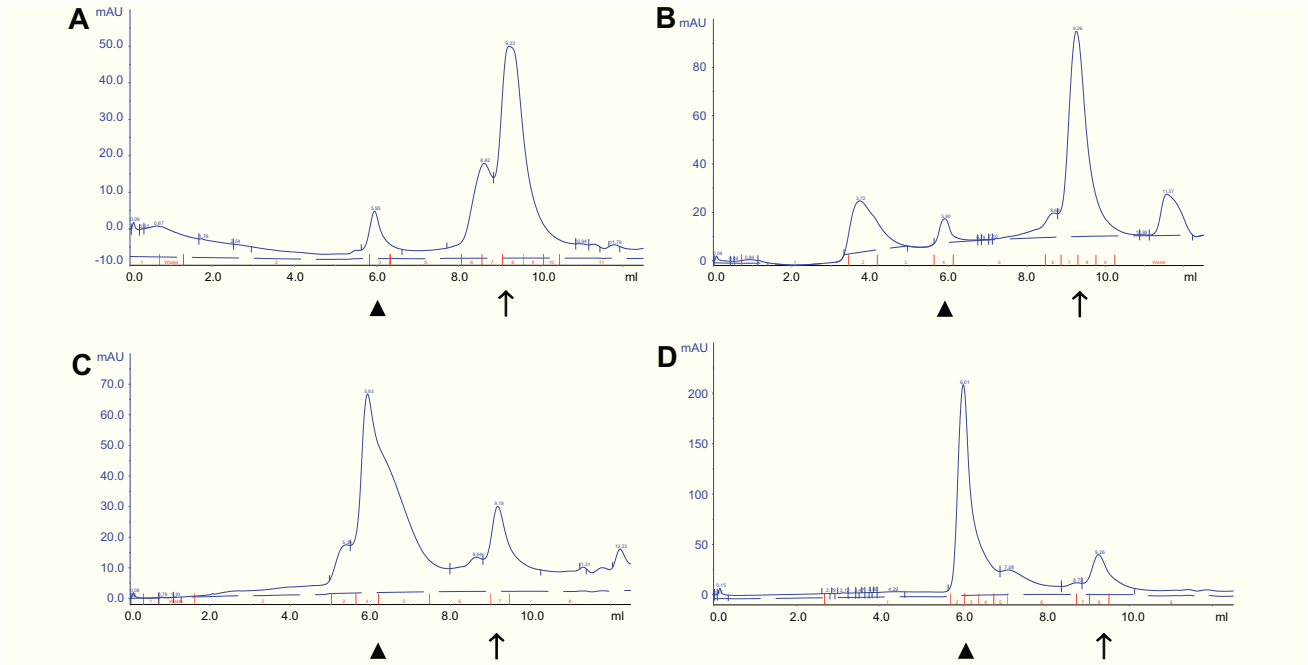

Fig. 2. Purification scheme of HisTrap purified 13-HSL on Bio-Sep SEC 3000. Panels on the left refer to 13-HSL expression in the presence of 20 mM benzyl alcohol; those on the right refer to 13-HSL expression in the presence of 50 mM trehalose + 400 mM NaCl. [A]–[B] 100 mM imidazole peak purification [C]–[D] 250 mM imidazole peak purification; [▲] represents aggregated protein; ↑ represents soluble protein.

revealed it to be comprised of 29% alpha helix and 18% beta sheet. The protein melted at 49 °C and was irreversible under the conditions used, likely due to cross-linking between the six cysteines present within the amino acidic sequence [26,27]. It is worth noting that the thermally denatured HSL at 75 °C still contains a substantial amount of secondary structure as calculated by DICHROWEB. The protein's transition curve is shown in Fig. S1. In order to investigate the influence of electrostatic interactions and solvent properties on the secondary structure of HSL, 1.0 and 1.5 M NaCl were added to HSL and thermal transition curves at 222 nm recorded. Because high concentrations of NaCl disrupt electrostatic interactions but stabilize hydrophobic interactions, they can be used as a method of testing which kind of interaction predominates [28]. In this case almost all secondary structure signals disappeared as temperature increased proving that residual secondary structure previously recorded was mainly due to electrostatic interactions. Also in this case the event was irreversible but the Tm registered was lower, being 43.5 °C indicating that the secondary structure is destabilized at high ionic strength [29].

3.2. Light scattering analysis

Size exclusion chromatography and light scattering analysis on native protein purified from benzyl alcohol treated cells clearly showed that HSL is monomeric in solution with a molar mass of 48 g/mol.

3.3. Enzymatic assays

The relationship between *Psy*HSL activity and temperature in the range 20–50 °C was investigated, using *p*NP-pentanoate as substrate. The apparent maximal activity was recorded at 35 °C, in good agreement with previous results [8]. *Psy*HSL thermal stability was evaluated in the range 35–45 °C (Fig. 3). Enzyme samples were incubated at any given temperature for up to 1 h and residual activity was measured. After 1 h incubation at 45 °C, the native protein still retained 10% of its enzymatic activity (Fig. 3), contrary to previous analyses of refolded *Psy*HSL which showed a dramatic drop in enzymatic activity after only 20 min incubation at 40 °C [8]. As far as specific activity of the enzyme is concerned, the recombinant native HSL showed a comparable specific activity of about 43 U/mg with those values obtained for the refolded *Psy*HSL (38 U/mg).

4. Discussion

Correct recombinant protein folding within the cell necessitates the presence, usually transient, of an array of molecular chaperones, either produced naturally or "induced" by the presence of additives which stimulate their endogenous production [21,24,30,31]. Cellular osmolytes act as chemical chaperones within the cell and are often produced naturally [11,21–23] to

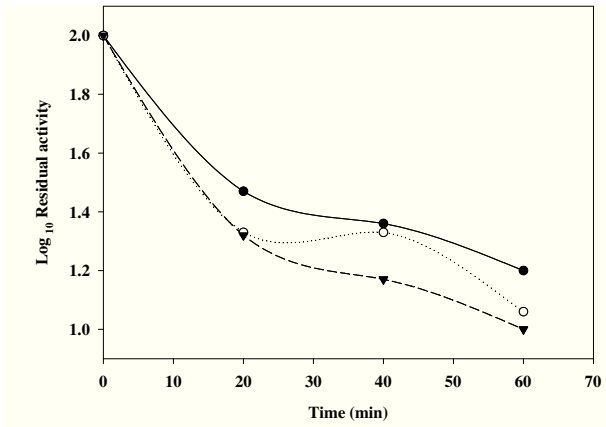

Fig. 3. Thermostability of *Psy*HSL at various temperatures: 35 °C [●], 40 °C [○], 45 °C [▼]. The enzyme was incubated in 0.1 M Tris–HCl pH 8.0 at the indicated temperatures for the times indicated. Residual activity was measured at 35 °C.

counteract a stressful environment, being composed of three classes of compounds. The first two classes include carbohydrates such as glycerol, sorbitol, trehalose and amino acids and derivatives such as alanine, taurine, γ-aminobutyric acid, which are compatible osmolytes and may accumulate in the cell at high concentration without affecting protein function. The third class is represented by methylamines such as betaine, trimethylamine N-oxide which are counteracting osmolytes which offset the adverse effects brought about by presence of inorganic ions such as urea. Normally the accumulation of cellular osmolytes is a relatively slow process, but interestingly it has been observed that the addition externally of a high concentration of NaCl leads to a rapid release of heat shock protein [11,21] and enhances the effect of using a cellular osmolyte alone, as observed here. In fact, in this study the use of additives to the bacterial growth media has had a determining effect in enabling us to produce enough full length *PsyHSL* native protein for extensive biochemical analyses. By comparison of CD spectra a significative shift of melting point was noted [8], highlighting the fact that in the conditions applied a more stable protein was produced. During thermal denaturation, secondary structure was disrupted only in the presence of high salt concentration, suggesting that solvent characteristics affect the conformational features of thermally treated HSL whilst residual secondary structure is influenced by electrostatic interactions [32].

Enzymatic assays performed at 40 °C revealed a more stable native *Psy*HSL, whilst the refolded protein lost its catalytic activity after only 20 min incubation at this temperature [8], despite the fact that the two forms of protein expressed had comparable specific activities. This may be due to the refolding process, leaving only a partially folded catalytically active enzyme unable to maintain its structure at higher temperature.

Catalytic activity was also tested at 45 °C, and unexpectedly the protein was at least 10% active after 1 h incubation confirming that the use of such chemical compounds represents an alternative strategy to obtain recombinant proteins in native form. The optimal temperature for native *Psy*HSL was 35 °C, the same as for the refolded enzyme, corroborating the psychrophilic character of *Psy*HSL.

In conclusion we have established a novel method for obtaining native HSL in *E. coli*. The native enzyme proved to be more stable during thermal denaturation compared to refolded inclusion bodies as shown by CD experiments and activity data.

Recent studies suggest that the relationship between enzymatic activity at low temperature and conformational stability is more complicated than that initially believed to be based on comparative activity and structural studies alone; in this case the native form of *Psy*HSL should allow us to better define its structure–function relationship especially with regard to its cold adaptation strategy, enabling it to be applied to a wide range of biotechnological processes.

Acknowledgments

This work was supported in part by italian PRIN grant 2008F5A3AF_001 (to G.A.).

Appendix A. Supplementary data

Supplementary data associated with this article can be found, in the online version, at doi:10.1016/j.bbrc.2012.03.028.

References

[1] I.J. Goldberg, Lipoprotein lipase and lipolysis: central roles in lipoprotein metabolism and atherogenesis, J. Lipid Res. 37 (1996) 693–707.
[2] D.W. Choo, T. Kurihara, T. Suzuki, K. Soda, N. Esaki, A cold-adapted lipase of an Alaskan psychrotroph, *Pseudomonas* sp. strain B11–1: gene cloning and enzyme purification and characterization, Appl. Environ. Microbiol. 64 (1998) 486–491.
[3] M. Royter, M. Schmidt, C. Elend, H. Höbenreich, T. Schäfer, U.T. Bornscheuer, G. Antranikian, Thermostable lipases from the extreme thermophilic anaerobic bacteria *Thermoanaerobacter thermohydrosulfuricus* SOL1 and *Caldanaerobacter subterraneus* subsp. *Tengcongensis*, Extremophiles 13 (2009) 769–783.
[4] P. Tirawongsaroj, R. Sriprang, P. Harnpicharnchai, T. Thongaram, V. Champreda, S. Tanapongpipat, K. Pootanakit, L. Eurwilaichitr, Novel thermophilic and thermostable lipolytic enzymes from a Thailand hot spring metagenomic library, J. Biotechnol. 133 (2008) 42–49.
[5] A. Houde, A. Kademi, D. Leblanc, Lipases and their industrial applications, an overview, Appl. Biochem. Biotechnol. 118 (2004) 155–170.
[6] F. Hasan, A.A. Shah, A. Hameed, Biotechnol. Adv. 27 (2009) 782–798.
[7] G. Feller, M. Thiry, J.L. Arpigny, C. Gerday, Cloning and expression in *Escherichia coli* of three lipase-encoding genes from the psychrotrophic antarctic strain *Moraxella TA144*, Gene 102 (1991) 111–115.
[8] C. De Santi, M.L. Tutino, L. Mandrich, M. Giuliani, E. Parrilli, P. Del Vecchio, D. de Pascale, The hormone-sensitive lipase from *Psychrobacter* sp. TA144: new insight in the structural/functional characterization, Biochimie 92 (2010) 949–957.
[9] D. Langin, H. Laurell, L.S. Holst, P. Belfrage, C. Holm, Gene organization and primary structure of human hormone-sensitive lipase: possible significance of a sequence homology with a lipase of *Moraxella TA144*, an antarctic bacterium, Proc. Natl. Acad. Sci. USA 90 (1993) 4897–4901.
[10] Z.S. Derewenda, U. Derewenda, Relationships among serine hydrolases: evidence for a common structural motif in triacylglyceride lipases and esterases, Biochem. Cell Biol. 69 (1991) 842–851.
[11] A. de Marco, L. Vigh, S. Diamant, P. Goloubinoff, Native folding of aggregation-prone recombinant proteins in *Escherichia coli* by osmolytes, plasmid- or benzyl alcohol-overexpressed molecular chaperones, Cell Stress Chap. 10 (2005) 329–339.
[12] T. Schultz, J. Liu, P. Capasso, A. de Marco, The solubility of recombinant proteins expressed in Escherichia coli is increased by *otsA* and *otsB* co-transformation, Biochem. Biophys. Res. Commun. 355 (2007) 234–239.
[13] J. Sambrook, E. F. Fritsch, T. Maniatis, Molecular cloning: a laboratory manual, 2nd ed. Cold Spring Harbor Laboratory, Cold Spring Harbor, New York, 1989.
[14] G. Georgiou, P. Valax, Expression of correctly folded proteins in *Escherichia coli*, Curr. Opin. Biotechnol. 7 (1996) 190–197.
[15] O. Kolaj, S. Spada, S. Robin, J.G. Wall, Use of folding modulators to improve heterologous protein production in *Escherichia coli*, Microb. Cell Fact. 8 (2009) 9.
[16] F. Baneyx, Recombinant protein expression in *Escherichia coli*, Curr. Opin. Biotechnol. 10 (1999) 411–421.
[17] A. Mogk, E. Deuerling, S. Vorderwülbecke, E. Vierling, B. Bukau, Small heat shock proteins, *ClpB* and the *DnaK* system form a functional triade in reversing protein aggregation, Mol. Microbiol. 50 (2003) 585–595.
[18] H.P. Sørensen, K.K. Mortensen, Soluble expression of recombinant proteins in the cytoplasm of *Escherichia coli*, Microb. Cell Fact. 4 (2005) 1.
[19] W.J. Welch, C.R. Brown, Influence of molecular and chemical chaperones on protein folding, Cell Stress Chap. 1 (1996) 109–115.
[20] A. Puig, H.F. Gilbert, Protein disulfide isomerase exhibits chaperone and anti-chaperone activity in the oxidative refolding of lysozyme, J. Biol. Chem. 269 (1994) 7764–7771.
[21] S. Diamant, D. Rosenthal, A. Azem, N. Eliahu, A.P. Ben-Zvi, P. Goloubinoff, Dicarboxylic amino acids and glycine-betaine regulate chaperone-mediated protein-disaggregation under stress, Mol. Microbiol. 49 (2003) 401–410.
[22] H.C. Tseng, D.J. Graves, Natural methylamine osmolytes, trimethylamine N-oxide and betaine, increase tau-induced polymerization of microtubules, Biochem. Biophys. Res. Commun. 250 (1998) 726–730.
[23] P.H. Yancey, Organic osmolytes as compatible, metabolic and counteracting cytoprotectants in high osmolarity and other stresses, J. Exp. Biol. 208 (2005) 2819–2830.
[24] D.H. Lee, M.D. Kim, W.H. Lee, D.H. Kweon, J.H. Seo, Consortium of fold-catalyzing proteins increases soluble expression of cyclohexanone monooxygenase in recombinant *Escherichia coli*, Appl. Microbiol. Biotechnol. 63 (2004) 549–552.
[25] K.S. Gunnarsen, E. Lunde, P.E. Kristiansen, B. Bogen, I. Sandlie, G.A. Løset, Periplasmic expression of soluble single chain T cell receptors is rescued by the chaperone *FkpA*, BMC Biotechnol. 10 (2010) 8.
[26] P. Del Vecchio, G. Graziano, G. Barone, L. Mandrich, M. Rossi, G. Manco, Temperature-induced denaturation of the Aes acetyl-esterase from *Escherichia coli*, Thermochimica Acta 441 (2006) 144–149.
[27] L. Tornatore, D. Marasco, N. Dathan, R.M. Vitale, E. Benedetti, S. Papa, G. Franzoso, M. Ruvo, S.M. Monti, Gadd45 beta forms a homodimeric complex that binds tightly to MKK7, J. Mol. Biol. 378 (2008) 97–111.
[28] S.H. Gerber, J. Rizo, T.C. Südhof, Role of electrostatic and hydrophobic interactions in Ca(2$^+$)-dependent phospholipid binding by the C(2)A-domain from synaptotagmin I, Diabetes 51 (2002) S12–18.
[29] K. Yamazaki, T. Iwura, R. Ishikawa, Y. Ozaki, Effects of ionic strength on the thermal unfolding process of granulocyte-colony stimulating factor, J. Biochem. 139 (2006) 41–49.
[30] A. de Marco, Strategies for successful recombinant expression of disulfide bond-dependent proteins in *Escherichia coli*, Microb. Cell Fact. 8 (2009) 26.
[31] F. Baneyx, M. Mujacic, Recombinant protein folding and misfolding in *Escherichia coli*, Nat. Biotechnol. 22 (2004) 1399–1408.
[32] B. Ibarra-Molero, J.A. Zitzewitz, C.R. Matthews, Salt-bridges can stabilize but do not accelerate the folding of the homodimeric coiled-coil peptide GCN4-p1, J. Mol. Biol. 336 (2004) 989–996.

Journal of Molecular Catalysis B: Enzymatic 82 (2012) 46–52

Contents lists available at SciVerse ScienceDirect

Journal of Molecular Catalysis B: Enzymatic

journal homepage: www.elsevier.com/locate/molcatb

Effect of low organic solvents concentration on the stability and catalytic activity of HSL-like carboxylesterases: Analysis from psychrophiles to (hyper)thermophiles

Luigi Mandrich*, Concetta De Santi, Donatella de Pascale, Giuseppe Manco

Institute of Protein Biochemistry, CNR, Via Pietro Castellino, 111, I-80131 Naples, Italy

ARTICLE INFO

Article history:
Received 11 January 2012
Received in revised form 17 May 2012
Accepted 2 June 2012
Available online xxx

Keywords:
Carboxylesterases
Enzyme kinetics
Organic solvent effect
Thermal stability

ABSTRACT

A comparative study aiming at analysing the catalytic activity and stability of four related enzymes belonging to the HSL family in the presence of several water-miscible organic solvents was performed. The studied enzymes were four carboxylesterases: *Psy*HSL (psychrophilic), Aes (mesophilic), EST2 (thermophilic) and AFEST (hyperthermophilic). The effect of the solvents on catalytic activity was measured by adding solvents up to 20% (v/v) to the assay mixture. For all enzymes at low solvent concentrations (4–5%) the catalytic activity (U/mg) increased up to 3–4-fold; only diethyl ether exerted a negative effect when compared to the reference value without solvent. EST2 and AFEST retained more than 100% of activity for concentrations of solvent >10% (v/v). Similar results were obtained for the stability analysis; in fact these two enzymes appeared more stable than the mesophilic and psychrophilic counterparts.

The kinetic parameters of *Psy*HSL, EST2 and AFEST in all the tested solvents showed an increase in k_{cat} but a negative effect on K_M values. In the case of *Psy*HSL the K_M increase was very low resulting in a substantial increase of the specific constant (S); in particular, the addition of dimethyl sulfoxide increased the k_{cat} and the s values about 4- and 3-fold, respectively. We tested the ability of the enzymes to synthesize esters with the aim to discriminate if the decrease of activity in the presence of organic solvents was due to protein denaturation or an inversion of the hydrolytic reaction toward synthesis. While for *Psy*HSL and Aes the synthesis was very low and completely abolished in presence of solvents, instead for EST2 and AFEST the esters synthesis increased up to 10-fold in the presence of solvents, although the hydrolytic activity dropped about 300-fold.

1. Introduction

The properties of an enzyme in organic solvents may differ dramatically with respect to those in aqueous environment [1]. It is accepted that water is essential for the maintenance of native conformation but it is also involved in several mechanisms of enzyme inactivation [2]. Irreversible thermo-inactivation of enzymes, in aqueous solution at 90–100 °C depends on covalent modifications at level of: cysteine residues (thiol-catalysed disulfide interchange, oxidation of –SH groups); asparagines and/or glutamine residues (deamidation); and hydrolysis of peptide bonds nearby aspartic acid residues [3,4]. In most of these thermo-inactivation processes water is one of the reactants as well as in heat-induced protein denaturation where aggregation of enzymes and incorrect structure formation are observed [3,4]. The presence of an organic solvent may alter these mechanisms and lead to improvement or worsening of the enzyme performance. In general, the activity and stability of enzymes depend on the nature of the solvent (water-miscible or immiscible, protic or aprotic, etc.) and the water content of the enzyme; biocatalysts which show increased activity and/or stability in organic solvents are considered attractive for biotechnological applications [5].

Normally, an enzyme shows enhanced thermostability when dispersed in pure water-immiscible organic solvents. This has been observed for porcine pancreatic lipase and lipase from *Candida cylindracea* ribonuclease, chymotripsin and several other enzymes [5,6]. Enzymes in dry organic solvents show a significant characteristic that is higher conformational rigidity, that prevents them to unfold and this could explain their increased thermostability compared to that in aqueous solution [7]. In organic solvents enzyme activity changes principally for the absence or drastic reduction of water which assure the required flexibility for catalysis.

Proteins in mixtures of water and water-miscible organic solvents (>20% of organic solvents) are known to be generally less stable and less active than in water only, even though some

* Corresponding author. Tel.: +39 081 6132581; fax: +39 081 6132277.
E-mail address: l.mandrich@ibp.cnr.it (L. Mandrich).

1381-1177/$ – see front matter © 2012 Elsevier B.V. All rights reserved.
http://dx.doi.org/10.1016/j.molcatb.2012.06.002

exception exist depending on the solvent or the protein [8,39,41]. Protein folding is a balance between non-covalent, hydrophobic and electrostatic interactions, and they are influenced by the surrounding conditions (temperature, ionic strength of the solvent) as well as type of enzyme. In the presence of organic solvents the hydrophobic interactions are disrupted and proteins aggregate or unfold [6,9]. Studies of the behaviour of enzymes of biotechnological interest in the presence of organic solvents are useful for further applications.

In this paper, we studied the effect of the increasing concentration of several water-miscible organic solvents on stability, catalytic activity, kinetic parameters and ester synthesis of four carboxylesterases, which cover a range of catalysis temperature from 5 to 85 °C: the psychrophilic *Psy*HSL from *Psychrobacter* sp. TA144 [10], the mesophilic Aes from *Escherichia coli* [11], the thermophilic EST2 from *Alicyclobacillus acidocaldarius* [12] and the hyperthermophilic AFEST from *Archaeoglobus fulgidus* [13]. These enzymes belong to the same group, the HSL family [14–17], from the classification by ESTHER DATABASE (http://bioweb.ensam.inra.fr/ESTHER/), that corresponds to the family IV of the classification by Arpigny and Jaeger [18]. Previously only kinetic parameters of EST2 in acetonitrile and alcohols such as methanol, ethanol and 2-propanol have been reported [25]. Since these enzymes were related, we studied not only their different behaviour with several solvents but also differences due to their altered thermal adaptation. The effect of organic solvents on the activity and stability of enzymes is not universal and seems to depend on the properties of the solvent and/or the considered enzyme. The organic solvents were selected for their different physico-chemical characteristics: polar aprotic (acetonitrile, dimethyl formamide, dimethyl sulfoxide), polar protic (methanol), polar poly-protic (ethylene glycol) and non polar (diethyl ether). In Table 1 are summarized the main features of these solvents.

In modern biotechnology, the application of microorganisms and enzymes to the production of chemicals, biopolymers, materials and fuels offers great opportunities for the industries. In the case of lipases/esterases their substrates and/or products are generally not miscible in water and the industrial biotransformation processes run under harsh conditions, such as high and low temperature, extremes of pH and high pressure, presence of salt, organic solvents and metals [24]. For these reasons, the organic solvent tolerance of enzymes is a relevant property, which show potential in biotechnological applications. In the case of the enzyme belonging to the HSL family some data about the organic solvent tolerance were reported [10,25]. Herein we reported a complete analysis on the effect of the six organic solvents on *Psy*HSL, Aes, EST2 and AFEST enzymes. Moreover we checked the effect of organic solvents on a reaction of biotechnological interest, namely the modification of EST2 enantioselectivity towards the substrate (*RS*)-*p*-nitrophenyl-2-chloropropionate. This substrate is used to produce (*S*)-2-chloropropionic acid, an intermediate in the synthesis of optically pure phenoxypropionic acid herbicides [26,27].

2. Experimental

2.1. Purification of proteins

Enzymes used in the experiments were expressed and purified as previously reported: the psychrophilic *Psy* HSL from *Psychrobacter* sp. TA144, see reference De Santi et al. [10]; the mesophilic Aes from *E. coli* [11,29]; the thermophilic EST2 from *A. acidocaldarius*, see reference Manco et al. [12]; and the hyperthermophilic AFEST from *A. fulgidus*, see reference Manco et al. [13].

2.2. Esterase activity

The time course of the esterase-catalysed hydrolysis of *p*NP-esters (C_5 and C_6 acyl chain length) was followed by monitoring of *p*-nitrophenol production at 405 nm, in 1-cm path-length cells with a Cary 100 spectrophotometer (Varian, Australia). Initial rates were calculated by linear least-squares analysis of time courses comprising less than 10% of the total substrate turnover. Assays were performed at the optimal temperature of each enzymes (35 °C for *Psy*HSL; 65 °C for Aes; 70 °C for EST2; 80 °C for AFEST) [10,12,13,29], in a mixture of 40 mM Tris–HCl pH 8.0 for *Psy*HSL and 40 mM buffer phosphate pH 7.1 for the other enzymes, 4% acetonitrile at the indicated pH (3% for *Psy*HSL), containing *p*NP-esters (100 μM). Stock solutions of *p*NP-esters, C_5 and C_6, were prepared by dissolving substrates in pure acetonitrile [10,12,13]. Samples of identical composition as the assay mixture, omitting the enzyme, provided suitable blanks. Assays were done in duplicate and results were means of two independent experiments. One unit of enzymatic activity was defined as the amount of the protein releasing 1 μM of *p*-nitrophenoxide/min from *p*NP-pentanoate or -hexanoate at indicated temperature. The absorption coefficient used for *p*-nitrophenoxide was 19,000 $M^{-1}\,cm^{-1}$ at 35 °C and pH 8.0 or 20,000 $M^{-1}\,cm^{-1}$ form 65 to 80 °C at pH 7.1.

2.3. Effect on enzymatic activity by organic solvents

Enzyme activity was evaluated in the optimal conditions of temperature and pH of each enzymes using the better reported substrate (100 μM final concentration), that are *p*NP-pentanoate for *Psy*HSL [10] and *p*NP-hexanoate for Aes, EST2 and AFEST [12,13,35]. Stock solutions of each substrate were prepared in all the solvents tested; the activity was measured using an increasing concentration of the solvents up to 20% (v/v) in the assay mixture. Results were reported as relative activity with respect to the value measured without solvents.

2.4. Stability to solvents

The stability to solvents of the enzymes was studied at the optimal temperature and pH of each enzyme incubated in a mixture containing 2.5, 5.0 and 10.0% (v/v) of each organic solvent. Pure enzymes (0.2 mg/ml) were incubated in sealed glass tubes at the appropriates temperatures. Aliquots were withdrawn at 15, 30, 60, 120, 240, and 360 min (in some case up to 24 h) and assayed at the optimal temperature of each enzymes, in the standard conditions described above.

2.5. Kinetic measurements

Initial velocity versus substrate concentration data were fitted to the Lineweaver–Burk transformation of the Michaelis–Menten equation, by weighted linear least-squares analysis with a personal computer and the GRAFIT program 3.0 [30]; *p*NP-pentanoate ranged from 1 to 200 μM and *p*NP-hexanoate from 1 to 150 μM. Assays were done in duplicate or triplicate and results for kinetic data were mean of two independent experiments. Kinetic parameters were calculated for each organic solvents (3%, v/v for *Psy*HSL and 4%, v/v for the other enzymes), dissolving *p*NP-pentanoate or -hexanoate in each pure organic solvent, and also without solvent, dissolving *p*NP-pentanoate or -hexanoate in water at their maximum of solubility. Measurements were done at the optimal pH and temperature of each enzymes.

Table 1
Main characteristics of the organic solvents used in this study.

Structure	Characteristics			
	Hydrophobicity, log P[a]	Denaturation capacity (DC)[b]	Polarity index, I[c]	Dielectric constant, ε[d]
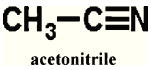 acetonitrile	−0.3	64.3	5.8	37
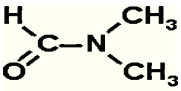 dimethyl formamide	−1.0	63.3	6.4	38
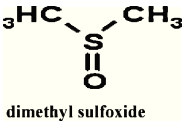 dimethyl sulfoxide	−1.3	60.3	7.2	47
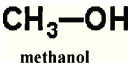 methanol	−0.76	30.5	5.1	33
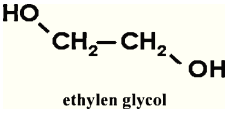 ethylen glycol	−1.8	18.7	5.4	38
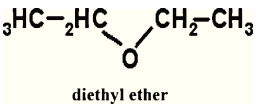 diethyl ether	−0.8	50.2	6.7	4.3

[a] The log P value were taken from, or calculated on the basis of Ref. [19].
[b] The denaturing capacities of the solvents were taken from Ref. [20].
[c] The polarity indexes of solvents were taken from Ref. [21].
[d] The dielectric constant value were taken from Refs. [22,23].

2.6. In vitro ester synthesis

The assays were carried out in buffered solutions with or without solvents as previously described [31]. Briefly, 50 μM *p*-nitrophenol and 500 μM hexanoic acid were added to a buffered solution containing or not the solvent, and after the addition of the enzymes the activity was recorded at 405 nm by following the decrease of absorbance due to ester synthesis. Each enzyme was tested at its optimal temperature and pH in the presence of 5 and 10% (v/v) solvent. Results are the mean of two independent experiments.

2.7. Enantioselectivity measurements

The assays were carried out in buffered solutions with or without 4% (v/v) solvent (as previously described [26]). The substrates were prepared dissolving (*R*)- or (*S*)-*p*-nitrophenyl-2-chloropropionate in pure organic solvents. Assays were done at 25 °C and in 50 mM sodium citrate buffer at pH 5.0. The kinetic determinations were performed only for EST2 wild type enzyme and for EST2 L212P mutant in acetonitrile [26]. Initial velocity versus substrate concentration data were fitted to the Lineweaver–Burk transformation of the Michaelis–Menten equation, by weighted linear least-squares analysis with a personal computer and the GRAFIT program 3.0 [30]. Assays were done in duplicate or triplicate and results for kinetic data were mean of two independent experiments.

3. Results and discussion

3.1. Activity and stability

In Table 1 are reported the six solvents used and their main characteristics; it has been considered their: (a) hydrophobicity, expressed as log P, that is empirically calculated $\log_{10}$ of the coefficient for solvent partitioning P between 1-octanol and water [19], log P could be used as a criterion to correlate organic solvents and their denaturating strength only for solvents of the same class such as alcohols [20]; (b) denaturation capacity, that is an index of thermodynamic stability of a protein obtained by taking into account the solvent concentration at the protein is half inactivated.

It has been experimentally verified that exists a linear relationships between DC of a solvent and half-inactivation of several proteins. Thus DC represents a good index of the denaturing strength of organic solvents [20]; (c) polarity index, that is a measure of the enzymes denaturation degree by the solvent, in other words solvents having polarity index of 5.8 and above if are used as cosolvents cause reversible conformational changes in the enzyme molecule up to a concentration of 50% (v/v). Solvents having polarity index of 5.0 and below cause irreversible conformational changes of the enzymes [21,22]; (d) dielectric constant, that is a rough measure of a solvents polarity. Solvents with a dielectric constant of less 15 are considered to be non polar [36]. The polar aprotic solvents, defined as solvents do not containing an –OH or –NH bond, were acetonitrile, dimethyl formamide and dimethyl sulfoxide; they have different values of hydrophobicity, polarity index and dielectric constant [19,21–23]. Methanol was used as polar protic solvent, defined as containing an –OH or –NH bond, and ethylene glycol as polar polyprotic; they differ in hydrophobicity and denaturation capacity values [19,20]; diethyl ether was used as apolar solvent. Polar aprotic solvents tend to have large dipole moment and solvate positively charged species via their negative dipole. For all enzymes, we measured the activity as function of the solvent percentage, up to 20% by the volume, and at different temperatures as follows: (i) at the reported optimal temperature of each enzyme, (ii) at the living temperature of the bacterium from which the enzymes have been isolated, (iii) at room

Table 2
Enzymes half-live. Acetonitrile stability was measured at three different solvent concentrations: 2.5, 5.0 and 10.0% (v/v). The stability was followed for different times of incubation at the optimal temperature and pH of each enzyme; *p*NP-pentanoate (*Psy*HSL) or *p*NP-hexanoate (Aes, EST2, AFEST) were used as substrates. The stability was reported as half life-time $t_{1/2}$ (min).

Enzymes	Acetonitrile concentration (v/v)		
	2.5%	5.0%	10.0%
*Psy*HSL	3 min	2 min	1 min
Aes	800 min	250 min	170 min
EST2	330 min	100 min	90 min
AFEST	105 min	95 min	60 min

temperature (25 °C) and (iv) at 50 °C. The stability of enzymes to solvents was measured at three different concentrations: 2.5, 5.0 and 10.0% (v/v), and at the optimal temperature and pH of each enzyme. The kinetic parameters were calculated in presence of 4% of each solvent and the rate of ester synthesis of each enzyme in all solvents were calculated aiming at verify if the decrease of activity at high concentration of solvent was due to denaturation or to some change of the equilibrium reaction.

3.2. Acetonitrile

Fig. 1 shows the results obtained for the enzyme activity as function of acetonitrile concentration and temperatures. In panel A (Fig. 1) is shown the profile obtained for *Psy*HSL: we observed a maximum increase of activity in presence of solvent at about 3% (v/v) at 35 °C; lower increments were recorded at 25 and 4 °C. At a concentration of acetonitrile ranging between 6 and 8%, the activity dropped down below the value measured without the solvent. For other enzymes (Aes panel B, EST2 panel C, AFEST panel D, Fig. 1), the maximum increase of activity was observed at 25 °C and in presence of about 6% of solvent; the temperature increasing was inversely related to the activity increasing. In the case of AFEST at 25 and 50 °C and up to 20% of acetonitrile we recorded enzyme activation with respect to the sample without solvent set as 100%. Instead EST2 appears to be more sensitive to high concentrations of acetonitrile at all temperatures tested.

As far as the enzyme stability in acetonitrile is concerned, it turned out that *Psy*HSL had low stability at all solvent concentrations tested, with a half-life of few minutes (Table 2), while the other enzymes seemed to be more stable, with a half-life of about 800 min for Aes at 2.5% (v/v) acetonitrile. A decreasing stability was recorded at higher solvent concentration for all the enzymes tested (Table 2).

3.3. Dimethyl sulfoxide

Concerning the addition of dimethyl sulfoxide, the greatest activation was obtained for *Psy*HSL (Supplemental data, Fig. S1A) and its behaviour was very similar to that of EST2; AFEST (Supplemental data, Fig. S1C and D), showed a relevant activity also at high solvent concentration, while for Aes was recorded a fast decrease of activity at concentrations over 6% (Supplemental data, Fig. S1B).

As for the enzyme stability in dimethyl sulfoxide, the behaviour was very similar to that obtained for acetonitrile at all concentrations analysed; *Psy*HSL was less stable than the others enzymes and Aes seemed to be less stable with respect to acetonitrile, showing half-lives of about 600 and 150 min in 2.5 or 10%, DMSO, respectively. EST2 seemed to be more stable than in acetonitrile showing half-lives of 500 and 90 min in 2.5% and 10% DMSO, respectively (Supplemental data, Table S1).

3.4. Dimethyl formamide

The analysis of activity in DMF shows that the maximum enhancement was obtained in the range of 2–6% of solvent for all

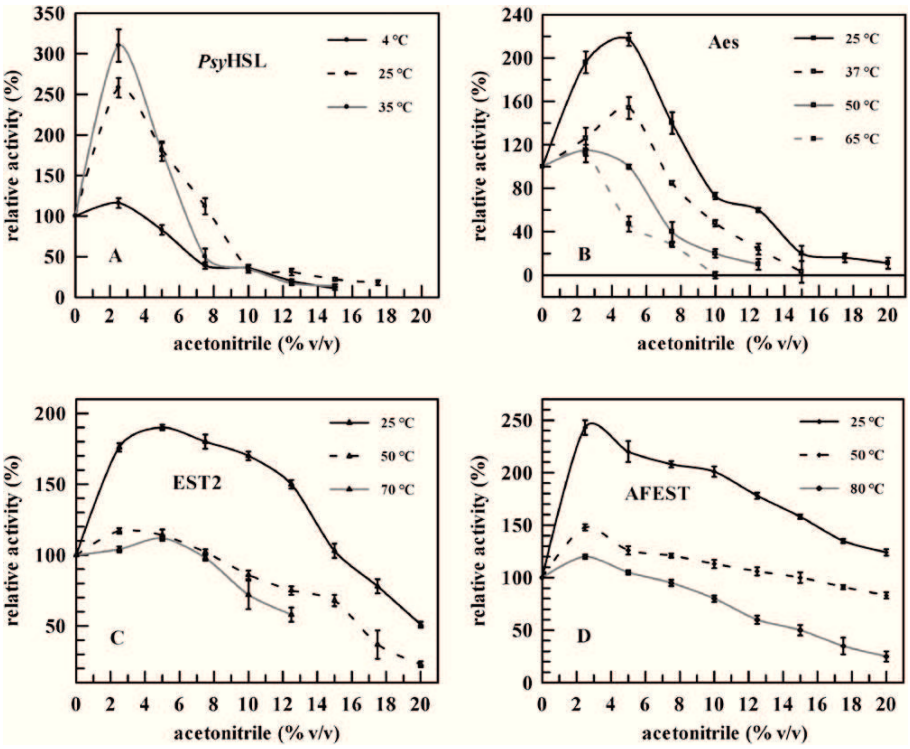

Fig. 1. Enzyme activity vs acetonitrile concentration (%, v/v). Data obtained for: (A) *Psy*HSL; (B) Aes; (C) EST2; (D) AFEST. For each enzyme the assays were done at the optimal pH, and using *p*NP-hexanoate as substrate.

Table 3
Ester synthesis. We followed spectrophotometrically the synthesis of *p*-NP-hexanoate, starting from *p*-nitrophenol and hexanoic acid, using a reaction mixture containing 5 or 10% of each solvents. Results obtained at 10% of solvent concentration are reported in parentheses. Results are mean of two different experiments. One unit of synthetic activity was defined as the amount of protein that synthesized 1 μmol of *p*NP-hexanoate/min.

Solvents	Enzymes activity (U/mg)			
	*Psy*HSL	Aes	EST2	AFEST
None	0.0051 ± 0.0002	0.012 ± 0.001	2.4 ± 0.1	1.10 ± 0.05
Acetonitrile	n.d.	0.0063 ± 0.0005 (n.d.)	6.9 ± 0.2 (4.3 ± 0.1)	2.8 ± 0.01 (2.1 ± 0.01)
Dimethyl sulfoxyde	0.0045 ± 0.0005 (0.0028 ± 0.0002)	0.015 ± 0.001 (0.0074 ± 0.0005)	n.d.	n.d.
Dimethyl formamide	0.0042 ± 0.0005 (n.d.)	0.010 ± 0.001 (n.d.)	3.3 ± 0.1 (n.d.)	2.5 ± 0.02 (n.d.)
Methanol	n.d.	n.d.	30.0 ± 5.0 (3.1 ± 0.1)	9.5 ± 0.1 (4.0 ± 0.2)
Ethylene glycol	n.d.	n.d.	n.d.	n.d.
Diethyl ether	n.d.	n.d.	n.d.	n.d.

enzymes; for additional increments of solvent the activity dropped down below the value measured in absence of solvent (Supplemental data, Fig. S2A–D).

By analysing all data regarding the enzyme stability in DMF, we could hypothesize a stronger denaturing action of this solvent most likely, due to the increased polarity with respect to the two solvents used before. This could destabilize charges present on the protein surface. Accordingly, *Psy*HSL showed half lives of few minutes, and even EST2 and AFEST were demonstrated to be less stable with respect to other solvents analysed (half lives of about 60 and 20 min at 2.5 and 10% DMF, respectively; Supplemental data, Table S2).

3.5. Methanol

The analysis of activity in methanol shows a behaviour similar to other solvents, with an increase of activity in the range 3–5% of methanol, which reached about 4-fold for *Psy*HSL (Supplemental data, Fig. S3). EST2 activation at 70 °C decreased rapidly above 10% methanol (Supplemental data, Fig. S3C). This result was confirmed also in terms of stability; in fact EST2 was demonstrated to be less stable in methanol with respect to the other solvents analysed, whereas Aes showed an excellent stability in this solvent (Supplemental data, Table S3). Since methanol is a strong protein denaturant, because it disrupt the hydrophobic interaction [38], we could speculate a general effect due to the high polarity of methanol; furthermore, for EST2 and AFEST, the denaturation effect was enhanced by the high temperatures used for the incubation, e.g. 70 and 80 °C.

3.6. Ethylene glycol

*Psy*HSL activity was dramatically affected by the presence of ethylene glycol; in fact, we observed a decrease of activity with respect to the control, in all tested conditions (Supplemental data, Fig. S4A). Concerning the addition of ethylene glycol to the other three enzymes, we observed that activity remained above the value measured without solvent for Aes and EST2 up to 12.5% of ethylene glycol (Fig. S4B); for AFEST this trend was maintained almost up to 20% of solvent (Supplemental data, Fig. S4B–D).

In terms of protein stability, in the presence of ethylene glycol, EST2 and Aes demonstrated to be very stable, with a half life of 240 and 360 min, respectively at 10% of solvent, whereas AFEST showed a moderate stability (Supplemental data, Table S4). Comparing the results obtained in ethylene glycol with that obtained with methanol, it turned out that the less destabilizing effect we observed in ethylene glycol could be ascribed to the lower "denaturation capacity" (Table 1) of the ethylene glycol with respect to methanol.

3.7. Diethyl ether

In Fig. S5 (Supplemental data) it is reported the effect of diethyl ether on the enzyme activities. In all the conditions tested, Aes, EST2 and AFEST proved to be less active than without solvent, while *Psy*HSL enzymatic activity increased at 25 and 37 °C up to 5% of solvent concentration (Supplemental data, Fig. S5A). Interestingly diethyl ether affects the stability of the same three enzymes in the same way as the solvent which shows the lower half-lives, with respect to the other solvents analysed, and at all the used percentages (2.5, 5.0 and 10.0%); in contrast the psychrophilic protein, *Psy*HSL appeared to be more stable in diethyl ether with respect to the other solvents tested here a result similar to the effect of methanol (Supplemental data, Table S5).

How may we explain these results? An hypothesis could be that being the structural core of (hyper)thermophilic enzymes much more stable with a overall less flexible structure due to a large number of ionic and hydrophobic interactions [32,33], an apolar solvent reaching the inner core of the protein might interfere with the protein hydrophobic interactions leading to protein unfolding.

On the other hand, psychrophilic enzymes are characterized by a high structural flexibility, due to a lower number of hydrophobic interactions [34], and as a consequence these proteins might be less sensitive to the presence of apolar solvents (diethyl ether in this case).

3.8. Kinetic parameters

The kinetic parameters were calculated at 4% final concentration of each solvent for Aes, EST2 and AFEST and 3% for *Psy*HSL. The results are summarized in Table S6 (Supplemental data). Fig. 2 shows the k_{cat} and $s = k_{cat}/K_M$ values as ratio of the value obtained in water and solvents used for each enzyme. A careful reading of the kinetic parameters pointed out an increase of enzymatic activity for all the tested enzymes, only exception being *Psy*HSL and Aes, for which a slight reduction was observed in diethyl ether (Fig. 2A). *Psy*HSL showed the strongest increases of k_{cat} (around 4-fold) with respect to the other enzymes, in dimethyl sulfoxide. Concerning Aes, we observed a large increase in k_{cat} (up to 3-fold) in DMF, ethylene glycol and methanol. Slighter increasing, up to 1.5-fold, were recorded for EST2 and AFEST (Fig. 2A); finally, for all the enzymes analysed, the addition of solvents increased the K_M values (Supplemental data, Table S6). In terms of specificity constants s (k_{cat}/K_M) the variations recorded correspond to a weak increase for Aes, a decrease for EST2 and AFEST and 2–3 fold increase for *Psy*HSL (Fig. 2B).

3.9. Ester synthesis

With the aim to understand if the decrease in enzymatic activity, observed after incubation in organic solvents, was due to a

Table 4
The parameters were calculated using (*R*)- or (*S*)-*p*-nitrophenyl-2-chloropropionate as substrate, in a mixture containing sodium citrate buffer 50 mM pH 5.0 and 10% of each solvents at 25 °C. Stock solution of the substrates dissolved in each solvent were prepared. The kinetic determinations were performed only for EST2.

Solvent	(*R*)-*p*-Nitrophenyl-2-chloropropionate			(*S*)-*p*-Nitrophenyl-2-chloropropionate			Ratio *Ss*/*Rs*
	k_{cat} (s^{-1})	K_M (mM)	k_{cat}/K_M (s^{-1} mM^{-1})	k_{cat} (s^{-1})	K_M (mM)	k_{cat}/K_M (s^{-1} mM^{-1})	
–	37.5 ± 1.5	0.100 ± 0.014	375 ± 60	52.6 ± 3.4	0.110 ± 0.030	480 ± 100	1.28 ± 0.27
Acetonitrile	53.5 ± 2.0	0.170 ± 0.020	314 ± 50	56.6 ± 2.5	0.076 ± 0.013	745 ± 80	2.37 ± 0.39
Dimethyl sulfoxide	39.0 ± 2.0	0.105 ± 0.015	371 ± 50	48.8 ± 2.4	0.124 ± 0.024	394 ± 50	1.06 ± 0.06
Dimethyl formamide	48.0 ± 1.0	0.230 ± 0.025	208 ± 27	36.7 ± 1.6	0.125 ± 0.025	293 ± 75	1.41 ± 0.39
Methanol	43.2 ± 1.0	0.190 ± 0.013	227 ± 18	35.5 ± 1.0	0.130 ± 0.015	273 ± 35	1.20 ± 0.20
Ethylene glycol	43.7 ± 2.3	0.190 ± 0.030	230 ± 40	41.5 ± 1.8	0.115 ± 0.020	360 ± 80	1.57 ± 0.55

denaturation process or to an inversion of the hydrolytic reaction, the rates of ester synthesis were calculated.

Our results (Table 3) show an excellent rate of ester synthesis for EST2 and AFEST in 5% methanol, while the increase of methanol percentage (10%) corresponds to a drastic decrease of synthetic reaction. Other esterases tested under the same conditions demonstrated a very poor catalytic rate of synthesis, suggesting that the presence of organic solvent led to the protein unfolding.

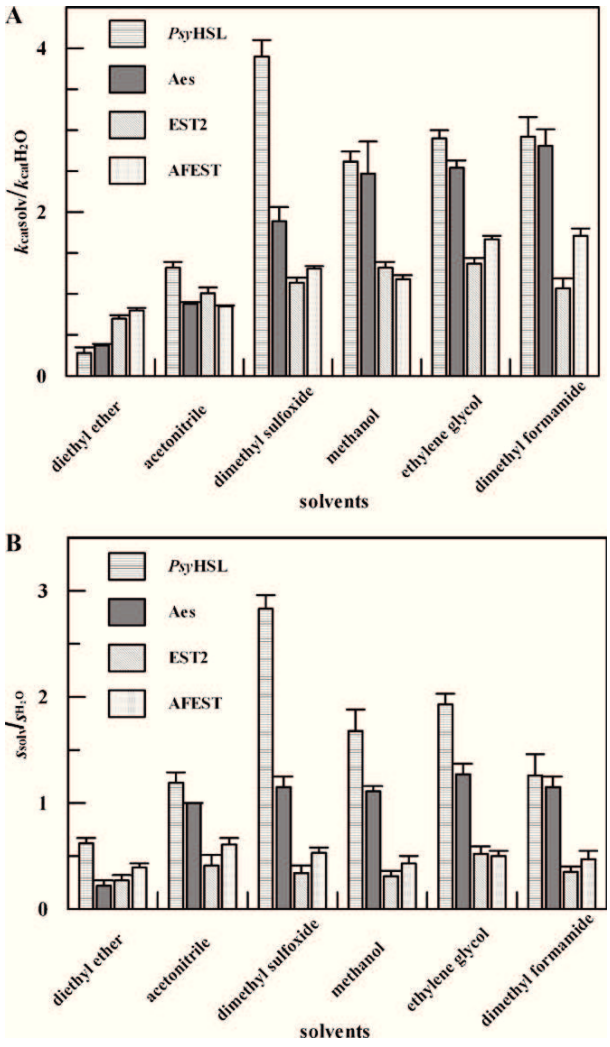

Fig. 2. Graphical representation of kinetic parameters reported in Table S6 (Supplemental data). Parameters were reported as ratio with respect to the value obtained in water. (A) k_{cat} solvent/k_{cat} H_2O values are reported; (B) $s_{solvent}/s_{H_2O}$ values are reported. To better understand the real difference in activity among the enzymes used, we report the value measured in H_2O: PsyHSL $k_{cat} = 19.0 \pm 1.3\ s^{-1}$, $s = 190 \pm 30\ s^{-1}\ mM^{-1}$; Aes $k_{cat} = 40.3 \pm 0.6\ s^{-1}$, $s = 260 \pm 10\ s^{-1}\ mM^{-1}$; EST2 $k_{cat} = 3800 \pm 80\ s^{-1}$, $s = 475 \pm 55$ $(\times 10^3)\ s^{-1}\ mM^{-1}$; AFEST $k_{cat} = 1530 \pm 5\ s^{-1}$, $s = 352 \pm 23$ $(\times 10^3)\ s^{-1}\ mM^{-1}$.

3.10. Enantioselectivity

To translate the information gathered on the solvents stability into a reaction/process of biotechnological interest, we used as a model reaction the EST2 hydrolysis of (*RS*)-*p*-nitrophenyl-2-chloropropionate to obtain (*S*)-2-chloropropionic acid, a compound used in the synthesis of optically pure phenoxypropionic acid herbicides [27]. Previously, it has been reported that EST2 is able to hydrolyse this compound, showing a slightly preference for the *S* form [26]; in the same work by a random mutagenic approach, consisting in error prone PCR of the EST2 gene, expression of the genes and screening for altered activities against the R or the S form of the substrate we isolated a mutated version of EST2, L212P that displayed about 6-fold increase of specificity for the *S* form [26]. In Table 4 are reported the kinetic parameters measured for EST2 in the different solvents, using the (*R*) or (*S*) forms of the substrate. In the presence of acetonitrile we measured the maximum difference in affinity for the *S* form, respect to the parameters measured without solvent showing a ratio between the specific constants *Ss*/*Rs* in acetonitrile of 2.37 (without solvent the ratio was 1.28, Table 4). In presence of acetonitrile the parameters measured on the *R* form of the substrate were the same obtained without solvent and the difference was due to a decrease of K_M value, corresponding an increase of affinity for the *S* form. Regarding DMF an inversion of ratio of activities was observed favouring the *R* form. Whereas using DMSO a decrease of ratio *Ss*/*Rs* was measured respect to the value without solvent (Table 4), due to a decrease of specific constant for the *S* form, remaining unchanged for the *R* form. Finally we tested the behaviour of the mutant L212P in acetonitrile, obtaining a slight increase of the ratio *Ss*/*Sr* with respect the value measured without solvents, from 6.6 to 7.4.

4. Conclusions

The study of behaviour of enzymes in different conditions such as temperature, pH, presence of salts and/or organic solvents may be a preparatory phase to understand the potential of enzymes in biotechnological application. By now, many enzymes have been described soluble in pure organic solvents, more stable there than in water and show different catalytic properties, generally reduced activity but altered specificity [39–41]. Systems made of homogeneous aqueous–organic solvent mixtures are used in catalysis when the substrates are not completely soluble in water, and they may alter the synthesis/hydrolysis equilibrium and the enantioselectivity [42]. In this light, the nature of organic solvent used causes changes in the properties of the reaction medium which can determine different conformational flexibility, deformation of the enzyme [43], and different solubility and polarization of the substrates.

The ester hydrolysis reaction is a nucleophilic substitution which involves a carbocation intermediate, anything that can facilitate this will speed up the catalytic reaction. The addition of solvents to the reaction can stabilize ionic intermediates in the case of aprotic solvents; and to solvate the leaving group in the case of protic solvents, among these there are water and alcohols, which will also act as nucleophiles [37]. In this work, we observed that ethylene glycol (polyprotic) is less destabilizing than methanol for all proteins; in fact, the half-lives were higher with respect to methanol (Tables S3 and S4), also the activity in the presence of increasing percentage of solvent (v/v) was higher in ethylene glycol than in methanol (Figs. S3 and S4). In the case of aprotic solvents no direct correlation was observed, for instance, while Aes showed an high half-life in both DMSO and DMF, EST2 half-life was similar to Aes in DMSO, but 10 fold less in DMF. In terms of kinetic parameters (Table S6) the aprotic solvents gave increased specific constants for *Psy*HSL and Aes due to essentially an increase in k_{cat}. In the case of EST2 and AFEST an increase of k_{cat} and K_M values was observed, with consequent decrease of specific constants.

The activity and stability of the tested enzymes was altered by all solvents tested; from a kinetic point of view, dimethyl formamide, dimethyl sulfoxide, methanol and ethylene glycol enhance the activity ($k_{cat)}$ of all enzymes; parallelly it was observed a general and slight increase in the K_M values suggesting a reduction of the substrate affinity. These effects are not unexpected because organic solvents might change local or global polarity of the enzyme and therefore they could stabilize the surface binding site for substrate or they might remove or change the distribution of water molecules in the active site that in turn could have an effect on k_{cat} and K_M. At substrate level, the solvents might give some conformational differences or have a mere inhibitory effect [28]. For the same reasons the organic solvents might have a different effect on the enantiomer substrate (*RS*)-*p*-nitrophenyl chloropropionate because the *R* or the *S* form could interact better with EST2 enzyme and as consequence give a different rate of hydrolysis or a different affinity. In the model case analysed here, the mutation L212P concerns an exposed residue in the active site likely to be involved in slight modifications [26], which in turn help the *S* form of substrate to have a better interaction with the enzyme ultimately leading to an increase of activity. These alterations could be easily mimicked by the so called "medium engineering" as reported here (Table 4). If we assume that for L212P mutant the enzyme conformation is optimized for the *S* form, the presence of organic solvents could have a negative or slight positive effect on the catalysis because the organic solvent could interfere with the optimal active site conformation.

In this light, we could explain why we obtained only a slight increase in affinity of *S* form in presence of acetonitrile for the mutant L212P and the inversion of ratio of activity when dimethyl formamide was used.

The highest protein stability of EST2 and AFEST in all tested solvents, is in good agreement with previous knowledge about properties of (hyper)thermophilic enzymes; accordingly *Psy*HSL seemed to be less stable in presence of solvents, in agreement with its lower thermal stability; in other words these two properties: thermal and solvent stability are strictly related suggesting a common denaturation pathway in which molecular flexibility is a fundamental determinant of enzyme denaturation, and worth to be taken into account when planning to study specific biotransformation reactions.

Appendix A. Supplementary data

Supplementary data associated with this article can be found, in the online version, at http://dx.doi.org/10.1016/j.molcatb.2012.06.002.

References

[1] A.M. Klibanov, Trends Biochem. Sci. 14 (1989) 141–144.
[2] A.M. Klibanov, Adv. Appl. Microbiol. 29 (1983) 1–28.
[3] T.J. Ahern, A.M. Klibanov, Science 228 (1985) 1280–1284.
[4] S.E. Zale, A.M. Klibanov, Biochemistry 25 (1986) 5432–5444.
[5] G. Carrea, S. Riva, Angew. Chem. Int. Ed. Engl. 39 (2000) 2226–2254.
[6] A. Zacks, A.M. Klibanov, Science 224 (1984) 1249–1251.
[7] D.B. Volkin, A. Staubli, R. Langer, A.M. Klibanov, Biothechnol. Bioeng. 37 (1991) 843–853.
[8] K. Xu, K. Griebenow, A.M. Klibanov, Biotechnol. Bioeng. 56 (1997) 485–491.
[9] L.M. Simon, M. Kotorman, G. Garab, I. Laczko, Biochem. Biophys. Res. Commun. 280 (2001) 1367–1371.
[10] C. De Santi, M.L. Tutino, L. Mandrich, M. Giuliani, E. Parrilli, P. Del Vecchio, D. de Pascale, Biochimie 92 (2010) 949–957.
[11] R. Peist, A. Koch, P. Bolek, S. Sewitz, T. Kolbus, W. Boos, J. Bacteriol. 179 (1997) 7679–7686.
[12] G. Manco, E. Adinolfi, F.M. Pisani, G. Ottolina, G. Carrea, M. Rossi, Biochem. J. 332 (1998) 203–212.
[13] G. Manco, E. Giosuè, S. D'Auria, P. Herman, G. Carrea, M. Rossi, Arch. Biochem. Biophys. 373 (2000) 182–192.
[14] E. Krejci, N. Duval, A. Chatonnet, P. Vincens, J. Maussoliè, Proc. Natl. Acad. Sci. U.S.A. 88 (1991) 6647–6651.
[15] D. Langin, H. Laurell, L. Stenson-Holst, P. Belfrage, C. Holm, Proc. Natl. Acad. Sci. U.S.A. 90 (1993) 4897–4901.
[16] H. Hemilä, T.T. Koivula, I. Palva, Biochem. Biophys. Acta 1210 (1994) 249–253.
[17] T. Hotelier, L. Renault, X. Cousin, V. Negre, P. Marchot, A. Chatonnet, Nucleic Acids Res. 32 (database issue) (2004) D145–D147.
[18] J.L. Arpigny, K.E. Jaeger, Biochem. J. 343 (1999) 177–183.
[19] R.F. Rekker, The Hydrophobic Fragmental Constant, Pharmacochemistry Library, vol. 1, Elsevier, New York, 1977.
[20] Y.L. Khmelnitsky, V.V. Mozhaev, A.B. Belova, M.V. Sergeeva, K. Martinek, Eur. J. Biochem. 198 (1991) 31–41.
[21] M.N. Gupta, R. Batra, R. Tyagi, A. Sharma, Biotechnol. Prog. 13 (1997) 284–288.
[22] C. Reichardt, Angew. Chem. Int. Ed. 18 (1979) 98–110.
[23] J.A. Riddick, W.B. Bunger, T.K. Sakano, Organic Solvents. Physical Properties and Methods of Purification, 4th ed., Wiley, New York, 1986.
[24] K. Egorova, G. Antranikian, Review 8 (2005) 649–655.
[25] G. Manco, L. Mandrich, M. Rossi, J. Biol. Chem. 276 (2001) 37482–37490.
[26] G. Manco, G. Carrea, E. Giosuè, G. Ottolina, G. Adamo, M. Rossi, Extremophiles 6 (2002) 325–331.
[27] A. Kurata, M. Fujita, A.M. Mowafy, H. Kamachi, T. Kurihara, N. Esaki, J. Biosci. Bioeng. 105 (2008) 429–431.
[28] G. Zandonella, L. Haalck, F. Spener, K. Faber, F. Faltauf, A. Hermetter, Eur. J. Biochem. 231 (1995) 50–55.
[29] L. Mandrich, E. Caputo, B.M. Martin, M. Rossi, G. Manco, J. Biol. Chem. 277 (2002) 48241–48247.
[30] R.J. Leatherbarrow, Staines, Erithacus Software, UK, 1992.
[31] L. Mandrich, G. Manco, M. Rossi, E. Floris, T. Jansen-van den Bosch, G. Smit, J.A. Wouters, Appl. Environ. Microbiol. 72 (2006) 3191–3197.
[32] P.J. Haney, J.H. Buldak, C.I. Reich, C.R. Wouse, G.J. Olsen, Proc. Natl. Acad. Sci. U.S.A. 96 (1999) 3578–3583.
[33] C. Veille, G.J. Zeikus, Microbiol. Mol. Biol. Rev. 65 (2001) 1–43.
[34] C. Gerday, M. Aittaleb, J.L. Arpigny, E. Baise, J.P. Chessa, G. Garsoux, I. Petrescu, G. Feller, Biochim. Biophys. Acta 1342 (1997) 119–131.
[35] T. Farias, L. Mandrich, M. Rossi, G. Manco, Protein Pept. Lett. 14 (2007) 165–169.
[36] T.H. Lowery, K.S. Richardson, Mechanism and Theory in Organic Chemistry, 3rd ed., Harper Collins Publisher, New York, 1987.
[37] K.S. Peters, Chem. Rev. 107 (2007) 859–873.
[38] Q. Shao, Y. Fan, L. Yang, Y. Qin Gao, J. Chem. Phys. 136 (2012) 115101–115109.
[39] S. Torres, G.R. Castro, Food Technol. Biotechnol. 42 (2004) 271–277.
[40] D.M. Ruiz, R.E. De Castro, J. Ind. Microbiol. Biotechnol. 34 (2007) 111–115.
[41] L. Costas, V.E. Bosio, A. Pandey, G.R. Castro, Appl. Biochem. Biotechnol. 151 (2008) 578–586.
[42] G.R. Castro, T. Knubovets, Crit. Rev. Biotechnol. 23 (2003) 195–231.
[43] K. Watanabe, S. Ueji, Biotechnol. Lett. 22 (2000) 599–603.

AIChE

Thermal Stabilization of Psychrophilic Enzymes: A Case Study of the Cold-Active Hormone-Sensitive Lipase from *Psychrobacter* sp. TA144

Concetta De Santi
Institute of Protein Biochemistry, CNR, Via Pietro Castellino 111, I-80131 Naples, Italy

Lorenzo Durante
Dept. of Structural and Functional Biology, University of Naples Federico II, Complesso Universitario Monte Sant'Angelo, Via Cintia 4, I-80126 Naples, Italy

Pompea Del Vecchio
Dept. of Chemical Sciences, University of Naples Federico II, Complesso Universitario Monte Sant'Angelo, Via Cintia 4, I-80126 Naples, Italy

Maria Luisa Tutino and Ermenegilda Parrilli
Dept. of Chemical Sciences, University of Naples Federico II, Complesso Universitario Monte Sant'Angelo, Via Cintia 4, I-80126 Naples, Italy

School of Biotechnological Sciences, University of Naples Federico II, Complesso Universitario Monte Sant'Angelo, Via Cintia 4, I-80126, Naples, Italy

Donatella de Pascale
Institute of Protein Biochemistry, CNR, Via Pietro Castellino 111, I-80131 Naples, Italy

DOI 10.1002/btpr.1574
Published online July 2, 2012 in Wiley Online Library (wileyonlinelibrary.com).

Cold-adapted enzymes possess high specific activity at low and moderate temperatures with respect to their mesophilic and thermophilic homologs; it is accepted that they have a less rigid and more flexible structure in the region surrounding the active site. However, the low stability of such molecules could represent the main barrier for their application in some industrial bioprocesses. The aim of this article was to investigate the ability of the naturally occurring osmolytes to increase the thermal stability and the specific activity of the cold-active lipase from Psychrobacter sp. TA144 (PsyHSL), which belongs to the hormone-sensitive lipase group. The effect of trimethylamine N-oxide (TMAO), betaine, and L-proline addition on the activity and thermal stability of PsyHSL was investigated by means of biochemical and biophysical techniques. It turned out that in the presence of 3 M TMAO, the enzyme specific activity enhanced up to 250% at 50°C, while the addition of 1 M TMAO increased the thermostability fivefold at 45°C. Our experiments demonstrated that, even in the case of a psychrophilic enzyme, osmoprotectants, particularly TMAO, addition may be considered an efficient strategy to improve the protein thermal stability and specific activity at higher temperatures. © 2012 American Institute of Chemical Engineers *Biotechnol. Prog.*, 28: 946–952, 2012
Keywords: psychrophilic enzymes, hormone-sensitive lipase, TMAO, betaine, L-proline

Introduction

The available data regarding psychrophilic enzymes pointed out that the high specific activity at low temperatures of these biocatalysts is often associated to a low thermostability, which makes them inclined to loose their activity at moderate and even high temperatures.[1] This feature is considered quite often a detrimental trait for the biotechnological use of such enzymes, and could represent a great limitation in their bioprocess applications.

Correspondence concerning this article should be addressed to Dr. D. de Pascale at d.depascale@ibp.cnr.it.

In naturally evolved enzymes, low temperature activity has been generally associated with low conformational stability as seen by the shift of the apparent temperature optima to lower temperatures and low stability vs. chemical denaturants. These observations suggested a necessary inverse relationship between low-temperature activity and structural stability and stimulated the investigation of structural factors responsible for these characteristics. Comparative investigations of numerous protein models and crystal structures revealed that cold-adapted enzymes tend to exhibit an attenuation of the strength and number of structural factors known to stabilize protein molecules.[2]

During these years, many researchers have centered their activity looking for new strategies to overcome the thermal

lability of psychrophilic proteins. The use of new methodologies (such as site-directed mutagenesis, directed evolution, etc.) led to increase the thermostability of psychrophilic enzymes and very often to decrease their cold-adaptation, that is, the activity at low temperatures.[3] Although the aforementioned are powerful methods, these approaches are laborious, time consuming, and need to be applied to each given biocatalyst. An alternative strategy could be represented by the use of osmolytes to enhance thermal stability of cold-active enzymes.

Osmolytes are small molecules known as chemically stabilizing solutes, and they are commonly found in nature to protect plants, animals, and microorganisms from environmental stresses; they could be divided into three main groups: sugars, amino acids and their derivatives, and methyl ammonium derivatives. The effect of these osmolytes on the protein stability is well known, as they promote the protein stabilization and also induce the refolding of misfolded proteins.[4] Moreover, the effect of osmolytes on the enzymatic activity of enzymes has also been investigated on a number of enzymes.

Jamal et al.[5] classified the osmolytes into two main groups based on their specific action: compatible and counteracting. Although amino acids belong to the first group, that promotes the protein stabilization without any influence on the activity, the counteracting osmolytes (methyl ammonium derivatives) protect proteins against inactivation/denaturation by urea and are believed to cause changes in protein enzymatic activity.[5]

In extremely cold environments, organisms tend to accumulate small organic compounds, such as osmolytes, that lower the colligative freezing point of the cytoplasm and thereby contribute to seasonal freezing resistance. These osmolytes are also called chemical chaperones, as they are able to promote and preserve protein folding and do so without any apparent specificity for protein structure and sequence. Despite recent advances in the understanding of the effect of such compound on the protein stability, little information is available on the role of osmolytes in the increase of thermal stability and enzymatic activity of psychrophilic enzymes.

Trimethylamine N-oxide (TMAO), betaine, and L-proline are naturally occurring osmolytes. The effect of these compounds as chemical chaperones is well known in organisms that withstand extreme environmental conditions[6] and they could help in avoiding cold-denaturation of proteins exposed to harsh conditions. TMAO and betaine belong to the counteracting osmolytes, whereas L-proline belongs to the compatible osmolytes. TMAO is widely used to analyze the effect of osmolytes on conformational stability.[7]

In this article, we report on the effect of several osmolytes, such as TMAO, betaine, and L-proline, on the enzymatic activity/thermal stability of the psychrophilic hormone-sensitive lipase from *Psychrobacter sp*. TA144 (after called *Psy*HSL),[8] which belongs to the "H" block in the ESTHER database (http://bioweb.ensam.inra.fr/ESTHER/general?what=index). We focused our attention on *Psy*HSL as the region surrounding the active site is homologous to the human HSL.[9] In our previous report, we established that, as most psychrophilic enzymes, *Psy*HSL showed a high catalytic activity at very low temperatures associated with a very low thermal stability at temperatures exceeding 40°C.

Herein, we report that the addition of TMAO and betaine increase the specific activity at higher temperatures and led the protein to be significantly more thermostable at 45°C up to 5 h of incubation.

Materials and Methods

Materials and analytical procedures

Tris–HCl buffer 20 mM pH 8.0 was used for CD spectra, whereas Tris–HCl buffer 100 mM pH 8.0 was used for kinetic measurements. The osmolytes TMAO, betaine (*N*,*N*,*N*-trimethylglycine), L-proline were purchased from Sigma Chemical and they were used at a concentration of 1 M and 3 M. Buffer solutions were prepared by use of distilled water at 18.3 MΩ and filtered through 0.22-μm filters before use.

SDS-PAGE (12.5%) was performed in nondenaturing conditions, without β-mercaptoehtanol and avoiding heat-denaturation treatment of the samples. The sample was incubated at 35°C for 1 h in the presence of 3 M TMAO just before loading. "Page ruler prestained protein ladder"(Fermentas) was used as the molecular weight standard.

PsyHSL purification

Recombinant *Psy*HSL was purified from inclusion bodies by use of the protocol as described in De Santi et al.[8] The purified enzyme was routinely stored at −20°C in the presence of 20% glycerol used as stabilizing agent.

Enzyme thermal stability: PsyHSL optimal temperature studies

The enzymatic activity of *Psy*HSL was assayed at 35, 40, 45, and 50°C in the absence and in the presence of TMAO, betaine, and L-proline at final concentrations of 1 and 3 M. The substrate used for this analysis was *p*NP-pentanoate, dissolved in acetonitrile, at a final concentration of 100 μM in a reaction mixture of 100 mM Tris–HCl pH 8.0, containing 3% acetonitrile. The amount of enzyme for each assay was 5 μg and the specific activity (U/mg) was calculated.[8]

PsyHSL thermostability studies

To study the effect of osmolytes on the thermostability of *Psy*HSL, pure enzyme (0.2 mg/mL) was incubated in sealed glass tubes at the different temperatures in 100 mM Tris–HCl pH 8.0 in the presence of TMAO, betaine, and L-proline at a final concentration of 1 M. The activity of the psychrophilic protein was then assayed in the range of temperature from 4°C to 50°C.

Aliquots were withdrawn each hour starting from 1 to 5 h and assayed at 35°C. All assays were done in duplicate and the residual percentage activity was determined. The measurement of esterase activity was performed using *p*NP-pentanoate, in standard condition as described above.

CD measurements

CD measurements were performed by means of a Jasco J-715 spectropolarimeter equipped with a Peltier type temperature control system (Model PTC-348WI). The molar ellipticity $[\theta]$ expressed in deg cm^2 dmol^{-1}, was calculated in the far-UV region from the equation: $[\theta] = (\theta)\text{obs}\cdot\text{mrw}/10\cdot l\cdot C$, where (θ)obs is the ellipticity measured in degrees, mrw is the mean residue molecular weight, (109.1 Da) for *Psy*HSL enzyme, C is the protein concentration in g mL^{-1} and l is

Table 1. Specific Activity of *Psy*HSL at Different Temperatures

Sample	Specific Activity (U/mg) 35°C	Specific Activity (U/mg) 40°C	Specific Activity (U/mg) 45°C	Specific Activity (U/mg) 50°C
*Psy*HSL buffer	41.3 ± 0.6	40.9 ± 0.1	22.2 ± 0.1	7.56 ± 0.3
1 M TMAO	25.6 ± 0.1	36.0 ± 0.2	40.1 ± 0.2	14.5 ± 0.1
3 M TMAO	16.3 ± 0.1	16.7 ± 0.2	17.1 ± 0.2	19.1 ± 0.1
1 M betaine	40.0 ± 0.2	37.9 ± 0.3	36.3 ± 0.1	6.18 ± 0.2
3 M betaine	25.6 ± 0.3	32.0 ± 0.1	34.1 ± 0.1	12.5 ± 0.1
1 M proline	3.7 ± 0.1	2.8 ± 0.3	0.80 ± 0.3	0.61 ± 0.1
3 M proline	2.8 ± 0.5	2.4 ± 0.4	2.38 ± 0.4	0.44 ± 0.2

The enzymatic assays were performed in the presence of different osmolytes. The activity was measured using *p*NP-pentanoate at a final concentration of 100 μM in 0.1 M Tris–HCl pH 8.0, containing 3% acetonitrile.

the optical path length of the cell in cm. In the near-UV region, the molar ellipticity $[\theta]$ was calculated per protein molar concentration (m) using the equation $[\theta] = (\theta)\text{obs}\cdot 100/\text{mL}$. CD spectra were recorded using 0.1-cm path length cells and a protein concentration of about 0.1 mg/mL in the far-UV region; 0.5-cm path length cells and protein concentration of about 2 mg/mL were instead used in the near-UV region. They were recorded at constant temperature with a time constant of 4 s, a 2-nm bandwidth, and a scan rate of 20 nm/min, signal-averaged over at least three scans, and baseline corrected by subtracting a buffer spectrum. Thermal unfolding curves were recorded in the temperature mode, by following the changes of the CD signal in the near-UV region, at 278 nm, with a scan rate of 1.0°C/min.

Results

Effect of osmolytes on the optimum assay temperature of PsyHSL

Standard assay conditions for *Psy*HSL were previously determined and the apparent optimal temperature resulted to be 35°C in standard assay conditions.[8] Osmolytes that are the object of this study (i.e., L-proline, betaine, and TMAO) were added to the standard assay buffer at two final concentrations (1 and 3 M) and *Psy*HSL specific activity was determined at four different temperatures (35, 40, 45, and 50°C). At temperatures lower than 30°C, the presence of tested osmolytes did not influence the *Psy*HSL specific activity (data not shown). The results are presented in Table 1, where kinetic data are reported as specific activity, and the *Psy*HSL specific activity was recorded at the respective temperature in standard conditions. In all tested conditions, the specificity of the enzyme resulted to be almost the same, demonstrating that the presence of osmolytes does not affect the enzyme substrate affinity (data not shown).

It turned out that L-proline addition had a drastic negative effect on *Psy*HSL activity at all tested temperatures. At temperatures 35°C and 40°C, TMAO or betaine addition (regardless of their respective final concentration) induced a slight reduction of *Psy*HSL specific activity. Interestingly, at the higher temperatures, the addition of either betaine or TMAO to the assay mix resulted in an increase of enzyme specific activity, up to 253%, for example, when the enzyme was tested in the presence of 3 M TMAO at 50°C.

Effect of osmolytes on thermal stability of PsyHSL

The thermal stability of *Psy*HSL was evaluated in the presence of osmolytes and the results obtained were compared to those obtained in the same buffer without osmoprotectants. As observed in Figure 1, the addition of all tested osmolytes induced a notable thermal stabilization of *Psy*HSL, the most efficient one being TMAO added at 1 M final concentration. Indeed, the enzyme retained its activity after 5 h incubation up to 45°C, whereas at 50°C and after 3 h of incubation the enzyme preparation was almost totally inactivated. A similar *Psy*HSL behavior was observed in the presence of 1 M betaine or 1 M L-proline; the addition of both osmolytes stabilized the enzyme, which retained its activity for 5 h up to 35°C. At higher temperatures, the added osmolytes only partially counteracted the enzyme thermal denaturation, and L-proline was found to be more effective than betaine because 2.5% residual activity was still detected after 5 h of incubation of *Psy*HSL at 50°C (Figure 1).

CD measurements

Circular dichroism measurements were performed to investigate on the changes in conformational stability of the enzyme induced by the presence of high concentrated solutions of osmolytes. Figure 2 shows the CD spectra obtained in the absence and in the presence of osmolytes and at different temperatures. In Figure 2A, we show the CD spectra of *Psy*HSL enzyme at pH 8.0 in a dilute buffer solution of 20 mM Tris–HCl, recorded at 5°C (filled circles) and 70°C (open circles). The analysis of the CD spectrum obtained at 5°C by means of Dichroweb[10,11,12] provided the values of 31% α-helix, 33% β-strand content for *Psy*HSL as previously reported.[8] The CD spectrum of *Psy*HSL recorded at 70°C appears different from a typical random coil spectrum, as it still showed a broad negative band in the far-UV region. This might be due to a residual non-native secondary structure or to the presence of soluble aggregates of the enzyme formed at high temperatures. Thermal denaturation curves recorded by following the change in the CD signal at 222 nm did not show a sigmoidal trend suggesting that the secondary structure gradually decreases at increasing of temperature. This prevented us from studying the thermal denaturation of *Psy*HSL by changes in the far-UV CD spectra. The CD spectra of *Psy*HSL enzyme at pH 8.0 in a diluted buffer solution of 20 mM Tris–HCl and 20% glycerol (filled squares), the same buffer in the presence of 1 M betaine (open squares), 1 M TMAO (open circles), 3 M TMAO (filled circles) are reported in Figure 2B. The comparison of spectra suggested that the protein secondary structure was unaffected by the presence of 1 M and 3 M TMAO as well as of 1 M betaine. The high absorption of 1 M L-proline solutions below 230 nm prevented the registration of trustworthy CD spectra of *Psy*HSL in the presence of that osmolyte. The CD spectra of *Psy*HSL in the presence of 1 M TMAO at the temperatures of the activity assay are reported in

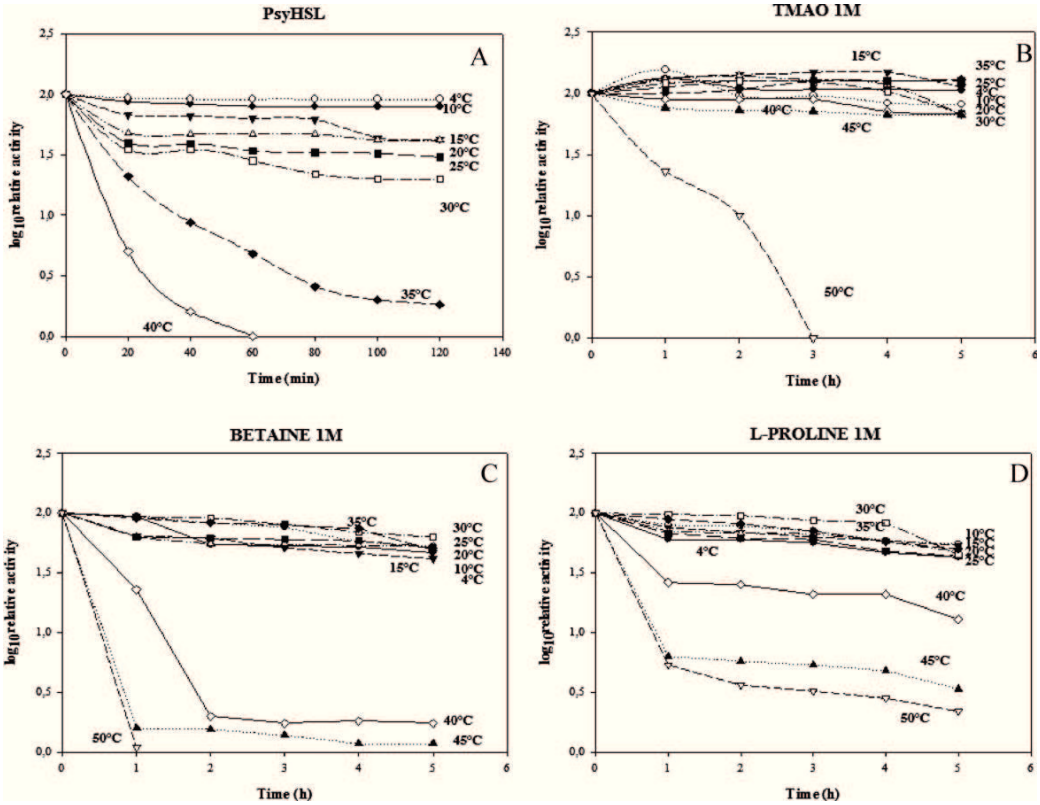

Figure 1. Thermostability of *Psy*HSL at various temperatures, such as 4°C (•), 10°C (○), 15°C (▼), 20°C (△), 25°C (■), 30°C (□), 35°C (◆), 40°C (◇), 45°C (▲), and 50°C (grad).

The enzyme was incubated, in the absence of any osmolyte (A), in the presence of TMAO 1 M (B), betaine 1 M (C), and L-proline 1 M (D), in 0.1 M Tris–HCl pH 8.0 at the indicated temperatures for the times indicated. The residual activity was measured at 35°C in standard condition.

Figure 2C. As can be observed, the negative CD band remains constant up to 50°C. The overall results of the *Psy*HSL far-UV CD spectra suggest that its secondary structure does not change in the presence of osmolytes and slightly changes at increasing temperature even in the presence of osmolytes. No thermal transition curves can be recorded by following changes of CD bands in that region. This finding is not surprising considering the high flexibility of psychrophilic proteins. The contribution of aromatic side chains to the near-UV CD spectra of proteins can be used as sensitive probe of protein conformation. *Psy*HSL possesses 14 tyrosine and six tryptophan residues, therefore, the near-UV CD spectrum is representative of the ordered spatial arrangement of these residues in the native protein conformation. The near-UV CD spectra at 5°C (thick line) and at 70°C (thin line) of *Psy*HSL enzyme at pH 8.0 in 100 mM Tris-HCl buffer and 20% glycerol are reported in Figure 3. The spectrum at 5°C is characterized by a large positive band centered at 278 nm that flattens at 70°C thus suggesting that the increase of temperature strongly perturbs the protein tertiary structure. Near-UV CD spectra of *Psy*HSL at 5°C in the presence of osmolytes (Figure 4; Panel A 1 M TMAO, Panel B 1 M Betaine, and Panel C 1 M L-proline) show the same large positive band centered at 278 nm showing that the tertiary structure does not change in the presence of osmolytes. Each spectrum shown in Figure 4 was recorded at the temperatures of the activity assay (see Figures 4A–C). These spectra highlight a decrease of the positive band at increasing temperature, suggesting the reduction of *Psy*HSL tertiary structure. Thermal denaturation profiles, recorded by following the CD signal at 278 nm at a constant scanning rate of 1°C/min, although appeared noisy, showed sigmoid patterns. Thermal denaturation curves of *Psy*HSL are reported in Figure 5. The experimental values are reported as fraction of unfolded molecules assuming that the CD signals at 5°C and 70°C correspond to the native and denatured state, respectively. The denaturation temperature values were evaluated from the inflection point of each sigmoid curve and are reported in Table 2. According to its psychrophilic nature, *Pys*HSL possesses a low thermal stability. In fact, its denaturation temperature at pH 8.0 in 20 mM Tris–HCl buffer was 35.5°C (see Table 2), whereas in the presence of 20% glycerol it increased to 43.5°C. The effect of osmoprotectants was tested in the presence of 20% glycerol. The addition of 1 M L-proline did not affect the denaturation temperature, which remained almost the same (43.5°C, Table 2). A further increase of the denaturation temperature was observed on the addition of 1 M betaine in the buffer, enhancing temperature up to 44.5°C. As far as the addition of 1 M TMAO was concerned, a significant increase in denaturation temperature was observed, where the value increased to 50.5°C (see Table 2). These results strongly suggest that in the presence of high concentration of osmolytes, the protein seems to be more resistant against the action of temperature. Among the osmolytes, TMAO emerged as the most effective. These observations agree

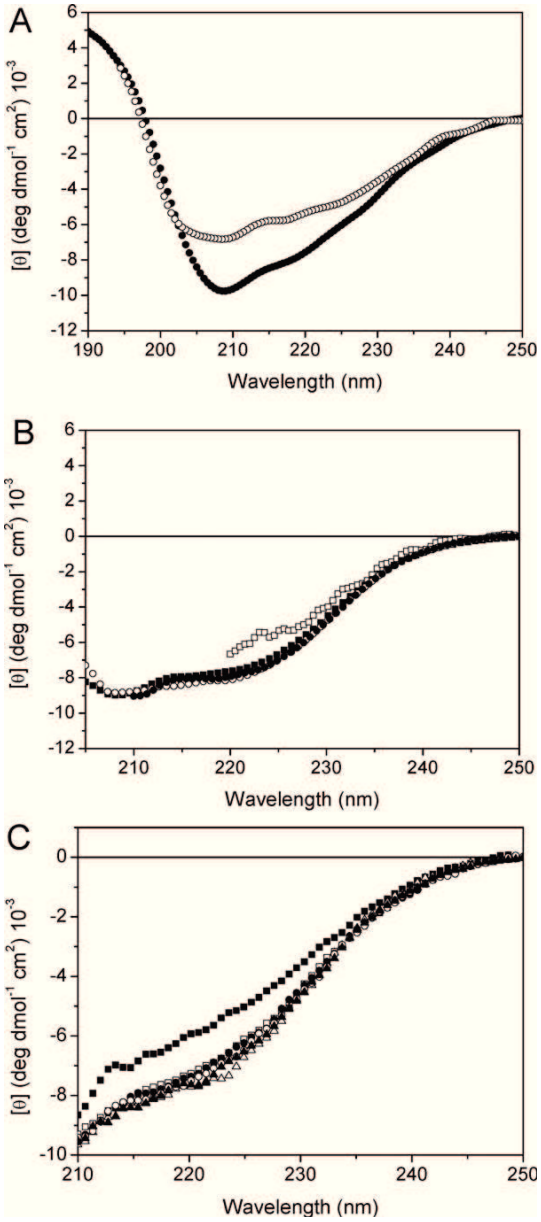

Figure 2. (A) Far-UV CD spectra of *Psy*HSL enzyme in 20 mM Tris–HCl buffer, pH 8 at 5°C (•) and at 70°C (○); (B) far-UV CD spectra at 5°C in 20 mM Tris–HCl, pH 8, 20% glycerol (■), 1 M betaine (□), 1 M TMAO (○), 3 M TMAO (•); (C) far-UV CD spectra of *Psy*HSL enzyme in 20 mM Tris–HCl buffer, pH 8 in the presence of 1 M TMAO at 5°C (△), 35°C (▲), 40°C (○), 45°C (•), 50°C (□), and 70°C (■).

with the results obtained from specific activity. The temperature-induced denaturation of *Psy*HSL was found to be irreversible, both in the absence and in the presence of osmolytes.

Discussion

Several reports have shown that the conformational stability of protein in vitro increased in the presence of osmolytes.[13–15] The mechanism, however, is not yet completely understood. The effect of the osmolytes on protein stability should be directed by a fine equilibrium between their ability

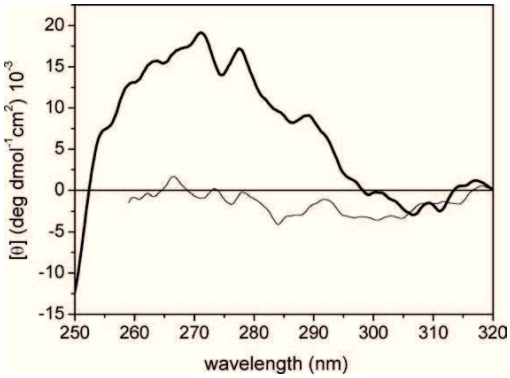

Figure 3. Near-UV CD spectra of *Psy*HSL in 100 mM Tris–HCl buffer, pH 8, 20% glycerol at 5°C (thick line) and 70°C (thin line).

to enhance/reduce the surface tension of water and their capability to either encourage preferential hydration for proteins or exert direct binding to the protein surface amino acids. Indeed, two models are used to describe the effect of osmolytes on protein stability.[5] The binding model speculates that an increase in the osmolyte-induced stability arises from the preferential hydration (or exclusion of the osmolyte) leading to a shift in the denaturation equilibrium, toward the native state.[16,17] The second model, the excluded volume model, is based on the idea that osmolytes limit the conformational freedom of proteins by driving them to their most compact native state (catalytically most efficient form). The decrease in conformational freedom arises from steric repulsions between the protein and the osmolyte.[5]

Despite significant advances in understanding the effect of osmolytes on protein stability, its consequent effects on the activity of enzymes has not been examined. In fact, protein stability and enzyme activity are strictly related, but up until today it is not clear how this link is retained in the presence of osmolytes.

Several reports demonstrated that hyperthermophilic and mesophilic enzymes are stabilized by the same osmolytes.[13,14,18] Concerning psychrophilic proteins, there is up to now only one recent report on the cold-adapted enzyme, Deseasin MCP-01,[19] in which the use of TMAO as a stabilizing agent is reported to increase the thermostability while keeping enzyme psychrophilic characters (such as structural flexibility and high catalytic efficiency at low temperatures). Indeed, to be active in cold environments, psychrophilic proteins often display a fragile structure and are generally considered to be less stable and more susceptible to heat- and cold-denaturation.[2]

The aim of this work was to explore the ability of the natural occurring osmolytes to increase thermal stability and the specific activity of the hormone sensitive lipase from *Psychrobacter sp*. TA144. *Psy*HSL was produced in *E. coli* cells and recovered in quite homogeneous form (about 90–95% pure).[8] The purified recombinant *Psy*HSL exhibited stability in the presence of 20% glycerol, and efficiently converted several substrates into products. The recombinant psychrophilic enzyme exhibited an apparent optimal temperature equal to 35°C with respect to the substrate *p*NP-pentanoate and when the optimal pH 8 was used. Stability studies demonstrated that the enzyme behaves as a classical psychrophilic one,[20] as it was characterized by a pronounced thermal-lability. Indeed, it retained almost 100% of activity

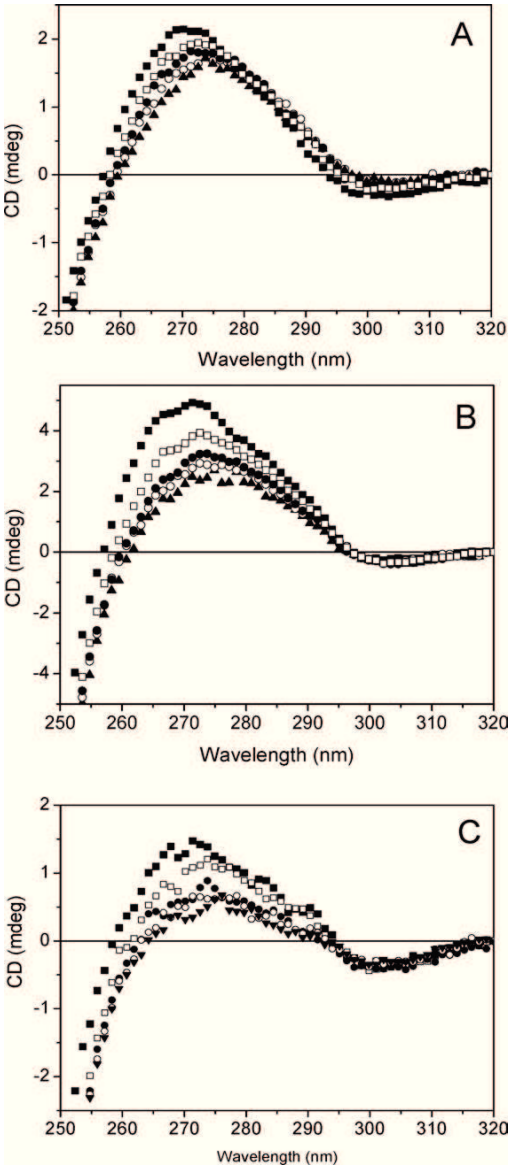

Figure 4. Near-UV CD spectra of *Psy*HSL enzyme in 20 mM Tris–HCl buffer in the presence of (A) 1 M TMAO, (B) 1 M betaine and (C) 1 M L-proline at 5°C (■), 35°C (□), 40°C (•), 45°C (○), and 50°C (▲).

after 2 h of incubation at 4°C, whereas a gradual loss of activity was observed when the enzyme was incubated at temperature above 30°C, with practically no remaining activity after only 20 min of incubation at 40°C (Figure 1A).

In this work, we investigated the ability of TMAO, betaine, and L-proline to alter the thermal stability and specific activity of *Psy*HSL. The addition of different osmolytes seemed to have different effects on the optimal temperature of *Psy*HSL, as TMAO and betaine addition at 1 M and 3 M at final concentration shifted the optimal temperature by about 15°C with respect to any compound addition. The best increase of *Psy*HSL specific activity was about 250% in the presence of TMAO (3 M) at 50°C (Table 1).

We also investigated the effect of osmolytes on thermostability of *Psy*HSL. Our results demonstrated that *Psy*HSL

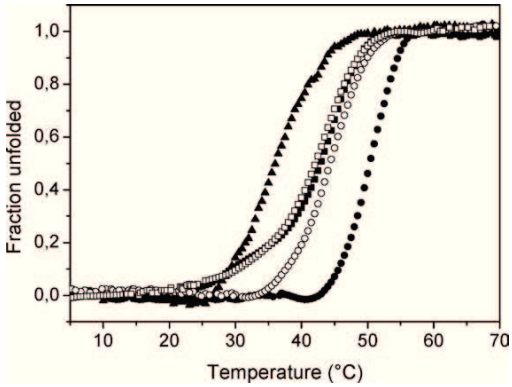

Figure 5. Thermal-induced unfolding profiles of *Psy*HSL in 20 mM Tris–HCl buffer, pH 8 (▲), 20 mM Tris–HCl buffer, pH 8, 20% glycerol without osmolyte (■), in 20 mM Tris–HCl buffer, pH 8 with 1 M L-proline (□), in 20 mM Tris–HCl buffer, pH 8 with 1 M betaine (○) and with 1 M TMAO (•). Measurements were performed as described in "Materials and Methods" section.

Table 2. Denaturation Temperature of *Psy*HSL Enzyme in Different Buffer Conditions at pH 8.0 and in the Presence of Different Osmolytes Obtained by Recording the Molar Ellipticity at 278 nm

	T_d (°C)
20 mM Tris-HCl	35.5
20 mM Tris-HCl + 20% glycerol (Buffer A)	43.5
Buffer A + L-proline 1 M	43.5
Buffer A + betaine 1 M	44.5
Buffer A + TMAO 1 M	50.5

retained its catalytic activity after 5 h of incubation at 45°C in the presence of 1 M TMAO (Figure 1B), whereas the cold-active enzyme displayed a narrow stability loosing its activity after 20 min of incubation at 40°C in the absence of any osmolytes (Figure 1A). The stabilization of *Psy*HSL by TMAO addition resulted in a noticeable increase of the protein thermostability ($t_{1/2}$), which enhanced by fivefold at 45°C (data not shown).

A *Psy*HSL CD spectroscopic analysis by far-UV CD spectra was performed (Figure 2), and it demonstrated that the osmolytes addition did not affect the *Psy*HSL secondary structure (Figure 2B). The near-UV spectra (Figure 3) demonstrated that the protein tertiary structure (recorded at 5°C) was destroyed at 70°C, thus allowing us to use the near-UV spectra to study the protein thermal denaturation profiles in the presence of osmolytes (Figure 4).

As shown in Table 2, *Psy*HSL displayed a melting temperature of 35.5°C, in good agreement with other cold-active enzymes.[20] When 20% glycerol was added, the melting temperature increased up to 43.5°C, and further addition of osmolytes, such as betaine and TMAO increased the melting temperature up to 44.5°C and 50.5°C, respectively (Figure 5). It has been previously demonstrated that osmolytes can independently affect proteins;[5] hence, their effects can be additive. This may be the reason why many organisms use multiosmolyte systems. Based on our findings, we can hypothesize that the presence of both glycerol and TMAO notably enhanced the melting temperature of the *Psy*HSL by about 15°C and thus its stability.

The overall results reported in this article show that the effects of osmolytes on the thermal stability and enzymatic

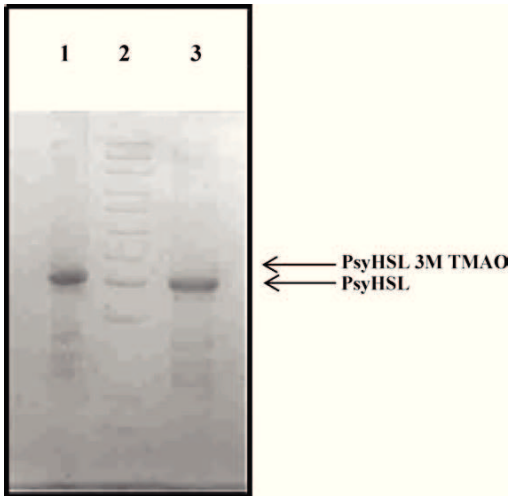

Figure 6. SDS-PAGE (12% acrylammide) of *Psy*HSL in the presence (Lane 1) and in the absence (Lane 3) of TMAO 3 M; Lane 2, molecular weight markers.

efficiencies were similar to those described for mesophilic enzymes.[15] In particular, it was demonstrated that TMAO improved the specific activity and protein thermal stability at high temperature. To clarify the molecular mechanisms responsible for TMAO effect on *Psy*HSL, the binding capability of TMAO to psychrophilic protein was investigated by nondenaturing SDS-PAGE gel electrophoresis (Figure 6), incubating the protein at 35°C for 1 h in the presence of 3 M TMAO before loading the sample. In the presence of TMAO, the protein showed a lower electrophoretic mobility, likely due to the TMAO holding capability (Figure 6) thus allowing us to hypothesize that TMAO shows preferential hydration in the vicinity of *Psy*HSL.

Our results suggest that TMAO molecules are inclined to be excluded from the enzymes surface and oblige the protein to assume a densely folded structure, with a minimum of surface area exposed to water molecules. The steric repulsions between the protein and the osmolytes limit the conformational freedom of proteins by driving them to their most compact native state. This hypothesis could justify the detrimental effect of TMAO addition on *Psy*HSL specific activity at moderate temperatures (35°C and 40°C), especially observed at higher TMAO concentration (3 M, see Table 1).

Our findings confirmed that TMAO can be used as an efficient stabilizing agent to boost the thermostability of cold-adapted enzymes. Compared with mutation and modification, addition of TMAO is an uncomplicated and consistent method to improve both thermostability and specific activity of a cold-adapted enzyme and it may represent a novel approach to increase the thermal stability of psychrophilic protein in view of their application in several bioprocesses. This provides new prospects for exploiting cold-adapted enzymes.

Acknowledgments

The authors thank Dr. Luigi Mandrich (Institute of Protein Biochemistry, National Research Council, Naples, Italy) for helpful discussion. This work was supported by P.N.R.A. (Programma Nazionale di Ricerche in Antartide 2009–2011).

Literature Cited

1. Tutino ML, di Prisco G, Marino G, de Pascale D. Cold-adapted esterases and lipases: from fundamentals to application. *Protein Pept Lett*. 2009;16:1172–1180.
2. Marx JC, Collins T, D'Amico S, Feller G, Gerday C. Cold-adapted enzymes from marine Antarctic microorganisms. *Mar Biotechnol*. 2007;9:293–304.
3. Siddiqui KS, Poljak A, Cavicchioli R. Improved activity and stability of alkaline phosphatases from psychrophilic and mesophilic organisms by chemically modifying aliphatic or amino groups using tetracarboxy-benzophenone derivatives. *Cell Mol Biol (Noisy-le-grand)*. 2004;50:657–667.
4. Holthauzen LM, Auton M, Sinev M, Rösgen J. Protein stability in the presence of cosolutes. *Methods Enzymol*. 2011;492:61–125.
5. Jamal S, Poddar NK, Singh LR, Dar TA, Rishi V, Ahmad F. Relationship between functional activity and protein stability in the presence of all classes of stabilizing osmolytes. *FEBS J*. 2009;276:6024–6032.
6. Gong H, Croft K, Driedzic WR, Ewart KV. Chemical chaperoning action of glycerol on the antifreeze protein in rainbow smelt. *J Thermal Biol*. 2011;36:78–83.
7. Attri P, Venkatesu P, Lee MJ. Influence of osmolytes and denaturants on the structure and enzyme activity of alpha-chymotrypsin. *J Phys Chem B*. 2010;114:1471–1478.
8. De Santi C, Tutino ML, Mandrich L, Giuliani M, Parrilli E, Del Vecchio P, de Pascale D. The hormone-sensitive lipase from Psychrobacter sp. TA144: new insight in the structural/functional characterization. *Biochimie*. 2010;92:949–957.
9. Hotelier T, Renault L, Cousin X, Negre V, Marchot P, Chatonnet A. ESTHER, the database of the alpha/beta-hydrolase fold superfamily of proteins. *Nucleic Acids Res*. 2004;32:D145–D147.
10. Compton LA, Johnson WC. Analysis of protein circular dichroism spectra for secondary structure using a simple matrix multiplication. *Anal Biochem*. 1986;155:155–167.
11. Whitmore L, Wallace BA. DICHROWEB: an online server for protein secondary structure analyses from circular dichroism spectroscopic data. *Nucleic Acids Res*. 2004;32:668–673.
12. Sreerama N, Woody RW. Estimation of protein secondary structure from circular dichroism spectra: comparison of CONTIN, SELCON, and CDSSTR methods with an expanded reference set. *Anal Biochem*. 2000;287:252–260.
13. Santos H, da Costa MS. Compatible solutes of organisms that live in hot saline environments. *Environ Microbiol*. 2002;4:501–509.
14. Faria TQ, Lima JC, Bastos M, Maçanita AL, Santos H. Protein stabilization by osmolytes from hyperthermophiles: effect of mannosylglycerate on the thermal unfolding of recombinant nuclease from *Staphylococcus aureus* studied by picosecond time-resolved fluorescence and calorimetry. *J Biol Chem*. 2004;279:48680–48691.
15. Mello CC, Barrick D. Measuring the stability of partly folded proteins using TMAO. *Protein Sci*. 2003;12:1522–1529.
16. Timasheff SN. The control of protein stability and association by weak interactions with water: how do solvents affect these processes? *Annu Rev Biophys Biomol Struct*. 1993;22:67–97.
17. Timasheff SN. Protein–solvent preferential interactions, protein hydration, and the modulation of biochemical reactions by solvent components. *Proc Natl Acad Sci USA*. 2002;99:9721–9726.
18. Mukaiyama A, Koga Y, Takano K and Kanaya S. Osmolyte effect on the stability and folding of a hyperthermophilic protein. *Proteins: Struct Funct Bioinform*. 2008;71:110–118.
19. He HL, Chen XL, Zhang XY, Sun CY, Zou BC, Zhang YZ. Novel use for the osmolyte trimethylamine N-oxide: retaining the psychrophilic characters of cold-adapted protease deseasin MCP-01 and simultaneously improving its thermostability. *Mar Biotechnol*. 2009;11:710–716.
20. Kulakova L, Galkin A, Nakayama T, Nishino T, Esaki N. Cold-active esterase from *Psychrobacter* sp. Ant300: gene cloning, characterization, and the effects of Gly>Pro substitution near the active site on its catalytic activity and stability. *Biochem Biophys Acta*. 2004;1696:59–65.

Manuscript received Dec. 6, 2011, and revision received Jun. 7, 2012.

Fish & Shellfish Immunology 33 (2012) 1183–1191

Contents lists available at SciVerse ScienceDirect

Fish & Shellfish Immunology

journal homepage: www.elsevier.com/locate/fsi

A piscidin-like antimicrobial peptide from the icefish *Chionodraco hamatus* (Perciformes: Channichthyidae): Molecular characterization, localization and bactericidal activity

Francesco Buonocore [a,*], Elisa Randelli [a], Daniela Casani [a], Simona Picchietti [a], Maria Cristina Belardinelli [a], Donatella de Pascale [b], Concetta De Santi [b], Giuseppe Scapigliati [b]

[a] Department for Innovation in Biological, Agro-food and Forest Systems, University of Tuscia, Largo dell'Università, 01100 Viterbo, Italy
[b] Institute of Protein Biochemistry, CNR, Via Pietro Castellino 111, 80131 Napoli, Italy

ARTICLE INFO

Article history:
Received 14 May 2012
Received in revised form
29 August 2012
Accepted 4 September 2012
Available online 13 September 2012

Keywords:
Antimicrobial peptides
Chionodraco hamatus
Real-time PCR
Mast cells
Bactericidal activity

ABSTRACT

Antimicrobial peptides (AMPs) are considered one of the most ancient components of the innate immune system. They are able to exert their protection activity against a variety of microorganisms, and are widely distributed in both vertebrates and invertebrates. In this paper we focused on an AMP identified in the Antarctic teleost *Chionodraco hamatus*, an icefish species. The cDNA sequence of the AMP, named chionodracine, is comprised of 515 bp and translates for a putative protein precursor of 80 amino acids, with a signal peptide of 22 amino acids. The structural features evidenced in the primary sequence of chionodracine lead to the inclusion of the peptide in the antimicrobial family of piscidins. The analysis by real-time PCR of the basal gene transcripts of chionodracine in different icefish tissues showed that the highest expression was found in gills, followed by head kidney. The chionodracine expression levels in head kidney leukocytes were up-regulated *in vitro* both by LPS and poly I:C, and *in vivo* by LPS. A putative chionodracine mature peptide was synthesized and employed to obtain a polyclonal antiserum, which was used in immunohistochemistry of gills sections and revealed a significant positivity associated with mast cells. The bactericidal activity of the peptide was investigated and found significant against Antarctic psychrophilic bacteria strains (*Psychrobacter* sp. TAD1 and TA144), the Gram-positive *Bacillus cereus*, and at a lesser extent against the Gram-negative *Escherichia coli*. Interestingly, the haemolytic activity of chionodracine was tested *in vitro* on human erythrocytes and no significant lysis occurred until peptide concentration of 50 μM.

1. Introduction

The antimicrobial peptides (AMPs) are considered as fundamental components of the innate immune system of eukaryotes, where they contribute actively to the control of microbial invasion [1–3]. The specificity of AMPs against pathogens is extremely wide towards species and strains of bacteria, fungi, parasites and viruses [4]. Due to their considerable genetic variability, AMPs cannot be easily classified on the base of size, structure or physico-chemical parameters, thus several categories have been described as peptides having common structures such as α-helices, β-sheets, extended structures and loop structures [5,6]. The expression of AMPs is usually high in primary barriers tissues of the organism, such as the skin in mammals, to prevent colonization by pathogens [4,7,8]. The potential use of AMPs as antimicrobial drugs can be significant [9,10], but it is actually limited by the knowledge of their mechanisms of action that has not been fully understood [11].

During recent years the research on fish AMPs showed an exponential increase, and a large number of AMPs sequences have been cloned and characterized (for a review see Ref. [12]). Among these it should be mentioned pleurocidin from winter flounder (*Pleuronectes americanus*) [13], piscidin or moronecidin from hybrid striped bass (white bass, *Morone chrysops*, female, x striped bass, *M. saxatilis*, male) [14] and dicentracine from sea bass (*Dicentrarchus labrax*) [15]. Fish AMPs have been shown to be biologically active against both bacterial and viral fish pathogens [16,17] and, therefore, could be of importance in fish farming for their impact on the immune system responses [18]. The tissue localization of fish AMPs has been performed in sea bream, where piscidin were demonstrated to be primarily present in mast cells and professional

* Corresponding author. Tel.: +39 0761 357644; fax: +39 0761 357111.
E-mail address: fbuono@unitus.it (F. Buonocore).

1050-4648/$ – see front matter © 2012 Elsevier Ltd. All rights reserved.
http://dx.doi.org/10.1016/j.fsi.2012.09.005

phagocytic granulocytes [19]. Other AMPs from fish, like hepcidins, have been shown to also function as iron regulators [20], thus suggesting others possible functional roles of these molecules.

The icefish *Chionodraco hamatus* is a teleost species belonging to the Channichthyidae family, one of the six extant families of Antarctic Perciformes [21]. These fishes display interesting physiological adaptations, like antifreeze glycoproteins [22] and peculiar immunoglobulins [23,24]. In addition, icefishes show a complete absence of haemoglobin and of functional blood erythrocytes [25]. Such peculiarities make *C. hamatus* an interesting model of study for the immune system adaptation to low environmental temperatures.

In this paper we describe in *C. hamatus* the identification of a cDNA coding for a piscidin-like AMP, named chionodracine, and investigated levels of gene expression in different tissues, as well as the *in vitro* and *in vivo* gene regulation after stimulation with LPS or poly I:C. Moreover, a polyclonal antibody has been produced against the putative mature sequence of the peptide and used to investigate the presence of chionodracine in the gills, a tissue in direct contact with the outside. Indeed, the gills are the major route of entry for pathogen invasion after epithelial damage [19,26–28] and thus are considered important immune organs capable of mounting robust immune responses [29]. Finally, we evaluated the bactericidal activity of chionodracine against both fish and human bacteria, for a possible use of the peptide as an antimicrobial drug.

2. Materials and methods

2.1. Cloning of an AMP from C. hamatus

C. hamatus specimens were collected with nets in January–February 2011 during the XXVI Italian Antarctic Expedition organized by the National Program of Antarctic Research (P.N.R.A.) at the Italian Antarctic Base, Terra Nova Bay, Ross sea (Mario Zucchelli Station). After collection, fish were placed in tanks, transported to aquaria and kept in running seawater.

Head kidney leukocytes were obtained from *C. hamatus* after disrupting the organ by teasing on a 100 μm cell strainer and total RNA was isolated from leukocytes using Trisure (Bioline). The RNA was resuspended in DEPC-treated water and cDNA prepared with the BioScript RNase H minus (Bioline) enzyme using the protocol described in Ref. [30]. Two degenerate primers (PISFW 5′-CT(T/C) TCTTGTGCT GTCGATGGT-3′ and PISRV 5′-GCA(A/T/G)GA(G/T/C) CAG(C/G)AAG(A/C)(T/G)C (G/A/T)GC-3′) corresponding to conserved regions of known AMP genes were used in PCR on the cDNA. Controls for the presence of DNA contamination were performed using the cDNA as template and with β-actin primers that span an intron. Reactions were conducted using a Mastercycler (Eppendorf). The cycling protocol was one cycle of 94 °C for 5 min, 35 cycles of 94 °C for 45 s, 48 °C for 45 s, 72 °C for 45 s, followed by one cycle of 72 °C for 10 min. PCR products (15 μl) were visualized on 1% (w/v) agarose gels containing ethidium bromide (10 ng/ml) using hyperladder IV (Bioline) as size marker. The PCR product was purified using a QIAquick Gel Extraction Kit (QIAgen), inserted into the pGEM-T Easy vector (Promega) and transformed into competent JM109 *Escherichia coli* cells. Plasmid DNA from at least five independent clones was purified using the Wizard Plus SV Minipreps DNA Purification System (Promega) and sequenced using MWG DNA Sequencing Services. Sequences generated were analysed for similarity with other known sequences using the BLAST [31] program.

Further primers were designed based on the initial icefish AMP sequence for 5′- and 3′-rapid amplification of cDNA ends (RACE-PCR) (3′AMFW: 5′-CTTTCTTGTGCTGTCGATGGT-3′ and 5′AMRV: 5′-GCAAGACCAGCAAGAGCGGC-3′). cDNA was synthesized from head kidney RNA with a First-strand cDNA Synthesis kit (GE Healthcare) following the manufacturer's instructions. For 3′ RACE-PCR, cDNA was transcribed using an oligo-dT adaptor primer (5′-CTCGA-GATCGATGCGGCCGCT$_{15}$-3′). PCR was performed with the 3′AMFW primer and the oligo-dT adaptor primer. For 5′ RACE-PCR, cDNA was transcribed from total RNA using the oligo-dT primer, treated with *E. coli* RNase H (Promega), purified using a PCR Purification Kit (QIAgen), and tailed with poly(C) at the 5′ end with terminal deoxynucleotidyl transferase (TdT, Promega). PCR was performed with 5′AMRW primer and an Oligo-dG primer (5′-GGGGGGIGG-GIIGGGIIG-3′). Sequencing of amplified products and similarity searches were performed as described above. The icefish AMP sequence was analysed for the presence of a signal peptide using SignalP software [32]. Alignment of the icefish AMP amino acid sequence to other known molecules from other species was carried out using the BioEdit sequence alignment package. A phylogenetic tree was constructed by the "neighbor joining" method using MEGA 4.1 Software [33] on full-length amino acid sequences using the normal default parameters and as test of reliability the bootstrap test with 10,000 replications and 60,000 random seeds. The identified AMP was named chionodracine.

2.2. Basal expression of chionodracine

To study the chionodracine basal expression, four icefishes were sampled and leucocytes from different tissues (spleen, head kidney (HK), gills, liver, gut) obtained as described above. Total RNA was isolated from each tissue separately with Trisure (Bioline), resuspended in DEPC-treated water and used for real-time quantitative PCR without pooling the tissue samples coming from the different fishes. For reverse transcription, the BioScript RNase H minus (Bioline) enzyme was used with the protocol described in Ref. [30]. The expression level of chionodracine transcripts was determined with an Mx3000P™ real-time PCR system (Stratagene) equipped with version 4.1 software and using the Brilliant SYBR Green Q-PCR Master Mix (Agilent Technologies) following the manufacturer's instructions, with ROX as internal passive reference dye. Specific PCR primers were designed for the amplification of about 200 bp products from chionodracine (AMPFW: 5′-CTTGTGCTGTCGATGGTGGT-3′; AMPRV: 5′-CTGCACCTTCATCGCT TCCC-3′) and 18 S ribosomal RNA (18SFW: 5′-CCAACGAGCTGCTGACC-3′; 18SRV: 5′-CCGTTACCCGTG-GTCC-3′), used as a house-keeping gene. Ten nanogram of cDNA template was used in each PCR reaction. The PCR conditions were: 95 °C for 10 min, followed by 35 cycles of 95 °C for 45 s, 52 °C for 45 s and 72 °C for 45 s. Triplicate reactions were performed for each template cDNA and the template was replaced with water in all blank control reactions. The analysis was carried out using the endpoints method option that causes the collection of the fluorescence data at the end of each extension stage of amplification. A relative quantitation has been performed, comparing the levels of the target transcript (chionodracine) to a reference transcript (calibrator, the tissue with the lowest chionodracine expression, in this case the liver). A normalizer target (18 S ribosomal RNA) is included to correct for differences in total cDNA input between samples. The results are expressed as the mean ± SD of the results obtained from the four considered fishes.

2.3. In vitro and in vivo expression of chionodracine after stimulations

The *in vitro* chionodracine expression was studied using leukocytes isolated from four icefishes (100 g of weight) head kidney (HK) cells cultured in L-15 medium (Gibco) containing 10% FCS, adjusted to 1×10^5 cells/ml and incubated for 4 h and 24 h with: (1) 5 μg ml^{-1} of lipopolysaccharide (LPS from *E. coli* 0127:B8, Sigma); (2) 50 μg ml^{-1} poly I:C (Sigma). The cell control samples were

stimulated with L-15 alone. Total RNA was isolated with Tripure (Roche), resuspended in DEPC-treated water and used for real-time quantitative PCR without pooling the samples coming from the different fishes. The primers and the real-time PCR conditions were the same as described in the above section, except that the calibrator for this experiment was the time 0 control.

The *in vivo* chionodracine expression was studied after intraperitoneally injection of 500 μl of L-15 medium (Gibco) brought to 600 mOsm kg^{-1}, that is the osmolarity of Antarctic Teleosts as determined in previous experiments and due to their particular adaptation to low temperatures, and containing 100 μg of LPS in four icefishes. The four control fishes were injected with L-15 only. After 24 h, leukocytes were isolated from head kidney and total RNA extracted as described above. The primers and the real-time PCR conditions were the same as described in the above section, except that the calibrator for this experiment was the time 0 control.

The results of all the experiments were expressed as the mean ± SD of the results obtained from four fishes and the differences from the control were considered significant if $p < 0.05$ using the two-way ANOVA analysis followed by the Bonferroni's post-test for the *in vitro* stimulations and the one-way ANOVA followed by the Bonferroni's post test for the *in vivo* stimulation.

2.4. Production of a polyclonal antibody, and enzyme-linked immunosorbent assay (ELISA)

Three Balb/C mice (eight weeks old from Charles River Laboratories, Lecco, Italy) were acclimatized for one week in the animal facilities of the University of Tuscia (Viterbo, Italy). These mice were immunized by intraperitoneal injection of the selected chionodracine peptide (22 amino acids long) conjugated with the carrier protein KLH (Primm srl, Milano, Italy). The immunization procedure was as follows: (1) $t = 1$ day injection of 50 μg of KLH-peptide diluted with 50 μl of PBS (Sigma) plus 50 μl of complete Freund's adjuvant; (2) $t = 13$ days and $t = 25$ days injection of 50 μg of KLH-peptide diluted with 50 μl of PBS (Sigma) plus 50 μl of complete Freund's adjuvant; (3) $t = 36$ days and $t = 47$ days injection of 50 μg of KLH-peptide diluted with 50 μl of PBS (Sigma); $t = 60$ days bled of the mice. The sera isolated by centrifugation contain the polyclonal antibodies against the chionodracine peptide. The sera from the three different mice were successively analysed by enzyme-linked immunosorbent assay (ELISA) to investigate their activity against the peptide. The procedure was similar as previously described [34]. Briefly, the 96-well microtitres plates (Cellstar, Greiner Bio-One) were filled with 100 μl/well of 50 mM carbonate–bicarbonate buffer (pH 9.4) containing 0.2 μg of the chionodracine peptide and coated overnight at 4 °C. After washing and blocking procedures, 100 μl of serial dilutions of mice serum (from 1:10 to 1:100) were added to the wells and incubated for 16 h at 25 °C. After washing, antibody binding was detected with horseradish peroxidase-conjugated goat anti-mouse IgG antibody (1: 200 dilution) using a colouration with H_2O_2 and 4-chloro-1-napthol. The results were recorded by reading the optical density (OD) value at 492 nm by an automated ELISA reader (Labsystems Multiskan MS). Each point was performed in triplicate.

2.5. Immunohistochemistry

Gills from three different fish were fixed for 7 h at 4 °C in Bouin's fixative. After embedding in paraplast, blocks were serially sectioned at a thickness of 7 μm. Some sections were stained with May-Grümwald Giemsa while others were used for the immunohistochemistry.

Immunohistochemistry (IHC) was performed by ABC-peroxidase with nickel enhancement as previously described [35]. In summary, serial sections 7 μm-thick were incubated for 18 h at room temperature with the mouse polyclonal antiserum named Pab Ch1 (diluted 1:100 in PBS 0.1 M, pH 7.3 containing 0.1% sodium azide) that recognizes the selected mature chionodracine peptide. Pre-immune serum substituted the primary antibody in negative controls. Thereafter, sections were incubated for 60 min with biotinylated horse anti-mouse IgG serum (Vector Labs., Burlingame, USA) diluted 1:1000 with PBS containing 0.1% sodium azide and 1% BSA, followed by incubation for 60 min with avidin-biotinylated peroxidase complex (ABC, Vectastain Elite, Vector). After rinses and staining (diaminobenzidine and nickel enhancement), sections were dehydrated, mounted and examined under bright-field illumination.

In each specimen, multiple sets of consecutive sections were differentially immunostained with the antibody above mentioned. Cell measurements were obtained using a computer-assisted image analysis system which includes a Zeiss microscope equipped with a colour video camera (Axio Cam MRC, Arese, Milano Italy) and a software package (KS 300 and AxioVision). Measurements of cell diameter (major axis) were performed in 5 specimens and pooled. Mean and SD were calculated.

2.6. Antibacterial activity assays

The antimicrobial activity of the chionodracine peptide was examined against four Gram-negative bacterial strains (*Psychrobacter* sp. TAD1, *Psychrobacter* sp. TA144, *Pseudomonas aeruginosa*, *E. coli* BL21(DE3)) and one Gram-positive bacterial strain (*Bacillus cereus*). The strains were kindly provided by the Department of Organic Chemistry and Biochemistry, University of Naples and the Institute of Protein Biochemistry, CNR, Naples. Luria Bertani (LB) medium was used for the growth of the four Gram-negative bacteria while peptone 1.5% was used for the growth of *B. cereus*. All bacteria were grown aerobically and cultured at different temperatures: 15 °C (*Psychrobacter* sp. TAD1, *Psychrobacter* sp. TA144) for 48 h, 25 °C (*E. coli* and *B. cereus*) for 48 h and 37 °C (*E. coli*, *B. cereus* and *P. aeruginosa*) for 16 h.

The peptide was dissolved in sterile deionized water to reach a final concentration of 1 mg/ml. The minimum inhibitory concentration (MIC) was determined by using serial dilutions of the peptide, with LB medium or Peptone 1.5%, using a volume of 500 μl per tube. The final concentration of the peptide ranged from 1.25 to 20 μM. Two internal controls were used: an *E. coli* BL21 (DE3) culture without the peptide and an *E. coli* culture with the peptide pOVA (as internal control) that has no antimicrobial properties. The tubes were inoculated with an appropriate bacterial cell suspension to reach a final concentration of 10^5 cfu/ml for each strain. After incubation at different temperatures (as reported above), the MIC was defined as the lowest concentration of the peptide that totally inhibited the growth.

To measure the minimum bactericidal concentration (MBC), an aliquot (200 μl) of the cell suspension was taken from the tubes above the MIC and the cell suspension was plated on an LB agar plate after incubation at the different temperatures (see above) for 48 h. MBC was defined as the lowest concentration of the peptide at which more than 99.9% of the cells were killed compared with a non-treated control.

2.7. Haemolytic activity assay

The haemolytic assay was performed as indicated by Belokoneva et al. [36]. In brief, a 2.5% (v/v) suspension of human red blood cells from healthy donors in PBS (Gibco) was incubated with serial

dilutions of the selected peptide. Red blood cells were counted by a haemocytometer and adjusted to approximately to about 8.0×10^6 cells/ml. Erythrocytes were successively incubated at 37 °C for 2 h with the chionodracine peptide in distilled water (positive control), PBS (negative control) and with the different concentrations of peptide (from 50 μM to 0.5 μM with seven dilutions). Each point has been made in triplicate. The supernatant was separated from the pellet with a centrifugation at $1500 \times g$ for 5 min; the absorbance was measured at 570 nm. The relative OD compared to that of the positive control defined the percentage of haemolysis.

3. Results

3.1. Chionodracine cloning and sequence analysis

The first PCR was made with primers PISFW and PISRV and gave only one product of the expected size (146 bp) that, after sequencing, showed homology with other known AMP sequences in Teleosts (data not shown). 3′-RACE-PCR performed with primer 3′AMFW (based on the initial 146 bp sequence) and oligo-dT adaptor primer gave a product of 407 bp. 5′-RACE-PCR performed with 5′AMRW (based on the initial 146 bp sequence) and the Oligo-dG primer gave a product of 289 bp. The full-length cDNA (EMBL accession number FR718953) of the chionodracine is comprised of 515 bp from the three overlapping products with a coding sequence of 240 bp and was confirmed by PCR using primers that amplify the complete coding sequence (data not shown). The 3′-UTR contained a polyadenylation signal (AATAAA) 18 bp upstream of the poly(A) tail. The presence of a putative signal peptide of 22 amino acids (cleavage site between Ala^{22} and Phe^{23}) and no N-glycosylation and O-glycosylation sites was evidenced using predictive methods.

A multiple alignment of the chionodracine amino acid sequence with other known AMP sequences from Teleosts was assembled (Fig. 1) to investigate the conserved amino acid residues. The chionodracine, due to its primary structure, should be included in the antimicrobial family of piscidins, which comprises moronecidins and pleurocidins [37]. Pleurocidin was found in the skin mucus of winter flounder (*P. americanus*) [13] and was predicted to assume an amphipathic alpha-helical conformation [38]. These AMPs are produced as pre-pro-peptides and, after secretion, the mature peptides should be obtained due to the processing of the pro-peptides by local proteases, as it happens in mammals [39]. From the alignment in Panel A of Fig. 1, it has been evidenced that only few amino acids are conserved between all the pleurocidin and moronecidin sequences and these amino acids are mainly located in the signal peptide region. In the Panel B of Fig. 1, the chionodracine has been aligned only with the components of the Moronidae family and, in this case, the number of conserved amino acids is much higher and they are present all along the sequence.

Phylogenetic analysis (Fig. 2) performed using amino acid sequences showed that chionodracine grouped with the AMP sequences of the other Teleosts belonging to the Perciformes Order. Another branch comprises the Teleosts of the Pleuronectiformes Order, whereas the two representatives of the Scorpaeniformes and Gadiformes Orders are in a separate cluster.

3.2. Basal and in vitro and in vivo chionodracine expression

Chionodracine mRNA basal levels have been analysed in different organs and tissues of *C. hamatus* specimens (Fig. 3). The products of real-time PCR were loaded on agarose gels to exclude the presence of non-specific amplicons and single bands of the expected sizes were obtained. The highest chionodracine expression was found in gills, followed closely by head kidney. The lowest mRNA levels were evidenced in liver, followed by gut. Chionodracine expression was studied on icefish leukocytes from head kidney after 4 h and 24 h of stimulation with LPS and poly I:C. The stimulation with LPS (Panel A, Fig. 4) shows a slight decrease of chionodracine expression after 4 h and a slight increase after 24 h, both being not statistically significant. The stimulation with poly I:C (Panel A, Fig. 4) shows a slight increase of chionodracine transcripts levels after 4 h and a much higher increase at 24 h, both being statistically significant. Differently, the *in vivo* treatment with LPS

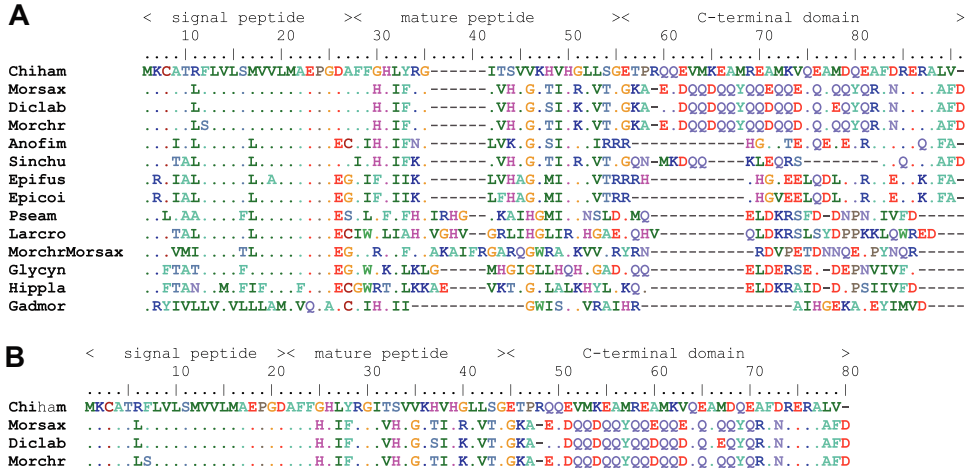

Fig. 1. Alignment of the predicted icefish AMP amino acid sequence with other known AMP molecules from Teleost fishes. The conserved amino acid residues in the different sequence are indicated by dots. The different identified domains are evidenced above the alignment. Accession numbers: dicentracine (sea bass, *Dicentrarchus labrax*) AAP58960; moronecidin (white bass, *Morone chrysops*) AAL57318; moronecidin (striped sea bass, *Morone saxatilis*) AF385583; moronecidin (Mandarin fish, *Siniperca chuatsi*) AAV65044; chionodracine (icefish, *Chionodraco hamatus*) FR718953; piscidin-like (brown-marbled grouper, *Epinephelus fuscoguttatus*) ADE06665; epinecidin (orange-spotted grouper, *Epinephelus coioides*) AY705494; dicentracin (sablefish, *Anoplopoma fimbria*) ACQ58110; piscidin-4 (*Morone chrysops* × *Morone saxatilis*) ADP37959; piscidin (Atlantic cod, *Gadus morhua*) FJ917596; pleurocidin-like (witch flounder, *Glyptocephalus cynoglossus*) AY273177; pleurocidin-like (Atlantic halibut, *Hippoglossus hippoglossus*) AAP55801; pleurocidin-like (winter flounder, *Pseudopleuronectes americanus*) AY282498; piscidin-like (large yellow croaker, *Larimichthys crocea*) EU741827. (For interpretation of the references to colour in this figure legend, the reader is referred to the web version of this article.)

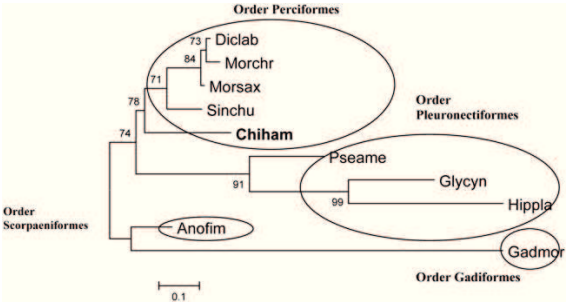

Fig. 2. Phylogenetic tree showing the relationship between chionodracine sequence with other known Teleosts AMP molecules. The tree was constructed by the "neighbour-joining" method using the bootstrap test with 10,000 replications. 0.1 Indicates the genetic distance.

(Panel B, Fig. 4) shows a significant and relevant increase of chionodracine expression after 24 h of stimulation.

3.3. Immunohistochemical detection of chionodracine in gills

The ELISA assay performed on sera of the three mice immunized with chionodracine revealed that mice responded to immunization with a medium serum titre of 1:100 (data not shown), and the one showing highest positivity in ELISA (Pab Ch1) was used for immunohistochemical detection in icefish gills.

The general morphology of the *C. hamatus* gill was characterized by thin and slender filament (or primary lamellae) with elongated secondary lamellae. An epithelial sheet covered filaments and secondary lamellae, in particular a pluristratified primary epithelium covered the filament while a monostratified secondary epithelium covered the secondary lamellae. In the primary and secondary epithelia among the different cell types could be observed immune cells such as lymphocytes and mast cells (Fig. 5). These latter were predominantly found in the primary lamellae and in the interlamellar regions (Fig. 5). They were also distributed in the secondary epithelium. Chionodracine-positive cells were identified by comparing serial sections of gills that were stained with May-Grümwald Giemsa or Pab Ch1 antibody. This comparison evidenced that mast cells were consistently chionodracine-positive and were localized within the primary lamellae, in the interlamellar regions and in the secondary lamellar epithelia (Fig. 5). These mast cells were very numerous large cells (cell diameter 8.43 ± 1.13) in which the immunostaining was distributed throughout the cytoplasm (Fig. 5). No reaction was observed in the control sections (Fig. 5).

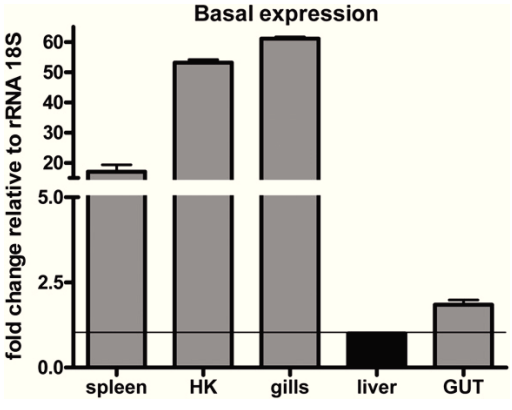

Fig. 3. Chionodracine basal expression in different tissues. Chionodracine mRNA levels were expressed as a ratio relative to rRNA 18 S levels in the same samples after real-time PCR analysis using the tissue with the lowest expression (liver) as calibrator. Data were expressed as the mean ± SD.

3.4. Antibacterial activity assays

The concentrations of the selected chionodracine peptide required to inhibit and to kill the bacterial strains (MIC) are summarized in the Table 1. Among all bacterial strains tested, *E. coli* and *B. cereus*, grown at 25 °C, were the most susceptible to the peptide followed, very closely, by psychrophilic bacteria. At 37 °C, the MIC value for *E. coli* and *B. cereus* were 4-fold and 2-fold higher, respectively, compared to their growth at 25 °C. MBC values were also determined and showed in Table 1. These values were the same of the corresponding MIC values except for *E. coli*. This indicates that the chionodracine peptide is able to exert bacteriostatic rather than bactericidal activity against these two strains.

3.5. Haemolytic activity assay

The haemolytic effect of the selected chionodracine peptide has been tested on human erythrocytes to investigate its capacity to induce membrane lysis. Seven concentrations have been used (starting from a concentration of 50 μM with successive dilutions) that correspond for the first point to 120 μg of peptide (Fig. 6). The percentage of haemolysis is very low for all tested concentrations and it reaches the maximum (0.8%) with the highest concentration value (50 μM).

4. Discussion

The resistance of pathogens to antibiotics is an increasing threat to public health, leading to a demand of new classes of antibiotics that may overcame this problem [11]. In turn, to avoid or delay as much as possible microbial resistance, it could be a strategy to search for antibiotic substances in environments where the ecology of microbial interactions are markedly different. In this view, and considering that different AMPs have already been discovered in fish species, the aim of our work was to investigate the presence of antibacterial peptides in Antarctic species, namely in the icefish *C. hamatus*.

We have thus identified in this species, by homology cloning, an AMP that we named chionodracine, belonging to the antimicrobial family of piscidins. The peptide displays a relative high sequence identity to its homologous in striped bass, sea bass and white bass.

Investigating basal expression analysis of chionodracine mRNA we evidenced highest levels in the gills. This is in agreement with the consideration that in fish the gills are a main portal for entry of pathogens [7] and, therefore, a strong local immune response is needed in this site to try to avoid the development of a disease. Comparing these results with other Teleosts, it could be evidenced that dicentracine in sea bass [15], epinecidin in orange-spotted grouper [16] and a piscidin from mandarin fish [37] appeared to be highly expressed in head kidney, whereas piscidin-4 peptides are present in high concentrations in gills of striped bass [40].

The expression of chionodracine was also studied *in vitro* and *in vivo* in leukocytes, and obtained results gave us the first clues on the possible biological activity of chionodracine. Indeed, we observed a significant up-regulation after 24 h of stimulation with LPS, a component of the external membrane of the *E. coli*, indicating an involvement of chionodracine in the innate immune responses against bacteria. In addition, also a stimulation with poly I:C, that mimics a double-stranded RNA molecule, was observed after 24 h,

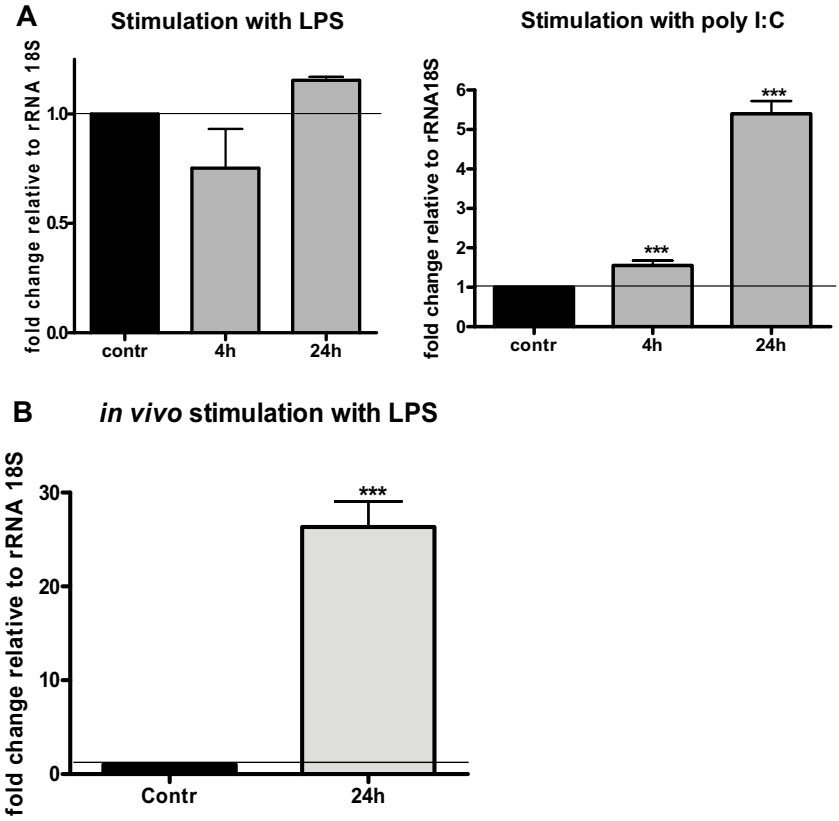

Fig. 4. Chionodracine expression analysis after *in vitro* stimulation with LPS and poly I:C and *in vivo* stimulation with LPS. Panel A: Chionodracine mRNA levels expressed as a ratio relative to rRNA 18 S levels in the same samples after real-time PCR analysis of HK leukocytes stimulated with L15 (control), with 5 μg/ml LPS for 4 and 24 h, and with 50 μg/ml of poly I:C for 4 and 24 h, and normalized against the non-stimulated 0 h control. Data were expressed as the mean ± SD and three asterisks indicates when $p < 0.001$ with respect to the time 0 control. Panel B: Chionodracine mRNA levels expressed as a ratio relative to rRNA 18 S levels after real-time PCR analysis of HK leukocytes stimulated *in vivo* with L15 (control) and with 100 μg of LPS for 24 h and normalized against the non-stimulated 0 h control. Controls and data expression are the same as indicated for Panel A.

thus suggesting an involvement in innate responses against viruses. Similar experiments have been performed *in vivo* in the orange-spotted grouper for epinecidin [16] and in the mandarin fish for a piscidin [37] and in both species a significant increase of expression was found after 6 h of stimulation.

After these encouraging results, we decided to investigate more in detail the putative amino acid sequence of chionodracine to evidence a possible mature antimicrobial peptide. In the alignment of Fig. 1 a prediction of putative mature AMP from the different species is evidenced, although a mature sequence is known only for winter flounder, where pleurocidin was purified from skin [13]. However, some structural features are well defined, as usually antimicrobial peptides are highly amphipathic molecules with hydrophobic and hydrophilic moieties present in different localizations on the surface of the peptide [41]. Therefore, we decided to analyse the primary sequence of our putative mature peptide using some web resources. The server for the prediction of antimicrobial peptides in a protein sequence (AntiBP server http://www.imtech.res.in/cgibin/antibp/antibp1.pl) should give an overall accuracy of about 92% in finding and designing peptide based antibiotics [42] and when used on our sequence the obtained score was quite high (0.817), suggesting a putative high antibacterial activity. Subsequently, the mature sequence has been investigated for its capacity to form an amphipathic α-helical conformation using the server http://rzlab.ucr.edu/scripts/wheel/wheel.cgi created by Don Armstrong and Raphael Zidovetzki. The obtained helical wheel projection is shown in Fig. 7. The chionodracine mature peptide shows two positive charged amino acids, which is a common aspect of most antimicrobial peptides, and it shows in the upper right side of the wheel hydrophobic and hydrophilic amino acids, whereas in the lower left side potentially charged amino acids: therefore the primary sequence possesses all the characteristics needed to form an amphipathic α-helical structure.

The results from structural analyses encouraged the synthesis of a mature peptide to be used for the production of a polyclonal antibody and for other studies. Thus, mice were immunized and a serum was obtained and employed to test by IHC the positivity to chionodracine in gills sections. As expected by the high mRNA expression data, a significant positivity was detected by IHC, and the chionodracine-positive cells resulted to be very similar to mast cells (MC) localized within the primary lamellae, in the inter-lamellar regions and in the secondary lamellar epithelia. This observation is in agreement with previous results, where AMPs were identified in teleost gill epithelial goblet cells [14,43] as well as in immune cells, including neutrophils [44], rodlet cells [45] and mast cells [46,47].

To better understand these results, it should be remembered that in teleosts, MC have been recognized to be important components of not specific immune defence, having populations heterogeneity with varied morphologies, granular content and

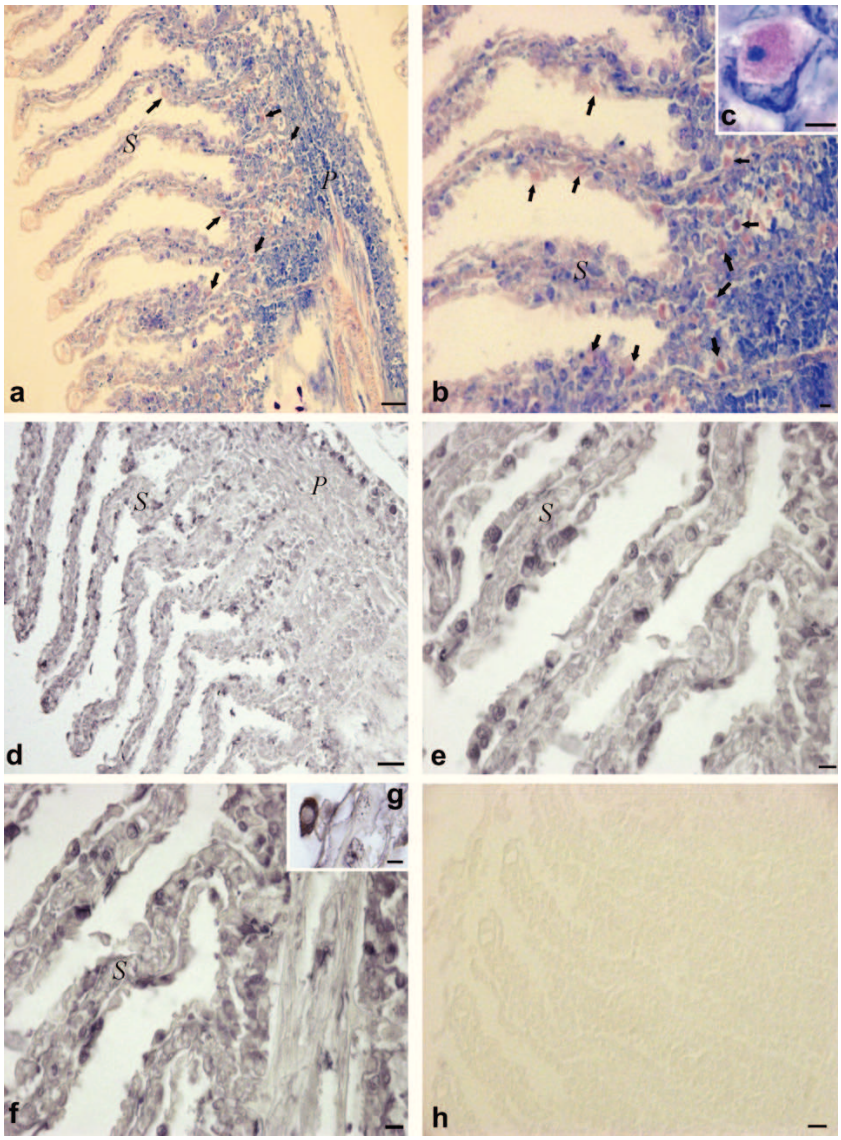

Fig. 5. Histological sections and immunohistochemical localization of chionodracine in the gills of *Chionodraco hamatus*. (a) May-Grümwald Giemsa (MGG) of gill showing within the primary and secondary lamellae several mast cells (arrows). Scale bar = 50 μm. (b) Higher magnification of figure (a) showing the mast cells within the interlamellar regions and in the secondary epithelium (arrows). Scale bar = 10 μm. (c) A mast cell is shown at higher resolution in the insert. Scale bar = 5 μm. (d) Chionodracine-positive cells in the primary and secondary lamellae (arrows). Scale bar = 50 μm. (e) Immunopositive cells prevalent localized in the secondary epithelium. Scale bar = 10 μm. (f) Immunoreactive cells in the interlamellar regions. Scale bar = 10 μm. A chionodracine-positive cell is shown at higher resolution in (g). Scale bar = 2 μm. (h) Negative control showing absence of chionodracine immunoreactivity in gill tissue treated with pre-immune serum. Scale bar = 20 μm. *Key*: *S*: secondary lamella; *P*: primary lamella.

Table 1
Minimum inhibitory concentration (MIC) and minimum bactericidal concentration (MBC) of the chionodracine mature peptide against mesophilic and psychrophilic bacteria at the three different tested temperatures.

Temperature	Species	Gram	MIC (μM)	MBC (μM)
15 °C	*Psychrobacter* sp. TAD1	–	10	10
15 °C	*Psychrobacter* sp. TA144	–	15	15
25 °C	*Escherichia coli*	–	5	30
25 °C	*Bacillus cereus*	+	5	5
37 °C	*Escherichia coli*	–	20	30
37 °C	*Bacillus cereus*	+	10	10
37 °C	*Pseudomonas aeruginosa*	–	ND	ND

response to stimuli, and diverse mediator molecules [48]. The MC have been identified in all vertebrate classes as single-lobed cells containing variable amounts of membrane-bound secretory granules, which store a large series of mediators that in teleost fish are tryptase and histamine. In particular histamine was detected in MC of Perciformes [19], while was absent in Pleuronectiformes, Salmoniformes, Anguilliformes, Cypriniformes and Lepidosireniformes, corroborating the high heterogeneity of MC populations. In addition, increasing evidence supported that in fish the MC are able to secrete AMPs among which the piscidins are the prototypical AMP present in piscine MC [8,14,19,40,43,45,49,50].

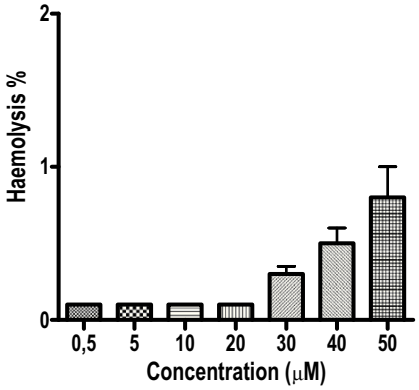

Fig. 6. Haemolytic activity of chionodracine selected peptide against human erythrocytes. Seven different concentrations have been tested, starting from 50 μM with successive dilutions. The values represent the mean ± SD ($n = 3$). A positive control was determined using distilled water and was considered as 100% of haemolysis.

The chionodracine peptide was also employed to investigate a possible biological activity as antibiotic substance, and thus we performed specific antimicrobial assays against two strains of psychrophilic bacteria (*Psychrobacter* sp. TAD1 and *Psychrobacter* sp. TA144), the Gram-negative bacteria *E. coli* and the Gram-positive bacteria *B. cereus* (see Table 1). Taking into consideration the low-temperature Antarctic environment, to study the chionodracine activity we decided to perform further assays growing the *E. coli* and *B. cereus* at lower temperatures than usual (25 °C instead of 37 °C). The result showed that the peptide was more active against both bacteria under these conditions. This could be a first indication that either the peptide is adapted to low temperatures, or that the membranes of the two bacteria change their conformations at low temperatures and could be therefore more easily affected by the peptide. These speculations need more experiments to better elucidate observed activities.

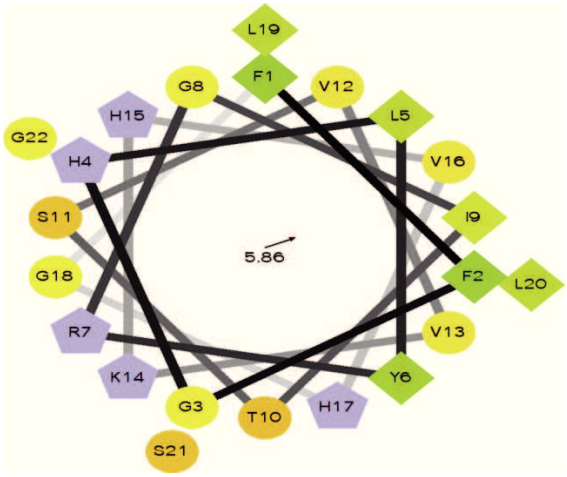

Fig. 7. Helical wheel projection of the chionodracine mature peptide. The hydrophilic residues are presented as circles, hydrophobic residues as diamonds, potentially negatively charged as triangles, and potentially positively charged as pentagons. Hydrophobicity is colour coded: the most hydrophobic residue is green, and the amount of green is decreasing proportionally to the hydrophobicity, with zero hydrophobicity coded as yellow. Hydrophilic residues are coded red with pure red being the most hydrophilic (uncharged) residue, and the amount of red decreasing proportionally to the hydrophilicity. The potentially charged residues are light blue. The black arrow stands for the helical hydrophobic moment. (For interpretation of the references to colour in this figure legend, the reader is referred to the web version of this article.)

For comparison with fish antibacterial peptides, piscidins have potent, broad-spectrum antibacterial and antifungal activity and have strong antiparasitic activity [8,45,49]. With regard to their mechanism of action, piscidins are thought to inhibit the synthesis of the cell wall, nucleic acids, and proteins or even inhibit enzymatic activity of pathogens [51]. Chionodracine, belonging to the family of piscidins, could be then directly involved in the destruction of pathogens as reported for the pleurocidin by Murray et al. [52]. The AMPs in fact have been recognized in regions of active inflammatory response especially due to parasitic and bacterial infections [47,53,54] and in this sense the gills can be considered one of the tissues first exposed to environmental challenges and pathogens, whose ability to mount an immune defence is crucial [8,52].

In the near future, the capacity of the peptide to kill microbes will be further studied on other fish bacteria (like *Vibrio anguillarum*, *Photobacterium damselae* subsp. *piscicida*, etc.) and viruses (like Betanodavirus, etc.) to test its possible use in aquaculture. Furthermore, its activity will be investigated on human bacteria (other than the already tested *P. aeruginosa*, which was not affected by the peptide), virus and fungi specific pathogens to verify the utility as a new antimicrobial drug. This idea was supported by the haemolytic activity assays, showing that the mature peptide did not induced membrane lysis on human erythrocytes at the tested peptide concentrations, thus providing a first pre-requisite for its possible use as antibiotic molecule.

Acknowledgements

This work was supported by the Italian Program of Antarctic Research (Project PROGDEF09_118) which allowed fish collection. Authors are indebted to Dr. Cristiano Papeschi for mouse care and immunization.

References

[1] Andreu D, Rivas L. Animal antimicrobial peptides: an overview. Biopolymers 1998;47:415–33.
[2] Zasloff M. Antimicrobial peptides of multicellular organisms. Nature 2002; 415:389–95.
[3] Bulet P, Stocklin R, Menin L. Anti-microbial peptides: from invertebrates to vertebrates. Immunol Rev 2004;198:169–84.
[4] Lehrer RI, Ganz T. Antimicrobial peptides in mammalian and insect host defence. Curr Opin Immunol 1999;11:23–7.
[5] Lai Y, Gallo RL. AMPed up immunity: how antimicrobial peptides have multiple roles in immune defense. Trends Immunol 2009;30:131–41.
[6] Guani-Guerra E, Santos-Mendoza T, Lugo-Reyes SO, Teran LM. Antimicrobial peptides: general overview and clinical implications in human health and disease. Clin Immunol 2010;135:1–11.
[7] Morris DJ, Adams A, Richards RH. In situ hybridisation identifies the gill as portal of entry for PKK (Phylum Myxozoa), the causative agent of proliferative kidney disease in salmonids. Parasitol Res 2000;86:950–6.
[8] Andrews M, Battaglene S, Cobcroft J, Adams M, Noga E, Nowak B. Host response to the chondracanthid copepod *Chondracanthus goldsmidi*, a gill parasite of the striped trumpeter, *Latris lineata* (Forster), in Tasmania. J Fish Dis 2010;33:211–20.
[9] Hancock RE, Sahl HG. Antimicrobial and host-defense peptides as new anti-infective therapeutic strategies. Nat Biotechnol 2006;24:1551–7.
[10] Easton DM, Nijnik A, Mayer ML, Hancock RE. Potential of immunomodulatory host defense peptides as novel anti-infectives. Trends Biotechnol 2009;27: 582–90.
[11] Wimley WC, Hristova K. Antimicrobial peptides: successes, challenges and unanswered questions. J Membr Biol 2011;239:27–34.
[12] Ravichandran S, Kumaravel K, Rameshkumar G, AjithKumar TT. Antimicrobial peptides from the marine fishes. Res J Immunol 2010;3:146–56.
[13] Cole AM, Weis P, Diamond G. Isolation and characterization of pleurocidin, an antimicrobial peptide in the skin secretions of winter flounder. J Biol Chem 1997;272:12008–13.
[14] Silphaduang U, Noga EJ. Peptide antibiotics in mast cells of fish. Nature 2001; 414:268–9.

[15] Salerno G, Parrinello N, Roch P, Cammarata M. cDNA sequence and tissue expression of an antimicrobial peptide, dicentracin: a new component of the moronecidin family isolated from head kidney leukocytes of sea bass, *Dicentrarchus labrax*. Comp Biochem Physiol B 2007;146:521–9.
[16] Pan C-Y, Chen J-Y, Cheng Y-SE, Chen C-Y, Ni I-H, et al. Gene expression and localization of the epinecidin-1 antimicrobial peptide in the grouper (*Epinephelus coioides*) and its role in protecting fish against pathogenic infection. DNA Cell Biol 2007;26:403–13.
[17] Chia T-J, Wu Y-C, Chen J-Y, Chi S-C. Antimicrobial peptides (AMP) with antiviral activity against fish nodavirus. Fish Shellfish Immunol 2010;28:434–9.
[18] Noga EJ, Ullal AJ, Corrales J, Fernandes JMO. Application of antimicrobial polypeptide host defenses to aquaculture: exploitation of downregulation and upregulation responses. Comp Biochem Physiol D 2011;6:44–54.
[19] Mulero I, Noga EJ, Meseguer J, Garcia-Ayala A, Mulero V. The antimicrobial peptides piscidins are stored in the granules of professional phagocytic granulocytes of fish and are delivered to the bacteria-containing phagosome upon phagocytosis. Dev Comp Immunol 2008;32:1531–8.
[20] Shi J, Camus AC. Hepcidin in amphibian and fishes: antimicrobial peptides or iron regulatory hormones. Dev Comp Immunol 2006;30:746–55.
[21] Near TJ. Estimating divergence times of notothenioid fishes using a fossil-calibrated molecular clock. Antarct Sci 2004;16:37–44.
[22] Bargelloni L, Ritchie PA, Patarnello T, Battaglia B, Lambert DM, Meyer A. Molecular evolution at subzero temperatures – mitochondrial and nuclear phylogenies of fishes from Antarctica (suborder Notothenioidei), and the evolution of antifreeze glycopeptides. Mol Biol Evol 1994;11:854–63.
[23] Scapigliati G, Chausson F, Cooper EL, Scalia D, Mazzini M. Qualitative and quantitative analysis serum immunoglobulins of four Antarctic fish species. Polar Biol 1997;18:209–13.
[24] Coscia MR, Morea V, Tramontano A, Oreste U. Analysis of a cDNA sequence encoding the immunoglobulin heavy chain of the Antarctic teleost *Trematomus bernacchii*. Fish Shellfish Immunol 2000;10:343–57.
[25] Ruud JT. Vertebrates without erythrocytes and blood pigment. Nature 1954; 173:848–50.
[26] Ellis AE. Innate host defense mechanisms of fish against viruses and bacteria. Dev Comp Immunol 2001;25:827–39.
[27] Holzer AS, Sommerville C, Wootten R. Tracing the route of *Sphaerospora truttae* from the entry locus to the target organ of the host, *Salmo salar* L., using an optimized and specific in situ hybridization technique. J Fish Dis 2003;26:647–55.
[28] Grove S, Johansen R, Reitan LJ, Press CM. Immune- and enzyme histochemical characterization of leukocyte populations within lymphoid and mucosal tissues of Atlantic halibut (*Hippoglossus hippoglossus*). Fish Shellfish Immunol 2006;20:693–708.
[29] Smith VJ, Fernandes MO. Antimicrobial peptides of the innate immune system. In: Zaccone G, Meseguer J, Garcia-Ayala A, Kapoor BG, editors. Fish defenses. Immunology, vol. 1. Enfield: Science Publishers; 2009. p. 241–75.
[30] Buonocore F, Randelli E, Bird S, Secombes CJ, Facchiano A, Costantini S, et al. Interleukin-10 expression by real-time PCR and homology modelling analysis in the European sea bass (*Dicentrarchus labrax* L.). Aquaculture 2007;270: 512–22.
[31] Altschul SF, Gish W, Miller W, Myers E, Lipman DJ. Best local alignment search tool. J Mol Biol 1990;215:403–10.
[32] Nielsen H, Engelbrecht J, Brunak S, von Heijne G. Identification of prokaryotic and eukaryotic signal peptides and prediction of their cleavage sites. Protein Eng 1997;10:1–6.
[33] Tamura K, Dudley J, Nei M, Kumar S. MEGA4: molecular evolutionary genetics analysis (MEGA) software version 4.0. Mol Biol Evol 2007;24:1596–9.
[34] Meloni S, Mazzini M, Buonocore F, Scapigliati G. Humoral immunity in Antarctic fish: serum immunoglobulins analysis in seven species and antigen-induced response in *Trematomus bernacchii* (Teleostea, Notothenioidea). Ital J Zool 2000;1:79–83.
[35] Abelli L, Gallo VP, Civinini A, Mastrolia L. Immunohistochemical and ultrastructural evidence of adrenal chromaffin cell subtypes in sea bass *Dicentrarchus labrax* (L.). Gen Comp Endocrinol 1996;102:113–22.
[36] Belokoneva OS, Villegas E, Corzo G, Dai L, Nakajima T. The hemolytic activity of six arachnid cationic peptides in affected by the phosphatidylcholine-to-sphingomyelin ratio in lipid bilayers. Biochim Biophys Acta 2003;1617:22–30.
[37] Sun BJ, Xie HX, Song Y, Nie P. Gene structure of an antimicrobial peptide from mandarin fish, *Siniperca chuatsi* (Basilewsky), suggests that moronecidins and pleurocidins belong in one family: the piscidins. J Fish Dis 2007;30:335–43.
[38] Syvitski RT, Burton I, Mattatall NR, Douglas SE, Jakeman DL. Structural characterization of the antimicrobial peptide pleurocidin from winter flounder. Biochemistry 2005;44:7282–93.
[39] Wiesner J, Vilcinskas A. Antimicrobial peptides: the ancient arm of the human immune system. Virulence 2010;1:440–64.
[40] Corrales J, Mulero I, Mulero V, Noga EJ. Detection of antimicrobial peptides related to piscidin 4 in important aquacultured fish. Dev Comp Immunol 2010;34:331–43.
[41] Toke O. Antimicrobial peptides: new candidates in the fight against bacterial infections. Biopolymers 2005;80:717–35.
[42] Lata S, Sharma BK, Raghava GPS. Analysis and prediction of antibacterial peptides. BMC Bioinforma 2007;8:263.
[43] Jia X, Patrzykat A, Devlin RH, Ackerman PA, Iwama GK, Hancock RE. Antimicrobial peptides protect Coho salmon from *Vibrio anguillarum* infections. Appl Environ Microbiol 2000;66:1928–32.
[44] Dezfuli BS, Lui A, Giovinazzo G, Boldrini P, Giari L. Intestinal inflammatory response of pawan *Coregonus lavaretus* (Pisces) to the presence of acanthocephalan infections. Parasitology 2009;136:929–37.
[45] Dezfuli BS, Pironi F, Giari L, Noga EJ. Immunocytochemical localization of piscidin in mast cells of infected seabass gill. Fish Shellfish Immunol 2010;28: 476–82.
[46] Dezfuli BS, Giari L, Simoni E, Menegatti R, Shinn AP, Manera M. Gill histopathology of cultured European sea bass, *Dicentrarchus labrax* (L.), infected with *Diplectanum aequans* (Wagener 1857) Diesing 1958 (Diplectanidae: Monogenea). Parasitol Res 2007;100:707–13.
[47] Dezfuli BS, Giovinazzo G, Lui A, Giari L. Inflammatory response to *Dentitruncus truttae* (Acanthocephala) in the intestine of brown trout. Fish Shellfish Immunol 2008;24:724–33.
[48] Reite OB, Evensen Ø. Inflammatory cells of teleostean fish: a review focusing on mast cells/eosinophilic granule cells and rodlet cells. Fish Shellfish Immunol 2006;20:192–208.
[49] Colorni A, Ullal A, Heinisch G, Noga EJ. Activity of the antimicrobial polypeptide piscidin 2 against fish ectoparasites. J Fish Dis 2008;31:423–32.
[50] Corrales J, Gordon WL, Noga EJ. Development of an ELISA for quantification of the antimicrobial peptide piscidin 4 and its application to assess stress in fish. Fish Shellfish Immunol 2009;27:154–63.
[51] Campagna S, Saint N, Molle G, Aumelas A. Structure and mechanism of action of the antimicrobial peptide piscidin. Biochemistry 2007;46:1771–8.
[52] Murray HM, Leggiadro CT, Douglas SE. Immunocytochemical localization of pleurocidin to the cytoplasmic granules of eosinophilic granular cells from the winter flounder gill. J Fish Biol 2007;70:336–45.
[53] Reimschuessel R, Bennett RO, May EB, Lipsky MM. Eosinophilic granular cell response to a microsporidian infection in a sergeant major fish, *Abudefduf saxatilis* L. J Fish Dis 1987;10:319–22.
[54] Sharp GJE, Pike AW, Secombes CJ. The immune response of wild rainbow trout *Salmo gairdneri* Richardson to naturally acquired plerocercoid of *Diphyllobothrium dendriticum* (Nitzsch 1824) and *D. ditremun* (Creplin 1825). J Fish Biol 1989;35:781–94.

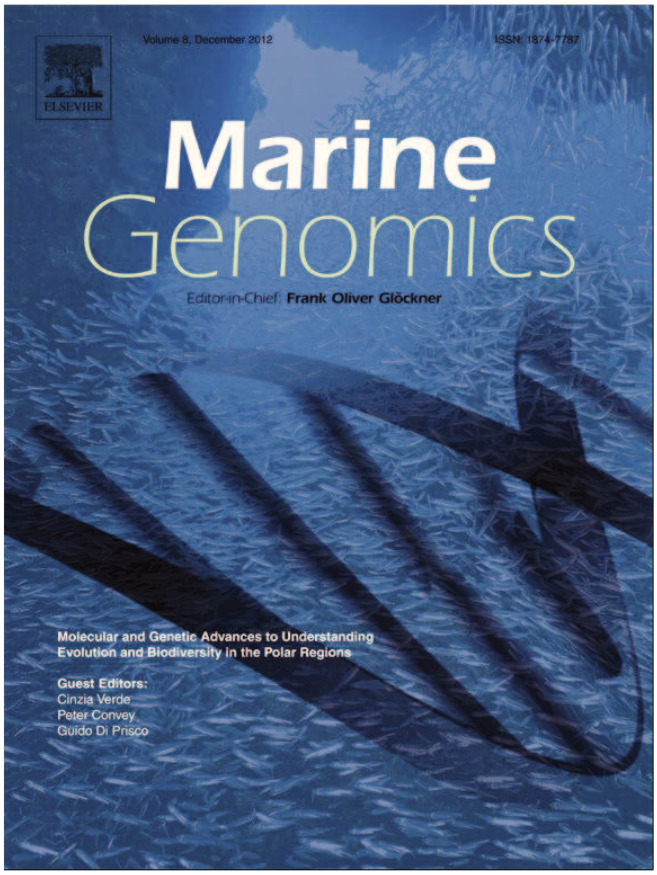

Marine Genomics 8 (2012) 15–22

Contents lists available at SciVerse ScienceDirect

Marine Genomics

journal homepage: www.elsevier.com/locate/margen

The microbial diversity of Polar environments is a fertile ground for bioprospecting

Donatella de Pascale [a,*], Concetta De Santi [a], Juan Fu [b], Bjarne Landfald [b]

[a] Institute of Protein Biochemistry, National Research Council, Via Pietro Castellino, 111, I-80134, Naples, Italy
[b] Norwegian College of Fishery Science, University of Tromsø, N-9037 Tromsø, Norway

ARTICLE INFO

Article history:
Received 2 February 2012
Received in revised form 5 April 2012
Accepted 10 April 2012

Keywords:
Bioprospecting
Prokaryotic
Polar
Metagenomics

ABSTRACT

The term bioprospecting has been adopted for systematic searches in nature for new bioactive compounds, genes, proteins, microorganisms and other products with potential for commercial use. Much effort has been focused on microorganisms able to thrive under harsh conditions, including the Polar environments. Both the lipid and protein cellular building blocks of Polar microorganisms are shaped by their adaptation to the permanently low temperatures. In addition, strongly differing environments, such as permafrost, glaciers and sea ice, have contributed to additional functional diversity. Emerging massive-parallel sequencing technologies have revealed the existence of a huge, hitherto unseen diversity of low-abundance phylotypes – the rare biosphere – even in the Polar environments. This realization has further strengthened the need to employ cultivation-independent approaches, including metagenomics and single-cell genomic sequencing, to get comprehensive access to the genetic diversity of microbial communities for bioprospecting purposes. In this review, we present an updated snapshot of recent findings on the molecular basis for adaptation to the cold and the phylogenetic diversities of different Polar environments. Novel approaches in bioprospecting are presented and we conclude by showing recent bioprospecting outcomes in terms of new molecules patented or applied by some biotech companies.

1. Introduction

Even though the development of new products by e.g. the pharmaceutical or biocatalyst industries increasingly leans on synthetic approaches, like combinatorial organic synthesis, rational design and directed evolution, natural compounds are still the main source of biomolecules with genuinely novel structural features and properties (Harvey et al., 2010). In recent years, the term bioprospecting has been coined for the systematic search in nature for novel bioactive molecules. Bioprospecting efforts are presently often characterized by high-throughput approaches, where robotized technologies are employed to screen systematically through large numbers of samples from specific environments or categories of organisms.

Microorganisms are essential in today's bioprospecting efforts, both as producers of secondary metabolites and biocatalysts. In the search for new enzymes, much effort has been directed towards extremophiles, i.e. microorganisms living in conditions on the margins of life and, therefore, anticipated to have evolved catalysts with correspondingly "extreme" properties. In Polar environments, the obvious extremophilic adaptation is to very low temperatures, a feature which distinguishes basically all kinds of environments in these regions. Furthermore, the cold is often combined with other kinds of challenging surroundings, such as the hypersalinity of sea ice brine channels, the extremely low free water and nutrient availability in permafrost soil and the unique light conditions in these high-latitude regions.

In this review the authors present an updated picture of the outcomes of prokaryotic bioprospecting in Polar environments, on the background of the distinctive molecular adaptations and microbial diversities found in these high-latitude areas. Phylogenetic and functional diversities are discussed in the light of new, powerful analytical tools, such as metagenomics. Our main focus will be on the permanently cold marine and terrestrial environments. Evidently mesophilic and thermophilic microbial environments of the Arctic and the Antarctica, including e.g. digestive tracts of warm-blooded animals, thermal springs and deep-sea hydrothermal vents, also harbor organisms that are interesting from a bioprospecting perspective, but we find such environments to be outside the scope of this review.

2. Low temperature has shaped evolution of biomolecules

Environmental temperature influences biological functions of poikilothermic organisms at all levels, from molecules to whole organisms, and differences in temperature regime have been considered as a strong selective force during evolution (Eanes, 1999; Watt and Dean, 2000). By living in the most permanently cold environments on the planet, microorganisms adapted to the Polar regions have been studied as evident cases both for elucidating the molecular characteristics of cold adaptation, in general, and for finding cold-adapted molecules with application potential. The microorganisms that survive and grow in the

* Corresponding author at: Institute of Protein Biochemistry, National Research Council, Via Pietro Castellino, 111, I-80131, Naples, Italy. Tel.: +39 0816132314; fax: +39 0816132249.
URL: d.depascale@ibp.cnr.it (D. de Pascale).

1874-7787/$ – see front matter
doi:10.1016/j.margen.2012.04.004

Polar regions have adopted a variety of adaptive strategies to maintain activity and metabolic function despite the challenging conditions. Cold adaptation has taken place both at the cellular and molecular levels and involves several phenotypic traits. These include changes in low-molecular weight compounds, such as carotenoid pigments and compatible solutes, the latter conventionally associated with osmotic stress response (Shivadji and Prakash, 2010). The most evident expressions of cold adaptation are, however, found in the changed composition of membrane lipids which facilitates the maintenance of membrane fluidity and in the structural changes of enzymes to retain sufficient catalytic capacity at temperatures around 0 °C (Casanueva et al., 2010).

2.1. Lipid adaptation

It has for a long time been known that adaptation to life at low temperature in poikilothermic organisms is manifested in their membrane fatty acid profiles, both as individual responses to environmental change and as evolutionary differences between related organisms in separate climate regimes (Hazel and Williams, 1990; Russell, 1997). As the most general feature, cold adaptation at both levels involves an increased fraction of mono- or polyunsaturated fatty acids at the expense of saturated fatty acids, thereby maintaining membrane fluidity at lowered temperatures. The long-chain n−3 polyunsaturated fatty acids, principally the eicosapentaenoic (EPA) and docosahexaenoic (DHA) acids, are common elements of the membranes in eukaryotic organisms in cold marine environments, either accumulated through *de novo* biosynthesis in protists or by grazing/predation in Metazoa (Brett and Muller-Navarra, 1997). In prokaryotes, the presence of EPA was first reported by Johns and Perry (1977), and a series of subsequent studies has associated *de novo* biosynthesis of n−3 PUFAs in prokaryotes with well-known lineages of marine gamma-proteobacteria, most conspicuously in *Shewanella*, *Moritella* and *Colwellia* (Russell and Nichols, 1999). Early studies indicated the n−3 PUFA accumulation was a characteristic of deep-sea bacteria (DeLong and Yayanos, 1986; Wirsen et al., 1987), suggesting that it was a barophilic as much as a low-temperature adaptation. The capacity for n−3 PUFA production has, however, later been found to be equally widespread in non-barophilic, cold-adapted bacteria (Henderson et al., 1993; Yano et al., 1997; Cho and Mo, 1999; Nichols, 2003; Frolova et al., 2011), including Arctic and Antarctic strains (Nichols et al., 1993; Jøstensen and Landfald, 1997; Bowman et al., 1998; Jadhav et al., 2010). Mutant studies have unequivocally associated PUFA production in bacteria with cold adaptation, as growth is impaired at low, but not elevated temperatures by knocking out this trait in e.g. EPA-producing *Shewanella* sp. (Sato et al., 2008). However, the beneficial role of the n−3 PUFA seems not to be restricted to bulk membrane fluidity stabilization, as it has been associated with membrane organization and cell division processes and possibly interaction with specific membrane proteins (Kawamoto et al., 2009). Interestingly, biosynthesis of EPA and DHA in prokaryotes, as well as in certain protists of the thraustochytrid group, is not the result of elongations and desaturations of intermediates of the conventional fatty acid biosynthesis pathways, as it is in animals and other groups of protists. Rather, the two PUFAs are synthesized in their entirety from acetate by separate, polyketide synthase like systems (Metz et al., 2001). Genomic analyses have recently identified homologues to these PKS-like gene clusters in a wide range of bacterial phyla, but the gene products are less clarified outside the well-established EPA and DHA producing genera (Shulse and Allen, 2011).

2.2. Proteins

As far as the psychrophilic microorganims are concerned, their ability to thrive close to the freezing point of water implies a vast array of adaptations in most cellular components. Investigations on the structural basis for enzymatic adaptation to different temperatures are largely based on comparative studies, since psychrophilic proteins display sequences and structures analogous with those of their meso- and thermo-philic counterparts. It is generally accepted that cold-adapted proteins have a less rigid, more flexible structure (Marx et al., 2007) and these comparative studies have also revealed a number of more specific structural characteristics in cold-active proteins.

Metpally and Reddy, 2009 systematically analyzed the compositional variation and substitution preferences of amino acids in proteomes of psychrophiles, as compared to those of mesophiles, in order to unveil the general proteome-wide characteristics for cold adaptation. In psychrophilic bacteria, serine, aspartic acid, threonine and alanine are over-represented in the coil regions of secondary structures, while glutamic acid and leucine are under-represented in the helical regions. Compared to mesophiles, psychrophiles comprise a significantly higher proportion of amino acids that contribute to high protein flexibility in the coil regions of proteins, i.e. those with tiny/small or neutral side chains. Amino acids with aliphatic, basic, aromatic and hydrophilic side chains are under-represented in the helical regions of proteins of psychrophiles.

To investigate the flexibility as a key characteristic of cold adaptation, other studies have been conducted on the cavities in psychrophilic enzymes. They were significantly different from the homologous mesophilic enzymes (Paredes et al., 2011), as the psychrophilic enzymes tend to be more solvated in the core and their cavity surfaces contain a higher proportion of acidic amino acids. This allows water molecules to stably exist within the cavities. Specifically these small adjustments include the reduction in the number of salt bridges, the reduction of aromatic interactions, a reduced hydrophobic clustering, the reduced content in the amino acids proline and arginine; together with additional loop-structures, and more solvent interaction (Feller, 2010).

From a thermodynamic point of view, an inevitable consequence of life at very low temperature is a decrease in the biocatalytic reaction rates. A decrease in temperature down to 0 °C results in about 10- to 60-fold reduction in the reaction rates, as suggested by the Arrhenius equation. Therefore, a consistent feature of psychrophilic enzymes is a lowered conformational stability, allowing the protein to be more flexible and thereby retaining sufficient catalytic rates in metabolically active organisms. This concept is clearly encapsulated by Cavicchioli et al. (2011): "….the high flexibility of cold-active enzymes enables increased complementarity between active site and substrates, at low energy cost, resulting in high specific activities at low temperatures".

The comparison of biophysical studies, X-ray crystal structures and whole genome analyses performed between (hyper)thermophilic proteins and psychrophilic counterparts has suggested that protein thermal stability under differing temperature regimes is largely achieved by an additive series of small changes. Therefore, a unique mechanism of stabilization does not exist (Metpally and Reddy 2009). Parameters that have been reported to be involved in stabilization at high temperatures are as follows: (1) decreased number of small residues such as glycine and alanine, which has been reported to be responsible for higher flexibility; (2) increased number of proline residues, in particular in loop regions; (3) decreased number of cysteine residues; (4) decreased number of putative deamidation sites; (5) increased percentage of charged amino acids, these residues are engaged in ion pairs on the protein surface, thereby being responsible for the "resilience" property of the protein; (6) increased electrostatic and hydrophobic interactions, and finally (7) decreased areas and volumes of cavities (de Pascale et al., 2008; Vieille and Zeikus, 2001; Pace, 2000; De Simone et al., 2001 and Mandrich et al., 2004).

Comprehensive statistical studies based on analyses of the increasing number of sequenced genomes and on solved three-dimensional structures, have given additional information on the patterns of temperature adaptation at the sequence and structural levels. In particular, these studies have confirmed an increased number of charged residues, especially lysine, arginine and glutamate and a decreased number of

polar residues, such as serine, aspartate and glycine, in thermophilic and hyper-thermophilic proteins (Osterlund et al., 1996; Shen et al., 1999, 2000; Lang et al., 1998). Moreover, these data are in agreement with some experimental evidence on the importance of salt bridges for protein stability. Recent findings demonstrate that thermal stability is not simply correlated with the number of ion pairs, but more interestingly, with optimized electrostatic interactions (Mandrich et al., 2005; Del Vecchio et al., 2005). It is important to underline that not all the above-mentioned changes should be expected to occur in a single protein molecule, since proteins may adopt several strategies in altering their stability and activity in response to environmental variations (Mandrich and de Pascale, 2011).

3. The cultivation-independent picture of prokaryotic diversity

Although cultivation of microorganisms has steadily grown more sophisticated, microscopic studies during the 1970s made it evident that the fraction of prokaryotic organisms receptive of laboratory cultivation constituted just a small fraction of all viable cells present in most natural environments (Staley and Konopka, 1985; Amann et al., 1995). This same picture emerged from basically any environment to be explored. The groundbreaking introduction of ribosomal RNA gene sequence analysis into microbial phylogeny studies by Carl Woese and co-workers (Fox et al., 1980) and the use of this approach on clone libraries of the 16S rRNA gene amplified from environmental DNA (Ward et al., 1990) confirmed that the uncultivated majority of prokaryotes, to a large extent, are made up of phylogenetic groups that differ from, and sometimes show very remote relationships with, hitherto cultivated bacteria (Giovannoni et al., 1990; Weisburg et al., 1991; Pace, 1997). From these early observations, cultivation-independent, molecular-phylogenetic approaches to microbial diversity studies have undergone spectacular developments the last two decades. The development has largely been driven by the technological leaps distinctive of the field of molecular biology in general. Most strikingly, it is illustrated by the development in gene sequencing technologies, where machine capacities and costs per base pair in obtaining sequence information have undergone strong inverse developments. The massive parallel sequencing technologies of today have made it possible to acquire, at an affordable cost, quantities of genetic information that were beyond imagination just a decade ago.

Early cultivation-independent studies of prokaryotic species' richness in terrestrial and marine samples by DNA re-association or 16S rRNA gene clone libraries indicated figures that were much higher than reflected in strain collections from corresponding environments (Torsvik et al., 2002; Rappe and Giovannoni, 2003). Recent massive parallel 16S rRNA gene sequencing projects have deepened this picture further by establishing the existence of two clearly discernible bacterial community components. On the one hand there are abundant phylotypes, which constitute a minor fraction of all phylotypes present, but a dominant fraction of the total 16S rRNA gene pool — implying that they also dominate by way of cell numbers. On the other hand, there is an overwhelming number of noticeably low-abundant phylotypes — "the rare biosphere" (Sogin et al., 2006; Bent and Forney, 2008), which, despite their diversity, make up a minor fraction of the total ribosomal gene pool. Confident estimates have not been established on the actual species' richness of the rare biospheres of globally dominant ecosystems, as even the most extensive sequencing efforts so far, have not reached comprehensive coverage of the phylotypes present (Kirchman et al., 2010; Pommier et al., 2010; Will et al., 2010; Bartram et al., 2011; Matcher et al., 2011).

A second important finding from cultivation-independent 16S rRNA gene based analyses is the ubiquitous presence of uncultivated representatives of the Archaea domain in non-extreme natural environments. By and large, archaeal numbers and species richness are lower than observed for their bacteria counterparts in the same environments, the exception being the deep ocean waters, where archaeal cell densities have been shown to match that of bacteria (DeLong, 2003). Seawater and soil samplings unequivocally point to the Crenarchaeota branch of the Archaea as numerically dominant (DeLong, 2003; Bates et al., 2011), and there are strong indications that crenarchaeotal groups are key players in the nitrogen cycling in these environments. For instance, the first "uncultivable" marine Archaea to be cultivated and characterized phenotypically was a Crenarchaeota which gains respiration energy from ammonia oxidation (Könneke et al., 2005). Marine sediments present a more mixed picture with significant presence of both Crenarchaeota and Euryarchaeota. This has been demonstrated both in deep-ocean and more shallow sediments. Not unexpectedly, the sediment euryarchaeal phylogroups frequently show closest relationship with established methanogenic lineages (Vetriani et al., 1999; Wang et al., 2010; Jiang et al., 2011; Nguyen and Landfald, unpublished results).

3.1. The prokaryotic diversities of selected Polar environments

Several Polar environments have been targeted for cultivation-independent diversity studies the last number of years. The main focus has been on the most unique environmental types within these regions, such as the surface and permafrost layers of the tundra, sea ice, cores from the large Greenland and Antarctica ice sheets and the utterly inhospitable dry valleys of the Antarctica. Additionally, the Polar regions have been included in comprehensive studies of the oceanic waters and sediments. Here, the Polar distinctiveness seems less pronounced, as the oceans, on a worldwide basis, exchange water masses e.g. through the global oceanic conveyor belt.

3.1.1. The terrestrial environment

The upper active layer of the tundra, alternating between a frozen winter state and a thawed summer state, and the underlying, much thicker permafrost layer offer widely different life conditions for the indigenous microbiotas, although several studies have demonstrated substantial numbers of viable microbial cells even in the permafrost (Panikova et al., 2006; Price and Sowers, 2004). In the summer season, the thawed active layer should be expected to select for opportunistic fast-growing organisms capable of exploiting the moderate temperatures and good nutrient availability. On the other hand, the permafrost, experiencing constant "winter" conditions with sub-zero temperatures and subsequent low water and nutrients availability, should rather select for oligotrophic organisms with low, but steady growth rates under such conditions. On this background, two recent studies from the Canadian high Arctic (Wilhelm et al., 2011; Yergeau et al., 2010) indicate surprisingly moderate differences in gross phylogenetic composition and profiles of functional genes between the thawed upper active layer and the permafrost layer below. Both layers were found to harbor the same phyla that are also characteristic of upper soils of boreal forest in the Northern hemisphere (Neufeld and Mohn, 2005). Newsham et al. (2010) have observed the same trend in the Antarctica by finding marginal differences in bacterial community structure between two soils differing in water content and nutrient composition.

Several studies have largely found Actinobacteria, and the various sub-phyla of the Proteobacteria to constitute more than 50% of classified operational taxonomic units in the tundra bacterial communities, while the frequencies of other ubiquitous groups, such as Bacteroidetes, Firmicutes, Acidobacteria and Gemmatimonas, seem more variable. Somewhat contrary to this phylogenetic stability, Mackelprang et al. (2011) have documented rapid shift in metabolic profile and community structure upon thawing of Alaskan permafrost soil while Zak and Kling (2006) have found distinct differences in community structure between different Arctic tundra ecosystems. Cyanobacteria have been shown as essential primary producers of both limnic and terrestrial environments in the Polar regions (Vincent, 2000; Jungblut et al., 2010).

Methanogenic Archaea in Polar terrestrial environments is essential in the conversion of thawed permafrost organic material into atmospheric methane, thereby contributing to a positive feedback in greenhouse

gas driven climatic change (McGuire et al., 2009). The prevalence of methanogenic Euryarchaeota among Archaea has been confirmed in high-arctic wetland by cultivation-independent approaches (Høj et al., 2005), but the hitherto uncultivated Crenarchaeota group I.b3 was also detected at two separate locations. Other Crenarchaeota groups have previously also been found in Kamtschatka tundra soil (Ochsenreiter et al., 2003). In two separate studies, Steven et al. (2007, 2008) have detected substantial fractions of both Eury- and Crenarchaeota in permafrost cores, i.e. 61 vs. 39% and 76 vs. 34%, respectively. In the upper active layer in the 2008 study, the dominance by Crenarchaeota was, however, complete.

3.1.2. The glacial and sub-glacial microbiota

Deep ice core samples from the Greenland ice sheet have confirmed the presence of tiny ultramicrobacteria – some being cultivable – even in layers that have been trapped in the glacial ice for 100,000 years or more (Priscu and Christner, 2004). Cultivable variants have largely been found to belong to the family Flavobacteriaceae (Loveland-Curtze et al., 2010). In sub-glacial material underneath the >3000 m ice sheet of the Eastern Antarctica, Lanoil et al. (2009) have found quite dense, but relatively low-diversity bacterial communities dominated by beta-proteobacterial lineages. Interestingly, these Antarctic phylogroups showed quite close relationships with both Arctic and alpine sub-glacial bacterial communities (Foght et al., 2004; Simon et al., 2009; Skidmore et al., 2005).

3.1.3. The sea ice microbiota

The seasonal sea ice which covers huge areas of both the southern and the northern circumpolar oceans during their respective cold periods, constitute unique ecosystems which form the basis of microbial communities that are distinct from both the glacial and pelagic counterparts. The bulk of organisms live in the brine channels, characterized by salinities which may exceed that of seawater several-fold. The salt concentration tends to vary through the ice layer, as it drops from the top layer exposed to the very cold winter atmosphere towards the interface with the underlying seawater at its freezing point of roughly −2 °C (Thomas and Dieckmann, 2002). Community structure studies have also indicated a seasonal variation: a study from the Canadian Arctic indicates the winter community in the sea ice to reflect the composition of the underlying seawater quite closely by being dominated by bacteria of the SAR11 clade and other typical planktonic groups (Collins et al., 2010). Contrary to this, several studies of spring and summer sea ice samples from both the Arctic and the Antarctica have demonstrated a surprisingly high prevalence, i.e. from 3% to more than 50% of total microscopic prokaryotic counts, of cultivable bacteria belonging to the well-known, easily cultivable genera within the γ-proteobacteria and Bacteroidetes groups in sea ice (Helmke and Weyland, 1995; Junge et al., 2002; Brakstad et al., 2008).

3.1.4. The Polar oceans and sediments below

Through the global ocean circulation systems, water masses are slowly exchanged between the world's oceans, also resulting in an exchange of planktonic microorganisms (Munn, 2011). Accordingly, the main oceanic realms of the world seem noticeably homogenous with regard to the composition of major phyla of planktonic bacteria (Wietz et al., 2010). Some dominant groups, most strikingly the alfaproteobacterial SAR11 group, seem omnipresent as a significant fraction of the overall picoplankton biomass, from warm, equatorial waters to the high-latitude oceans. Other ubiquitous contributors to the bacterioplankton are various lineages of the Gamma-proteobacteria (e.g. the SAR86 group) and some representatives of the Bacteroides phylum. The Polar oceans are no exception to this pattern (Kirchman et al., 2010; Murray and Grzymski, 2007).

Recent high-throughput sequencing efforts have confirmed a large rare biosphere diversity also in the Arctic Ocean. Galand et al. (2009) have found the 1.5% most abundant of altogether nearly 8000 phylotypes of bacteria to constitute more than half of all 16S rRNA gene sequence tags, while the 86% phylotypes defined as rare (<0.01% each of total phylotypes) made up just 6% of the total sequence pool. The same rank-abundance pattern was even more pronounced within the Archaea, however at a far lower level of overall richness. Distinct biogeographical and water depth partitions were observed between phylotypes.

4. Traditional cultivation and "-omics" technologies in bioprospecting

4.1. The importance of isolates

As for other kinds of environments, our knowledge of the phenotypes and systematics of prokaryotic microorganisms in the Polar regions is historically based on meticulous collection, isolation and phenotypic characterization of strains. Before World War 2, just a few sporadic descriptions of bacteria from Antarctic environments were available, with Ekelöf (1908) being the first. However, more systematic studies were commenced from the 1950s onwards, as research expeditions to the Polar regions became more regular phenomena. Over time, the microbiologists' interests also turned from purely descriptive studies of the prevalence and systematics of bacteria in these extreme environments to elucidating the evolutionary adaptations to the cold surroundings. Antarctic and Arctic strains have been essential in studies of cold adaptation in microbes from the 1960s onwards (Morita, 1975; Gounot, 1986; D'Amico et al., 2006).

Collection of new isolates is still the basis for most microbiological bioprospecting efforts – also in the Polar regions – as this both gives access to the totality of genomic information in new microorganisms and makes the study of their phenotype possible in the laboratory. More sophisticated media and cultivation conditions (Vartoukian et al., 2010), as well as physical access to new habitats (e.g. from glacial and permafrost core samples or underneath sea ice by diving) have steadily brought new phylotypes of cold-adapted prokaryotes into the stock culture collections.

A further extension of possibilities offered by cultivation has come with the emergence of genomics and transcriptomics studies. These technologies imply access to the sequence information of the complete genome from interesting isolates. With the new massive-parallel sequencing technologies, this can be obtained at a price that is affordable for increasing numbers of laboratories. Various bioinformatic tools may subsequently be used to identify promising genes for amplification, cloning, expression and characterization of gene products.

A common strategy for bioprospecting through isolates collection is to employ selective media and cultivation conditions for phylogenetic groups which, from experience, are highly likely to potentially possess interesting bioactivities. The Actinomycetes – traditionally isolated from terrestrial, but more recently increasingly from marine environments (Fenical and Jensen, 2006) – have been prime targets for bioprospecting efforts, as they are frequent producers of secondary metabolites. Later the Cyanobacteria have also been shown as particularly interesting in this respect (Burja et al., 2001; Nunnery et al., 2010; Kehr et al., 2011). However, bioprospecting efforts targeting secondary metabolites from Arctic or Antarctic isolates have so far been very limited, the study by Biondi et al. (2008) on cyanobacteria being an exception. To date most screening projects on Polar bacteria have focused on the search for cold-adapted enzymes.

4.2. Diving into the uncultivated majority by metagenomics and metatranscriptomics

Besides the advances in sequencing technologies, other recent developments in high-throughput molecular biology techniques, such as robotized handling of large numbers of clones and screenings for bioactivities, have paved the way for metagenomic approaches to

microbial bioprospecting. The term metagenomics was introduced by Handelsman et al. (1998) and, in principle, implied an extension of the genomics approach into the complete microbial gene pool of selected environments — possibly after separation into size group characteristic of specific organisms, e.g. bacteria, protists or viruses. Consequently, the term metatranscriptomics covers the analogous cDNA-based approach. However, the uncovering of the tremendous diversity of the rare biosphere, as mentioned previously, has made complete coverage of the diversity of microbial communities a daunting task in most natural environments — even by today's most high-capacity sequencing technologies. The outcome of metagenomic sequencing efforts tends to be a strong representation – even resulting in near-complete or complete genome sequences – of the most abundant phylotypes in the communities (Venter et al., 2004), while organisms of the rare biosphere are randomly represented by genomic fragments.

In essence, metagenomics comprises the collection and purification of environmental DNA followed by cloning of the DNA into a suitable vector/host system on a large scale or – more recently – simply sequencing the collected DNA on a massive scale by one of the presently available massive-parallel sequencing technologies (Simon and Daniel, 2011). Although more labor intensive and costly than straightforward sequencing, the cloning strategy offers some distinct advantages, in particular related to subsequent use of the metagenomic material for bioprospecting. Firstly, clone libraries may be used for functional screening, i.e. to do large-scale searches for recombinant expression of specific activities in the cloned genomic material. This kind of searches work most efficiently towards single-peptide chain enzymes, but occasionally also more complex proteins or even biosynthetic pathways are coded and expressed from the same clone. Secondly, the cloning approach gives genomic fragments varying in length from a few kilobasepairs with conventional plasmid vectors up to around 100 kbp with BAC vectors, harboring corresponding stretches of contiguous gene sequence information. In contrast, the combination of short read lengths from the massive parallel sequencing technologies of today with the extreme diversities of many environmental microbial communities tends to give lots of short, non-contiguous sequence information which covers just fragments of individual genes and, therefore, has limited value in bioprospecting (Wommack et al., 2008).

Recently, technologies have also been developed to obtain genomic information from individual cells of the uncultivated bacteria. After picking out individual cells by micromanipulation devices or flow-cytometry cell sorting, multiple-displacement DNA amplification is employed to generate sufficient DNA for shotgun genome sequencing. Interesting candidates may be singled out by prior sequencing of the 16S rRNA or other phylogenetically informative genes (Woyke et al., 2009; Eloe et al., 2011; Siegl et al., 2011; Youssef et al., 2011).

5. The outcome of microbial bioprospecting in Polar regions, so far

Research on Polar microorganisms to find new bioproducts has been focused on four main areas, including 1) enzymes for use in a range of industrial processes, including food technology, 2) bioremediation and other pollution control technologies, 3) dietary supplements, with a particular focus on polyunsaturated fatty acids (PUFAs) and 4) antifreeze proteins.

Organisms thriving in permanently cold habitats, like the Polar zones, are a vast reservoir of cold-adapted enzymes. Such enzymes may be employed in a series of industrial applications (Aguilar, 1996; Morita et al., 1997), including as ingredient in cleaning agents, in the biodegradation of xenobiotic compounds in cold areas, in leather processing, in some food processes, such as cheese manufacturing, bakeries, meat tenderization, fermentation and confectionery, and in some molecular biology techniques, e.g. in heterologous gene expression systems or the use of heat-labile Antarctic alkaline phosphatase (Rina et al., 2000; Margesin and Schinner, 1999). The use of cold adapted enzymes can minimize undesirable side reactions taking place at higher temperatures and allow reactions involving heat-sensitive substrates (Jeon et al., 2009). These properties play an important role in the food and feed industries, where it is important to preserve the nutritional value and flavor of the products. Enzymes of Polar origin have also shown application potential in mixed aqueous-organic or non-aqueous solvents. Esterases and lipases have been found to exhibit a high level of stereospecificity that may be used for synthesizing chiral drugs (Jeon et al., 2009). Furthermore, genetic or chemical modifications offer useful and interesting ways for modifying the properties of enzymes to intensify their performance or augment their properties. Direct evolution was used to generate a cold-adapted Lipase B from *Candida antarctica*, where the half-life of enzyme inactivation and the activity were both significantly improved (Zhang et al., 2003).

A recent study has also demonstrated that it is possible to improve the productivity at low temperature by reducing uncompetitive substrate inhibition (Siddiqui et al., 2009). The modified enzymes will not be subject to substrate inhibition and this can be particularly valuable for those industrial processes that are operated with high substrate concentrations.

Specific classes of cold-active enzymes have been investigated, i.e. hydrolytic enzymes, comprising esterases, lipases, cellulases, glycosidases and proteases. Recently, a novel cold-adapted cellulase from an earthworm living in a cold environment was discovered that could convert cellulose directly into glucose (Ueda et al., 2010). This might be an important discovery regarding the efficient production of biofuels from cellulosic waste at low temperatures. For all the mentioned types of enzymes, functional screening methods are currently available which allow simple screening for novel biocatalysts both from microbial isolates and metagenomic libraries. Table 1 summarizes several enzymes recently isolated through metagenomic studies from Polar environments and Table 2 reports some example of enzymes and molecules from Polar environments recently utilized in industrial applications.

Polar regions are mostly uninhabited, but even the low level of human activities often involves the use of petroleum hydrocarbons, i.e. fuel for aviation, power generation, heating and operation of vehicles and ships. Further, the contamination by PCBs and polychlorinated biphenyls may constitute a great problem in these areas, among other factors due to the presence of several military bases, especially in the Arctic. Numerous studies have demonstrated that cold-active microorganisms may be employed for biodegrading hydrocarbons, and when optimized, the biological treatment of contaminated soil is less expensive than alternative ways to decontaminate, such as incineration, storage, or concentration (Eriksson et al., 2001).

One of the most noteworthy research projects on decontamination of hydrocarbon-contaminated soils by using Arctic genetic resources has been developed jointly by the Russian Federation, the United Nations Environment Programme (UNEP), and the Global Environment Facility (GEF). They have launched a program entitled: "Russian-Federation Support to the National Program of Action for the Protection of the Arctic Marine Environment". This pilot project is mainly concentrated on acquiring new technologies for implementing bioremediation processes based on some marine algae and bacteria from the Arctic. Recent studies of Polar bacterial communities have demonstrated a high prevalence of bacterial strains (many γ-Proteobacteria) that

Table 1
Enzymes recently isolated by metagenomics screening from Polar environments.

Enzyme	Source	Reference
Esterase	Arctic sediment	Jeon et al., 2009
Lipase	Antarctic soil	Cieśliński et al., 2009
β-galactosidase	*Arthrobacter* sp.20B	Białkowska et al., 2009
β-galactosidase	*Alkalilactibacillus ikkense*	Schmidt and Stougaard, 2010
α-amilase	*Pseudoalteromonas arctica* GS230	Lu et al., 2010
β-galactosidase	*Arthrobacter* sp. ON14	Xu et al., 2011
Chitinase	*Glaciozyma antarctica* PI12	Ramli et al., 2011
Esterase	Arctic soil	Yu et al., 2011

Table 2
Molecules and enzymes, from Polar environments, recently patented and implied by several biotech companies.

Enzyme	Source	Company
Glicoprotein	*Pseudoalteromonas antarctica*	Lipotec S.A. [SP]
Beta-galactosidase	*Pseudoalteromonas haloplanktis*	University of Liege [BE]
Alkaline phosphatase	Bacterium HK-47	Patent n. US4720458
Antifreeze Lipoprotein	*Moraxella* sp.	Kansai University [JP]
Lipase-catalyzed esther hydrolysis	*Pseudomonas* sp.	Nippon Paper Industries [JP], Novozymes [DK]
Anti-freeze proteins	*Marinomonas*, *Pseudomonas* sp.	Unilever [UK]
Enzymes xylanolytic activity	*Pseudoalteromonas haloplanktis*	Puratos Naamloze Vennootschap [BE]
Polyunsaturated fatty acid (PUFA) synthase systems	*Shewanella japonica* and *Shewanella olleyana*	Martek Biosciences Corporation [US]
Dehydrogenases	*Arthrobacter* sp., *Micrococcus* sp.	University of London [UK]
Detergent compositions enzymes	*Psychrophilic bacteria* sp.	Procter & Gamble [US]
Chlamysin B antibacterial protein	*Chlamys islandica*	Biotec ASA [NO]
Thermostable isomerase	*Thermoanaerobacter mathranii*	Bioneer A/S [DK]

are able to produce polyunsaturated fatty acids. The majority is psychrophilic (requiring low temperatures for growth) and halophilic (requiring the presence of salts for growth) in contrast to the bacteria present in the underlying water. PUFA-producing bacteria may represent an alternative source for human use. A significant advantage is that bacteria generally contain only one long-chain PUFA (usually eicosapentaenoic or docosahexaenoic acid) rather than the multiple components present in fish or algal oils.

Birds, fishes, amphibians, insects and plants have evolved several strategies to cope with extremely low temperatures in their natural habitats. The mechanisms involved also provide some valuable insight into bacterial cold tolerance. One of the major strategies adopted by the multicellular organisms is the production of specific proteins, which help them to maintain their body fluids in the liquid state at subzero temperatures. In general, such proteins are called antifreeze proteins (AFPs), although other terms such as antifreeze glycoproteins and antifreeze polypeptides are also used to denote the structural features of these cryoprotectants (Chattopadhyay, 2006).

The presence of AFPs in bacteria was firstly demonstrated by Duman and Olsen, 1993. Since then, a number of cold-adapted bacteria (e.g. *Pseudomonas putida*, *P. fluorescens*, *Marinomonas protea* have been found to possess AFPs and the first Antarctic bacterium found to be rich in AFPs was a strain of *Moraxella* (Chattopadhyay, 2006). A significant fraction of them are Antarctic isolates. In general, the bacterial proteins display less freeze protection than those found in AFPs from animals. Hence it is believed that AFPs in animals work by the mechanism of freeze avoidance, whereas freeze tolerance is the strategy used by plants and bacteria. The AFPs isolated from bacteria have a wide range of biotechnological applications, such as improving the cold storage and cryopreservation properties of cells and tissue, thereby reducing or preventing microbial contamination of frozen food (Venketesh and Dayananda, 2008). One of the most promising examples of application of these proteins in the food industry is the use of AFPs in the production of low-fat ice cream by the Unilever (Leary, 2008). For many years, the company has utilized anti-freeze protein to control the ice formation and structure in this product range. This food processing use of AFPs has been controversial, but it is noteworthy that anti-freeze proteins are naturally present in a wide range of organisms consumed as part of the established human diet, including fish, carrots, cabbage and Brussels sprouts (Breton et al., 2000).

Acknowledgments

This work was partially supported by P.N.R.A. (Programma Nazionale di Ricerche in Antartide 2009––2011) and by the University of Tromsø.

References

Aguilar, A., 1996. Extremophile research in the European Union: from fundamental aspects to industrial expectations. FEMS Microbiol. Rev. 18, 89–92.
Amann, R.I., Ludwig, W., Schleifer, K.H., 1995. Phylogenetic identification and in-situ detection of individual microbial-cells without cultivation. Microbiol. Rev. 59, 143–169.
Bartram, A.K., Lynch, M.D.J., Stearns, J.C., Moreno-Hagelsieb, G., Neufeld, J.D., 2011. Generation of multimillion-sequence 16S rRNA gene libraries from complex microbial communities by assembling paired-end illumina reads. Appl. Environ. Microbiol. 77, 3846–3852.
Bates, S.T., Berg-Lyons, D., Caporaso, J.G., Walters, W.A., Knight, R., Fierer, N., 2011. Examining the global distribution of dominant archaeal populations in soil. ISME J. 5, 908–917.
Bent, S.J., Forney, L.J., 2008. The tragedy of the uncommon: understanding limitations in the analysis of microbial diversity. ISME J. 2, 689–695.
Białkowska, A.M., Cieśliński, H., Nowakowska, K.M., Kur, J., Turkiewicz, M., 2009. A new beta-galactosidase with a low temperature optimum isolated from the Antarctic Arthrobacter sp. 20B: gene cloning, purification and characterization. Arch. Microbiol. 191, 825–835.
Biondi, N., Tredici, M.R., Taton, A., Wilmotte, A., Hodgson, D.A., Losi, D., Marinelli, F., 2008. Cyanobacteria from benthic mats of Antarctic lakes as a source of new bioactivities. J. Appl. Microbiol. 105, 105–115.
Bowman, J.P., Gosink, J.J., McCammon, S.A., Lewis, T.E., Nichols, D.S., Nichols, P.D., Skerratt, J.H., Staley, J.T., McMeekin, T.A., 1998. *Colwellia demingiae* sp. nov., *Colwellia hornerae* sp. nov., *Colwellia rossensis* sp. nov. and *Colwellia psychrotropica* sp. nov.: psychrophilic Antarctic species with the ability to synthesize docosahexaenoic acid (22: 6 omega 3. Int. J. Syst. Bacteriol. 48, 1171–1180.
Brakstad, O.G., Nonstad, I., Faksness, L.G., Brandvik, P.J., 2008. Responses of microbial communities in Arctic sea ice after contamination by crude petroleum oil. Microb. Ecol. 55, 540–552.
Breton, G., Danyluk, J., Ouellet, F., Sarhan, F., 2000. Biotechnological applications of plant freezing associated proteins. Biotechnol. Annu. Rev. 6, 59–101.
Brett, M.T., Muller-Navarra, D.C., 1997. The role of highly unsaturated fatty acids in aquatic food web processes. Freshw. Biol. 38, 483–499.
Burja, A.M., Banaigs, B., Abou-Mansour, E., Burgess, J.G., Wright, P.C., 2001. Marine cyanobacteria — a prolific source of natural products. Tetrahedron 57, 9347–9377.
Casanueva, A., Tuffin, M., Cary, C., Cowan, D.A., 2010. Molecular adaptations to psychrophily: the impact of 'omic' technologies. Trends Microbiol. 18, 374–381.
Cavicchioli, R., Charlton, T., Ertan, H., Mohd Omar, S., Siddiqui, K.S., Williams, T.J., 2011. Biotechnological uses of enzymes from psychrophiles. Microb. Biotechnol. 4, 449–460.
Chattopadhyay, M.K., 2006. Mechanism of bacterial adaptation to low temperature. J. Biosci. 31, 157–165.
Cho, K.W., Mo, S.J., 1999. Screening and characterization of eicosapentaenoic acid-producing marine bacteria. Biotechnol. Lett. 21, 215–218.
Cieśliński, H., Białkowskaa, A., Tkaczuk, K., Długołecka, A., Kur, J., Turkiewicz, M., 2009. Identification and molecular modeling of a novel lipase from an Antarctic soil metagenomic library. Pol. J. Microbiol. 58, 199–204.
Collins, R.E., Rocap, G., Deming, J.W., 2010. Persistence of bacterial and archaeal communities in sea ice through an Arctic winter. Environ. Microbiol. 12, 1828–1841.
D'Amico, S., Collins, T., Marx, J.C., Feller, G., Gerday, C., 2006. Psychrophilic microorganisms: challenges for life. EMBO Rep. 7, 385–389.
de Pascale, D., Cusano, A.M., Autore, F., Parrilli, E., di Prisco, G., Marino, G., Tutino, M.L., 2008. The cold-active Lip1 lipase from the Antarctic bacterium *Pseudoalteromonas haloplanktis* TAC125 is a member of a new bacterial lipolytic enzyme family. Extremophiles 12, 311–323.
De Simone, G., Menchise, V., Manco, G., Mandrich, L., Sorrentino, N., Lang, D., Rossi, M., Pedone, C., 2001. The crystal structure of a hyper-thermophilic carboxylesterase from the archaeon *Archaeoglobus fulgidus*. J. Mol. Biol. 314, 507–518.
Del Vecchio, P., Graziano, G., Granata, V., Farias, T., Barone, G., Mandrich, L., Rossi, M., Manco, G., 2005. Denaturant-induced unfolding of the acetyl-esterase from *Escherichia coli*. Biochemistry 43, 14637–14643.
DeLong, E.F., 2003. Oceans of Archaea. Asm News 69, 503–511.
Delong, E.F., Yayanos, A.A., 1986. Biochemical function and ecological significance of novel bacterial lipids in deep-sea prokaryotes. Appl. Environ. Microbiol. 51, 730–737.
Duman, J.G., Olsen, T.M., 1993. Thermal hysteresis protein activity in bacteria, fungi and phylogenetically diverse plants. Cryobiology 3, 322–328.
Eanes, W.F., 1999. Analysis of selection on enzyme polymorphisms. Annu. Rev. Ecol. Syst. 30, 301–326.
Ekelöf, E., 1908. Bakteriologische Studien während der Schwedischen Südpolar-Expedition 1901–1903, vol. 4. Bonnier, Stockholm.
Eloe, E.A., Fadrosh, D.W., Novotny, M., Zeigler Allen, L., Kim, M., Lombardo, M.J., Yee-Greenbaum, J., Yooseph, S., Allen, E.E., Lasken, R., Williamson, S.J., Bartlett, D.H., 2011. Going deeper: metagenome of a hadopelagic microbial community. PLoS One 6, 20388.
Eriksson, M., Ka, J.O., Mohn, W.W., 2001. Effects of low temperature and freeze–thaw cycles on hydrocarbon biodegradation in Arctic tundra soil. Appl. Environ. Microbiol. 11, 5107–5112.

Feller, G., 2010. Protein stability and enzyme activity at extreme biological temperatures. J. Phys. Condens. Matter 22, 323101.

Fenical, W., Jensen, P.R., 2006. Developing a new resource for drug discovery: marine actinomycete bacteria. Nat. Chem. Biol. 2, 666–673.

Foght, J., Aislabie, J., Turner, S., Brown, C.E., Ryburn, J., Saul, D.J., Lawson, W., 2004. Culturable bacteria in subglacial sediments and ice from two southern hemisphere glaciers. Microb. Ecol. 47, 329–340.

Fox, G.E., Stackebrandt, E., Hespell, R.B., Gibson, J., Maniloff, J., Dyer, T.A., Wolfe, R.S., Balch, W.E., Tanner, R.S., Magrum, L.J., Zablen, L.B., Blakemore, R., Gupta, R., Bonen, L., Lewis, B.J., Stahl, D.A., Luehrsen, K.R., Chen, K.N., Woese, C.R., 1980. The phylogeny of prokaryotes. Science 209, 457–463.

Frolova, G.M., Gumerova, P.A., Romanenko, L.A., Mikhailov, V.V., 2011. Characterization of the lipids of psychrophilic bacteria *Shewanella frigidimarina* isolated from sea ice of the Sea of Japan. Microbiology 80, 30–36.

Galand, P.E., Casamayor, E.O., Kirchman, D.L., Lovejoy, C., 2009. Ecology of the rare microbial biosphere of the Arctic Ocean. Proc. Natl. Acad. Sci. U. S. A. 106, 22427–22432.

Giovannoni, S.J., Britschgi, T.B., Moyer, C.L., Field, K.G., 1990. Genetic diversity in sargasso sea bacterioplankton. Nature 345, 60–63.

Gounot, A.M., 1986. Psychrophilic and psychrotrophic microorganisms. Experientia 42, 1192–1197.

Handelsman, J., Rondon, M.R., Brady, S.F., Clardy, J., Goodman, R.M., 1998. Molecular biological access to the chemistry of unknown soil microbes: a new frontier for natural products. Chem. Biol. 5, R245–R249.

Harvey, A.L., Clark, R.L., Mackay, S.P., Johnston, B.F., 2010. Current strategies for drug discovery through natural products. Expert Opin. Drug Discov. 5, 559–568.

Hazel, J.R., Williams, E.E., 1990. The role of alterations in membrane lipid-composition in enabling physiological adaptation of organisms to their physical-environment. Prog. Lipid Res. 29, 167–227.

Helmke, E., Weyland, H., 1995. Bacteria in sea-ice and underlying water of the eastern Weddell sea in midwinter. Mar. Ecol. Prog. Ser. 117, 269–287.

Henderson, R.J., Millar, R.M., Sargent, J.R., Jostensen, J.P., 1993. Transmonoenoic and polyunsaturated fatty-acids in phospholipids of a vibrio species of bacterium in relation to growth-conditions. Lipids 28, 389–396.

Høj, L., Olsen, R.A., Torsvik, V.L., 2005. Archaeal communities in High Arctic wetlands at Spitsbergen, Norway (78 degrees N) as characterized by 16S rRNA gene fingerprinting. FEMS Microbiol. Ecol. 53, 89–101.

Jadhav, V.V., Jamle, M.M., Pawar, P.D., Devare, M.N., Bhadekar, R.K., 2010. Fatty acid profiles of PUFA producing Antarctic bacteria: correlation with RAPD analysis. Ann. Microbiol. 60, 693–699.

Jeon, J.H., Kim, J.T., Kang, S.G., Lee, J.H., Kim, S.J., 2009. Characterization and its potential application of two esterases derived from the arctic sediment metagenome. Mar. Biotechnol. 11, 307–316.

Jiang, L.J., Zheng, Y.P., Chen, J.Q., Xiao, X., Wang, F.P., 2011. Stratification of Archaeal communities in shallow sediments of the Pearl River Estuary, Southern China. Antonie Van Leeuwenhoek 99, 739–751.

Johns, R.B., Perry, G.J., 1977. Lipids of marine bacterium flexibacter-polymorphus. Arch. Microbiol. 114, 267–271.

Jøstensen, J.P., Landfald, B., 1997. High prevalence of polyunsaturated-fatty-acid producing bacteria in arctic invertebrates. FEMS Microbiol. Lett. 151, 95–101.

Jungblut, A.D., Lovejoy, C., Vincent, W.F., 2010. Global distribution of cyanobacterial ecotypes in the cold biosphere. ISME J. 4, 191–202.

Junge, K., Imhoff, F., Staley, T., Deming, J.W., 2002. Phylogenetic diversity of numerically important arctic sea-ice bacteria cultured at subzero temperature. Microb. Ecol. 43, 315–328.

Kawamoto, J., Kurihara, T., Yamamoto, K., Nagayasu, M., Tani, Y., Mihara, H., Hosokawa, M., Baba, T., Sato, S.B., Esaki, N., 2009. Eicosapentaenoic acid plays a beneficial role in membrane organization and cell division of a cold-adapted bacterium, *Shewanella livingstonensis* Ac10. J. Bacteriol. 191, 632–640.

Kehr, J.C., Picchi, D.G., Dittmann, E., 2011. Natural product biosyntheses in cyanobacteria: a treasure trove of unique enzymes. Beilstein J. Org. Chem. 7, 1622–1635.

Kirchman, D.L., Cottrell, M.T., Lovejoy, C., 2010. The structure of bacterial communities in the western Arctic Ocean as revealed by pyrosequencing of 16S rRNA genes. Environ. Microbiol. 12, 1132–1143.

Könneke, M., Bernhard, A.E., de la Torre, J.R., Walker, C.B., Waterbury, J.B., Stahl, D.A., 2005. Isolation of an autotrophic ammonia-oxidizing marine archaeon. Nature 437, 543–546.

Lang, D.A., Mannese, M.L., deHaas, G.H., Verheij, H.M., Dijkstra, B.W., 1998. Structural basis of the chiral selectivity of *Pseudomonas cepacia* lipase. Eur. J. Biochem. 254, 333–340.

Lanoil, B., Skidmore, M., Priscu, J.C., Han, S., Foo, W., Vogel, S.W., Tulaczyk, S., Engelhardt, H., 2009. Bacteria beneath the west Antarctic ice sheet. Environ. Microbiol. 11, 609–615.

Leary, D., 2008. Bioprospecting in the Arctic. United Nation University-Institute of Advanced Study Report (UNU-IAS 2008 Report), pp. 1–45. Nishi-ku, Yokohama, Japan.

Loveland-Curtze, J., Miteva, V., Brenchley, J., 2010. Novel ultramicrobacterial isolates from a deep Greenland ice core represent a proposed new species, *Chryseobacterium greenlandense* sp. nov. Extremophiles 14, 61–69.

Lu, M., Wang, S., Fang, Y., Li, H., Liu, S., Liu, H., 2010. Cloning, expression, purification, and characterization of cold-adapted α-amylase from *Pseudoalteromonas arctica* GS230. Protein J. 29, 591–597.

Mackelprang, R., Waldrop, M.P., De Angelis, K.M., David, M.M., Chavarria, K.L., Blazewicz, S.J., Rubin, E.M., Jansson, J.K., 2011. Metagenomic analysis of a permafrost microbial community reveals a rapid response to thaw. Nature 480, 368–371.

Mandrich, L., de Pascale, D., 2011. An overview on thermal adaptation of esterases and lipases belonging to the HSL family: new insight by computational analysis. Curr. Chem. Biol. 5, 17–28.

Mandrich, L., Pezzullo, M., Del Vecchio, P., Barone, G., Rossi, M., Manco, G., 2004. Analysis of thermal adaptation in the HSL enzyme family. J. Mol. Biol. 335, 357–369.

Mandrich, L., Merone, L., Pezzullo, M., Cipolla, L., Nicotra, F., Rossi, M., Manco, G., 2005. Role of the N terminus in enzyme activity, stability and specificity in thermophilic esterases belonging to the HSL family. J. Mol. Biol. 345, 501–512.

Margesin, R., Schinner, F., 1999. Biotechnological Applications of Cold-Adapted Organisms. Springer-Verlag, Berlin, p. 338.

Marx, J.C., Collins, T., D'Amico, S., Feller, G., Gerday, C., 2007. Cold-adapted enzymes from marine Antarctic microorganisms. Mar Biotechnol (NY) 93, 293–304.

Matcher, G.F., Dorrington, R.A., Henninger, T.O., Froneman, P.W., 2011. Insights into the bacterial diversity in a freshwater-deprived permanently open Eastern Cape estuary, using 16S rRNA pyrosequencing analysis. Water Sa 37, 381–390.

McGuire, D., Anderson, L.G., Christensen, T.R., Dallimore, S., Guo, L., Hayes, D.J., Heimann, M., Lorenson, T.D., Macdonald, R.W., Roulet, N., 2009. Sensitivity of the carbon cycle in the Arctic to climate change. Ecol. Monogr. 79, 523–555.

Metpally, R.P., Reddy, B.V., 2009. Comparative proteome analysis of psychrophilic versus mesophilic bacterial species: Insights into the molecular basis of cold adaptation of proteins. BMC Genomics Jan 8. 10, 11.

Metz, J.G., Roessler, P., Facciotti, D., Levering, C., Dittrich, F., Lassner, M., Valentine, R., Lardizabal, K., Domergue, F., Yamada, A., Yazawa, K., Knauf, V., Browse, J., 2001. Production of polyunsaturated fatty acids by polyketide synthases in both prokaryotes and eukaryotes. Science 293, 290–293.

Morita, R.Y., 1975. Psychrophilic bacteria. Bacteriol. Rev. 39, 144–167.

Morita, Y., Nakamura, T., Hasan, Q., Murakami, Y., Yokoyama, K., Tamiya, E., 1997. Cold-active enzymes from cold-adapted bacteria. J. Am. Oil Chem. Soc. 74, 441–444.

Munn, C., 2011. Marine Microbiology: Ecology and Applications. Garland Science, New York.

Murray, A.E., Grzymski, J.J., 2007. Diversity and genomics of Antarctic marine microorganisms. Philos. Trans. R. Soc. Lond. B Biol. Sci. 362, 2259–2271.

Neufeld, J.D., Mohn, W.W., 2005. Unexpectedly high bacterial diversity in arctic tundra relative to boreal forest soils, revealed by serial analysis of ribosomal sequence tags. Appl. Environ. Microbiol. 71, 5710–5718.

Newsham, K.K., Pearce, D.A., Bridge, P.D., 2010. Minimal influence of water and nutrient content on the bacterial community composition of a maritime Antarctic soil. Microbiol. Res. 165, 523–530.

Nichols, D.S., 2003. Prokaryotes and the input of polyunsaturated fatty acids to the marine food web. FEMS Microbiol. Lett. 219, 1–7.

Nichols, D.S., Nichols, P.D., McMeekin, T.A., 1993. Polyunsaturated fatty-acids in Antarctic bacteria. Antarct. Sci. 5, 149–160.

Nunnery, J.K., Mevers, E., Gerwick, W.H., 2010. Biologically active secondary metabolites from marine cyanobacteria. Curr. Opin. Biotechnol. 21, 787–793.

Ochsenreiter, T., Selezi, D., Quaiser, A., Bonch-Osmolovskaya, L., Schleper, C., 2003. Diversity and abundance of Crenarchaeota in terrestrial habitats studied by 16S RNA surveys and real time PCR. Environ. Microbiol. 5, 787–797.

Osterlund, T., Danielsson, B., Degerman, E., Contreras, J.A., Edgren, G., Davis, R.C., Schotz, M.C., Holm, C., 1996. Domain-structure analysis of recombinant rat hormone-sensitive lipase. Biochem. J. 319, 411–420.

Pace, N.R., 1997. A molecular view of microbial diversity and the biosphere. Science 276, 734–740.

Pace, C.N., 2000. Single surface stabilizer. Nat. Struct. Biol. 7, 345–346.

Panikova, N.S., Flanaganb, P.W., Oechelc, W.C., Mastepanovd, M.A., Christensend, T.R., 2006. Microbial activity in soils frozen to below-39 degrees C. Soil Biol. Biochem. 38, 785–794.

Pommier, T., Neal, P.R., Gasol, J.M., Coll, M., Acinas, S.G., Pedros-Alio, C., 2010. Spatial patterns of bacterial richness and evenness in the NW Mediterranean Sea explored by pyrosequencing of the 16S rRNA. Aquat. Microb. Ecol. 61, 212–224.

Price, P.B., Sowers, T., 2004. Temperature dependence of metabolic rates for microbial growth, maintenance, and survival. Proc. Natl. Acad. Sci. U. S. A. 101, 4631–4636.

Priscu, J.C., Christner, B.C., 2004. Earth's icy biosphere. In: Bull, A.T. (Ed.), Microbial Diversity and Bioprospecting. ASM Press, Washington DC, pp. 130–145.

Ramli, A.N., Mahadi, N.M., Rabu, A., Murad, A.M., Bakar, F.D., Illias, R.M., 2011. Molecular cloning, expression and biochemical characterisation of a cold-adapted novel recombinant chitinase from Glaciozyma antarctica PI12. Microb. Cell Fact. 34, 2618–2630.

Rappe, M.S., Giovannoni, S.J., 2003. The uncultured microbial majority. Annu. Rev. Microbiol. 57, 369–394.

Rina, M., Pozidis, C., Mavromatis, K., Tzanodaskalaki, M., Kokkinidis, M., Bouriotis, V., 2000. Alkaline phosphatase from the Antarctic strain TAB5. Eur. J. Biochem. 267, 1230–1238.

Russell, N.J., 1997. Psychrophilic bacteria — molecular adaptations of membrane lipids. Comp. Biochem. Physiol. A Mol. Integr. physiol. 118, 489–493.

Russell, N.J., Nichols, D.S., 1999. Polyunsaturated fatty acids in marine bacteria — a dogma rewritten. Microbiology-UK 145, 767–779.

Sato, S., Kurihara, T., Kawamoto, J., Hosokawa, M., Sato, S.B., Esaki, N., 2008. Cold adaptation of eicosapentaenoic acid-less mutant of Shewanella livingstonensis Ac10 involving uptake and remodeling of synthetic phospholipids containing various polyunsaturated fatty acids. Extremophiles 12, 753–761.

Schmidt, M., Stougaard, P., 2010. Identification, cloning and expression of a cold-active beta-galactosidase from a novel Arctic bacterium, *Alkalilactibacillus ikkense*. Environ. Technol. 31, 1107–1114.

Shen, W.J., Sridhar, K., Bernlohr, D.A., Kraemer, F.B., 1999. Interaction of rat hormone-sensitive lipase with adipocyte lipid-binding protein. Proc. Natl. Acad. Sci. U. S. A. 96, 5528–5532.

Shen, W.-J., patel, S., Hong, R., Kraemer, F.B., 2000. Hormone-sensitive lipase functions as an oligomer. Biochemistry 39, 2392–2398.

Shivadji, S., Prakash, J.S.S., 2010. How do bacteria sense and respond to low temperature? Arch. Microbiol. 192, 85–95.

Shulse, C.N., Allen, E.E., 2011. Widespread occurrence of secondary lipid biosynthesis potential in microbial lineages. PLoS One 6.

Siddiqui, K.S., Parkin, D.M., Curmi, P.M., De Francisci, D., Poljak, A., Barrow, K., 2009. A novel approach for enhancing the catalytic efficiency of a protease at low temperature: reduction in substrate inhibition by chemical modification. Biotechnol. Bioeng. 103, 676–686.
Siegl, A., Kamke, J., Hochmuth, T., Piel, J., Richter, M., Liang, C., Dandekar, T., Hentschel, U., 2011. Single-cell genomics reveals the lifestyle of Poribacteria, a candidate phylum symbiotically associated with marine sponges. ISME J. 5, 61–70.
Simon, C., Daniel, R., 2011. Metagenomic analyses: past and future trends. Appl. Environ. Microbiol. 77, 1153–1161.
Simon, C., Wiezer, A., Strittmatter, A.W., Daniel, R., 2009. Phylogenetic diversity and metabolic potential revealed in a glacier ice metagenome. Appl. Environ. Microbiol. 75, 7519–7526.
Skidmore, M., Anderson, S.P., Sharp, M., Foght, J., Lanoil, B.D., 2005. Comparison of microbial community compositions of two subglacial environments reveals a possible role for microbes in chemical weathering processes. Appl. Environ. Microbiol. 71, 6986–6997.
Sogin, M.L., Morrison, H.G., Huber, J.A., Mark, A., Welch, D., Huse, S.M., Neal, P.R., Arrieta, J.M., Herndl, G.J., 2006. Microbial diversity in the deep sea and the underexplored "rare biosphere". Proc. Natl. Acad. Sci. U. S. A. 103, 12115–12120.
Staley, J.T., Konopka, A., 1985. Measurement of in situ activities of nonphotosynthetic microorganisms in aquatic and terrestrial habitats. Annu. Rev. Microbiol. 39, 321–346.
Steven, B., Briggs, G., McKay, C.P., Pollard, W.H., Greer, C.W., Whyte, L.G., 2007. Characterization of the microbial diversity in a permafrost sample from the Canadian high Arctic using culture-dependent and culture-independent methods. FEMS Microbiol. Ecol. 59, 513–523.
Steven, B., Pollard, W.H., Greer, C.W., Whyte, L.G., 2008. Microbial diversity and activity through a permafrost/ground ice core profile from the Canadian high Arctic. Environ. Microbiol. 10, 3388–3403.
Thomas, D.N., Dieckmann, G.S., 2002. Antarctic Sea ice — a habitat for extremophiles. Science 295, 641–644.
Torsvik, V., Ovreas, L., Thingstad, T.F., 2002. Prokaryotic diversity — magnitude, dynamics, and controlling factors. Science 296, 1064–1066.
Ueda, M., Goto, T., Nakazawa, M., Miyatake, K., Sakaguchi, M., Inouye, K., 2010. A novel cold-adapted cellulase complex from Eisenia foetida: characterization of a multienzyme complex with carboxymethylcellulase, beta-glucosidase, beta-1,3 glucanase, and beta-xylosidase. Comp. Biochem. Physiol. B Biochem. Mol. Biol. 26–32.
Vartoukian, S.R., Palmer, R.M., Wade, W.G., 2010. Strategies for culture of 'unculturable' bacteria. FEMS Microbiol. Lett. 1, 1–7.
Venketesh, S., Dayananda, C., 2008. Properties, potentials, and prospects of antifreeze proteins. Crit. Rev. Biotechnol. 28, 57–82.
Venter, J.C., Remington, K., Heidelberg, J.F., et al., 2004. Environmental genome shotgun sequencing of the Sargasso Sea. Science 304, 66–74.
Vetriani, C., Jannasch, H.W., MacGregor, B.J., Stahl, D.A., Reysenbach, A.L., 1999. Population structure and phylogenetic characterization of marine benthic archaea in deep-sea sediments. Appl. Environ. Microbiol. 65, 4375–4384.
Vieille, C., Zeikus, G.J., 2001. Hyperthermophilic enzymes: sources, uses, and molecular mechanisms for thermostability. Microbiol. Mol. Biol. Rev. 65, 1–43.
Vincent, W.F., 2000. Cyanobacterial dominance in the polar regions. In: Whitton, B.A., Potts, M. (Eds.), The Ecology of Cyanobacteria: Their Diversity in Time and Space. Kluwer Academics Publishers, Dordrecht, London, Boston, pp. 321–340.
Wang, P., Li, T., Hu, A.Y., Wei, Y.L., Guo, W.T., Jiao, N.Z., Zhang, C.L., 2010. Community structure of Archaea from deep-sea sediments of the South China Sea. Microb. Ecol. 60, 796–806.
Ward, D.M., Weller, R., Bateson, M.M., 1990. 16S rRNA sequences reveal numerous uncultured microorganisms in a natural community. Nature 345, 63–65.
Watt, W.B., Dean, A.M., 2000. Molecular-functional studies of adaptive genetic variation in prokaryotes and eukaryotes. Annu. Rev. Genet. 34, 593–622.
Weisburg, W.G., Barns, S.M., Pelletier, D.A., Lane, D.J., 1991. 16s ribosomal DNA amplification for phylogenetic study. J. Bacteriol. 173, 697–703.
Wietz, M., Gram, L., Jorgensen, B., Schramm, A., 2010. Latitudinal patterns in the abundance of major marine bacterioplankton groups. Aquat. Microb. 61, 179–189.
Wilhelm, R.C., Niederberger, T.D., Greer, C., Whyte, L.G., 2011. Microbial diversity of active layer and permafrost in an acidic wetland from the Canadian High Arctic. Can. J. Microbiol. 57, 303–315.
Will, C., Thurmer, A., Wollherr, A., Nacke, H., Herold, N., Schrumpf, M., Gutknecht, J., Wubet, T., Buscot, F., Daniel, R., 2010. Horizon-specific bacterial community composition of german grassland soils, as revealed by pyrosequencing-based analysis of 16S rRNA genes. Appl. Environ. Microbiol. 76, 6751–6759.
Wirsen, C.O., Jannasch, H.W., Wakeham, S.G., Canuel, E.A., 1987. Membrane-lipids of a psychrophilic and barophilic deep-sea bacterium. Curr. Microbiol. 14, 319–322.
Wommack, K.E., Bhavsar, J., Ravel, J., 2008. Metagenomics: read length matters. Appl. Environ. Microbiol. 74, 1453–1463.
Woyke, T., Xie, G., Copeland, A., González, J.M., Han, C., Kiss, H., Saw, J.H., Senin, P., Yang, C., Chatterji, S., Cheng, J.F., Eisen, J.A., Sieracki, M.E., Stepanauskas, R., 2009. Assembling the marine metagenome, one cell at a time. PLoS One 4 (4), e5299.
Xu, K., Tang, X., Gai, Y., Mehmood, M., Xiao, X., Wang, F., 2011. Molecular characterization of cold-inducible beta-galactosidase from Arthrobacter sp. ON14 isolated from Antarctica. J. Microbiol. Biotechnol. 21, 236–242.
Yano, Y., Nakayama, A., Yoshida, K., 1997. Distribution of polyunsaturated fatty acids in bacteria present in intestines of deep-sea fish and shallow-sea poikilothermic animals. Appl. Environ. Microbiol. 63, 2572–2577.
Yergeau, E., Hogues, H., Whyte, L.G., Greer, C.W., 2010. The functional potential of high Arctic permafrost revealed by metagenomic sequencing, qPCR and microarray analyses. ISME J. 4, 1206–1214.
Youssef, N.H., Blainey, P.C., Quake, S.R., Elshahed, M.S., 2011. Partial genome assembly for a candidate division OP11 single cell from an anoxic spring (zodletone spring, Oklahoma). Appl. Environ. Microbiol. 77, 7804–7814.
Yu, E.Y., Kwon, M.A., Lee, M., Oh, J.Y., Choi, J.E., Lee, J.Y., Song, B.K., Hahm, D.H., Song, J.K., 2011. Isolation and characterization of cold-active family VIII esterases from an arctic soil metagenome. Appl. Microbiol. Biotechnol. 90, 573–581.
Zak, D.R., Kling, G.W., 2006. Microbial community composition and function across an arctic tundra landscape. Ecology 87, 1659–1670.
Zhang, N., Suen, W.C., Windsor, W., Xiao, L., Madison, V., Zaks, A., 2003. Improving tolerance of *Candida antarctica* lipase B towards irreversible thermal inactivation throught directed evolution. Protein Eng. Des. Sel. 16, 599–605.

Biochimie 95 (2013) 1795–1806

Contents lists available at SciVerse ScienceDirect

Biochimie

journal homepage: www.elsevier.com/locate/biochi

Research paper

Characterization of the first eukaryotic cold-adapted patatin-like phospholipase from the psychrophilic *Euplotes focardii*: Identification of putative determinants of thermal-adaptation by comparison with the homologous protein from the mesophilic *Euplotes crassus*

Guang Yang [a], Concetta De Santi [b], Donatella de Pascale [b], Sandra Pucciarelli [a], Stefania Pucciarelli [a], Cristina Miceli [a,*]

[a] School of Biosciences and Biotechnology, University of Camerino, Italy
[b] Institute of Protein Biochemistry, CNR, Naples, Italy

ARTICLE INFO

Article history:
Received 12 November 2012
Accepted 13 June 2013
Available online 22 June 2013

Keywords:
Patatin-like phosholipase
Molecular cold adaptation
Site-directed mutagenesis
Psychrophilic enzymes

ABSTRACT

The ciliated protozoon *Euplotes focardii*, originally isolated from the coastal seawaters of Terra Nova Bay in Antarctica, shows a strictly psychrophilic phenotype, including optimal survival and multiplication rates at 4–5 °C. This characteristic makes *E. focardii* an ideal model species for identifying the molecular bases of cold adaptation in psychrophilic organisms, as well as a suitable source of novel cold-active enzymes for industrial applications. In the current study, we characterized the patatin-like phospholipase from *E. focardii* (*Ef*PLP), and its enzymatic activity was compared to that of the homologous protein from the mesophilic congeneric species *Euplotes crassus* (*Ec*PLP). Both *Ef*PLP and *Ec*PLP have consensus motifs conserved in other patatin-like phospholipases.

By analyzing both esterase and phospholipase A_2 activity, we determined the thermostability and the optimal pH, temperature dependence and substrates of these enzymes. We demonstrated that *Ef*PLP shows the characteristics of a psychrophilic phospholipase. Furthermore, we analyzed the enzymatic activity of three engineered versions of the *Ef*PLP, in which unique residues of *Ef*PLP, Gly_{80}, Ala_{201} and Val_{204}, were substituted through site-directed mutagenesis with residues found in the *E. crassus* homolog (Glu, Pro and Ile, respectively). Additionally, three corresponding mutants of *Ec*PLP were also generated and characterized. These analyses showed that the substitution of amino acids with rigid and bulky charged/hydrophobic side chain in the psychrophilic *Ef*PLP confers enzymatic properties similar to those of the mesophilic patatin-like phospholipase, and *vice versa*.

This is the first report on the isolation and characterization of a cold-adapted patatin-like phospholipase from eukaryotes. The results reported in this paper support the idea that enzyme thermal-adaptation is based mainly on some amino acid residues that influence the structural flexibility of polypeptides and that *Ef*PLP is an attractive biocatalyst for industrial processes at low temperatures.

1. Introduction

Psychrophiles are organisms living at cold temperatures, colonizing about 70% of earth's biosphere, such as polar and alpine regions or deep-sea waters [1]. The ability of psychrophiles to survive in the cold is the result of molecular evolution and adaptations which, together, overcome the deleterious effects of low energy environments and the freezing of water [1]. One of the essential adaptive properties of psychrophiles is represented by their cold-active enzymes, which have received a great deal of attention in fundamental research for understanding the molecular basis underlying cold-adaptation [2], and for their potential utilization in certain industrial applications [3]. Cold-adapted enzymes have evolved a range of molecular features that confer a high level of structural flexibility, particularly around the active site that are translated into low activation enthalpy. This property can be useful to

Abbreviations: PLP, patatin-like phospholipase; RATE, rapid amplification of telomeric ends; pNP, p-nitrophenyl; *Di*C_3PC, 1,2-dipropinoyl-sn-glycero-3-phosphocholine; *Di*C_4PC, 1,2-dibutanoyl-*sn*-glycero-3-phosphocholine; *Di*C_6PC, 1,2-dihexanoyl-*sn*-glycero-3-phosphocholine.

* Corresponding author. Dipartimento di Biologia Molecolare, Cellulare e Animale, University of Camerino, Via Gentile III da Varano, 62032 Camerino (MC), Italy. Tel.: +39 0737 40 32 55; fax: +39 0737 40 32 90.
E-mail address: cristina.miceli@unicam.it (C. Miceli).

0300-9084/$ – see front matter © 2013 Elsevier Masson SAS. All rights reserved.
http://dx.doi.org/10.1016/j.biochi.2013.06.008

improve the efficiency of industrial processes by lowering the energetic costs [3,4].

Lipases are one of the most investigated groups of enzymes because they display both hydrolysis and synthesis activity toward many useful ester compounds. Lipases catalyze esterification, trans-esterification, interesterification, acidolysis, alcoholysis, and aminolysis, in addition to the hydrolytic activity on triglycerides. Thus, they constitute a potential source of biotechnologically interesting substances and have emerged as key enzymes for a wide variety of different industrial applications, including synthesis of biopolymer and biodiesel, production of pharmaceutical and detergents, food processing, chemical transformation, and cosmetics. In this contest, cold-adapted lipases have lately attracted attention because their high activity at low temperature is a favorable property for the production of relatively frail compounds [5].

A family of lipolytic enzymes designated as patatin-like phospholipases (PLPs, EC = 3.1.1.3, PFAM accession number: PF01734) has been previously proposed as key biocatalysts [6]. The PLPs are nonspecific lipid acyl hydrolases predominately found in potato tubers [7–9], where are essentially storage proteins with catalytic properties [10]. These proteins catalyze the nonspecific hydrolysis of phospholipids, glycolipids, sulfolipids, and mono- and diacylglycerols [11–14]. Furthermore, PLPs appear to be involved in signal transduction and to function as bioactive enzymes that protect plants from parasites [15,16]. Sequence homology studies [16,17], together with crystal structure study of a isozyme of patatin, and alanine-scanning mutagenesis study [17,18], have shown that PLPs share conserved blocks with the animal calcium-independent phospholipase A_2 ($iPLA_2$) and cytosolic phospholipase A_2 ($cPLA_2$), and possess an active dyad site instead of the Ser-His-Asp/Glu triad common of other lipolytic enzymes [19].

PLPs were intensively studied in plants, bacteria and vertebrates [20–22]. Most of these works focused mainly on subfamily classification of the *PLP* genes and on the characterization of the biological roles by informatics approaches. Relatively few PLPs have been characterized biochemically so far.

In this paper, we report the biochemical characterization of the first eukaryotic PLP from *Euplotes focardii* (*Ef*PLP), a ciliated protozoon endemic of Antarctic coastal seawaters. Ciliates provide excellent material to study adaptive evolution to cold, since they are single cells directly exposed to environmental cues. We choose *E. focardii* as model organism for this study because this eukaryotic microbe shows strictly psychrophilic phenotypes: its optimal temperature of survival and reproduction is 4–5 °C; it lacks a transcriptional response of the *Hsp70* genes to thermal shock [23,24]; it possesses cold-stable microtubules [25,26] and modified ribosomal proteins [27].

By analyzing enzymatic activities, we determined optimal pH, temperature dependence, thermostability and substrates specificity of *Ef*PLP, in comparison with the activities of a PLP from the evolutionary close mesophilic species *Euplotes crassus* (*Ec*PLP). We demonstrated that *Ef*PLP shows the characteristics of a psychrophilic phospholipase, because it is active in the cold, whereas *Ec*PLP is not. Furthermore, we analyzed the enzymatic activity of three engineered versions of the *Ef*PLP, in which unique residues of *Ef*PLP, Gly_{80}, Ala_{201} and Val_{204}, were substituted through site-directed mutagenesis by Glu, Pro and Ile, respectively (i.e. residues found in the *E. crassus* homolog). These analyses indicated that the introduction in the *Ef*PLP of amino acids with rigid and bulky charged/hydrophobic side chains confer enzymatic properties more similar to those of the mesophilic PLPs. For obtaining further support of our findings, we also carried out the reverse procedures by replacing Glu_{81}, Pro_{202} and Ile_{205} residues of *Ec*PLP with Gly, Ala and Val, respectively. Following, the effects of temperatures on enzyme properties of those variants were examined and catalytic efficiency was also investigated. These results indicate that enzyme thermal-adaptation is based on amino acid residues that influence the structural flexibility of polypeptides. Furthermore, we demonstrated that PLPs are enzymes that can display both esterase and phospholipase A_2 (PLA_2) activities, a characteristic that makes these molecules promising for industrial applications even at low temperatures.

2. Materials and methods

2.1. Materials

Restriction enzymes, recombinant *Taq* DNA polymerase and *Pfu* DNA polymerase were purchased from Fermentas (Milan, Italy). Ampicillin, Isopropyl-β-D-thio-galactoside (IPTG), 5-bromo-4-chloro-indolyl-β-D-galactopyranoside (X-Gal) and *p*-Nitrophenyl (*p*NP) esters were purchased from Sigma–Aldrich (USA). Arachidonoyl thio-PC was obtained from Cayman Chemical Co. (Ann Arbor, MI, USA). 1,2-dipropinoyl-sn-glycero-3-phosphocholine (*Di*C_3PC), 1,2-dibutanoyl-*sn*-glycero-3-phosphocholine (*Di*C_4PC) and 1,2-dihexanoyl-*sn*-glycero-3-phosphocholine (*Di*C_6PC) were purchased from Avanti Polar Lipids (Alabama, USA). All chemicals were reagent grade. All oligonucleotide primers used in this study were synthesized by Sigma (Milan, Italy).

2.2. Cell strains and growth conditions

Cultures of *E. focardii* strain TN1 [28] and *E. crassus* strain G1 were used. *E. focardii* strain TN1 represents type-species material chosen from a number of wild-type strains isolated from sediment and seawater samples collected from the coastal waters of Terra Nova Bay, Antarctica (temperature −1.8 °C, salinity 35 *f* and pH 8.1–8.2). It was grown and maintained in a cold room at 4 °C. The *E. crassus* strain G1 used in this study was kindly obtained from the strain collection of Luporini's laboratory at the University of Camerino. It is a close relative species of *E. focardii* and represents the mesophilic counterpart. In a phylogenetic tree of *Euplotes* species based on 18S rDNA these two *Euplotes* belong to the same cluster (data not shown). Both cell lines were fed with the green alga *Dunaliella tertiolecta* as food.

2.3. Isolation of Euplotes PLPs nanochromosomes from macronuclear DNA via PCR and rapid amplification of telomeric ends (RATE)

E. focardii macronuclear DNA was purified as described [29]. To obtain the primary partial *E. focardii PLP* gene (*EfPLP*) sequence, we based our PCR strategy on degenerate oligonucleotide primers designed from *Euplotes EfPLP* consensus sequence (obtained by the alignment of homologous genes from *E. crassus*, which were kindly provided by the laboratory of Professor Gladyshev, Harvard Medical School, USA). Degenerate oligonucleotide primers were designed according to the improved CODEHOP primer design method [30]. The forward primer, 5′-GTKTCTGCHGGWTCCCTMAACACTTTAGGTCT-3′, covered codons 59–68 plus two nucleotides from 69, and the reverse primer, 5′- GATGTCVATSTTVCARATTACTCCACCATCAA-3′, corresponded to two nucleotides of codon 190 plus triplets 200–191. Amplification was performed using touchup PCR strategies: 95 °C for 2 min, followed by 10 cycles of 95 °C for 30 s, from 45 °C annealing temperature gradually rise 1 °C each cycle for 30 s to 54 °C, and 72 °C for 30 s, followed by 25 cycles of 95 °C for 30 s, 55 °C for 30 s, and 72 °C for 30 s, and finally a final extension at 72 °C for 5 min. The amplification products were expected to be about 1270 bp long.

Based on the organization of nanochromosomes in *Euplotes* spp. [31], RATE PCR [29] was carried out for obtaining the sequences of

N-terminal and C-terminal coding regions and the 5′- and 3′-UTRs. The forward primer, 5′- GCAGATAACTTAGGTGACAGAACTCT-3′ and reverse primer, 5′- AGAGTTCTGTCACCTAAGTTATCTGC-3′ were individually used in combination with the telomeric oligonucleotide 5′-$(C_4A_4)_4$-3′ in RATE PCR. Amplified products were cloned into pTZ57R/T vector (Fermentas, Milan, Italy) and further transformed into *Euplotes coli* DH5α. Clones containing the *EfPLP* recombinant plasmids were sequenced in both strands (BMR Genomics, Padova, Italy).

The *E. crassus PLP* gene (*EcPLP*) was amplified from *E. crassus* genomic DNA. Oligonucleotides *Ec*NdeI (5′-CATATGAGGAAATGTAGAGCATTAGCCCT-3′) and *Ec*XhoI (5′-CTCGAGTTGAGACTCAGATTTTGGTTGTTTT-3′) were used as forward and reverse primers, respectively. The amplification primer *Ec*NdeI and *Ec*XhoI were designed to introduce an NdeI restriction site upstream from the initiation site, and an XhoI restriction site downstream from the stop codon of *EcPLP*, respectively. Amplification was performed using standard conditions: 30 cycles at 95 °C for 30 s, 59 °C for 30 s and 72 °C for 70 s. After the amplification, the reaction was further incubated at 72 °C for 10 min and stored at 4 °C. The PCR product was ligated into pTZ57R/T vector (Fermentas, Milan, Italy) and further transformed into *E. coli* DH5α, and clones containing *EcPLP* recombinant plasmids were sequenced in both strands (BMR Genomics, Padova, Italy).

E. coli DH5α was used as host for cloning whereas *E. coli* BL21 (DE3) harbored the recombinant plasmids for gene expression. *E. coli* strains were routinely grown in LB medium at 37 °C. When required, antibiotics and chromogenic substrates were added at the following concentrations: 100 μg/mL ampicillin and 30 μg/mL 5-bromo-4-chloro-indolyl-β-D-galactopyranoside (X-Gal). The complete *Euplotes PLPs* sequences are available on GeneBank™ by accession numbers: JX257001 (*EfPLP*) and JX257002 (*EcPLP*).

2.4. Subcloning of Euplotes PLPs into the expression vector pET-22b(+)

In order to facilitate heterologous expression of *Ef*PLP protein in *E. coli*, the gene without predicted signal peptide (resulting from the deletion of the gene region encoding the first 18 amino acids) was synthesized with *E. coli* codon usage by a gene synthesis distributor (Mr. Gene, Regensburg, DE). Restriction sites NdeI and XhoI were introduced to the 5′- and 3′- respectively. The synthesized *EfPLP* gene was cloned into pET-22b(+) expression vector (Novagen, USA) previously digested by NdeI and XhoI restriction enzymes to construct an expression plasmid pET-*EfPLP*. Similarly, the *EcPLP* recombinant plasmid was digested by NdeI and XhoI restriction enzymes and *EcPLP* was cloned into pET-22b(+) expression vector previously digested by NdeI and XhoI restriction enzymes in order to obtain a pET-*EcPLP* expression vector. The expression cassette includes an in-frame C-terminal fusion purification 6× His-Tag. The DNA sequence of the resulting construct was verified by bidirectional DNA sequencing.

2.5. Plasmid constructions of mutants

The site-directed mutants were prepared by the overlap extension method [32]. It yielded six expression plasmids: pET-*EfPLP*-G80E, pET-*EfPLP*-A201P and pET-*EfPLP*-A201P/V204I for generating variants of *Ef*PLP; pET-*EcPLP*-E81G, pET-*EcPLP*-P202A and pET-*EcPLP*-P202A/I205V for obtaining mutants of *Ec*PLP. The polymerase chain reactions were carried out by using the plasmids pET-*EfPLP* and pET-*EcPLP*, respectively as templates, *Pfu* DNA polymerase, and two complementary mutagenic primers for each site-specific mutation. The sequences of the oligonucleotides used were as shown in Table 1. Each amplification reaction was performed with 30 cycles of 94 °C for 30 s, 68 °C for 1 min, and 72 °C for 10 min. The final amplified products were verified by bidirectional DNA sequencing.

2.6. Overexpression and purification of wild-type and mutant Euplotes PLPs

E. coli BL21 (DE3) cells carrying wild-types or mutants plasmids were grown overnight at 37 °C in LB medium supplemented with 100 μg/mL ampicillin. The overnight cultures were diluted to a cell density of about 0.08 OD_{600} in 600 mL of LB medium supplemented with 100 μg/mL ampicillin using a 2 L flask. Cultivation took place in a 2 L flask at 30 °C under vigorous stirring and aeration. The induction procedures were carried out when cultures reached 0.6–0.8 at OD_{600} by addition of filter-sterilized IPTG to a final concentration of 1 mM. The cultures were grown for overnight post-induction. Cells were harvested by centrifugation at 5000 *g* at 4 °C for 20 min, divided into 0.50 g aliquots and frozen at −80 °C.

2.7. Purification of PLPs from E. coli BL21 (DE3) cells

IPTG induction of recombinant *E. coli* BL21 (DE3)/PLPs cells resulted in the accumulation of recombinant wild-type and mutant proteins as inclusion bodies. To recover of PLPs from inclusion bodies, the bacterial cell pellet (0.50 g) was frozen and thawed twice, resuspended in 3 mL TE buffer (50 mM Tris–HCl, pH 8 and 40 mM EDTA). 0.75 g sucrose and 0.6 mg lysozyme were added and the solution was incubated at 37 °C for 30 min. An osmotic shock was performed by the addition of 3 mL ice-cold TE buffer. The solution was again homogenized and incubated for 30 min at 37 °C. The cells were subjected to sonication for 5 for 1 min with intervals of 2 min to prevent overheating. Subsequently, Triton-X100 was

Table 1
Nucleotide sequences of primers used for site-directed mutagenesis and generated recombinant plasmids.

Directed mutation	Primer sequence[a]	Generated plasmid
*Ef*PLP-G80E	FW: 5′-ACTGACGTTGAGGaAGCAAGCGAGTTC-3′ RV: 5′-GAACTCGCTTGCTtCCTCAACGTCAGT-3′	pET-*EfPLP*-G80E
*Ef*PLP-A201P	FW: 5′-ATCGACATTcCTTCGGCTGTTCGTCGTTGT-3′ RV: 5′-ACAACGACGAACAGCCGAAGgAATGTCGAT-3′	pET-*EfPLP*-A201P
*Ef*PLP-A201P/V204I	FW: 5′-ATCGACATTcCTTCGGCTaTTCGTCGTTGT-3′ RV: 5′-ACAACGACGAAtAGCCGAAGgAATGTCGAT-3′	pET-*EfPLP*-A201P/V204I
*Ec*PLP-E81G	FW: 5′-CAGAGGAAGTTGAAGgAGCCACTGAATTC-3′ RV: 5′-GAATTCAGTGGCTcCTTCAACTTCCTCTG-3′	pET-*EcPLP*-E81G
*Ec*PLP-P202A	FW: 5′-AACATCGACATTgCTTCAGCTATCAGAAGGT-3′ RV: 5′-ACCTTCTGATAGCTGAAGcAATGTCGATGTT-3′	pET-*EcPLP*-P202A
*Ec*PLP-P202A/I205V	FW: 5′-CATCGACATTgCTTCAGCTgTCAGAAGGTG-3′ RV: 5′-CACCTTCTGAcAGCTGAAGcAATGTCGATG-3′	pET-*EcPLP*-P202A/I205V

[a] Mismatch sites for site-directed mutagenesis are in small letters.

added to a final concentration of 0.1% (w/v) and the solution was sonicated again for 1 min. The inclusion bodies were collected by centrifugation (20 min, 6726 *g*, 4 °C) and washed with 4 mL TE buffer. After centrifugation, the pellet was suspended in 2 mL of 10 mM Tris–HCl (pH 8). After 10 min centrifugation at 15,000 *g*, the pellet containing inclusion bodies was solubilized in 10 mL of 8 M urea and 5 mM glycine (pH 9) at room temperature. To remove the insoluble material, the solution was centrifuged 20 min at 10,000 *g*. The resulting supernatant was dialyzed in 200 mL of 20 mM glycine (pH 9), 20 mM beta-mercaptoethanol and 5 mM EDTA, at 4 °C, to allow the unfolded protein to refold. The buffer was changed three times in 24 h. Finally, the solution was dialyzed again at 4 °C against 200 mL 20 mM Tris–HCl (pH 8) to remove beta-mercaptoethanol and EDTA. Then, the refolded protein was stored at −20 °C in presence of 10% glycerol. All isolation steps were performed at 4 °C (unless otherwise specified).

2.8. SDS-polyacrylamide gel electrophoresis (PAGE) and protein concentration determination

SDS-PAGE was performed according to the method of Laemmli using 5% polyacrylamide-stacking gel and 12% polyacrylamide-resolving gel with a Bio-Rad Mini-Protean II cell unit, at room temperature. The protein concentration was determined according to the Bradford method with bovine serum albumin as the standard [33]. The protein content was measured by monitoring the optical density at 595 nm.

2.9. N-terminal sequencing of the Euplotes PLPs recombinant protein

Electroblotting was performed using PVDF membrane with 25 mM Tris Base, 192 mM glycine (pH 9) transfer buffer in the presence of 10% methanol. The membrane stained with Coomassie Brilliant Blue and destained to achieve protein band from membrane. Recombinant protein identification was carried out by N-terminal sequencing (AB Procise 49X cLC Protein Sequencing System) of the electroblotted protein band.

2.10. Enzyme assays

The esterase activities of the PLPs were measured spectrophotometrically at 405 nm by detection of *p*-nitrophenoxide released from *p*NP esters in 1-cm path-length cells with a Cary 100 spectrophotometer (Varian, Australia) equipped with a temperature controller. Assays were performed in 1 mL mixture containing purified enzyme (30 μg/mL), Teorell–Stenhagen buffer (50 mM boric acid, 10 mM phosphoric acid, 2.5 mM citric acid, adjust pH by NaOH) [34] at pH 10.5, 3% acetonitrile, and *p*NP esters at different concentrations. Stock solutions of *p*NP esters were prepared by dissolving the substrates in pure acetonitrile. Enzyme activities were determined at 25 °C for *Ef*PLP, *Ef*PLP-G80E and *Ec*PLP-P202A/I205V, at 30 °C for *Ef*PLP-A201P and *Ec*PLP-P202A, and at 35 °C for *Ec*PLP, *Ec*PLP-E81G and *Ef*PLP-A201P/V204I, respectively. Assays were carried out in duplicate or triplicate, and the results were expressed as the means of two or three independent experiments. One unit enzymatic activity was defined as the amount of protein that released 1 μmol of *p*-nitrophenoxide/min from *p*NP esters. The absorption coefficient used for *p*-nitrophenoxide was 19,000 M^{-1} cm^{-1}.

2.11. Determination of optimal pH and temperature of wild-type and mutant PLPs

The pH dependence of the esterase activity was monitored at 348 nm (the pH-independent isosbestic point of *p*-nitrophenol and the *p*-nitrophenoxide ion), with *p*NP butyrate (100 μM) as substrate. A molar absorption coefficient of 5000 M^{-1} cm^{-1} at 25 °C was introduced. The universal Teorell-Stenhagen buffer over a broad range of pH (pH 8–12) was used. Data were analyzed as described by Dixon and Webb [35]. The temperature optimum was determined by analyzing the esterase activity in the range of temperature from 0 to 50 °C in Teorell-Stenhagen buffer (pH 10.5), containing 3% acetonitrile, using *p*NP butyrate (100 μM) as substrate.

2.12. Determination of the thermostability

Half-lives of thermal inactivation were determined for purified wild-types and variants PLPs by incubating the enzymes (30 μg/mL) at 40, 55 and 70 °C for 30–180 min with regular time intervals. Initial and residual activities were measured under the standard assay conditions previously described. The first-order rate constant, k_d, of irreversible thermal denaturation was obtained from the slope of the plots of ln (initial activity/residual activity) versus time, and the half-lives ($t_{1/2}$) were calculated as $\ln 2/k_d$.

2.13. Measurement of PLA_2 activity of wild-types and mutants

PLA_2 activities toward the substrate arachidonoyl thio-PC were estimated colorimetrically by determining the release of thiol groups. Substrate in ethanol was bubbled under a gentle stream of nitrogen and then solubilized in assay buffer (80 mM HEPES, pH 7.4, 150 mM NaCl, 10 mM $CaCl_2$, 4 mM Triton X-100, 30% v/v glycerol, and 1 mg/mL bovine serum albumin) and vortexed until completely dissolved. A solution in 6 mL of assay buffer contained arachidonoyl thio-PC at a final concentration of 1.5 mM. The PLA_2 assay was conducted using a 96 well microplate with a total assay volume of 225 μL. The reaction mixture contained assay buffer, arachidonoyl thio-PC substrate and purified enzyme (30 μg/mL). Reactions were initiated by the addition of purified enzyme to the wells followed by incubation for 1 h at 23 °C. Assays were stopped by addition of a mixture of 25 mM 5,5′-dithio-bis (2-nitrobenzoic acid) (DTNB) and 475 mM EGTA. Color was developed for 5 min and then absorbance was measured at 414 nm in a Multiskan Spectrum microplate reader (Thermo Labsystems). The determination of PLA_2 activity was calculated by following substrate manufacturer's instructions.

The PLA_2 activities toward substrates 1,2-dipropanoyl-*sn*-glycero-3-phosphocholine (or 1,2-dihexanoyl-*sn*-glycero-3-phosphocholine or 1,2-dibutanoyl-*sn*-glycero-3-phosphocholine) were determined titrimetrically at pH 10.5 and at 25 °C with a pH-stat T50 (Mettler Toledo). Substrates in chloroform were bubbled under a gentle stream of nitrogen and then solubilized in distilled water with sonication. The standard condition contained distilled water and 10 mM substrate in a final volume of 4 mL. Substrate mix was pre-equilibrated with NaOH (0.1 mM) to pH 10.5 and pre-incubated at 25 °C for 10 min. Assays were initiated by adding enzymes to the final concentration of 30 μg/mL into substrate mix, the enzyme activities were measured by continuously monitoring the temperature amount of acid liberated from hydrolysis using the pH stat. One unit of PLA_2 activity was defined as 1 μM of fatty acid liberated under standard condition.

2.14. Kinetic measurements

The kinetic parameters K_M and k_{cat} of enzymes were measured using *p*NP esters as substrates at the condition described in the *Enzyme Assays* section. The initial velocities of substrate hydrolysis were monitored for a minimum of six substrate concentrations. The following substrate concentration ranges were used: *p*NP acetate (C_2, 100–1500 μM), *p*NP propionate (C_3, 100–1500 μM), *p*NP butyrate (C_4, 100–1700 μM), *p*NP valerate (C_5, 100–1500 μM), *p*NP

caprylate (C_8, 50–700 μM), *p*NP caprate (C_{10}, 50–700 μM). All kinetic data were analyzed by nonlinear regression using Origin 8.0. The Standard Error (S.E.) value of each parameter was estimated from the curve fitting. Assays were done in duplicate or triplicate, and results for kinetic data were mean of two independent experiments.

2.15. Sequence analysis and comparative modeling

Sequence alignment between the putative amino acid sequences of *EfPLP* and *EcPLP* was initiated by the EMBOSS Needle Pairwise Sequence Alignment. Sequence similarity and analysis for conserved blocks were performed using BLAST programs on the National Center for Biotechnology Information (NCBI) website (http://www.ncbi.nlm.nih.gov). Sequence alignments were performed using the tools of the T-Coffee server (http://www.ebi.ac.uk/Tools/msa/tcoffee/) and ClustalW2 (http://www.ebi.ac.uk/Tools/msa/clustalw2/). The N-terminal signal peptide was predicted using SignalP 3.0 server (http://www.cbs.dtu.dk/services/SignalP/). Molecular weights were determined using Protein Calculator V3.3 (http://www.scripps.edu/~cdputnam/protcalc.html). Comparative homology model of the *E. focardii* PLP was obtained by the program SWISS-MODEL [36,37], using the patatin from *Solanum cardiophyllum* (PDB: 1OXW) as a specific template, and the sequence identity between template and target is 19%.

3. Results

3.1. Subcloning the Euplotes PLP genes

Euplotes macronuclear DNA consists of short linear molecules (nanochromosomes) ranging in size from 0.3 to 40 kbp, each of which is present in multiple copies and generally encodes a single genetic function [38]. These nanochromosomes have telomeres at their ends that consist of repeats of the C_4A_4 motif (schematically represented in Fig. 1A). By our RATE-PCR-based cloning strategy (described under "Materials and Methods"), we obtained two entire PLP nanochromosomes from *E. focardii* and *E. crassus*, that we named *EfPLP* and *EcPLP*. These nanochromosomes were 1156 bp and 1229 bp long respectively, without introns. The coding regions were 1071 bp and 1074 bp long, respectively, and the predicted proteins of 357 and 358 amino acids, respectively. The *EfPLP* coding region was flanked by 56 and 29 bp untranslated regions at the 5′ and 3′ sides respectively. The *EcPLP* coding region was flanked by 59 and 37 bp untranslated regions at the 5′ and 3′ sides respectively.

Blastp searches of the *EfPLP* predicted amino acid sequence revealed similarity with PLPs from other protists, including three PLPs from *Tetrahymena thermophila* (XP_001014319.1, XP_001014317.1, XP_001011026.1) with 57% positives (E-value 6e-59), 51% positives (E-value 1e-51), 50% positives (E-value 9e-39), respectively, and a hypothetical patatin from the Ichthyosporea fish parasite *Capsaspora owczarzaki* ATCC 30864 (EFW47637.1) with 51% positives (E-value 1e-33). Each of the bacterial patatin-like conserved blocks [39] was identified in both *Ef*PLP and *Ec*PLP (indicated as blocks I, II, III and IV in Fig. 1B). Block I consists of a Gly-rich region, which probably serves as an oxyanion hole. Block II represents a typical lipase nucleophilic elbow Gly-X-Ser-X-Gly containing the putative active-site Ser (Gly_{59}–Val_{60}–Ser_{61}–Ala_{62}–Gly_{63} in *Ef*PLP and Gly_{60}–Val_{61}–Ser_{62}–Ala_{63}–Gly_{64} in *Ec*PLP), which is located 10–20 AA downstream the Block I. Block III contains a conserved ASXXXP motif of unknown function. Block IV contains the active-site Asp (Asp_{191} in *Ef*PLP and Asp_{192} in *Ec*PLP) that, together with the active-site Ser, forms the catalytic Ser–Asp dyad.

Further sequence analysis performed using SignalP 3.0 server indicated the presence of a signal peptide typical of secreted proteins with a putative cleavage site located between Ser_{18} and Lys_{19} in *Ef*PLP and Ala_{19} and Arg_{20} in *Ec*PLP. Molecular weight of the cleaved mature *Ef*PLP and *Ec*PLP proteins were calculated as 37.6 kDa and 37.9 kDa, respectively. The *Ef*PLP and *Ec*PLP amino acid sequences were 80.2% identical.

3.2. Sequence analysis

Cold active enzymes have been reported to be structurally modified by an increasing flexibility of the polypeptide chain enabling an easier accommodation of substrates at low temperature [3,40]. Therefore, to characterize unique characteristics of *Ef*PLP that may be responsible for cold-adaptation, we chose to focus our attention to residue substitutions which were found in the *Ef*PLP with respect to *Ec*PLP from sequence comparison, and would be expected to increase intramolecular flexibility: 1) Pro to Ala in position 201; 2) charged residue to Val/Gly/Asn/Ala in positions 49/80/96/347, respectively; 3) Ile to Val/Val/Gly in positions 204/229/317, respectively. The substitutions of bulky/rigid amino acid with small ones have been observed for cold-adapted variants of several proteins and are expected to increase intramolecular flexibility [25,27,41]. In addition, these substitutions are similar to those that transform mesophilic subtilisin-like proteases into cold-active variants [42]. Fig. 2A′ and A″ show the low-resolution homology model of *Ef*PLP (see Materials and Methods) that give an approximation of the three-dimensional organization of the conserved residues that compose the catalytic dyad, the conserved block domains, and the localization of the mutated residues. We observed, that three of the unique residues of *Ef*PLP, Gly_{80}, Ala_{201} and Val_{204} (underlined in Fig. 1B), that surround the catalytic sites, may be potential candidates for cold adaptation of *Ef*PLP. To test this hypothesis, we decided to compare the enzymatic activity of *Ef*PLP and *Ec*PLP, and to investigate the activity of three engineered versions of *Ef*PLP and *Ec*PLP, respectively. In the former three mutants, *E. focardii* residues were substituted as they were in the *E. crassus* sequence: 1- *Ef*PLP-G80E, in which Gly_{80} was substituted by Glu; 2- *Ef*PLP-A201P, in which the Ala_{201} was substituted by Pro; 3- *Ef*PLP-A201P/V204I, in which the Ala_{201} and Val_{204} were substituted by Pro and Ile, respectively. In the latter three mutants, the Gly, Ala and Val together of *Ef*PLP were introduced into *Ec*PLP. Therefore, these mutants were named as *Ec*PLP-E81G, *Ec*PLP-P202A and *Ec*PLP-P202A/I205V.

Wild-types and six mutants were subcloned in the expression vectors pET-22b(+), as described under "Materials and Methods". After confirming the correct ORF and mutations by DNA sequencing, the plasmids were transformed into *E. coli* BL21 (DE3) cells for protein expression and purification. As estimated from SDS-PAGE (Fig. 2B) the purified proteins were about 95% pure.

3.3. Esterase activity of the PLP wild-types and mutants: pH dependence, thermophilicity and thermostability

As a first step, we determined the optimal pH for the esterase activity of the *Euplotes* PLPs using *p*NP butyrate as a substrate. Kinetics was followed spectrophotometrically at 348 nm in the pH range of 8.0–12.0, which is the pH independent isosbestic wavelength between the *p*-nitrophenol and *p*-nitrophenolate ion produced by the reaction. As shown in Fig. 3, the maximum activities for both wild-type *Ef*PLP and *Ec*PLP were recorded at pH 10.5 in Teorell-Stenhagen buffer. Similar results were obtained using the mutated versions of the *Ef*PLP and *Ec*PLP (data not shown).

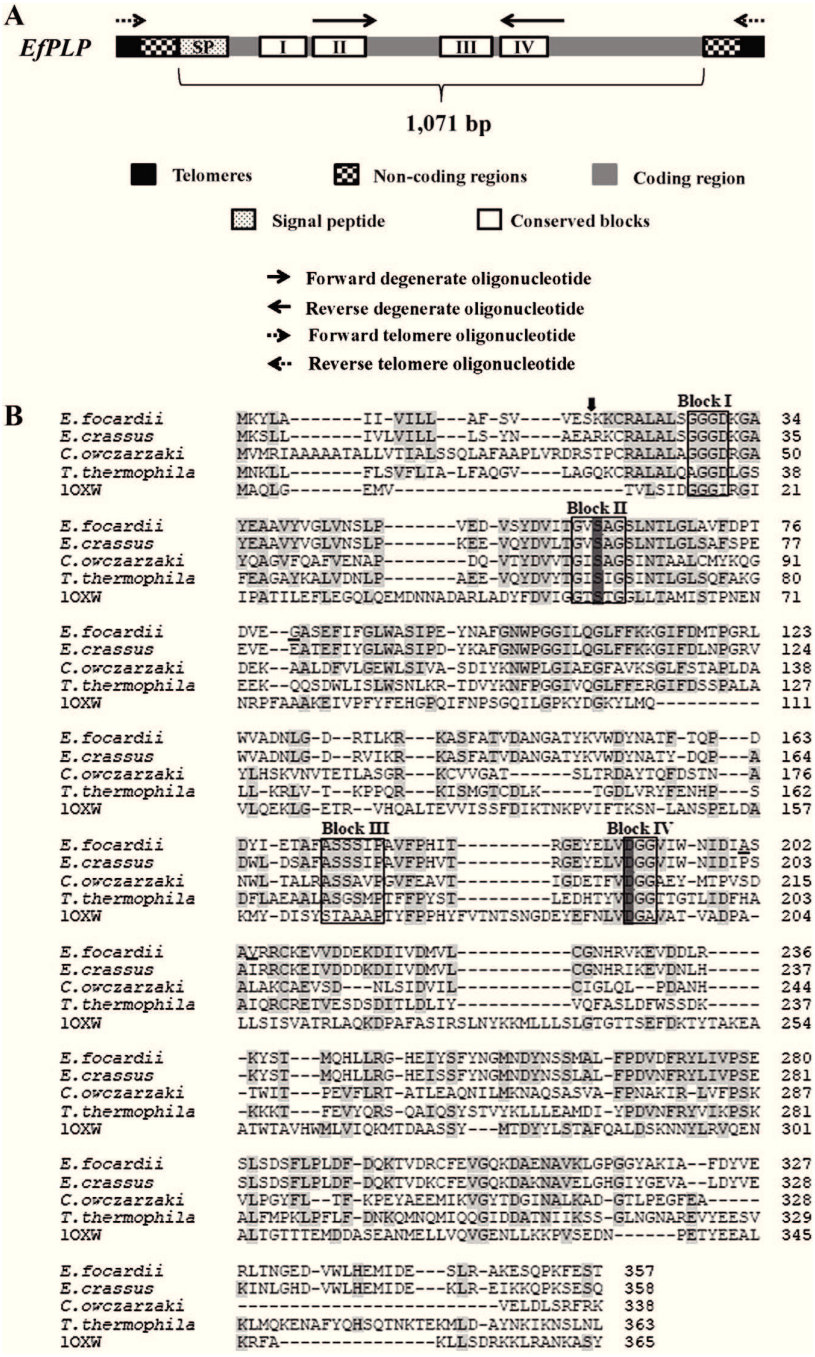

Fig. 1. *EfPLP* sequence analysis. (A) Schematic representation of the *EfPLP* macronuclear gene. The coding regions (gray squares) are flanked by non-coding regions (chequered squares) of differing lengths that terminate in telomeres composed of four repetition of the C_4A_4/G_4T_4 motif (black squares). The telomeric sequence can be used as template of oligonucleotides for PCR amplification in combination with oligonucleotides that bind DNA sequence of the coding region, indicated by horizontal arrows (see text). Signal peptide (SP) and conserved blocks (I, II, III, IV) are also represented; (B) Alignment of the predicted amino-acid sequences of *EfPLP* (JX257001) and *EcPLP* (JX257002) with the homologs from *T. thermophila* (XP_001014319.1), *C. owczarzaki* (EFW47637.1) and *Solanum cardiophyllum* (PDB accession code: 1OXW). Conserved residues are light shaded. Gray shaded Ser and Asp constitute the PLPs catalytic dyad. The conserved patatin block domains (Block I, Block II, Block III and Block IV) are boxed. The putative cleavage site of signal peptide between Ser_{18} and Lys_{19} are labeled with an arrow. The residues that are substituted by site-directed mutagenesis are underlined.

The effect of temperatures on esterase activity for both wild-types and mutants was determined using *p*NP butyrate as substrate in the temperature range of 0–50 °C. As shown in Fig. 4A, about 50% of the hydrolytic activity of *Ef*PLP was found at 0 °C. The highest percentage activity was observed at 25 °C. No activity was detected at 50 °C. In contrast, *Ec*PLP showed no activity at 0 °C, the highest activity was found at 35 °C, and the enzyme was still active at 50 °C (Fig. 4A).

The analysis of the esterase activity of the *Ef*PLP-G80E mutant showed that it behaved similarly to the wild-type, i.e. about 50% of

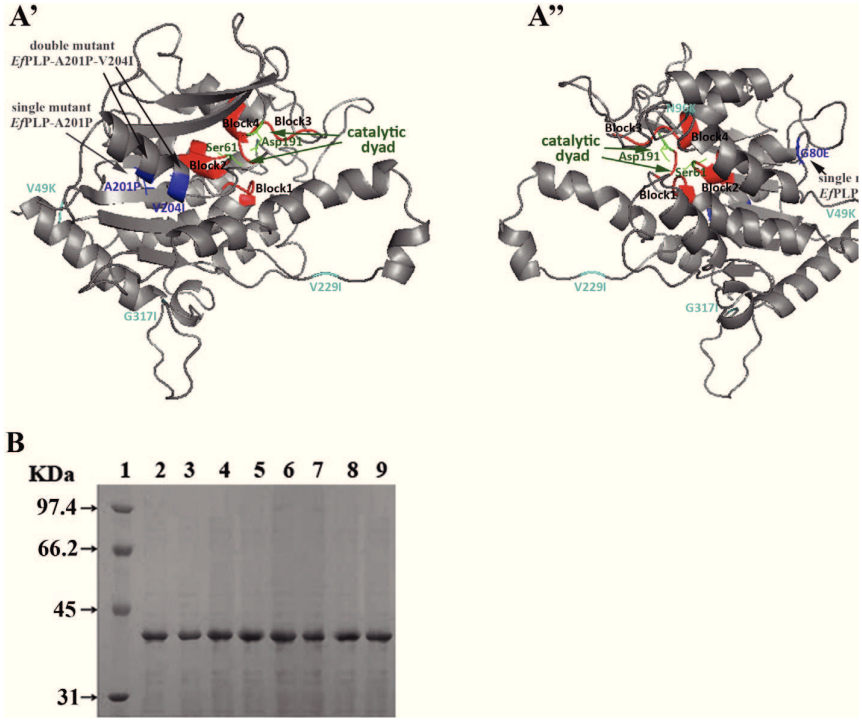

Fig. 2. (A′) Low-resolution homology model of *Ef*PLP. Side chains of the catalytic dyad aspartate and serine are shown in green; the conserved patatin block domains (Block I, Block II, Block III and Block IV) are shown in red; the mutated residues are shown in blue; other substitutions of amino acids that may influence the intramolecular flexibility are shown in light blue; (A″) Reverse side of Fig. A′; (B) Sodium dodecyl sulfate (SDS)-polyacrylamide gel electrophoresis (PAGE) analysis of recombinant proteins *Ef*PLP (lane 2), *Ec*PLP (lane 3), *Ef*PLP-G80E (lane 4), *Ef*PLP-A201P (lane 5), *Ef*PLP-A201P/V204I (lane 6), *Ec*PLP-E81G (lane 7), *Ec*PLP-P202A (lane 8), *Ec*PLP-P202A/I205V (lane 9) at the end of purification procedure. Five-microliter aliquots were withdrawn from each samples and loaded on a 12% SDS-PAGE gel in a Mini Protean III cell gel electrophoresis unit (Bio-Rad). The bands in the gel were revealed by Coomassie blue staining. Molecular mass markers (in kDa) are shown on the left (lane 1).

the activity at 0 °C, and the maximum activity at 25 °C, as shown in Fig. 4B. However, about 35% of the *Ef*PLP-G80E activity was maintained at 50 °C, whereas the wild-type showed no activity at this temperature. Also the *Ef*PLP-A201P mutant displayed activity at 0 °C similar to *Ef*PLP, but the maximum activity was recorded at 30 °C (Fig. 4B). The double mutant *Ef*PLP-A201P/V204I showed about 50% of maximum activity at 0 °C (Fig. 4B). However, the optimal temperature was 35 °C, and it maintained about 60% of activity at 50 °C as for *Ec*PLP, suggesting that the insertion of

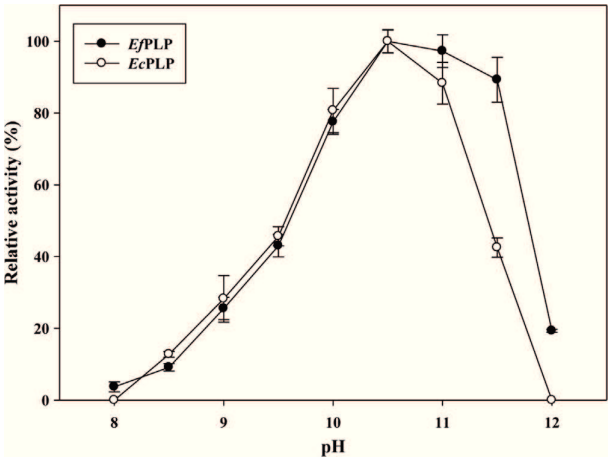

Fig. 3. Effect of pH on the esterase activity of wild-types.

E. crassus residues into *Ef*PLP conferred the capacity to efficiently exercise his enzymatic function at higher temperature than the cold-adapted variant of the PLPs.

When compared to the wild-type, the *Ec*PLP-E81G mutant showed an increased activity of about 20% at lower temperatures (15–25 °C) and decreased activity of about 10% at 40–50 °C (Fig. 4C). In contrast, the *Ec*PLP-P202A mutant displayed a dramatically increased activity at low temperature, in particular at 20–25 °C, when compared to the wild-type, and reached the highest activity at 30 °C (Fig. 4C). The double site mutant *Ec*PLP-P202A/I205V showed a 20% of activity at 0 °C, and its maximum activity was recorded at 25 °C (Fig. 4C). The double site mutant displayed a 30% loss of activity at 50 °C with respect to the wild-type. These results indicate that the residues chosen for mutations have a role in the temperature dependence of the enzyme activity.

To analyze the thermostability of the wild-type PLPs and their variants, we incubated the enzymes at 40, 55 and 70 °C for 30–180 min before measuring the residual esterase activities at their optimal temperatures, using *p*NP butyrate as substrate (Fig. 5A, B and C). As shown in Table 2, compared to *Ec*PLP which showed 3.38 and 3.11 h half-lives at 40 and 55 °C respectively, the psychrophilic counterpart *Ef*PLP displayed higher stability at the same temperatures with 3.72 and 3.65 h as half-lives. However, when the incubation temperature increased to 70 °C, *Ef*PLP showed a lower stability with 2.07 h half-life compared to *Ec*PLP which recorded 2.57 h half-life at the same temperature. All variants of *Ef*PLP with replacement of *Ec*PLP residues exhibited increased stability at 70 °C, with 2.21, 2.19 and 2.31 h half-lives for *Ef*PLP-G80E, *Ef*PLP-A201P and *Ef*PLP-A201P/V204I respectively. In contrast,

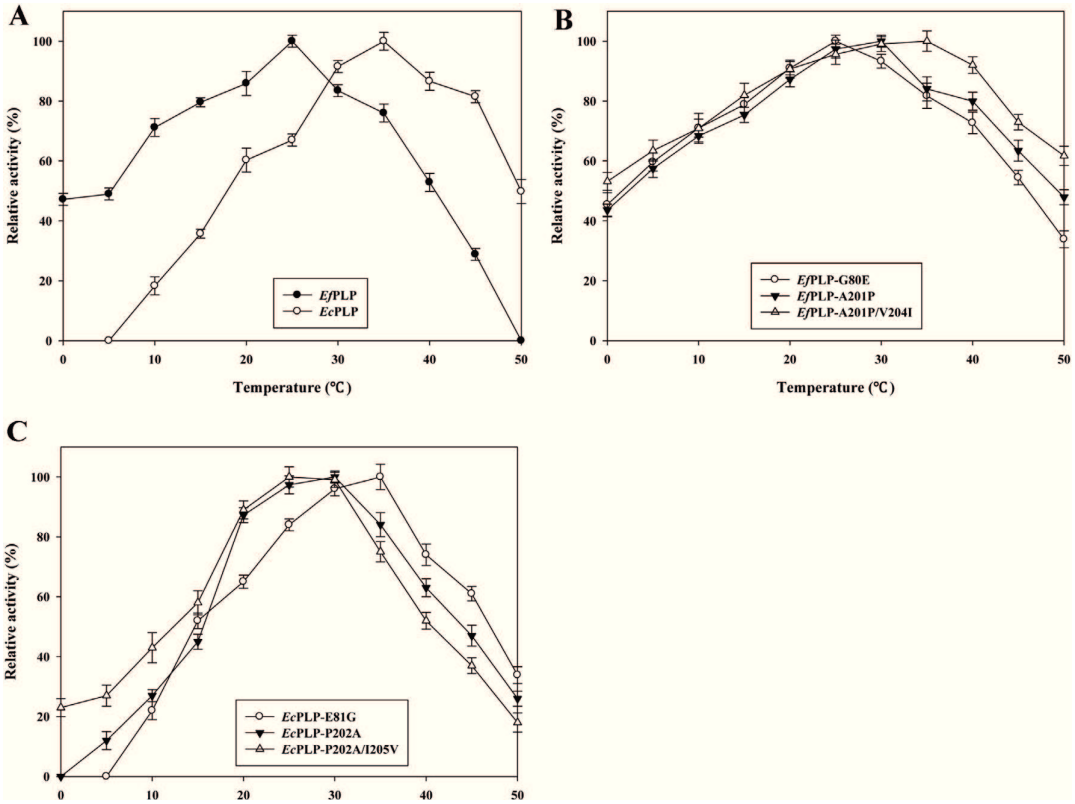

Fig. 4. Effect of temperature on the esterase activity of wild-types and mutants. (A) Temperature dependence of *Ef*PLP and *Ec*PLP; (B) temperature dependence of *Ef*PLP-G80E, *Ef*PLP-A201P and *Ef*PLP-A201P/V204I; (C) temperature dependence of *Ec*PLP-E81G, *Ec*PLP-P202A and *Ec*PLP-P202A/I205V.

mutants *Ec*PLP-E81G, *Ec*PLP-P202A and *Ec*PLP-P202A/I205V showed decreased stability at 70 °C with 2.45, 2.48 and 2.28 h half-lives respectively, when compared to their wild-type parent. To conclude, the introduction of *Ec*PLP residues into *Ef*PLP resulted to an increase of the thermostability of this protein, and *vice versa*.

3.4. PLA_2 activity of wild-types and mutants

To investigate the PLA_2 activity of *Ef*PLP, *Ec*PLP and mutants, we used the synthetic substrates *Di*C_3PC, *Di*C_4PC, *Di*C_6PC and arachidonoyl thio-PC in our assays (described under "Materials and Methods"). As shown in Table 3, *Ef*PLP, *Ec*PLP-E81G and *Ec*PLP-P202A/I205V showed increased activities with increase of substrate acyl chain length. In contrast, the *Ec*PLP and *Ef*PLP-A201P/V204I displayed higher activities toward substrates with shorter acyl chain length, and showed slightly decrease of activities with the increasing of the acyl chain length of substrates. When the substrate arachidonoyl thio-PC was used in the assay, *Ef*PLP displayed a distinct low activity compared to *Ec*PLP (Fig. 6). The double site mutant *Ef*PLP-A201P/V204I showed an increased activity compared to the *Ef*PLP. In contrast, all mutants of *Ec*PLP exhibited decreased activity compared to the wild-type; however, the double site mutant *Ec*PLP-P202A/I205V showed similar activity with *Ef*PLP.

3.5. Kinetic analysis of wild-types and mutants

Table 4 reports the kinetic constants of wild-types and mutants measured against six substrates of *p*NP esters with different acyl chain length. In general, all enzymes recorded the highest catalytic efficiency (k_{cat}/K_M) toward *p*NP butyrate as substrate. Three variants of *Ef*PLP exhibited slightly increase in esterase activity with all substrates and the most considerable increase of catalytic efficiency was observed with the double site mutants *Ef*PLP-A201P/V204I (1.9-fold increase in catalytic efficiency toward *p*NP caprate, compared to the wild type). Whereas variants of *Ec*PLP showed a minor decrease in catalytic efficiency with most of the substrates and the most marked decrease was recorded with the double site mutant *Ec*PLP-P202A/I205V (0.8-fold decrease toward *p*NP caprate, compared to the wild type). In spite of the fact that compared to the wild-type enzymes, the changes of catalytic efficiency of mutants were not substantially different. It is still remarkable that all these changes showed the trend to converting the thermal-adapted enzymes to their opposite counterparts. In general the k_{cat} of the cold adapted enzyme *Ef*PLP is lower than that of the mesophilic homolog (we should remind that the values reported in Table 4 are relative to the optimal temperature for any enzyme which is 25 °C for *Ef*PLP and 35 °C for *Ec*PLP). On the other hand from Table 4 it can be observed that *Ef*PLP shows higher substrate specificity, in comparison with *Ec*PLP, toward *p*NP butyrate (C_4 in the Table 4) among all the other tested substrates.

4. Discussion

In this study, we report the biochemical characterization of the PLP from the Antarctic ciliated protozoa *E. focardii* and that from *E. crassus*, its mesophilic counterpart. To our knowledge, this is the first biochemical characterization of an eukaryotic cold-active PLP.

The PLP from *E. focardii* shows most of the characteristics of a psychrophilic enzyme. It is 50% active at 4 °C, and it displays the

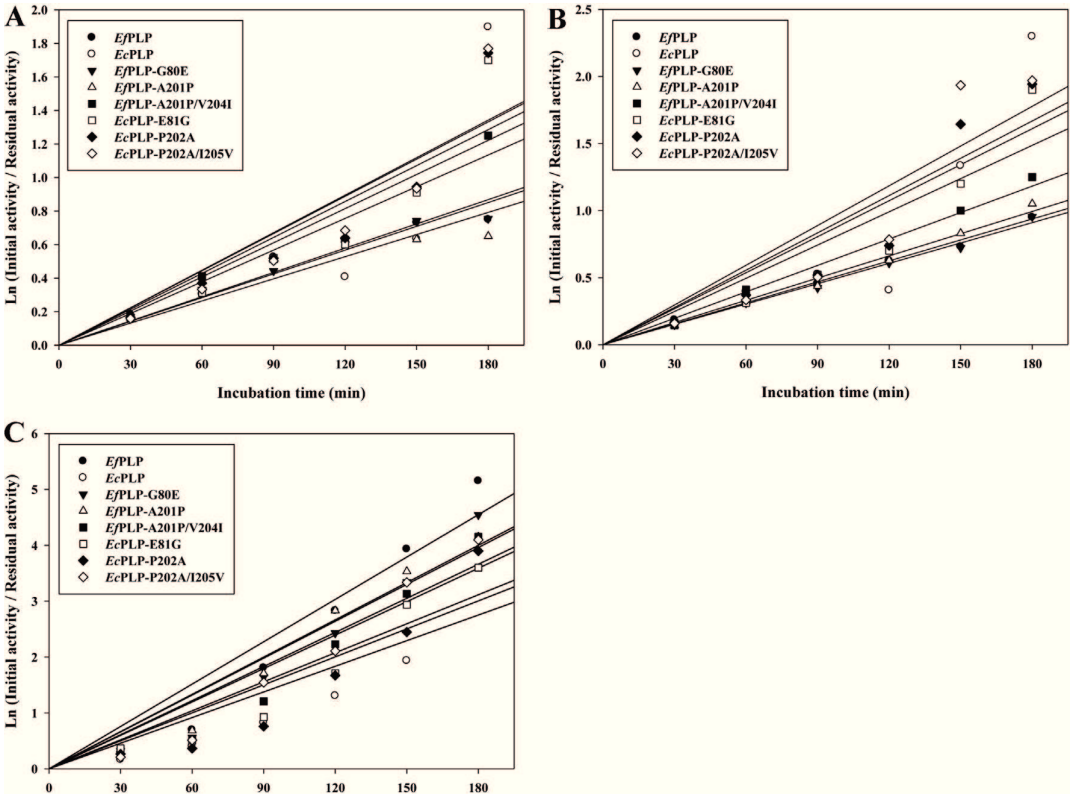

Fig. 5. Thermostability of wild-types and mutants. All enzymes were incubated at 40 °C (A), 55 °C (B) and 70 °C (C), samples were removed and assayed with *p*NP butyrate (100 μM) as substrate at regular time intervals at their optimal temperatures.

highest esterase activity at 25 °C. No activity was measured at 50 °C. In contrast, the PLP from the mesophilic *E. crassus* is not active at 4 °C, the highest activity is displayed at 35 °C and 50% of activity is maintained at 50 °C. We hypothesize that these features of cold-adaptation are consequence of adaptive substitutions of *Ef*PLP that confer structural flexibility to the polypeptide chain. This belief is first supported by the evidence that three mutants of *Ef*PLP (*Ef*PLP-G80E, *Ef*PLP-A201P, and *Ef*PLP-A201P/V204I) in which small amino acids are substituted by rigid and bulky amino acids, display esterase activities similar to the *E. crassus* phospholipase. In particular, *Ef*PLP-A201P/V204I shows its maximum activity at 35 °C, and 60% of its activity is maintained at 50 °C, whereas the wild-type showed no activity at 50 °C. These results suggest that the rigid side chain of Pro and the larger bulky hydrophobic side chain of Ile introduced by mutagenesis affected the structural flexibility of the *E. focardii* phospholipase, requiring an increase of the optimal temperature for the enzymatic activity. Furthermore, the single mutant *Ef*PLP-G80E displays the highest esterase activity at 25 °C as the wild type, but it shows 40% of activity at 50 °C, whereas the wild-type does not, suggesting that the single substitution of the *E. focardii* Gly_{80} with Glu confers enzymatic properties similar to the mesophilic *Ec*PLP without affecting its ability to function in the cold. It is noteworthy that the double site mutant *Ef*PLP-A201P/V204I displays esterase activity in a wide range of temperature, from 0 to 50 °C, a characteristic that makes it an attractive enzyme for industrial applications. In contrast, the substitution of Pro and Ile into Ala and Val in the *Ec*PLP clearly confer characteristics of a cold adapted enzyme, since the optimal temperature of *Ec*PLP-P202A/I205V was at 25 °C, but not 35 °C as for the wild-type. This evidence confirms that small residues confer an increased structural molecular flexibility to enzymes allowing to better function at low temperatures.

Table 2
Stability properties (half-lives) of wild-type PLPs and mutants.

Enzyme	$t_{1/2}$ (40 °C, h)	$t_{1/2}$ (55 °C, h)	$t_{1/2}$ (70 °C, h)	T_{opt} (°C)
*Ef*PLP	3.72 ± 0.06	3.65 ± 0.03	2.07 ± 0.07	25
*Ec*PLP	3.38 ± 0.13	3.11 ± 0.17	2.57 ± 0.15	35
*Ef*PLP-G80E	3.75 ± 0.04	3.68 ± 0.02	2.21 ± 0.07	25
*Ef*PLP-A201P	3.82 ± 0.07	3.59 ± 0.02	2.19 ± 0.06	30
*Ef*PLP-A201P/V204I	3.46 ± 0.04	3.42 ± 0.03	2.31 ± 0.08	35
*Ec*PLP-E81G	3.33 ± 0.11	3.19 ± 0.11	2.45 ± 0.09	35
*Ec*PLP-P202A	3.31 ± 0.11	3.07 ± 0.11	2.48 ± 0.13	30
*Ec*PLP-P202A/I205V	3.29 ± 0.11	3.01 ± 0.13	2.28 ± 0.08	25

Table 3
PLA_2 activity of wild-types and mutants toward different PC substrates.

Enzyme	Activity (μmol/min/ml)		
	DiC_3PC	*Di*C_4PC	*Di*C_6PC
*Ef*PLP	930 ± 32	1217 ± 32	1348 ± 22
*Ec*PLP	1329 ± 53	1084 ± 31	1078 ± 57
*Ef*PLP-G80E	1183 ± 23	985 ± 59	1024 ± 38
*Ef*PLP-A201P	1156 ± 49	977 ± 36	1038 ± 47
*Ef*PLP-A201P/V204I	1209 ± 43	1059 ± 35	1003 ± 38
*Ec*PLP-E81G	1076 ± 39	1123 ± 52	1181 ± 40
*Ec*PLP-P202A	1236 ± 54	1028 ± 47	1095 ± 29
*Ec*PLP-P202A/I205V	1103 ± 37	1144 ± 33	1230 ± 59

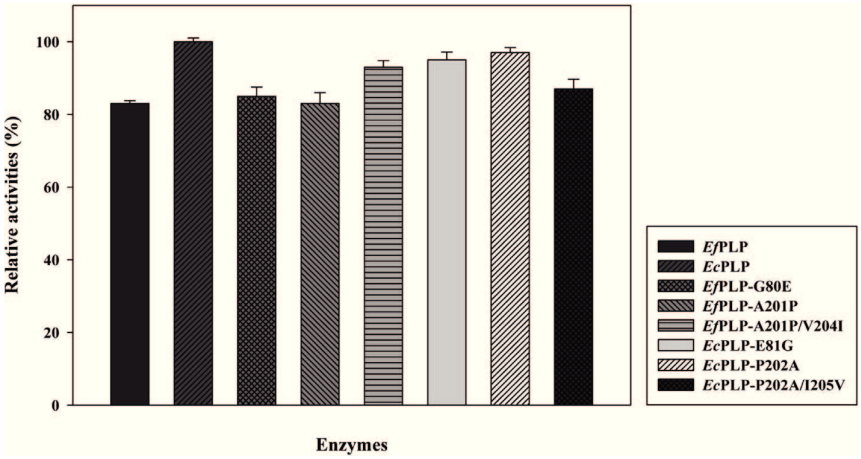

Fig. 6. Phospholipase A_2 activity of wild-types and mutants toward synthetic substrate arachidonoyl thio-PC.

The observation that mutants of *Ef*PLP behave more similarly to *Ec*PLP than the wild-type is confirmed by the kinetic analysis of these mutated enzymes, which showed a slightly increased catalytic efficiency (k_{cat}/K_M) compared to the wild-type *Ef*PLP (Table 4). However, the changes on catalytic efficiency of all mutants are relatively low to the previous reported researches [43–45], thus suggesting that the mutation sites may not directly be involved in the conformation of the catalytic core of the enzymes, which is also confirmed by the modeling analysis of *Ef*PLP (Fig. 2A′ and A″). The optimal pH for both *Ef*PLP and *Ec*PLP esterase activity is about pH 10.5, which indicates that these two proteins may be considered as alkaline phospholipases. However, *Ef*PLP displays a wider range of optimal pH with respect to *Ec*PLP, as demonstrated in Fig. 3, it maintained about 90% maximal activity at pH 11.5, a property that makes *Ef*PLP even more attractive for industrial applications.

Another remarkable property of *Ef*PLP is its higher thermostability after incubation at 40 °C and 55 °C when compared with *Ec*PLP. Furthermore, *Ef*PLP possesses relatively high thermostability showing 2.07 h half-life even after incubation at 70 °C. This is in contrast to many cold-active lipases from *Moraxella TA144* [46], *Acinetobacter baumannii* [47], *Candida albicans* [48], *Aspergillus nidulans* [49], and *Pseudomonas* spp. [50] which show decreased activity only after 20 min incubation at 40–50 °C. In other words, *Ef*PLP shows higher stability at moderate temperatures compared to its mesophilic counterpart, and also to most of the reported cold active enzymes [3]. This result is noteworthy considering the fact that cold-active enzymes usually possess a high level of structural flexibility, generally accompanied by a trade-off heat-lability [4]. However, the behavior of *Ef*PLP is not contradictory: it has been previously proposed that structural flexibility and rigidity of psychrophilic enzymes may co-exist in the same molecule, as only

Table 4
Kinetic constants of wild-types and mutants of *Euplotes* PLPs against six substrates of *p*NP esters with different acyl chain length.

Enzyme	Constant[a]	Substrate					
		C_2	C_3	C_4	C_5	C_8	C_{10}
***Ef*PLP**	k_{cat} (s^{-1})	**7.3**	**6.0**	**14.5**	**5.9**	**0.7**	**0.4**
	K_M (μM)	**373**	**405**	**566**	**366**	**194**	**183**
	k_{cat}/K_M (s^{-1} mM^{-1})	**19.6**	**14.8**	**25.6**	**16.1**	**3.6**	**2.2**
***Ec*PLP**	k_{cat} (s^{-1})	**11.5**	**7.0**	**19.2**	**7.7**	**0.8**	**0.7**
	K_M (μM)	**377**	**325**	**594**	**434**	**135**	**255**
	k_{cat}/K_M (s^{-1} mM^{-1})	**30.5**	**21.5**	**32.3**	**17.7**	**5.9**	**2.7**
***Ef*PLP-G80E**	k_{cat} (s^{-1})	**6.9**	**7.2**	**15.5**	**5.9**	**0.8**	**0.6**
	K_M (μM)	**311**	**420**	**555**	**357**	**129**	**164**
	k_{cat}/K_M (s^{-1} mM^{-1})	**22.2**	**17.1**	**27.9**	**16.5**	**6.2**	**3.7**
***Ef*PLP-A201P**	k_{cat} (s^{-1})	**12.8**	**8.0**	**22.1**	**6.9**	**1.5**	**0.7**
	K_M (μM)	**405**	**531**	**684**	**401**	**244**	**164**
	k_{cat}/K_M (s^{-1} mM^{-1})	**31.6**	**15.1**	**32.3**	**17.2**	**6.1**	**4.3**
***Ef*PLP-A201P/V204I**	k_{cat} (s^{-1})	**13.3**	**9.3**	**23.9**	**7.6**	**1.7**	**0.7**
	K_M (μM)	**410**	**541**	**695**	**408**	**260**	**169**
	k_{cat}/K_M (s^{-1} mM^{-1})	**32.4**	**17.2**	**34.4**	**18.6**	**6.5**	**4.1**
***Ec*PLP-E81G**	k_{cat} (s^{-1})	**10.4**	**6.2**	**17.9**	**7.2**	**0.7**	**0.5**
	K_M (μM)	**334**	**301**	**548**	**418**	**125**	**204**
	k_{cat}/K_M (s^{-1} mM^{-1})	**31.1**	**20.6**	**32.7**	**17.2**	**5.6**	**2.4**
***Ec*PLP-P202A**	k_{cat} (s^{-1})	**10.2**	**5.9**	**16.3**	**6.5**	**0.7**	**0.5**
	K_M (μM)	**348**	**275**	**530**	**401**	**118**	**197**
	k_{cat}/K_M (s^{-1} mM^{-1})	**29.3**	**21.4**	**30.7**	**16.2**	**5.9**	**2.5**
***Ec*PLP-P202A/I205V**	k_{cat} (s^{-1})	**9.1**	**5.8**	**15.2**	**6.3**	**0.6**	**0.4**
	K_M (μM)	**336**	**259**	**519**	**389**	**108**	**173**
	k_{cat}/K_M (s^{-1} mM^{-1})	**27.1**	**22.4**	**29.3**	**16.2**	**5.5**	**2.3**

[a] The standard error was not higher than 5%.

protein domains involved in the conformational changes during catalysis need to be flexible [51]. This hypothesis has been supported by several researches on characterization of cold-active enzymes [52–55].

Both wild-types and mutants show broad substrate specificity toward short and long acyl chain-length (C_2–C_{10}) of *p*NP esters, and higher activities were showed on short acyl chain-length (C_2–C_5). These results contrast sharply with those obtained for other patatins [17] which showed maximum relative activity on decanoate (C_{10}, 100%) and moderate activity on palmitate (C_{16}, 40%), and very low activities toward butyrate (C_4, 4%) and hexanoate (C_6, 25%) esters. In particular, for what concerns the K_M and k_{cat} values (Table 4), the affinity constants decreased on both short (C_2) and long (C_8, C_{10}) acyl chain length of substrates for both wild-type enzymes. In parallel the k_{cat} values become much lower for the same substrates, resulting in a decrease of the catalytic efficiency. Consequently, k_{cat}/K_M values displayed a trend, leading to *p*NP butyrate (C_4) as the most preferable substrate for both enzymes. The increased substrate specificity toward *p*NP butyrate (C_4) is thus manifested more by an increase in k_{cat} than by a decrease in K_M, that is, by an increase in maximum rate rather than by an increase in substrate binding. This behavior is an example of the so called "induced fit" phenomenon, in which the enzyme works better when is able to bind more tightly the transition-state than the ground-state of the substrate. Furthermore, comparing the substrate specificity between two wild-types, we can observe that the *Ec*PLP showed a higher activity toward all *p*NP esters used for test. This result can be explained by the previous finding that mesophilic enzymes have a higher kinetic efficiency compared with psychrophilic ones at their respective optimal conditions [4].

Besides esterase activities of *Ef*PLP and *Ec*PLP, the enzymes were also found to be active toward diacylphospholipids (*Di*C_3PC, *Di*C_4PC and *Di*C_6PC) and arachidonoyl thio-PC. The results showed an increased activity for *Ef*PLP according to the increase of substrates chain length, in contrast to *Ec*PLP which displayed a decreased activity when the substrates chain length increased (Table 3). By comparing the activities on arachidonoyl thio-PC, the double site mutant *Ef*PLP-A201P/V204I and the mesophilic enzyme *Ec*PLP showed higher efficiency than the psychrophilic counterpart *Ef*PLP (Fig. 6), probably because the mutant was constructed by replacing the specific residues of *Ef*PLP with those of *Ec*PLP. Additionally, the decreased activity of three variants of *Ec*PLP again confirmed that the trend of the shifted catalytic behavior of mutants toward the wild type enzyme from which they obtained the substituted residues.

Patatins are known as the major storage protein in potato tubers [18]. Plant PLPs were originally defined as vacuolar enzymes [9], but several of these molecules were found in the cytoplasm or partially bound to chloroplasts and other endomembranes, suggesting a potential role in signal transduction [16]. However, the hydrolase and in particular the galactolipase activity of plant patatins have been implicated in the mechanisms of defenses against parasites [56]. Actually, PLPs in *Arabidopsis* have been characterized as pathogen-inducible enzymes and were identified to be active in a context of pathogen defense [57]. Relatively few indications are available about the localization and the physiological role of PLPs in protozoans. For example, it has been reported that a patatin-like from *Toxoplasma* is localized in the cytosol and it may function as storage protein, like patatin in potato tuber, to aid parasite survival during physiological stress conditions [58]. However, this patatin-like lacks phospholipase activity [58]. Research on phospholipases isolated from the extracellular medium of the ciliate *T. thermophila* demonstrated that these enzymes possess hemolytic activity suggesting that they may serve to destroy competitors and predators [59]. The phospholipase activity and the putative signal peptide typical of secreted proteins of both *Ef*PLP and *Ec*PLP, suggest that they may represent extracellular enzymes, which are translocated to the extracellular environment in response to predators' attack as defense or to facilitate ciliate's feeding. However, the evidence that *Euplotes* PLPs possess both phospholipase and esterase activity suggest that they may be involved in key metabolic events such as membrane turnover and signal transduction, as well diverse functions in the degradation of food and fat [60]. Further study will help to unravel the physiological role of *Euplotes* PLPs.

PLPs have been used in industrial applications especially in food production, such as emulsification for mayonnaise, sauces, and salad dressings production [61,62]. These processes are based on enzymes expressed in microorganisms and produced in large quantities, making them cost competitive. Furthermore, with the development of protein engineering, it is possible to produce tailor-made phospholipases of characteristics and specificity for many applications [61]. The PLP from *E. focardii* possesses both phospholipase and esterase activity, and can work in the cold and wide range of pH conditions making it a good candidate for the implementation of new and harsh industrial applications.

To conclude, the PLP from the Antarctic ciliate *E. focardii* shows the characteristics of a psychrophilic enzyme. These characteristics appear related to amino acid residues that confer structural flexibility to the polypeptides; mutations at some of these residues are able to influence the thermal-adaptation of the enzyme. Furthermore, *Ef*PLP shows high thermostability, a characteristic that distinguishes this enzyme from other cold-adapted lipases, and make it an interesting biocatalyst for industrial applications.

Acknowledgments

This research was supported by grants from the Italian "Programma Nazionale di Ricerche in Antartide" (PNRA) and from the Italian "Ministero dell'Istruzione, dell'Università e della Ricerca" (MIUR) (PRIN 2008) to CM. We acknowledge the COST (action BM1102) for supporting part of this work.

References

[1] A. Casanueva, M. Tuffin, C. Cary, D.A. Cowan, Molecular adaptations to psychrophily: the impact of 'omic' technologies, Trends in Microbiology 18 (2010) 374–381.
[2] E. Papaleo, M. Pasi, M. Tiberti, L. De Gioia, Molecular dynamics of mesophilic-like mutants of a cold-adapted enzyme: insights into distal effects induced by the mutations, PLoS ONE 6 (2011) e24214.
[3] B. Joseph, P.W. Ramteke, G. Thomas, Cold active microbial lipases: some hot issues and recent developments, Biotechnology Advances 26 (2008) 457–470.
[4] K.S. Siddiqui, R. Cavicchioli, Cold-adapted enzymes, Annual Review of Biochemistry 75 (2006) 403–433.
[5] P.W.R. Babu Joseph, George Thomas, Nitisha Shrivastava, Standard review cold-active microbial lipases: a versatile tool for industrial applications, Biotechnology and Molecular Biology Reviews 2 (2) (June 2007) 039–048.
[6] A. Macrae, J. Visicchio, A. Lanot, Application of potato lipid acyl hydrolase for the synthesis of monoacylglycerols, Journal of the American Oil Chemists' Society 75 (1998) 1489–1494.
[7] S. Prat, W.B. Frommer, R. Hofgen, M. Keil, J. Kossmann, M. Koster-Topfer, X.J. Liu, B. Muller, H. Pena-Cortes, M. Rocha-Sosa, et al., Gene expression during tuber development in potato plants, FEBS Letters 268 (1990) 334–338.
[8] R. Höfgen, L. Willmitzer, Biochemical and genetic analysis of different patatin isoforms expressed in various organs of potato (*Solanum tuberosum*), Plant Science 66 (1990) 221–230.
[9] S. Rosahl, R. Schmidt, J. Schell, L. Willmitzer, Isolation and characterization of a gene from *Solanum tuberosum* encoding patatin, the major storage protein of potato tubers, Molecular and General Genetics 203 (1986) 214–220.
[10] D.L. Andrews, B. Beames, M.D. Summers, W.D. Park, Characterization of the lipid acyl hydrolase activity of the major potato (*Solanum tuberosum*) tuber protein, patatin, by cloning and abundant expression in a baculovirus vector, The Biochemical Journal 252 (1988) 199–206.
[11] O. Hirayama, H. Matsuda, H. Takeda, K. Maenaka, H. Takatsuka, Purification and properties of a lipid acyl-hydrolase from potato tubers, Biochimica et Biophysica acta 384 (1975) 127–137.
[12] D.A. Wardale, Lipid-degrading enzymes from potato tubers, Phytochemistry 19 (1980) 173–177.

[13] D. Racusen, Esterase specificity of patatin from two potato cultivars, Canadian Journal of Botany 64 (1986) 2104–2106.
[14] K. Senda, H. Yoshioka, N. Doke, K. Kawakita, A cytosolic phospholipase A2 from potato tissues appears to be patatin, Plant & Cell Physiology 37 (1996) 347–353.
[15] J.A. Strickland, G.L. Orr, T.A. Walsh, Inhibition of diabrotica larval growth by patatin, the lipid acyl hydrolase from potato tubers, Plant Physiology 109 (1995) 667–674.
[16] A. Holk, S. Rietz, M. Zahn, H. Quader, G.F. Scherer, Molecular identification of cytosolic, patatin-related phospholipases A from Arabidopsis with potential functions in plant signal transduction, Plant Physiology 130 (2002) 90–101.
[17] H.J. Hirschberg, J.W. Simons, N. Dekker, M.R. Egmond, Cloning, expression, purification and characterization of patatin, a novel phospholipase A, European Journal of Biochemistry/FEBS 268 (2001) 5037–5044.
[18] T.J. Rydel, J.M. Williams, E. Krieger, F. Moshiri, W.C. Stallings, S.M. Brown, J.C. Pershing, J.P. Purcell, M.F. Alibhai, The crystal structure, mutagenesis, and activity studies reveal that patatin is a lipid acyl hydrolase with a Ser-Asp catalytic dyad, Biochemistry 42 (2003) 6696–6708.
[19] J.D. Schrag, M. Cygler, Lipases and alpha/beta hydrolase fold, Methods in Enzymology 284 (1997) 85–107.
[20] P.C. Kienesberger, M. Oberer, A. Lass, R. Zechner, Mammalian patatin domain containing proteins: a family with diverse lipolytic activities involved in multiple biological functions, Journal of Lipid Research 50 (Suppl) (2009) S63–S68.
[21] G.F. Scherer, S.B. Ryu, X. Wang, A.R. Matos, T. Heitz, Patatin-related phospholipase A: nomenclature, subfamilies and functions in plants, Trends in Plant Science 15 (2010) 693–700.
[22] S. Banerji, A. Flieger, Patatin-like proteins: a new family of lipolytic enzymes present in bacteria? Microbiology 150 (2004) 522–525.
[23] A. La Terza, G. Papa, C. Miceli, P. Luporini, Divergence between two Antarctic species of the ciliate Euplotes, E. focardii and *E. nobilii*, in the expression of heat-shock protein 70 genes, Molecular Ecology 10 (2001) 1061–1067.
[24] A. LA TERZA, C. MICELI, P. LUPORINI, The gene for the heat-shock protein 70 of *Euplotes focardii*, an Antarctic psychrophilic ciliate, Antarctic Science 16 (2004) 23–28.
[25] F. Chiappori, S. Pucciarelli, I. Merelli, P. Ballarini, C. Miceli, L. Milanesi, Structural thermal adaptation of beta-tubulins from the Antarctic psychrophilic protozoan *Euplotes focardii*, Proteins 80 (2012) 1154–1166.
[26] S. Pucciarelli, A. La Terza, P. Ballarini, S. Barchetta, T. Yu, F. Marziale, V. Passini, B. Methe, H.W. Detrich 3rd, C. Miceli, Molecular cold-adaptation of protein function and gene regulation: the case for comparative genomic analyses in marine ciliated protozoa, Marine Genomics 2 (2009) 57–66.
[27] S. Pucciarelli, F. Marziale, G. Di Giuseppe, S. Barchetta, C. Miceli, Ribosomal cold-adaptation: characterization of the genes encoding the acidic ribosomal P0 and P2 proteins from the Antarctic ciliate *Euplotes focardii*, Gene 360 (2005) 103–110.
[28] A. Valbonesi, P. Luporini, Description of two new species of Euplotes and *Euplotes rariseta* from Antarctica, Polar Biol 11 (1990) 47–53.
[29] S. Pucciarelli, C. Miceli, Characterization of the cold-adapted alpha-tubulin from the psychrophilic ciliate *Euplotes focardii*, Extremophiles: Life Under Extreme Conditions 6 (2002) 385–389.
[30] T.M. Rose, E.R. Schultz, J.G. Henikoff, S. Pietrokovski, C.M. McCallum, S. Henikoff, Consensus-degenerate hybrid oligonucleotide primers for amplification of distantly related sequences, Nucleic Acids Research 26 (1998) 1628–1635.
[31] D.C. Hoffman, R.C. Anderson, M.L. DuBois, D.M. Prescott, Macronuclear gene-sized molecules of hypotrichs, Nucleic Acids Research 23 (1995) 1279–1283.
[32] S.N. Ho, H.D. Hunt, R.M. Horton, J.K. Pullen, L.R. Pease, Site-directed mutagenesis by overlap extension using the polymerase chain reaction, Gene 77 (1989) 51–59.
[33] N.J. Kruger, The Bradford method for protein quantitation, Methods in Molecular Biology 32 (1994) 9–15.
[34] E.T.S. Teorell, Universal buffer over the pH range 2.0 to 12.0, Biochemische Zeitschrift 299 (1938) 416–419.
[35] M. Dixon, E.C. Webb, Enzymes, Academic Press, New York, 1964.
[36] K. Arnold, L. Bordoli, J. Kopp, T. Schwede, The SWISS-MODEL workspace: a web-based environment for protein structure homology modelling, Bioinformatics 22 (2006) 195–201.
[37] L. Bordoli, F. Kiefer, K. Arnold, P. Benkert, J. Battey, T. Schwede, Protein structure homology modeling using SWISS-MODEL workspace, Nature Protocols 4 (2009) 1–13.
[38] F. Jonsson, J. Postberg, H.J. Lipps, The unusual way to make a genetically active nucleus, DNA and Cell Biology 28 (2009) 71–78.
[39] R. Salacha, F. Kovacic, C. Brochier-Armanet, S. Wilhelm, J. Tommassen, A. Filloux, R. Voulhoux, S. Bleves, The *Pseudomonas aeruginosa* patatin-like protein PlpD is the archetype of a novel Type V secretion system, Environmental Microbiology 12 (2010) 1498–1512.
[40] S. D'Amico, T. Collins, J.C. Marx, G. Feller, C. Gerday, Psychrophilic microorganisms: challenges for life, EMBO Reports 7 (2006) 385–389.
[41] S. Pucciarelli, S.K. Parker, H.W. Detrich 3rd, R. Melki, Characterization of the cytoplasmic chaperonin containing TCP-1 from the Antarctic fish *Notothenia coriiceps*, Extremophiles: Life Under Extreme Conditions 10 (2006) 537–549.
[42] P.L. Wintrode, K. Miyazaki, F.H. Arnold, Cold adaptation of a mesophilic subtilisin-like protease by laboratory evolution, The Journal of Biological Chemistry 275 (2000) 31635–31640.
[43] B. Jaouadi, N. Aghajari, R. Haser, S. Bejar, Enhancement of the thermostability and the catalytic efficiency of *Bacillus pumilus* CBS protease by site-directed mutagenesis, Biochimie 92 (2010) 360–369.
[44] Y. Nakagawa, A. Hasegawa, J. Hiratake, K. Sakata, Engineering of *Pseudomonas aeruginosa* lipase by directed evolution for enhanced amidase activity: mechanistic implication for amide hydrolysis by serine hydrolases, Protein Engineering, Design & Selection: PEDS 20 (2007) 339–346.
[45] I. Kauffmann, C. Schmidt-Dannert, Conversion of *Bacillus thermocatenulatus* lipase into an efficient phospholipase with increased activity toward long-chain fatty acyl substrates by directed evolution and rational design, Protein Engineering 14 (2001) 919–928.
[46] C. De Santi, M.L. Tutino, L. Mandrich, M. Giuliani, E. Parrilli, P. Del Vecchio, D. de Pascale, The hormone-sensitive lipase from *Psychrobacter sp.* TA144: new insight in the structural/functional characterization, Biochimie 92 (2010) 949–957.
[47] I.H. Park, S.H. Kim, Y.S. Lee, S.C. Lee, Y. Zhou, C.M. Kim, S.C. Ahn, Y.L. Choi, Gene cloning, purification, and characterization of a cold-adapted lipase produced by *Acinetobacter baumannii* BD5, Journal of Microbiology and Biotechnology 19 (2009) 128–135.
[48] D.M. Lan, N. Yang, W.K. Wang, Y.F. Shen, B. Yang, Y.H. Wang, A novel cold-active lipase from *Candida albicans*: cloning, expression and characterization of the recombinant enzyme, International Journal of Molecular Sciences 12 (2011) 3950–3965.
[49] I. Mayordomo, F. Randez-Gil, J.A. Prieto, Isolation, purification, and characterization of a cold-active lipase from *Aspergillus nidulans*, Journal of Agricultural and Food Chemistry 48 (2000) 105–109.
[50] D.W. Choo, T. Kurihara, T. Suzuki, K. Soda, N. Esaki, A cold-adapted lipase of an Alaskan psychrotroph, *Pseudomonas* sp. strain B11-1: gene cloning and enzyme purification and characterization, Applied and Environmental Microbiology 64 (1998) 486–491.
[51] T. Lonhienne, C. Gerday, G. Feller, Psychrophilic enzymes: revisiting the thermodynamic parameters of activation may explain local flexibility, Biochimica et Biophysica Acta (BBA) – Protein Structure and Molecular Enzymology 1543 (2000) 1–10.
[52] A.E. Fedoy, N. Yang, A. Martinez, H.K. Leiros, I.H. Steen, Structural and functional properties of isocitrate dehydrogenase from the psychrophilic bacterium *Desulfotalea psychrophila* reveal a cold-active enzyme with an unusual high thermal stability, Journal of Molecular Biology 372 (2007) 130–149.
[53] P. Gatti-Lafranconi, A. Natalello, S. Rehm, S.M. Doglia, J. Pleiss, M. Lotti, Evolution of stability in a cold-active enzyme elicits specificity relaxation and highlights substrate-related effects on temperature adaptation, Journal of Molecular Biology 395 (2010) 155–166.
[54] H.K. Leiros, A.L. Pey, M. Innselset, E. Moe, I. Leiros, I.H. Steen, A. Martinez, Structure of phenylalanine hydroxylase from *Colwellia psychrerythraea* 34H, a monomeric cold active enzyme with local flexibility around the active site and high overall stability, The Journal of Biological Chemistry 282 (2007) 21973–21986.
[55] L. Kulakova, A. Galkin, T. Nakayama, T. Nishino, N. Esaki, Cold-active esterase from *Psychrobacter* sp. Ant300: gene cloning, characterization, and the effects of Gly–>Pro substitution near the active site on its catalytic activity and stability, Biochimica et Biophysica acta 1696 (2004) 59–65.
[56] S. Dhondt, P. Geoffroy, B.A. Stelmach, M. Legrand, T. Heitz, Soluble phospholipase A2 activity is induced before oxylipin accumulation in tobacco mosaic virus-infected tobacco leaves and is contributed by patatin-like enzymes, The Plant Journal: For Cell and Molecular Biology 23 (2000) 431–440.
[57] S. La Camera, P. Geoffroy, H. Samaha, A. Ndiaye, G. Rahim, M. Legrand, T. Heitz, A pathogen-inducible patatin-like lipid acyl hydrolase facilitates fungal and bacterial host colonization in Arabidopsis, The Plant Journal: For Cell and Molecular Biology 44 (2005) 810–825.
[58] D.G. Mordue, C.F. Scott-Weathers, C.M. Tobin, L.J. Knoll, A patatin-like protein protects *Toxoplasma gondii* from degradation in activated macrophages, Molecular Microbiology 63 (2007) 482–496.
[59] J. Florin-Christensen, M. Florin-Christensen, J. Knudsen, L. Rasmussen, Phospholipases and phosphonolipids in a ciliate: an attack and defence system? Trends in Biochemical Sciences 11 (1986) 354–355.
[60] R.D. Schmid, R. Verger, Lipases: interfacial enzymes with attractive applications, Angewandte Chemie 37 (1998) 1608.
[61] L. De Maria, J. Vind, K.M. Oxenboll, A. Svendsen, S. Patkar, Phospholipases and their industrial applications, Applied Microbiology and Biotechnology 74 (2007) 290–300.
[62] J. Mansfeld, Plant phospholipases A2: perspectives on biotechnological applications, Biotechnology Letters 31 (2009) 1373–1380.

Appl Biochem Biotechnol
DOI 10.1007/s12010-013-0713-1

A New Alkaliphilic Cold-Active Esterase from the Psychrophilic Marine Bacterium *Rhodococcus* sp.: Functional and Structural Studies and Biotechnological Potential

Concetta De Santi · Pietro Tedesco · Luca Ambrosino · Bjørn Altermark · Nils-Peder Willassen · Donatella de Pascale

Received: 25 October 2013 / Accepted: 25 December 2013

Abstract The special features of cold-adapted lipolytic biocatalysts have made their use possible in several industrial applications. In fact, cold-active enzymes are known to be able to catalyze reactions at low temperatures, avoiding side reactions taking place at higher temperatures and preserving the integrity of products. A lipolytic gene was isolated from the Arctic marine bacterium *Rhodococcus* sp. AW25M09 and expressed in *Escherichia coli* as inclusion bodies. The recombinant enzyme (hereafter called *Rh*Lip) showed interesting cold-active esterase activity. The refolded purified enzyme displayed optimal activity at 30 °C and was cold-active with retention of 50 % activity at 10 °C. It is worth noting that the optimal pH was 11, and the low relative activity below pH 10 revealed that *Rh*Lip was an alkaliphilic esterase. The enzyme was active toward short-chain *p*-nitrophenyl esters (C2–C6), displaying optimal activity with the butyrate (C4) ester. In addition, the enzyme revealed a good organic solvent and salt tolerance. These features make this an interesting enzyme for exploitation in some industrial applications.

Keywords Esterase · Cold-active · Alkaliphilic · Biotechnological applications

Introduction

Esterases (EC 3.1.1.1) are hydrolytic enzymes that catalyze the hydrolysis of esters into alcohol and acid. They generally differ from lipases (EC 3.1.1.3) regarding the substrate

Concetta De Santi and Pietro Tedesco contributed equally to this work.

C. De Santi · P. Tedesco · L. Ambrosino · D. de Pascale (✉)
Institute of Protein Biochemistry, National Research Council, Via P. Castellino, 111, 80131 Naples, Italy
e-mail: d.depascale@ibp.cnr.it

B. Altermark · N.-P. Willassen
NorStruct, Department of Chemistry, Faculty of Science and Technology, University of Tromsø, Tromsø, Norway

Published online: 01 February 2014

specificity. By now, it is well recognized that esterases catalyze the hydrolysis and the synthesis of short-chain esters (less than 10 carbon atoms), while lipases act on substrates with long chains of carbon atoms (more than 10) [1]. These enzymes belong to the α/β-hydrolase superfamily and possess a highly conserved catalytic triad formed by Ser, His, and Asp [2]. Lipolytic enzymes are employed in a wide range of industrial applications including the food industry and detergent production as well as biocatalysts for chemical synthesis [3]. In particular, cold-active lipolytic enzymes are extremely appealing for industrial uses. It is generally accepted that cold-active biocatalysts have a more flexible structure [4] compared to mesophilic and thermophilic counterparts, and this high flexibility enables increased complementarity between active site and substrates, resulting in high specific activity at low temperatures [5]. Thus, the use of cold-adapted biocatalysts can minimize undesirable side reactions taking place at higher temperatures and allow reactions involving heat-sensitive substrates [6]. These properties are important for exploitation in the food industry, where the preservation of the nutritional value and flavor of the food is fundamental. Furthermore, thanks to their relatively low thermostability, these enzymes can often easily be inactivated.

Therefore, bioprospecting, looking for cold-active lypolitic enzymes from Arctic regions, has become an active and expanding discipline. In fact, organisms living in an extremely cold habitat have adopted several strategies to survive and thrive in these challenging environments, and these include the expression of enzymes able to efficiently catalyze reactions at temperatures close to 0 °C [7].

In this paper, we present the purification and characterization of a cold-active esterase from the marine psychrophilic actinobacterium *Rhodococcus* sp. AW25M09. This bacterium was isolated from the intestines/stomach of an Atlantic hagfish (*Myxine glutinosa*) captured on the cold seafloor during sampling performed in Hadsel Fjord, North Norway. Its genome was recently published [8]. The *lip3* gene was selected for its unique amino acid sequence and its homology with other lipases/esterases. The gene was amplified by PCR then cloned and recombinantly expressed in *Escherichia coli*, and the protein, aggregated as inclusion bodies, was refolded and extensively characterized.

Materials and Methods

Isolation of a Lipolytic Gene

The genome of the cold-adapted *Rhodococcus* sp. AW25M09 has been sequenced and has been deposited at DDBJ/EMBL/GenBank under accession number CAPS00000000. The genome was analyzed using the Artemis [9] with the aim to identify new genes encoding for esterases and lipases to be expressed in *E. coli*. Sequence analysis revealed an open reading frame (ORF) of 1,056 bp, the *lipR* lipolytic gene that encodes for a protein of 352 amino acids.

lipR Gene Cloning

Rhodococcus sp. AW25M09 was grown in Marine 2216 broth (Difco, Sparks, USA) at 20 °C, and the genomic DNA was purified with Sigma's GenElute Bacterial Genomic Kit according to the manufacturer's instruction and was used as template for the *lipR* gene amplification by PCR.

Two primers containing NdeI and NotI restriction sites were designed: 5′-AATACATATG TACCGCAGCAACGACTCCAACG-3′ and 5′-AATAGCGGCCGCGCAGTTGGACGGTG CAGGCACT-3′.

PCR was performed by using Mastercycler personal (Eppendorf, New York, USA). The reaction conditions used were as follows: 1 cycle (94 °C for 3 min), 30 cycles (94 °C for 30 s, 60 °C for 30 s, and 72 °C for 1 min), and a final cycle of 72 °C for 7 min. The amplified PCR product of 1,056 bp was cloned into pET-22b expression vector previously digested by NdeI and NotI restriction enzymes (New England BioLabs, Ipswich, MA, USA) including an in-frame C-terminal fusion purification 6×His-Tag. *E. coli* DH5-α competent cells were first transformed through the ligation reaction, and the construct was verified by bidirectional DNA sequencing. The isolated plasmid was then used to transform *E. coli* strain BL21(DE3) competent cells.

*Rh*Lip Recombinant Production in *E. coli* Cells

E. coli BL21(DE3) carrying pET-22b-*lipR* vector was grown in a shake flask containing Luria Bertani broth (LB) medium supplemented with 100 μg/mL ampicillin at 37 °C for 16 h. Growing culture was diluted to a cell density of about 0.05 OD_{600} in a 1-L shake flask containing 200 mL of LB medium supplemented with 100 μg/mL ampicillin. *Rh*Lip induction was performed when the culture density reached 0.5–0.6 at OD_{600} by the addition of filter-sterilized isopropyl-β-D-1-thiogalactopyranoside (IPTG) to a final concentration of 0.1 mM. Culture was carried out at constant agitation (220 rpm) at 20 °C for 16 h post-induction. Cells were then harvested by centrifugation at 6,000 rpm for 20 min at 4 °C, divided into 0.5-g aliquots, and frozen at −20 °C.

*Rh*Lip Purification and Refolding from Inclusion Bodies

The bacterial pellet (0.5 g) was frozen and thawed twice, and resuspended in 4 mL of Tris-EDTA (TE) buffer (20 mM Tris-HCl pH 8.0, 5 mM EDTA pH 8.0), and 0.6 mg of lysozyme and 0.75 g sucrose were added to the suspension; the suspension was incubated at 37 °C. After 30 min, 4 mL ice-cold TE buffer was added to the suspension and the suspension was incubated for 30 min at 37 °C; then, cells were subjected to sonication. Sonicated cells were centrifuged at 6,700 rcf for 20 min at 4 °C; then, the pellet was washed with 4 mL TE buffer and centrifuged and washed with 2 mL of 20 mM Tris-HCl pH 8.0. The extract was finally centrifuged for 10 min at 4 °C at 10,000 rcf. The pellet was resuspended in 10 mL of 6 M urea, 20 mM Tris-HCl pH 8.0, 15 mM β-mercaptoethanol, and 5 mM EDTA pH 8.0 at 4 °C with gentle shaking for 2 h. The insoluble material was removed by centrifugation at 15,000 rcf for 30 min at 4 °C. Renaturation of the supernatant containing the *Rh*Lip was achieved by a 30-fold dilution of the denaturant in 20 mM Tris-HCl pH 8.0, 500 mM arginine, 0.6 mM GSH, and 12 mM GSSG, and the solution was concentrated to about 10 mL using an Amicon ultrafiltration cell (Millipore, Billerica, USA) equipped with a 10-kDa membrane and abundantly dialyzed against 20 mM Tris-HCl pH 8.0. The protein was finally aliquoted and stored at −20 °C in the presence of 20 % glycerol.

Electrophoretic Analysis

Electrophoretic runs were performed with a Mini-Protean II cell (Bio-Rad, Hercules, CA) unit at room temperature. Twelve percent SDS-PAGE was made as described by Laemmli [10]. Marker XL-OPTI Protein 2.8 (ABM, Richmond, BC, Canada) was used as molecular weight standard.

*Rh*Lip Determination of pH and Temperature Optima

The esterase activity was monitored at 348 nm (the pH-independent isosbestic point of *p*-nitrophenol and *p*-nitrophenoxide ion) with *p*NP-pentanoate (100 μM) as substrate. The kinetic measurements were performed at 25 °C, and the buffers used were 0.1 M Na-phosphate over the pH range of 7.0–7.5, 0.1 M Tris-HCl over the pH range of 7.5–9.5, and 0.1 M CAPS over the pH range of 9.5–12.0. The assays were carried out in duplicate or triplicate, and the results were the means of two or three independent experiments. Due to the high self-degradation rate of the *p*NP-esters at high pH values, all further characterizations were performed at pH 10.0. The dependence of activity on temperature was studied over the range of 10–60 °C, with *p*NP-pentanoate (100 μM) as substrate, in a reaction mixture 0.1 M CAPS pH 10.0, containing 3 % acetonitrile (standard conditions).

*Rh*Lip Thermostability

The thermal stability of *Rh*Lip was studied over the range of 5–50 °C. Pure enzyme (0.2 mg/mL in a 0.1 M CAPS buffer pH 10.0) was incubated in tubes at different temperatures. Aliquots were withdrawn after 30, 60, 90, and 120 min and assayed at 30 °C in standard condition described above, using *p*NP-pentanoate as substrate.

*Rh*Lip Esterase Activity

The time course of the esterase-catalyzed hydrolysis of *p*NP-esters was followed by monitoring of *p*-nitrophenoxide production at 405 nm, in 1-cm path-length cells with a Cary 100 spectrophotometer (Varian, Mulgrave, Australia). Initial rates were calculated by linear least-squares analysis of time courses comprising less than 10 % of the substrate turnover. Assays were performed at 30 °C in a mixture of 0.1 M CAPS pH 10, 3 % acetonitrile, containing *p*NP-esters (100 μM). Stock solutions of *p*NP-butanoate (C4), *p*NP-pentanoate (C5), and *p*NP-hexanoate (C6) (Sigma-Aldrich, MO, USA) were prepared by dissolving substrates in pure acetonitrile. Assays were performed in duplicate, and the results were the mean of two independent experiments. One unit of enzymatic activity was defined as the amount of the protein releasing 1 μM of *p*-nitrophenoxide/min from *p*NP-esters. The absorption coefficient used for *p*-nitrophenoxide was 19,000 at 30 °C and pH 10.

Kinetic Measurements and Analysis

Initial velocities versus substrate concentration data were fitted to the Michaelis-Menten equation using the software GraphPad Prism version 5.00 (GraphPad software, La Jolla, USA). The concentration of *p*NP-butanoate and *p*NP-pentanoate ranged from 0.05 to 2 mM, while *p*NP-hexanoate were varied from 0.1 to 1 mM. Assays were done in duplicate and the results were the mean of two independent experiments. The kinetic experiments were performed using acetonitrile as solvent.

Effect on Enzymatic Activity by Organic Solvents, Detergents, Metals, and NaCl

Enzyme activity was evaluated in the standard assay (0.1 M CAPS pH 10, 3 % acetonitrile, 30 °C) using *p*NP-pentanoate as substrate. The activity was measured using an increasing concentration of the solvents such as acetonitrile, dimethyl sulfoxide (DMSO), diethyl ether,

and dimethyl formamide (DMFA) from 0 to 20 % (*v*/*v*) in the assay mixture. Results were reported as relative activity with respect to the value measured without solvents.

The effect of detergents on enzymatic activity of *Rh*Lip was evaluated by incubating 0.1 mg/mL of pure protein in the presence of 5 mM Triton X-100, Tween-20, and Tween-80 at 5 °C for 1 h. The residual enzymatic activity was measured in the standard condition as described above. Preferences for metal cations were analyzed by adding them separately to 0.1 mg/mL of pure protein at a final concentration of 5 mM and equilibrate at 5 °C for 1 h. The residual enzymatic activity was then measured in the standard condition as described above. The effect of NaCl on enzymatic activity was evaluated by increasing the salt concentration in a range of 0–1 M at 30 °C in standard assay conditions.

Modeling of *Rh*Lip

The three-dimensional model of *Rh*Lip was performed by a comparative modeling strategy using the structure of *Candida antarctica* lipase A as template (CAL A, PDB code 3GUU). The sequence alignment was calculated by the CLUSTALW program [11]. The MODELLER 9v11 program [12] was used to build 100 full atom models of *Rh*Lip structure setting 4.0 Å as root mean square deviation (RMSD) among initial models and by full model optimization. Structure validation was carried out using the pictorial database PDBsum [13]. The structure of the generated model was uploaded to the PDBsum server, and structural analyses, including PROCHECK plots [14], were generated. Moreover, the *Z* score of the *Rh*Lip model and *C. antarctica* lipase A (CAL A) structure was calculated by the web server WhatIf [15]. The *Z* score expresses how well the backbone conformations of all residues correspond to the known allowed areas in the Ramachandran plot. Furthermore, the solvent-accessible surface areas (SASAs) of *Rh*Lip model and CAL A structure were calculated using the POPS algorithm [16].

Molecular Dynamics

Molecular dynamics (MD) simulations were performed with GROMACS software package (v4.5.5) [17]. The model was inserted in a dodecahedron box filled with SPC216 water molecules using GROMOS43a1 all-atom force field. Simulations were carried out at different pH values. Imposing different protonation states according to the number of titratable groups reproduced neutral and basic pH conditions. The simulations were carried out by adding 26 sodium ions to have a value of zero for the net electrostatic charge of the system. The systems were subjected to several cycles of energy minimizations and position restraints to equilibrate the protein and the water molecules around the protein. Particle mesh Ewald (PME) algorithm was used for the electrostatic interactions with the cutoff of 1 nm. The time step was 2 fs, and the temperature was kept constant at 300 K using a modified Berendsen thermostat with a time constant of 0.1 ps. The simulation time for each dynamic was 10 ns. GROMACS routines were used to analyze the trajectories in terms of RMSD, RMSF, and gyration radius.

Results and Discussion

Purification and Refolding from Inclusion Bodies

In this work, we present a biochemical characterization of a new alkaliphilic esterase from *Rhodococcus* sp. The *lip3* gene was cloned into a pET-22b expression vector, and the

construct was transferred into *E. coli* BL21(DE3) calcium competent cells. Several expression conditions were investigated, but IPTG induction of *E. coli* cells resulted in the accumulation of recombinant *Rh*Lip as inclusion bodies (IB). The induction at 20 °C was effective in producing the highest amount of *Rh*Lip compared to the other contaminant proteins. The IBs were purified and the protein refolded as described in the "Materials and Methods" section. According to the structural analysis, two disulfide bridges were detected, and the refolding protocol was optimized by adding GSSG (oxidized glutathione) and GSH (reduced glutathione) to the refolding solution. Using this protocol, about 8 mg of pure enzyme was obtained from 0.5 g of *E. coli* cell pellet.

Purity of the protein preparation was evaluated by SDS-PAGE analysis. As shown in Fig. 1, a single band was observed with an apparent mass of about 38 kDa.

*Rh*Lip Functional Characterization

The dependence of *Rh*Lip activity in the function of pH was estimated using *p*NP-pentanoate as substrate (Fig. 2a). The absorption of *p*-nitrophenol changes at different pH values because of variations in equilibrium between *p*-nitrophenol and *p*-nitrophenoxide. In this work, we monitored the release of *p*-nitrophenol at 348 nm, that is, the isosbestic point of *p*-nitrophenol and *p*-nitrophenoxide. The maximum activity of

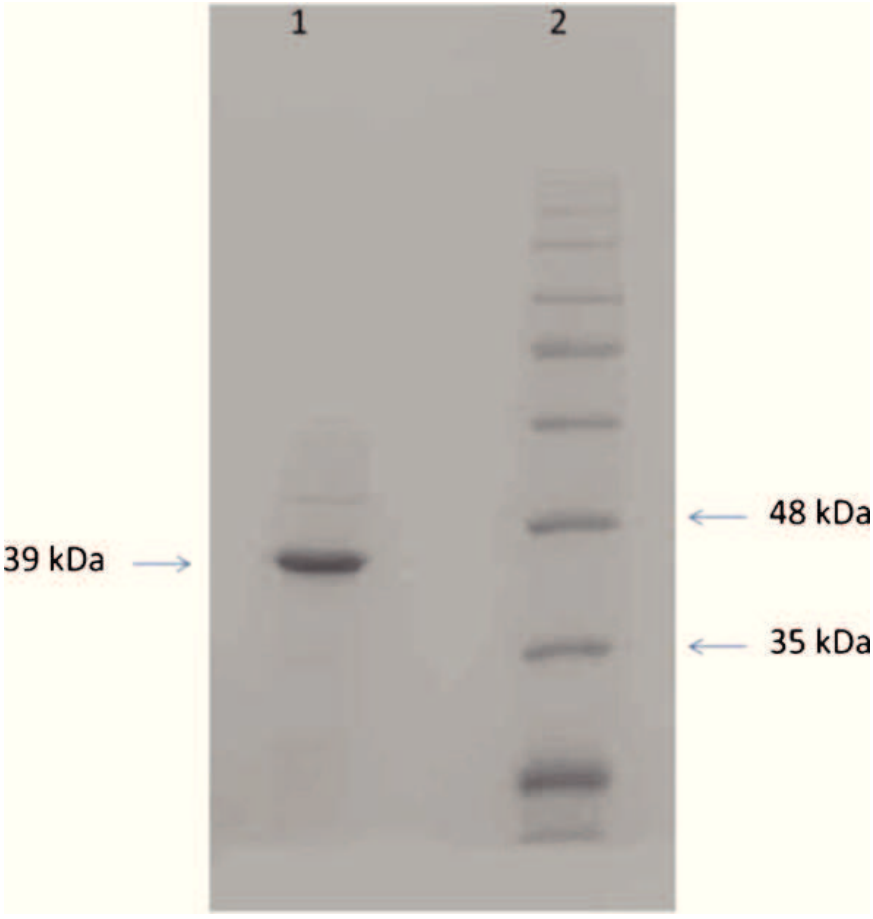

Fig. 1 SDS-PAGE (12 % acrylamide) of *Rh*Lip after the denaturation-refolding procedures. *Lane 1*, purified *Rh*Lip; *lane 2*, molecular weight marker

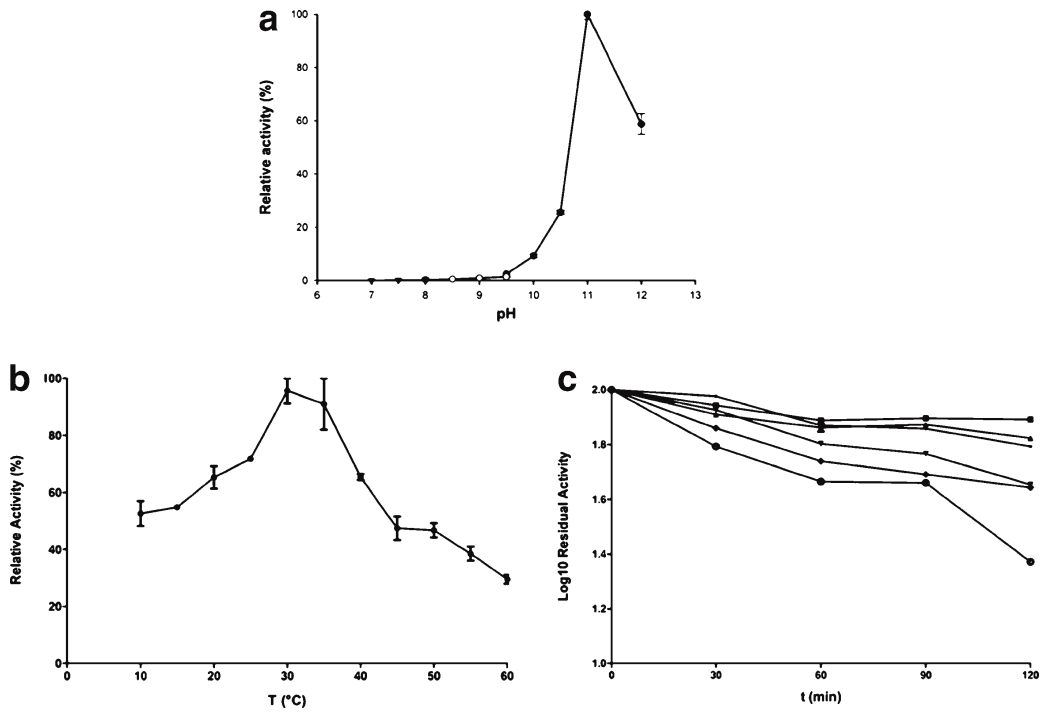

Fig. 2 **a** Effect of pH on the esterase activity. **b** Effect of temperature on the esterase activity. **c** Thermostability of *Rh*Lip, at various temperatures, such as 5 °C (*black circles*), 10 °C (*black squares*), 20 °C (*black up-pointing triangles*), 30 °C (*black down-pointing triangles*), 40 °C (*black diamonds*), and 50 °C (*white circles*). The enzyme was incubated in 0.1 M CAPS pH 10.0 at the indicated temperatures and times. The residual activity was measured at 30 °C using *p*NP-pentanoate as substrate

*Rh*Lip was recorded at pH 11 in 0.1 M CAPS, and the relatively low activity between pH 7 and pH 9 suggests that the enzyme was a highly alkaliphilic esterase. Other alkaliphilic esterases have been identified from genomic and metagenomic sources so far [18] including two other cold-active esterases with optimal pH >10 [19–21]. The relationship between *Rh*Lip activity and temperature was evaluated in the range of 10–60 °C using *p*NP-pentanoate as substrate (Fig. 2b). The apparent maximal activity was recorded at 30 °C, and the activity detected at 10 °C remained approximately the 50 % of the maximum activity.

The *Rh*Lip thermal stability was evaluated in the range of 5–50 °C. Enzyme samples were incubated at any given temperature for different lengths of time, and the residual activity was recorded at 30 °C. This study demonstrated that *Rh*Lip presented a typical behavior as other psychrophilic enzymes, showing a low kinetic stability at temperature higher than 30 °C [22, 23].

In fact, as shown in Fig. 2c, we observed a very low decrease in activity after 2 h of incubation at 5, 10, and 20 °C, while when the temperature increased up to 30 and 40 °C, we noted a significant decrease in activity. After 2 h of incubation at 50 °C, only 20 % of enzymatic activity was still recorded.

Kinetics Studies

We investigated the activity of *Rh*Lip toward different synthetic substrates by using several *p*NP-esters with different acyl chain lengths. Activity was assessed in the presence of 0.1 M CAPS pH 10 instead of the optimum pH buffer (0.1 M CAPS pH 11) due to the instability of

the various substrates at alkaline pH value. All the characterization was also performed at 30 °C and in the presence of 3 % acetonitrile. Concerning the affinity values, we observed that Km values decrease when acyl chain length increases, and this suggests that *Rh*Lip possesses a high affinity with longer aliphatic chain substrates. Instead, the Kcat and Kcat/Km values show the opposite behavior: in our standard conditions, the enzyme displays the highest Kcat and Kcat/Km on *p*NP-butanoate with values of 1.63 s^{-1} and 2.16 s^{-1} mM^{-1}, respectively (Table 1). The biochemical characterization of the recombinant enzyme revealed *p*NP-butanoate (C4) as the preferred substrate, and the hydrolytic activity significantly decreased as the chain length increased above C8, with very little activity toward *p*NP-tetradecanoate (C14) (data not shown), suggesting that the enzyme was an esterase and not a lipase.

Effect on Enzymatic Activity by Organic Solvents, Detergents, Metals, and NaCl

The effect of the presence of water-miscible solvents on *Rh*Lip enzymatic activity on *p*NP-pentanoate at 30 °C in 0.1 M CAPS pH 10.0 was investigated. For all the solvents tested, except DMFA, we observed a similar behavior as shown in Fig. 3a. The increasing concentration of organic solvent in the assay mixture enlarged *Rh*Lip catalytic activity up to a critical concentration, and further addition of solvents led to a gradual protein inactivation. These results are coherent to what were observed for other esterases belonging to hormone-sensitive lipase protein family, as demonstrated by Mandrich and coworkers [24].

We reported the best enzymatic activation (more than 200 % of the relative activity) in the presence of 5 % diethyl ether. This behavior has been explained in literature as the ability of the organic solvents to stabilize ionic intermediates in the case of aprotic solvents [25]. *Rh*Lip was incubated in the presence of various denaturants or metal ions for 1 h, and the residual activity was measured using *p*NP-pentanoate as substrate at 30 °C. The resulting values are summarized in Table 2, which demonstrated that few tested compounds had an inhibitory effect on *Rh*Lip activity, although at various extents. The strongest inhibitory effect was observed in the presence of Ca^{2+} ions suggesting the absence of a Ca^{2+}-binding motif sequence. A similar effect of enzymatic inactivation was detected in the presence of Tween-80. On the contrary, a strong activation was observed by incubating the *Rh*Lip in the presence of Tween-20 and EDTA. Tween 20 was more easily hydrolysed than Tween-80, indicating that the chain length may play an important role on substrate specificity [26].

The effect of the presence of NaCl on *Rh*Lip enzymatic activity was evaluated on *p*NP-pentanoate in 0.1 M CAPS pH 10.0 at 30 °C. We observed an improved activity with the highest concentration of 1 M NaCl (Fig. 3b). A similar behavior may be explained as the ability of salt to enhance the hydrophobic interaction between enzyme and substrate [27].

Table 1 Kinetic parameters

	Km (mM)	Kcat (1/s)	Kcat/Km (1/s*mM)
*p*NP-butanoate	0.753±0.098	1.63±0.19	2.16±0.25
*p*NP-valerate	0.691±0.090	0.69±0.09	0.99±0.11
*p*NP-caproate	0.276±0.036	0.14±0.01	0.45±0.04

All parameters were calculated at 30 °C, in 0.1 M CAPS pH 10.0, containing acetonitrile at a final concentration of 3 %

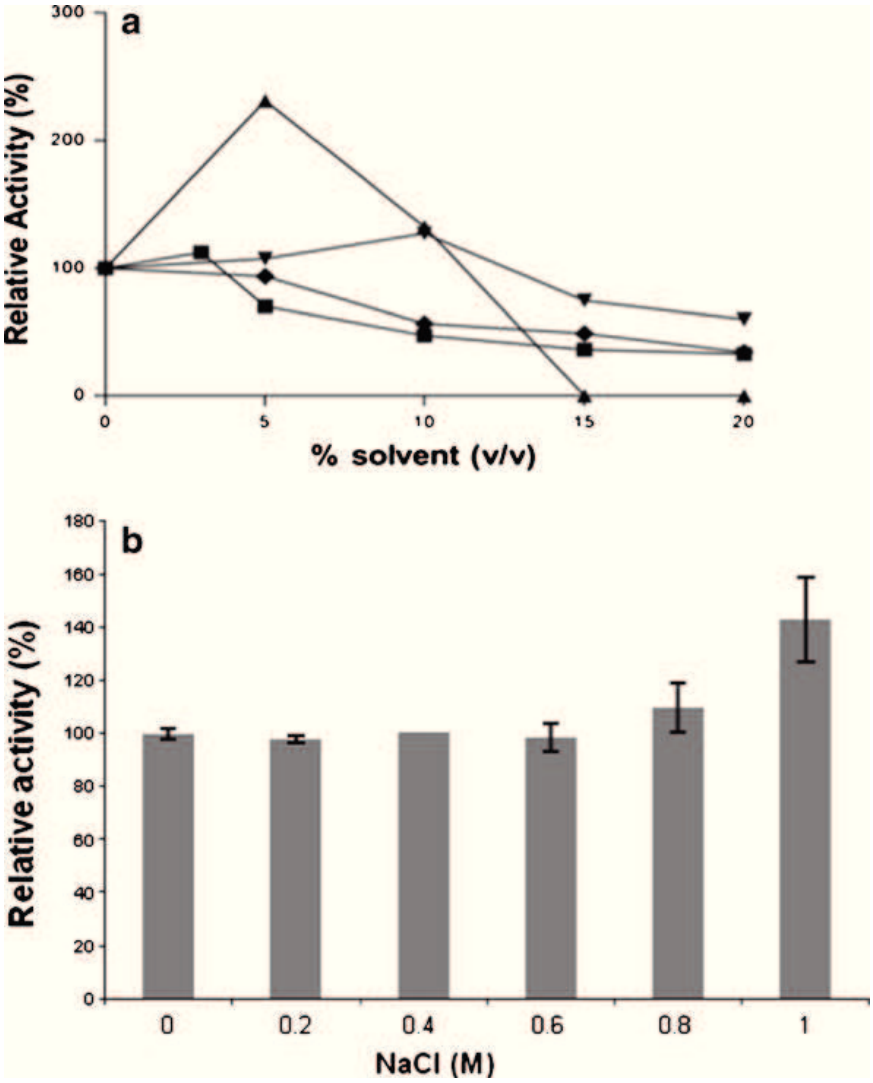

Fig. 3 **a** Effect of organic solvents on the esterase activity. Enzyme activity was evaluated in the presence of increasing concentration of acetonitrile (*black squares*), diethyl ether (*black up-pointing triangles*), DMSO (*black down-pointing triangles*), and DMFA (*black diamonds*). The relative activity was measured at 30 °C in 0.1 M CAPS pH 10.0 using *p*NP-pentanoate as substrate. **b** Effect of NaCl on the esterase activity. Enzyme activity was evaluated in the presence of increasing concentrations of NaCl. The relative activity was measured at 30 °C in 0.1 M CAPS pH 10.0 with *p*NP-pentanoate as substrate

*Rh*Lip Model

The three-dimensional modeling of *Rh*Lip was performed by a homology modeling approach using the *C. antarctica* lipase A (PDB ID: 3GUU) structure as template. The CAL A structure was chosen due to sequence identity of 30 % between the *Rh*Lip sequence and the template. The multiple alignments between *Rh*Lip and the best scoring templates are shown in Fig. 4. Starting from the alignment of *Rh*Lip sequence with the reference structure, a set of 100 all-atom models was generated. The best model (Fig. 5a) was selected in terms of energetic and stereochemical quality. In details, it had 89.2 % of

Table 2 Effect of various compounds on *Rh*Lip activity

Compounds (5 mM)	Relative activity (%)
No addition	100
$CaCl_2$	40.77±2
$CuCl_2$	101.94±9
$MgCl_2$	124.27±17
$LiCl_2$	130.10±1
EDTA	195.14±6
Tween-20	151.46±15
Tween-80	0
Triton X-100	98.06±10

The residual activity was measured in 0.1 M CAPS pH 10.0 with *p*NP-pentanoate at 30 °C

residues in most favored regions of the Ramachandran plot according to PROCHECK program and a WhatIf *Z* score of 0.050. These values, compared with those of the template structure, i.e., *Z* score=−1.181 and 88.6 % of residues in most favored regions of the Ramachandran plot, indicated that the quality of the model was really high. The *Rh*Lip model showed an alpha-beta structure characterized by 13 α-helices (H3, H5–H16), three 3_{10} helices (H1, H2, and H4), and nine beta-strands (B1–B9), corresponding to 39.6 and 14.5 % of the sequence, respectively. *Rh*Lip secondary structures are represented in Fig. 6. *Rh*Lip was stabilized by two disulfide bonds as well as the template structure (Cys47–Cys224, Cys299–Cys351). The SASAs of *RhLip* model and CAL A structure calculated by POPS algorithm showed a hydrophobic area of 61.23 % and a hydrophilic area of 38.77 % for *Rh*Lip, while a hydrophobic area of 49.83 % and a hydrophilic area of 50.17 % for CAL A. Hydrophobicity of the surface exposed to the solvent is an important feature of lipases and esterases because these classes of enzymes work at the interface between a polar and an apolar phase. Structural analysis was carried out by analyzing the most conserved residues of *Rh*Lip multiple alignment (Fig. 7). Ser137, Asp283, and His323 form the catalytic triad of *Rh*Lip (Fig. 5b). These three amino acids are located in three different loops connecting three strands to three α-helices. In particular, Ser137 is within a conserved motif (GTSXGG), and the presence of the glycines gives some flexibility at this area. The side chain atoms NE2 and ND1 of H323 make two h-bonds (2.69 and 3.19 Å) with the side chain atom OG of S137 and the side chain atom OD2 of D283. These bonds hold together the members of the catalytic triad. Moreover, carbonyl oxygen of His323 makes a hydrogen bond (2.58 Å) with the hydroxyl group of Tyr136, another conserved residue located in a strand of beta-sheet B. This bond further helps this β-strand to keep close to the catalytic triad.

Molecular Dynamics

Since the three-dimensional model accurately described the structural organization of this protein, we tried to have a more dynamic view of its structure. We have subjected the best *Rh*Lip model to molecular dynamics simulations in order to evaluate its stability. These studies were made at neutral as well as at alkaline pH because the sequence of this protein

Fig. 4 Multiple sequence alignment among *Rh*Lip sequence and other four templates, which demonstrated to display the best score. The intensity of blue color is proportional to the identity percentage. The conservation level of residues and the consensus is also shown

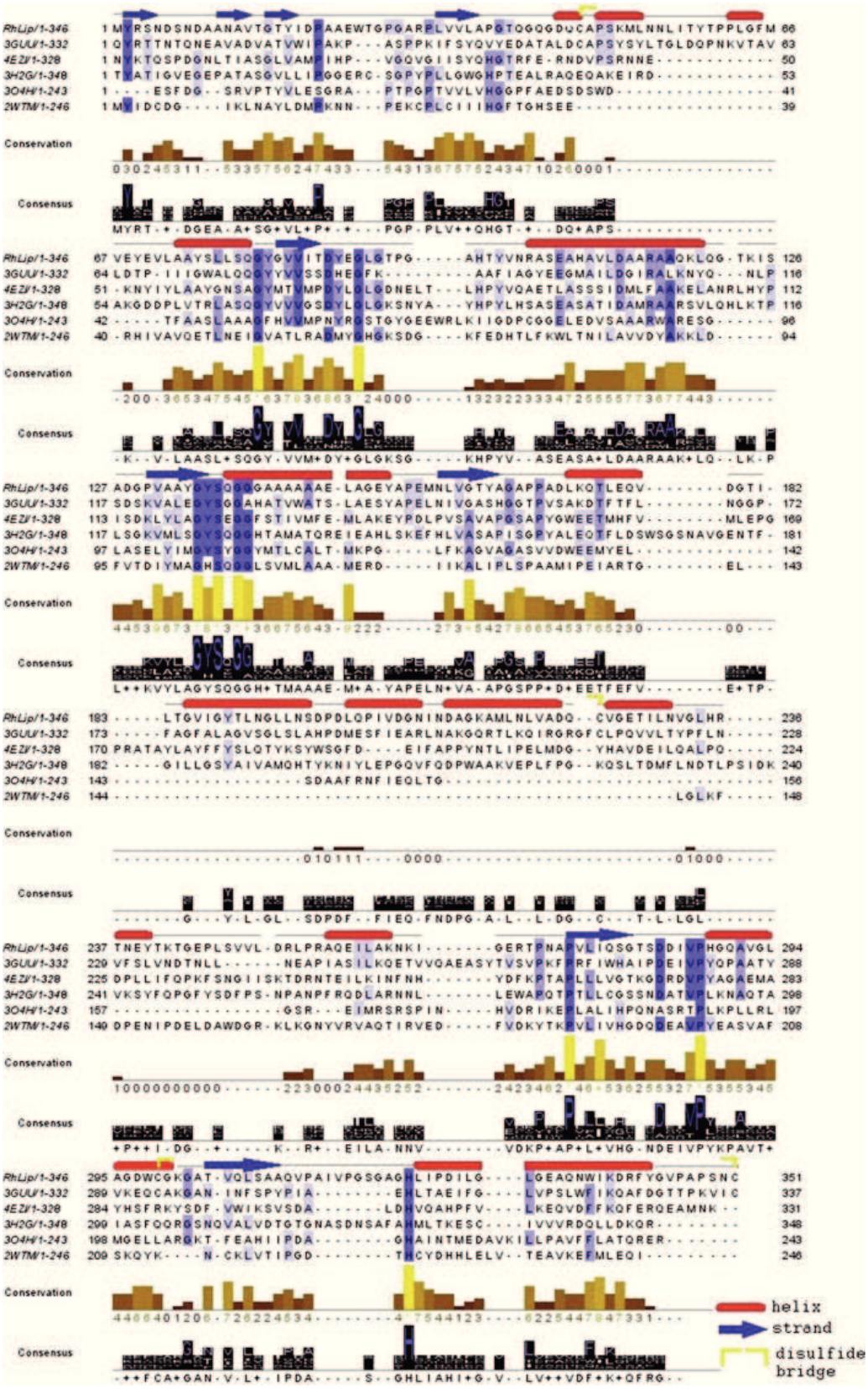
RhLip/1-346
3GUU/1-332
4EZI/1-328
3H2G/1-348
3O4H/1-243
2WTM/1-246
Conservation
Consensus
helix
strand
disulfide bridge

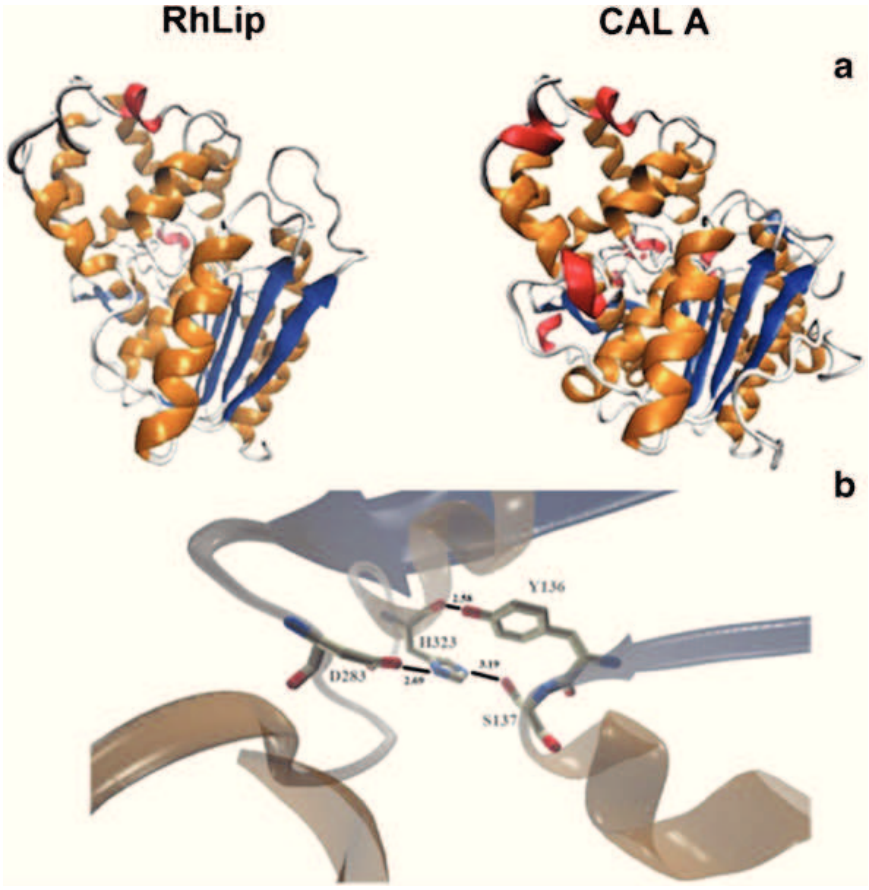

Fig. 5 **a** Graphical representation of *Rh*Lip and CAL A (PDB ID: 3GUU) structures. Alpha helices are shown in *orange*, 3–10 helices are shown in *red*, and beta-strands are shown in *blue*. **b** Graphical representation of *Rh*Lip catalytic triad. Hydrogen bond length is displayed in angstroms

shows many positively and negatively charged residues sensitive to pH changes. The *Rh*Lip model reached a stable equilibrated state after 6 ns simulation at both pH levels; in fact, the related RMSD values (Fig. 7a), computed by superposing the various structures obtained during the simulations and the initial structure at time zero, were almost constant in the remaining simulation time. However, we noted that the fluctuations observed at alkaline pH levels in the first 3–4 ns were slightly more severe in comparison with the simulation computed at neutral pH (Fig. 7b). This behavior highlighted a different way for the protein to reach an equilibrium state compared to the results at neutral pH. Then, in order to compare the overall size of the two systems at different pH levels, we computed the gyration radius concerning all atoms of 346 residues (Fig. 8). The gyration radius trend showed a quite similar evolution in the simulations, and practically, no variation in molecule compactness was observed.

Finally, the superposition of the RMS fluctuations at neutral and alkaline pH revealed that the residues with a high degree of flexibility fell in the loop region. This was due to the high presence of charged residues in these regions that, at neutral and alkaline pH, behaved differently. This suggests the important functional role played by these flexible loops in *Rh*Lip at structural as well as at functional levels.

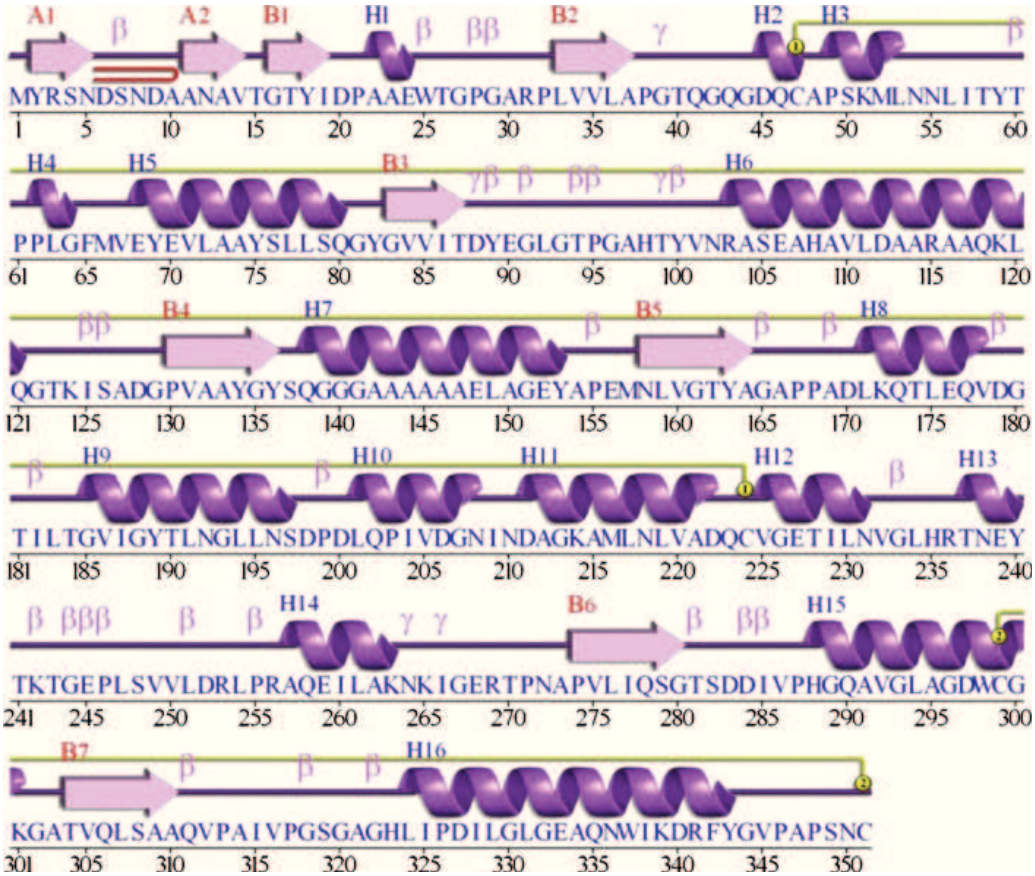

Fig. 6 *Rh*Lip secondary structure representation. Helices are labeled from H1 to H15. Beta-strands are labeled according to the beta-sheet they belong (**a** or **b**). Turns are labeled with β or γ. The disulfide bridge is represented in *yellow*

Conclusion

The present study shed light on a new lypolitic cold-adapted enzyme, which was demonstrated to possess interesting features and various potential applications, as additive for detergent production and biocatalyst for regio- and stereoselective reactions in chemical synthesis [6]. The recombinant enzyme was successfully purified from the inclusion body and characterized. *Rh*Lip was revealed to be an extremely alkaliphilic and cold-adapted esterase. As other psychrophilic enzymes, *Rh*Lip showed a low thermostability at temperature higher than 30 °C, and this heat lability can be exploited in several applications, especially in the food industry. In this case, an industrial process catalyzed by an esterase can be easily stopped by a little increase in temperature, preserving food integrity and flavor.

The enhanced catalytic activity in tested organic solvents could make it useful for some industrial purposes such as production of chemicals, biopolymers, and fuels [28]. *Rh*Lip also showed an improved activity in the presence of 1 M NaCl. This evidence could be useful for industrial application of food processing in the presence of a high concentration of salt. The analysis of the *Rh*Lip model revealed some structural features of the catalytic site of this enzyme, showing the three-dimensional arrangement and the interactions between residues of

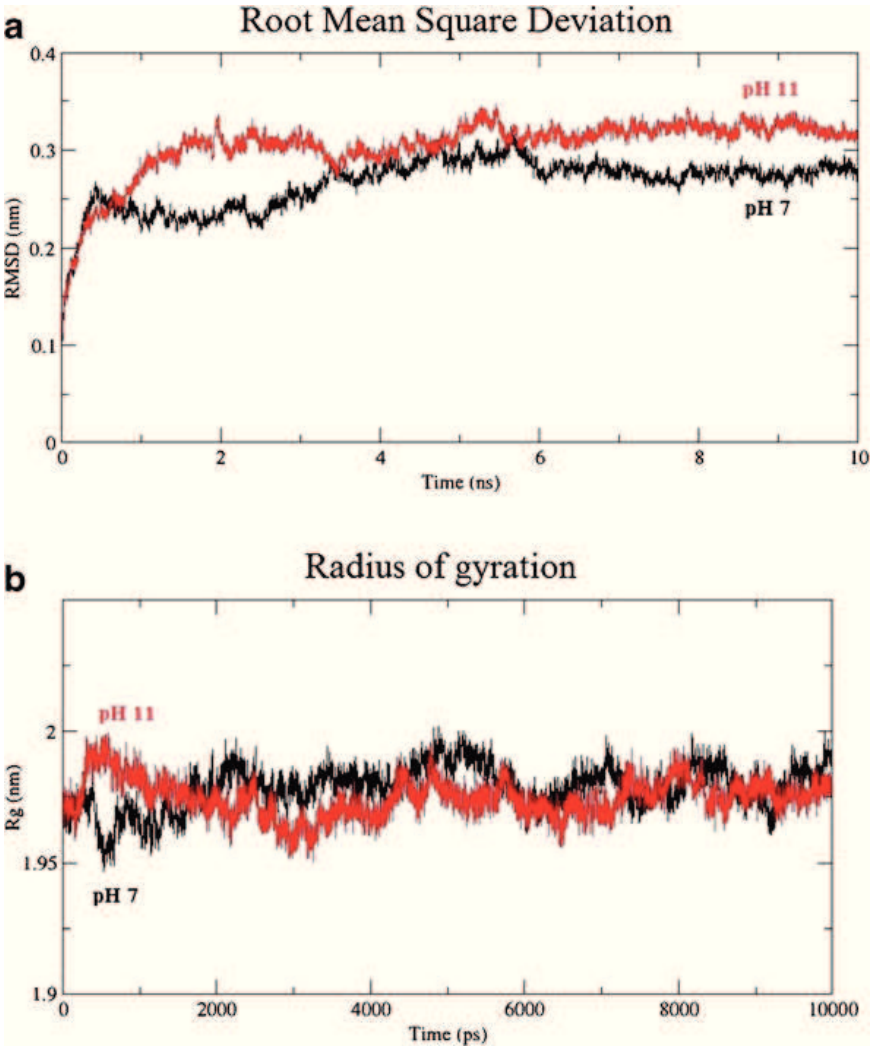

Fig. 7 **a** Trend of root–mean–square deviation (RMSD) for *Rh*Lip structure at pH 7 (*black*) and at pH 11 (*red*) during the molecular dynamic simulations. **b** Trend of gyration radius at pH 7 (*black*) and at pH 11 (*red*)

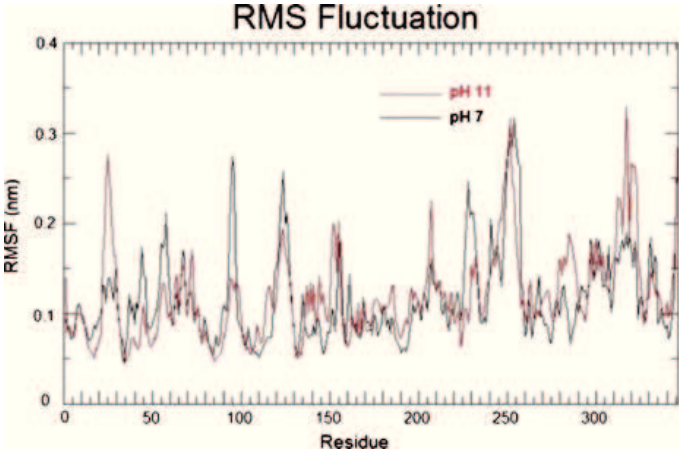

Fig. 8 Root mean square fluctuations at neutral (*black*) and alkaline (*red*) pH at the end of the molecular dynamic simulations

the catalytic triad. Moreover, results of MD simulations highlighted that the protein seems to be quite stable at neutral as well as at alkaline pH. Further developments of this study could be directed to identify potential targets for site-directed mutagenesis to improve protein stability and catalytic activity.

Acknowledgments This work was supported by P.N.R.A. (Italian National Antarctic Research Programme) 2009–2011. We also thank the Yggdrasil application grants 2011–2012 and 2012–2013, funded by the National Research Council of Norway, for supporting the research activities of Dr. Concetta De Santi.

References

1. Rhee, S. K., Liu, X., Wu, L., Chong, S. C., Wan, X., & Zhou, J. (2004). *Applied and Environmental Microbiology, 70*, 4303–4317.
2. Gupta, R., Gupta, N., & Rathi, P. (2004). *Applied Microbiology and Biotechnology, 64*, 763–781.
3. Aurilia, V., Parracino, A., & D'Auria, S. (2008). Microbial carbohydrate esterases in cold adapted environments. *Gene, 410*, 234–240.
4. Paredes, D. I., Watters, K., Pitman, D. J., Bystroff, C., & Dordick, J. S. (2011). *BMC Structural Biology, 11*, 42.
5. Cavicchioli, R., Charlton, T., Ertan, H., Mohd Omar, S., Siddiqui, K. S., & Williams, T. J. (2011). *Microbial Biotechnology, 4*, 449–460.
6. Jeon, J. H., Kim, J. T., Kang, S. G., Lee, J. H., & Kim, S. J. (2009). *Marine Biotechnology (NY), 11*, 307–316.
7. de Pascale, D., De Santi, C., Fu, J., & Landfald, B. (2012). *Marine Genomics, 8*, 15–22.
8. Hjerde, E., Pierechod, M. M., Williamson, A. K., et al. (2013). *Genome Announcements, 7*(1). e0005513.
9. Rutherford, K., Parkhill, J., Crook, J., Horsnell, T., Rice, P., Rajandream, M. A., et al. (2000). *Bioinformatics, 16*, 944–945.
10. Laemmli, U. K. (1970). *Nature, 227*, 680–685.
11. Thompson, J. D., Higgins, D. G., & Gibson, T. J. (1994). *Nucleic Acids Research, 22*, 4673–4680.
12. Sali, A., & Blundell, T. L. (1993). *Journal of Molecular Biology, 234*, 779–815.
13. Laskowski, R. A. (2001). *Nucleic Acids Research, 29*, 221–222.
14. Laskowski, R. A., MacArthur, M., Moss, D. S., & Thornton, J. M. (1993). *Journal Applied Crystallography, 26*, 283–291.
15. Vriend, G. (1990). *Journal of Molecular Graphics, 8*(29), 52–56.
16. Cavallo, L., Kleinjung, J., & Fraternali, F. (2003). *Nucleic Acids Research, 31*, 3364–3366.
17. Hess, B., Kutzner, C., van der Spoel, D., & Lindhal, E. (2008). *Journal of Chemical Theory and Computation, 4*, 435–447.
18. Kademi, A., Ait-Abdelkader, N., Fakhreddine, L., & Baratti, J. (2000). *Applied Microbiology and Biotechnology, 54*, 173–179.
19. Park, H. J., Jeon, J. H., Kang, S. G., Lee, J. H., Lee, S. A., & Kim, H. K. (2007). *Protein Expression and Purification, 52*, 340–347.
20. Hu, X. P., Heath, C., Taylor, M. P., Tuffin, M., & Cowan, D. (2012). *Extremophiles : Life Under Extreme Conditions, 16*, 79–86.
21. Kim, Y. H., Kwon, E. J., Kim, S. K., Jeong, Y. S., Kim, J., Yun, H. D., et al. (2010). *Biochemical and Biophysical Research Communications, 393*, 45–49.
22. De Santi, C., Tutino, M. L., Mandrich, L., Giuliani, M., Parrilli, E., Del Vecchio, P., et al. (2010). *Biochimie, 92*, 949–957.
23. Wang, Q., Hou, Y., Ding, Y., & Yan, P. (2012). *Molecular Biology Reports, 39*, 9233–9238.
24. Mandrich, L., De Santi, C., de Pascale, D., & Manco, G. (2012). *Journal of Molecular Catalysis B Enzymatic, 83*, 46–52.
25. Peters, K. S. (2007). *Chemical Reviews, 107*, 859–873.
26. Gandolfi, R., Marinelli, F., Lazzarini, A., & Molinari, F. (2000). *Journal of Applied Microbiology, 89*, 870–875.
27. Morimoto, K., Furuta, E., Hashimoto, H., & Inouye, K. (2006). *Journal of Biochemistry, 139*, 1065–1071.
28. Egorova, K., & Antranikian, G. (2005). *Current Opinion in Microbiology, 8*, 649–655.